

Iterative Detection for Overloaded Multiuser MIMO OFDM Systems

Min Chen

PhD Thesis

University of York
Department of Electronics

August 2013

Abstract

Inspired by *multiuser detection* (MUD) and the ‘Turbo principle’, this thesis deals with *iterative interference cancellation* (IIC) in overloaded multiuser *multiple-input multiple-output* (MIMO) *orthogonal frequency division multiplexing* (OFDM) systems.

Linear detection schemes, such as *zero forcing* (ZF) and *minimum mean square error* (MMSE) cannot be used for the overloaded system because of the rank deficiency of channel matrix, while the optimal approach, the *maximum likelihood* (ML) detection has high computational complexity. In this thesis, an iterative interference cancellation (IIC) multiuser detection scheme with matched filter and convolutional codes is considered. The main idea of this combination is a low complexity receiver. *Parallel interference cancellation* (PIC) is employed to improve the multiuser receiver performance for overloaded systems. A *log-likelihood ratio* (LLR) converter is proposed to further improve the reliability of the soft value converted from the output of the matched filter. Simulation results show that the *bit error rate* (BER) performance of this method is close to the optimal approach for a two user system. However, for the four user or more user system, it has an error floor of the BER performance. For this case, a channel selection scheme is proposed to distinguish whether the channel is good or bad by using the mutual information based on the *extrinsic information transfer* (EXIT) chart. The mutual information can be predicted in a look-up table which greatly reduces the complexity. For those ‘bad’ channels identified by the channel selection, we introduce two adaptive transmission methods to deal with such channels: one uses a lower code rate, and the other is multiple transmissions. The use of an IIC receiver with the *interleave-division multiple access* (IDMA) to further improve the BER performance without any channel selection is also investigated. It has been shown that this approach can remove the error floor.

Finally, the influence of channel accuracy on the IIC is investigated. Pilot-based Wiener filter channel estimation is used to test and verify how much the IIC is influenced by the channel accuracy.

Contents

List of Figures	v
List of Tables	xi
Acknowledgements	xii
Declaration	xiii
Publications	xiv
Chapter 1 Introduction	1
1.1 Motivation	2
1.2 Single-user Detection vs Multiuser Detection.....	3
1.3 Underloaded System vs Overloaded System.....	4
1.4 Summary of Contributions	5
1.5 Outline of This Thesis	6
1.6 Conclusion.....	8
Chapter 2 Fundamental Techniques	9
2.1 MIMO Systems	10
2.1.1 Space-time Coding	11
2.1.2 Spatial Multiplexing	11
2.2 OFDM	13
2.2.1 Introduction of OFDM.....	15

2.2.2 OFDM System Model	19
2.3 MIMO OFDM Systems	22
2.4 Multiuser Detection	23
2.4.1 Matched Filter Detector	25
2.4.2 ZF Detector	26
2.4.3 MMSE Detector	26
2.4.4 ML Detector	27
2.4.5 Parallel Interference Cancellation	27
2.4.6 Performance Comparison between MUD Schemes	29
2.5 Convolutional Code	30
2.5.1 Convolutional Encoding	32
2.5.2 Convolutional Decoding	34
2.6 Turbo Code	35
2.6.1 Turbo Encoding	36
2.6.2 Interleaver	38
2.6.3 Turbo Decoding	40
2.7 EXIT Chart	42
2.8 Interleave-Division Multiple Access (IDMA)	45
2.9 Simulations	46
2.10 Conclusions	54
Chapter 3 Low Complexity Iterative Detection for Overloaded Multiuser MIMO OFDM systems	55

3.1 Introduction	56
3.2 Turbo Multiuser Detection	57
3.3 System Model.....	59
3.4 Multiuser Receiver for AWGN Channel.....	60
3.4.1 Iterative PIC Receiver.....	64
3.4.2 Performance of Iterative PIC Receiver in AWGN Channels	66
3.5 Multiuser Receiver for Flat Fading Channels	70
3.5.1 Performance of Iterative PIC Receiver in Block Fading Channels.....	71
3.6 Multiuser Receiver for Frequency Selective Channels	72
3.6.1 Performance of Iterative PIC Receiver in Frequency Selective Fading Channels	75
3.7 Iterative Interference Cancellation (IIC) Receiver	76
3.7.1 LLR Scaling Factor.....	79
3.7.2 Iterative Interference Cancellation MUD	81
3.7.3 Iterative MAP MUD	84
3.7.4 Performance Comparison between Iterative MAP MUD and IIC MUD.....	87
3.8 Performance of IIC MUD.....	88
3.9 Conclusions	96
Chapter 4 Channel Selection for Iterative Interference Cancellation Multiuser Detection	97
4.1 Introduction	98
4.2 Channel Selection Criterion	99
4.3 Adaptive Transmissions	105
4.4 System Model for Different Channels using Different Code Rates	106
4.5 System Model for Multiple Transmissions	108

4.6 Simulation Results.....	110
4.7 Conclusions	116
Chapter 5 Iterative Interference Cancellation for IDMA Systems	117
5.1 Introduction	118
5.2 The IDMA System Model.....	120
5.3 The Elementary Signal Estimator (ESE).....	121
5.4 Simulation Results.....	125
5.5 Conclusions	130
Chapter 6 Channel Estimation for Iterative Interference cancellation Multiuser Detection	131
6.1 Introduction	132
6.2 Wiener Filter	133
6.3 Iterative Channel Estimation by Wiener Filter.....	138
6.4 Iterative Channel Estimation for MIMO Systems.....	140
6.5 Simulation Results.....	142
6.6 Conclusions	149
Chapter 7 Conclusions and Future Work.....	151
7.1 Summary of Work.....	152
7.2 List of Contributions	153
7.3 Future Work	154
Glossary	155
Bibliography	158

List of Figures

2.1	Block diagram of a MIMO system.....	10
2.2	Alamouti's two transmit diversity scheme with one or two receive antennas	11
2.3	A basic structure of VBLAST transmitter.....	12
2.4	Horizontal encoding (a) and vertical encoding (b) for spatial multiplexing	12
2.5	Principle of OFDM [32].....	16
2.6	OFDM system block diagrams.....	17
2.7	CP insertion.....	18
2.8	Function of CP	18
2.9	BER performances of OFDM system with/out CP and with/out equalization (the channel is perfect known at the receiver, with 4 taps multipath block fading channel (channel coefficients [1 0.9 0.7 0.5]), data length 10000, 128 subcarriers, and CP length 10).....	19
2.10	$N_T \times N_R$ MIMO-OFDM system.....	23
2.11	Multiple access communication system with K users	25
2.12	Comparison of linear and non-linear detections for MIMO (2-by-2) OFDM system .	30
2.13	Code structure of general convolutional code	31
2.14	Structures of convolutional encoder	33
2.15	The basic Turbo encoding structure.....	37
2.16	Basic structure of an iterative Turbo decoder.....	40

2.17 Iterative decoder for parallel concatenated codes.....	43
2.18 Structure of the IDMA system	46
2.19 SISO system of AWGN, block fading and fast fading channel with/out convolutional code (1/2 rate).....	47
2.20 Comparison of BER performance for SISO system using convolutional code with different generator polynomials (with the same code rate 1/2) in a block fading channel	47
2.21 2-by-2 system of fading channel using convolutional code (1/2 rate) with/out interleaver, hard decision decoding is considered.....	48
2.22 BER performance of ML hard decision and MAP soft decision of 2-by-2 system with fast fading channel using convolutional code (1/2 rate).....	49
2.23 BER performance of SISO system of AWGN, block fading and fast fading channel using convolutional code (1/2 rate) and turbo code (1/2 rate).....	50
2.24 BER performance of data bits and parity bits of SISO system of AWGN, block fading and fast fading channel using convolutional code (1/2 rate).....	50
2.25 BER performance of data bits and parity bits of SISO system of AWGN, block fading and fast fading channel using turbo code (symmetric PCC rate 1/2 rate)	51
2.26 Extrinsic information transfer characteristics of soft in/soft out decoder for rate 1/2 convolutional code and simulated trajectory of iterative decoding at 0.5dB	52
2.27 Extrinsic information transfer characteristics of soft in/soft out decoder for rate 1/2 convolutional code and simulated trajectory of iterative decoding at 0.8dB	52
2.28 Extrinsic information transfer characteristics of soft in/soft out decoder for rate 1/2 convolutional code and simulated trajectory of iterative decoding at 1.2dB	53
2.29 Extrinsic information transfer characteristics of soft in/soft out decoder for rate 1/2 convolutional code and simulated trajectory of iterative decoding at 3dB	53
3.1 The structure of overloaded multiuser MIMO system	60
3.2 Matched filter multiuser receiver for overloaded MIMO system.....	61
3.3 Threshold used to convert LLR to soft estimate	64

LIST OF FIGURES

3.4	Structure diagram of the iterative PIC receiver.....	65
3.5	BER performance of iterative PIC receiver for two user (one transmitter for each user) two receiver system in AWGN channel.....	67
3.6	BER performance of iterative PIC receiver for three user (one transmitter for each user) three receiver system in AWGN channel.....	68
3.7	BER performance of iterative PIC receiver for four user (one transmitter for each user) four receiver system in AWGN channel.....	68
3.8	BER performance of iterative PIC receiver for two user (one transmitter for each user) one receiver system in AWGN channel.....	69
3.9	BER performance of iterative PIC receiver for two user (one transmitter for each user) one receiver system in AWGN channel with unequal power (1, 0.5).....	69
3.10	BER performance of iterative PIC receiver for two user (one transmitter for each user) two receiver system in Rayleigh flat fading channel.....	71
3.11	BER performance of iterative PIC receiver for two user (one transmitter for each user) one receiver system in Rayleigh flat fading channel.....	72
3.12	The transmitter structure of overloaded multiuser MIMO OFDM system.....	73
3.13	The receiver structure of overloaded multiuser MIMO OFDM system.....	74
3.14	BER performance of iterative PIC receiver for two user (one transmitter for each user) two receiver system in frequency selective fading channel.....	75
3.15	BER performance of iterative PIC receiver for two user (one transmitter for each user) one receiver OFDM system in frequency selective fading channel.....	76
3.16	PDFs of the MRC output and hard to soft converter output for the two user one receiver system in frequency selective fading channel (2 taps delay model).....	78
3.17	PDFs of the LLR converter output for two user one receiver system in frequency selective fading channel (2 taps delay model).....	80
3.18	The structure of IIC-MUD scheme.....	82
3.19	Structure of iterative MAP receiver.....	84
3.20	Four combinations for two user case.....	85

3.21 BER performance of IIC MUD for 2×1 OFDM system.....	87
3.22 BER performances of IIC MUD for 2×1 OFDM system using Turbo code ([5 7], 1/2 code rate) and convolutional code ([5 7], 1/2 code rate).....	88
3.23 BER performances of IIC MUD for 2×1 and 2×2 OFDM system.....	89
3.24 EXIT charts for two specific cases: (a) bad channel and (c) good channel, while (b) shows the whole iterative process which is like a figure of eight	90
3.25 BER performance (a) and FER performance (b) for 4×2 OFDM system, compared with the optimal approach (IMAP).....	91
3.26 BER performances of IIC MUD for 4×2 OFDM system using Turbo code ([5 7], 1/2 code rate) and convolutional code ([5 7], 1/2 code rate).....	92
3.27 EXIT chart of IIC MUD for 4×2 OFDM system using Turbo code ([5 7], 1/2 code rate) and convolutional code ([5 7], 1/2 code rate)	93
3.28 BER performance for the four user two receiver system with different transmit power (0, 0,-3 and -3dB)	94
3.29 BER performance of IIC MUD for fixed channel multipath (2 taps) under different OLFs using 1/3 code rate.....	94
3.30 BER performance of IIC MUD for fixed code rate (1/3) and OLF (4.5) under different channel taps	95
3.31 BER performance of IIC MUD for fixed OLF (5) under different channel taps and code rates.....	95
4.1 The structure of IIC MUD with channel analyzer and selector.....	100
4.2 EXIT chart for a bad channel (a) and a good channel (b)	102
4.3 The structure of adaptive system for different channels using different code rates .	107
4.4 The adaptive receiver structure for different channels using different code rates....	107
4.5 The structure of adaptive system for multiple transmissions	108
4.6 The adaptive receiver structure for multiple transmissions.....	109
4.7 Rejected channel rate (RCR) and errored channel rate (ECR).....	111

4.8	BER (a) and FER (b) performance for the four user two receiver system using IIC-MUD with channel selection	112
4.9	BER performance for the eight user four receiver system using IIC-MUD with channel selection under different channel taps (2, 3, 4 taps)	113
4.10	Throughput vs SNR for two adaptive schemes	114
4.11	BER (a) and FER (b) performance for the four user two receiver system using lower code rate (1/3) and adaptive transmission for bad channels compared to the IIC with and without channel selection	115
5.1	The structure of a MIMO-OFDM IDMA system.....	120
5.2	The structure of ESE receiver	121
5.3	BER performance of the 4×1 OFDM-IDMA system with rate-1/4 repetition code (1/8 total rate), ESE, IIC, and MAP approaches are compared.....	125
5.4	BER performance of the 4×2 OFDM-IDMA system with rate-1/2 repetition code (1/4 total rate), ESE, IIC, and MAP approaches are compared.....	126
5.5	EXIT chart of the 4×2 OFDM-IDMA system with rate-1/2 repetition code (1/4 total rate); With IDMA and without IDMA are compared.....	127
5.6	BER performance of OFDM-IDMA system with rate-1/4 repetition code (1/8 total rate) for different users; With ESE (a) and with IIC (b) are compared	128
5.7	BER performance of OFDM-IDMA system with rate-1/2 repetition code (1/4 total rate) for different users; With ESE (a) and with IIC (b) are compared	129
5.8	BER performance of OFDM-IDMA system for ten user case: 10-by-1 with rate-1/6 repetition code (1/12 total rate) and 10-by-2 with rate-1/4 repetition code (1/8 total rate).....	130
6.1	BER performance of IIC with non-perfect channel knowledge	133
6.2	Pilot insertion structures: (a) using one whole OFDM symbol for transmitting pilots, and (b) using interpolation during one OFDM symbol	134
6.3	Two structures of Channel estimation by Wiener filtering: (a) using one whole OFDM symbol for transmitting pilots, and (b) using interpolation during one OFDM symbol	135

6.4	System structure of iterative channel estimation and signal detection.....	139
6.5	Pilots insertion for MIMO system.....	140
6.6	Receiver structure of channel estimation for MIMO system	141
6.7	MSE performance for SISO OFDM system by Wiener filter	143
6.8	MSE performance for 2-by-1 OFDM system by Wiener filter, with only one iteration	143
6.9	BER performance of 2-by-1 OFDM system with only one iteration channel estimation	144
6.10	MSE performance of iterative channel estimation for 2-by-1 OFDM system by Wiener filter, using different length of pilots (16, 32, 64, 128, 256), compared with different MSE references (data length 256 + pilot length).....	144
6.11	BER performance of iterative channel estimation for 2-by-1 OFDM system by Wiener filter	145
6.12	MSE performance of iterative channel estimation with interference cancellation method and pseudo-inverse method for 2-by-1 OFDM system by Wiener filter.....	146
6.13	BER performance of iterative channel estimation with interference cancellation method and pseudo-inverse method for 2-by-1 OFDM system by Wiener filter.....	146
6.14	MSE performance of non-iterative vs iterative channel estimation for 4-by-2 OFDM system by Wiener filter, without channel selection.....	147
6.15	BER performance of 4-by-2 OFDM system with non-iterative vs iterative channel estimation by Wiener filter, without channel selection	148
6.16	MSE performance of non-iterative vs iterative channel estimation for 4-by-2 OFDM system by Wiener filter, with channel selection.....	148
6.17	BER performance of 4-by-2 OFDM system with iterative vs non-iterative channel estimation by Wiener filter, with channel selection	149

List of Tables

3.1 Complexities of Iterative PIC Receiver in AWGN channel	66
3.2 Complexities of IIC Receiver in frequency selective fading channel.....	83
4.1 Look-up table for mean value vs mutual information.....	104
5.1 Complexity comparison between IIC and ESE for 4-by-2 system using BPSK: $N_T = 4, N_R = 2$, iteration no.=8.....	124
5.2 Complexity comparison between IIC and ESE for 10-by-2 system using BPSK: $N_T = 10, N_R = 2$, iteration no.=8.....	125
6.1 Complexities comparison between interference cancellation and pseudo inverse method for channel estimation.....	142

Acknowledgement

I would like to express my most sincere gratitude to my supervisor, Professor Alister G. Burr. Thank you for your heuristic ideas, valuable supervision, patient instructions and continuous encouragement during my PhD study. You have successfully kept my research progress and conducted my work into a right direction. Without your help much of this work would not have been possible. Thank you for your great work and precious time on correcting my English.

I would like to thank my thesis advisor, Dr. Yuriy Zakharov, who gives me useful comments and helpful suggestions.

I would also like to deliver my grateful thanks to my thesis advisor, Dr. Rodrigo de Lamare. Thank you for always being supportive and providing valuable advice on my annual research progress report.

More thanks go to my colleagues and friends in Communications Research Group, for your help and support throughout my research and my life.

Finally, my deepest gratitude is expressed to my dear parents, who are far away in China, but always care about me, encourage me and try their best to support me. Thank you for your selfless love and unconditional support.

Declaration

Some of the research presented in this thesis has resulted in some publications. These publications are listed at the end of the thesis.

All work presented in this thesis as original is so, to the best knowledge of the author. References and acknowledgements to other researchers have been given as appropriate.

Publications

1. Min Chen and A. G. Burr, “Low-Complexity Iterative Interference Cancellation Multiuser Detection Based Channel Selection,” the second round of review for IET Communications, 2013.
2. Min Chen and A. G. Burr, “Low-Complexity Channel selection and Iterative Detection for Overloaded Uplink Multiuser MIMO OFDM System,” presented at IEEE Vehicular Technology Conference (VTC’13-Spring), Dresden, Germany, June 2013.
3. Min Chen and A. G. Burr, “Low-Complexity Iterative Interference Cancellation Multiuser Detection for Overloaded MIMO OFDM IDMA System,” presented at International ITG Workshop on Smart Antennas (WSA’13), Stuttgart, Germany, March 2013.
4. Min Chen and A. G. Burr, “Low-Complexity Iterative Detection for Overloaded Uplink Multiuser MIMO OFDM System,” presented at International ITG Workshop on Smart Antennas (WSA’12), Dresden, Germany, March 2012.

Chapter 1

Introduction

Contents

1.1 Motivation.....	2
1.2 Single-user Detection vs Multiuser Detection.....	3
1.3 Underloaded System vs Overloaded System.....	4
1.4 Summary of Contributions	5
1.5 Outline of This Thesis	6
1.6 Conclusion.....	8

1.1 Motivation

Recently, due to the current trend of personal wireless communication, it is widely acknowledged that the tremendous demand for higher spectral efficiency, higher data rate, and higher channel capacity, constitutes a significant challenge in next generation wireless communications. However, it is restricted by the limited bandwidth resource that is available for wireless communications. Therefore, much research has been performed to improve the efficiency of the spectrum use. *Multiple-input and multiple-output* (MIMO) systems, which apply multiple antennas at both the transmitter and the receiver, are one of the hottest research topics in this area [1] [2]. MIMO techniques can in principle provide capacity in multiple antenna wireless communication links proportional to the minimum number of transmit and receive antennas, and hence can greatly improve performance compared to single antenna links. The performance benefits can be characterized as multiplexing gain and/or diversity gain [2], and a wide range of techniques, including space time coding and spatial multiplexing are available to exploit these gains.

For multipath fading channel, most conventional modulation techniques are sensitive to inter-symbol interference unless the channel symbol rate is small compared to the delay spread of the channel. Multicarrier techniques provide the solution for wireless communication and fulfil the demands of the wireless channel. *Orthogonal Frequency Division Multiplexing* (OFDM), which has drawn a lot of attention in the field of radio communications, is significantly less sensitive to inter-symbol interference. This is because OFDM splits a high rate data stream into a number of lower rate streams that are transmitted simultaneously over a number of subcarriers, and hence the rate on each OFDM subcarrier is reduced relative to the delay spread while the total symbol rate is equal to that of a single-carrier system. Another reason for this is that a guard time is introduced for each OFDM symbol, which is chosen to be larger than the expected maximum delay. This technique has been considered to be a candidate to support multimedia services in mobile radio communication, to provide higher capacity over conventional access techniques.

In a frequency-selective fading channel, the bit errors of OFDM are normally concentrated in a few severely faded subcarriers. In the rest of the subcarriers, there are normally no bit errors. Therefore the overall *bit error rate* (BER) performance of such

systems is close to that of the poorest channels, which could be rather poor on a fading channel. For this reason a *forward error-control* (FEC) code and interleaver is employed, resulting in a scheme which is widely known as coded OFDM. The FEC code should be powerful enough to correct the sampled errors lying in the severely faded channel, so that higher channel capacity can be obtained. Hence in OFDM, that a code minimum distance significantly greater than the channel order is required to achieve full diversity. Convolutional codes and Turbo codes are used in this thesis and there is a brief introduction to both codes in chapter 2.

The combination of these three technologies, MIMO OFDM with FEC code system, is the great solution for the wireless communication. In recent years, *multiuser detection* (MUD), which can also increase the spectral efficiency, is therefore of great interest. In wireless communications, as a set of advanced MIMO technologies, multiuser MIMO exploits the availability of multiple independent transmit antennas in order to enhance the communication capabilities of each individual user.

It is well known [52] that multi-user MIMO techniques are capable of significantly increasing throughput compared to traditional MIMO wireless systems where F/TDMA is used, especially in asymmetric systems, where the number of antennas at the *base station* (BS) exceeds the number on each terminal. In most cases it is assumed that the number of receive antennas at the BS is greater than or equal to the total number of transmit antennas across all users, but in some cases it may be possible to increase system capacity by allowing a larger number of users, resulting in a so-called *overloaded* system.

However, the known linear MUDs, such as *zero-forcing* (ZF) and *minimum mean square error* (MMSE), due to the rank deficient channel matrix, cannot work for the overloaded system. The optimal and sub-optimal MUDs are of too high computational complexity. The motivation of this thesis is to find suitable detection schemes for overloaded multiuser MIMO OFDM systems, which should be of low complexity, easy implementation, and with good performance.

1.2 Single-user Detection vs Multiuser Detection

Conventional single-user receivers achieve inferior performance in a multiuser system, since they are designed to operate in thermal noise without *co-channel interference*

(CCI) or *multiple access interference* (MAI). Multiuser receivers, however, can exploit the structure of the multiuser signal, detect all users' data simultaneously, and suppress or cancel the multiuser interference effectively, so that they substantially outperform single-user receivers in a multiuser environment.

Many types of MUD techniques have been developed to extract the interference structure by using the *channel impulse responses* (CIR). The optimal approaches based on *maximum likelihood* (ML) or *maximum a posteriori probability* (MAP) algorithm are of too computational complex, although their performance can approach the performance in a single-user system (single-user bound).

Thereby some sub-optimal MUD algorithms have been investigated, which have much lower complexity. Among them, ZF detection and MMSE detection can suppress the interference by means of linear processing, which therefore are referred to as linear detection. Another class of sub-optimal MUD is *successive interference cancellation* (SIC) and *parallel interference cancellation* (PIC), referred to as decision-feedback MUD. The PIC detector is an iterative multiuser detector, which can perform as many iterations as needed. This iterative structure can combine the MUD with the channel decoding. A more detailed introduction to the MUD technique will be given in Chapter 2.

MUD requires knowledge of all users, including both the desired user and the interferers, therefore cannot be used to combat unknown interference. When all the users are desired and their information is known, we can perform MUD to achieve the most desirable detection performance. However, when the interferers' data which may come from other cells or other wireless systems operating in the same waveband is undesired or their information is unknown, advanced single-user receivers [3] can be employed to achieve substantial performance gain over the conventional single-user receiver, instead of multiuser receivers. This thesis will focus on MUD techniques, rather than single-user detection.

1.3 Underloaded System vs Overloaded System

MIMO systems employ multiple antennas at both the transmitter and the receiver. They can roughly be divided into two categories: under-loaded system and overloaded system.

For under-loaded system, the number of receive antennas is greater than or equal to the total number of transmit antenna across all users. Many research works for MIMO technologies are based on this kind of system. The above MUD schemes are also on the basis of this system.

However, when the number of receive antennas is less than the total number of transmit antennas, we call it an overloaded system. For overloaded systems, the interference is more serious, the useful information from received signal is much less than that of under-loaded system. Due to the rank deficient channel, most linear MUD schemes cannot work. In this case, new MUD method should be developed.

1.4 Summary of Contributions

To begin with, this section will briefly introduce the novel contributions of this thesis. Furthermore, more details will be given in individual chapters and then they will be summarized in the last chapter.

1. A low complexity *iterative interference cancellation* (IIC) multiuser detection scheme is proposed for overloaded multiuser MIMO OFDM system. Based on the iterative principle, joint detection and decoding with simple matched filter and convolutional code is used. For the overloaded system, the number of receive antennas is fewer than that of the transmit antennas, the received signal contains too much interference, so that the *log-likelihood ratio* (LLR) is unreliable and will cause problems in decoding. In order to obtain reliable LLR, a LLR convertor is proposed, where a scaling factor which is calculated from the available channel information is applied. In addition to the calculation of the channel covariance, this method requires a low complexity, and for a two user system, the BER performance is very close to that of the optimal approach (MAP detection).
2. For four or more users' case, the matched filter will result in an error floor of the BER performance. A channel selection scheme is proposed to solve this problem. This scheme is based on the EXIT chart. We choose a good or bad channel based on the mutual information. The mutual information is also calculated directly from the channel information. Without the influence of bad channels, the BER performance of the proposed method is close to the MAP detection.
3. For the channel selection scheme, we propose two adaptive methods to process the so-called bad channels. One is using lower code rate for bad channels. According to

the *overloading factor* (OLF), the other method divides the transmitters into several groups for transmission at the non-convergent channels; this method can reduce the interference significantly. Simulation results show that both schemes can remove the error floor and achieve almost the optimal BER performance.

4. The attractive feature of *Interleave-division multiple access* (IDMA) is that it allows the use of a low complexity iterative multiuser detection technique. Combined with IDMA, our proposed IIC can achieve almost the optimal performance without any channel selection. Compared to the *elementary signal estimator* (ESE) [107], which is widely used for IDMA systems, our IIC has nearly the same level of complexity, but achieves much better performance.
5. The scaling factor and channel selection both are based on the assumption that the channel state information is perfectly known at the receiver. Therefore, the influence of channel accuracy on the IIC performance is investigated. By using the Wiener filter, both non-iterative and iterative channel estimation are derived. Simulation results show that although the non-iterative channel estimation can result in a high IIC performance, the performance is further improved when using the iterative channel estimation. The IIC with iterative channel estimation can achieve the performance of the IIC with perfect channel knowledge.

1.5 Outline of This Thesis

After a brief introduction of the motivation and contributions, the rest of the thesis is organised into the following chapters:

Chapter 2: Fundamental Techniques

This chapter introduces the fundamental techniques which are used in this thesis: MIMO, OFDM, Multiuser Detection, Convolutional codes, and Turbo codes. This introduction will mainly focus on the approaches employed to construct the iterative receiver, which are the matched filter, the PIC detector, and the convolutional codes.

Chapter 3: Low Complexity Iterative Detection for Overloaded Multiuser MIMO OFDM Systems

In this chapter, we focus on the overloaded system. Combined with the matched filter, and PIC, an iterative interference cancellation (IIC) MUD is built. A scaling factor is introduced to provide reliable LLRs, which is based on the channel matrix and is used

to make the output of the matched filter close to the Gaussian-like distribution, so that the decoder can obtain the information from the LLRs effectively. IIC can work well for 2-by-1 system. For 4-by-2 and more overloaded systems, the IIC requires lower code rate.

Chapter 4: Channel Selection for Iterative Interference Cancellation Multiuser Detection

In this chapter, a channel selection scheme is introduced for more users and much more overloaded systems, which is based on the EXIT chart. We find the relationship between the mutual information and the mean value from channel, so that a look-up table is obtained. We can select the channel directly using the CHANNEL INFORMATIONs. For the selected channel, the 4-by-2 system can work well. Moreover for the rejected channel, we propose two adaptive methods: one is using low code rate, and the other is multiple transmission. Both methods require low feedback, and work well.

Chapter 5: Iterative Interference Cancellation for Interleave-Division Multiple Access Systems

In this chapter, IDMA is employed. Due to the advantage of IDMA, our low complexity IIC can work very well for the overloaded system. It can obtain more gain compared to the ESE. Combined with IDMA, the IIC can work for high OLF systems, and achieve good performance.

Chapter 6: Channel Estimation for IIC MUD

This chapter presents the relationship between the IIC MUD and channel estimation. Pilot-based channel estimation by Wiener filter is introduced. The simulation show the non-iterative channel estimation is good enough for the IIC MUD. Meanwhile the iterative channel estimation takes the channel estimator, detector and the decoder as an iterative cycle, works in an iterative manner, makes full use of information between those components, and obtains much better performance than non-iterative channel estimation.

Chapter 7: Conclusions and Future Work

This chapter concludes whole thesis in terms of the work presented in the thesis. It summarizes the contributions of this thesis and provides some suggestions for future research based on current work.

1.6 Conclusions

In this chapter, an introduction to the motivation of this work is first given. Based on the interference environment, the two types of receivers are compared: multiuser receiver and single-user receiver. Multiuser receivers usually yield better performance than the single-user ones, but require information of all users. Hence when the receiver needs to detect all users and channels are obtainable, MUD is encouraged. The contribution of this thesis is then presented, and finally shows the outline of this thesis.

Chapter2

Fundamental Techniques

Contents

2.1 MIMO Systems.....	10
2.2 OFDM	13
2.3 MIMO OFDM Systems	22
2.4 Multiuser Detection.....	23
2.5 Convolutional Code.....	30
2.6 Turbo Code.....	35
2.7 EXIT Chart.....	42
2.8 Interleave-Division Multiple Access (IDMA)	45
2.9 Simulations	46
2.10 Conclusions	54

In this chapter, some fundamental techniques used in this thesis are introduced: MIMO, OFDM, MIMO OFDM, *multiuser detection* (MUD), convolutional code, Turbo code, and the *extrinsic information transfer* (EXIT) chart.

2.1 MIMO Systems

In recent years, in order to support reliable high-rate transmissions for wireless communications, a large amount of research has addressed multiple antenna systems, by using multiple antennas both at the transmitter and the receiver. *Multiple-input multiple-output* (MIMO) techniques are becoming the method of choice to achieve the required spectral and power efficiency as well as the reliability of communication [1] [2]. MIMO systems can in principle provide capacity in multiple antenna wireless communication links proportional to the minimum number of transmit and receive antennas, and hence can greatly improve performance compared to *single-input single-output* (SISO) systems [3][4]. The performance benefits of the MIMO channel can be characterized as multiplexing gain and/or diversity gain [5]. Hence, the most important design objective for the MIMO transmission technique is to optimally exploit these benefits in a communication system in order to mitigate the impairments of the wireless channel.

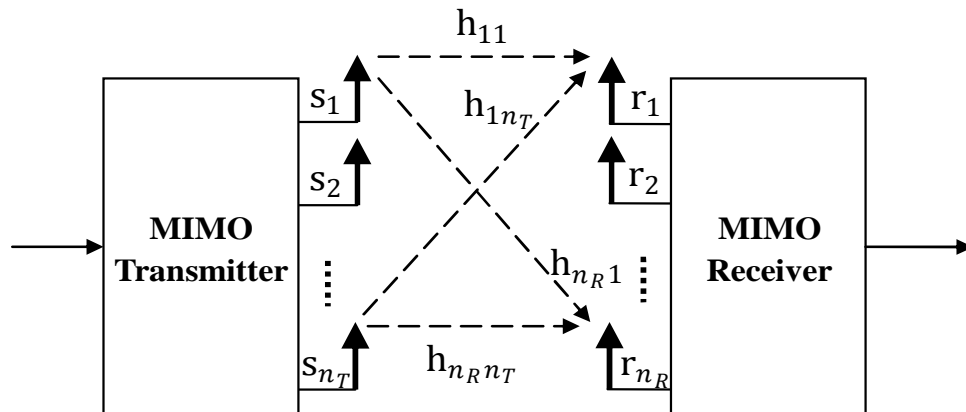


Figure 2.1 Block diagram of a MIMO system

The original idea of MIMO goes back to 1970, proposed by Kaye and George [6]. In 1976, two *maximum likelihood* (ML) vector sequence estimation algorithms for multiple channel transmission systems were then presented [7].

The general construction of a MIMO system is depicted in Fig. 2.1 with arrays of n_T transmit and n_R receive antennas. It is clearly shown that there are $n_T \times n_R$ potentially independent diversity branches between pairs of transmitting and receiving antennas, which can provide multiple individual fading paths for the same information message.

2.1.1 Space-time Coding

In 1998, in order to maximize the diversity gain of a MIMO system, space-time coding was proposed [8], where multiple copies of a data stream are transmitted across a number of antennas and various versions of the data are received, to combat the effects of channel fading and improve the reliability of data transmission. Some of the received copies of the data will be ‘better’ than others, due to the fact that the multiple copies are transferred through different fading channels. This redundancy leads to a higher chance to correctly decode the received signal, by using one or more of the received copies of the data.

Considering a system with n_T transmit and n_R receive antennas, the maximum diversity gain $n_T \times n_R$ can be possibly realized through designing suitable transmit signals over multiple independently fading paths in the absence of channel knowledge at the transmitter.

According to the coding structures, there are two main types of space-time codes: *space-time trellis codes* (STTC) [8][9], and *space-time block codes* (STBC) [10].

STTC, which is quite similar to trellis-coded modulation, uses trellis structure to ensure that redundant copies of data are distributed over time and space. Compared to STBC, it provides better gain at the cost of complex Viterbi detection at the receiver.

The key idea of STBC is orthogonal designs. For STBC, transmit symbols are arranged in an orthogonal way so that they can still be detected at the receiver without any co-antenna interference, even after the MIMO channel. In Fig. 2.2, a system that has two transmit antennas and one (or two) receive antenna(s) is shown.

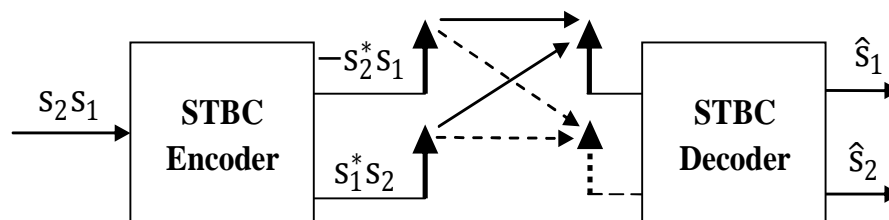


Figure 2.2 Alamouti’s two transmit diversity scheme with one or two receive antennas

2.1.2 Spatial Multiplexing

In spatial multiplexing, the transmit data is de-multiplexed into sub-streams and sent from different antennas. Such as *layered space-time* (LST) codes, which use multiple

antennas to exploit spatial multiplexing in order to obtain high spectral efficiencies and enhance the system capacity [11][12][13]. To some extent, spatial multiplexing can be considered as space time codes to exploit the multiplexing gains [5].

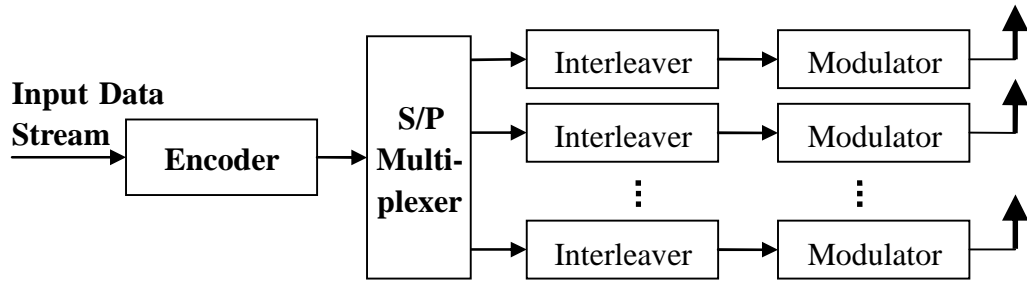
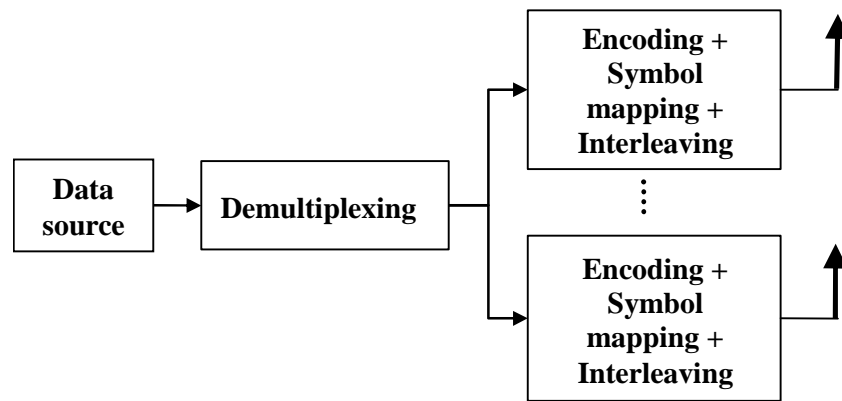
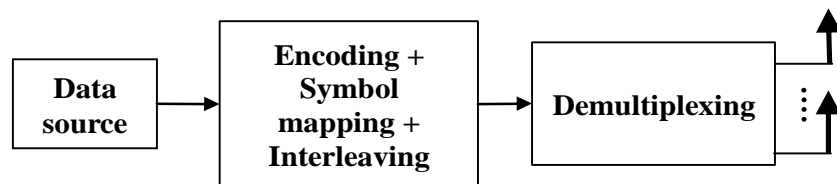


Figure 2.3 A basic structure of VBLAST transmitter



(a)



(b)

Figure 2.4 Horizontal encoding (a) and vertical encoding (b) for spatial multiplexing

The primary objective of spatial multiplexing is to linearly increase channel capacity with $\min(n_T, n_R)$ without additional power or bandwidth expenses. The corresponding gain is therefore attained by transmitting independent modulated signals from the individual antennas.

LST codes are an effective solution for enormous bit rates, which can realize a significant portion of the MIMO channel capacity with comparatively small implementation complexity. Each sub-stream is transmitted simultaneously by an

individual transmit antenna in the same frequency band. The receiver uses at least the same number of receive antennas to separate and detect each sub-stream based on a combination processing of interference suppression and interference cancellation. The separated signal can be decoded by conventional decoding algorithms with lower complexity compared with the conventional ML decoding approach. According to the application of error control coding and the assignment of modulated symbols over different antennas, various LST architectures are proposed. One of the most important forms is called *vertical Bell Laboratories LST* (VBLAST) which is shown in Fig. 2.3.

Bell Laboratories LST (BLAST) transmitter is one of the most promising methods, which includes *vertical encoding* (VE) and *horizontal encoding* (HE). For HE, as shown in Fig. 2.4(a), the bit stream to be transmitted is first de-multiplexed into several separate data streams. Each stream undergoes independent encoding, symbol mapping and interleaving, and then is transmitted from the corresponding antennas.

For VE, as shown in Fig. 2.4(b), the bit stream first undergoes encoding, symbol mapping and interleaving, and then is de-multiplexed into several separate streams transmitted from the individual antennas. This architecture can achieve full diversity gain since each information bit can be spread across all the transmit antennas.

2.2 OFDM

OFDM, which is short for Orthogonal Frequency Division Multiplexing, is a special type of Frequency Division Multiplexing, designed to maximize the use of the spectrum, while minimizing the amount of interference between adjacent frequencies. It can effectively mitigate *intersymbol interference* (ISI) caused by the delay spread of wireless channels, has gained increased interest in the last years for its advantages in digital transmissions over frequency-selective fading channels. Therefore, it has been widely used in many wireless systems and adopted by various standards [14].

OFDM scheme is a special form of *multicarrier* (MC), which was first proposed for dispersive fading channels [15]. It is pointed out that orthogonal band limited carrier waves generated by band pass filter set can overlap each other without causing inter-symbol interference and inter-carrier interference between them.

The multicarrier system employing *orthogonal quadrature amplitude modulation* (O-QAM) of the carriers was studied in 1967 [16]. In the classic parallel data

transmission systems [15][16], the frequency domain bandwidth is divided into a number of non-overlapping subchannels, each of which hosts a specific carrier widely referred to as a subcarrier. The early OFDM schemes [15]-[18] required banks of sinusoidal subcarrier generators and demodulators, which imposed a high implementation complexity.

This drawback limited the application of OFDM to military systems until 1971, when the *discrete Fourier transform* (DFT) was suggested that can be used for the OFDM modulation and demodulation processes [19], which significantly reduces the implementation complexity of OFDM. Since then, more practical OFDM research has been carried out. The capacity of OFDM was investigated in [20] and [21].

In 1985, the feasibility of OFDM was first investigated in mobile communications [22]. By using pilots, OFDM can improve the system performance in Rayleigh fading channel significantly. Also this technique can provide added protection against delay spread with interpolated pilots.

Furthermore, OFDM was employed for digital broadcasting in 1987 [23]. [24] studied the performance and complexity of MC modulation and concluded that the time for MC has come. After that, more and more OFDM implementations were suggested. OFDM has been used in *digital audio broadcasting* (DAB) and *digital video broadcasting* (DVB), *wireless local area network* (WLAN) (802.11a/g/n and so on) and also in the proposal of the *long term evolution* (LTE) and *Worldwide Interoperability for Microwave Access* (WiMax) system.

OFDM uses multiple carriers to transmit data, can help to take advantage of frequency diversity and cope with severe channel conditions, by dividing a frequency selective fading channel into a set of frequency flat fading channels. Furthermore, channel equalization is greatly simplified, with only a single equaliser tap applied on each subchannel in an OFDM system. In order to make it robust to *inter-carrier interference* (ICI) and ISI, the low symbol rate at the sub-channels makes the use of a guard interval or *cyclic prefix* (CP) between symbols affordable [25].

OFDM has lots of advantages, including its robustness to ISI and its superiority to cope with frequency selective fading channel. However it still has some disadvantages, such as high *peak to average power ratio* (PAPR) and sensitivity to frequency errors between transmitters and receivers. Researchers have presented many ways to deal with these

problems. [26] introduced a block coding scheme for the reduction of the peak to mean envelope power ratio of multi-carrier systems like OFDM. A selective scrambling technique for reducing the peak to average power ratio was proposed in *quadrature phase-shift keying* QPSK-OFDM systems [27], while incurring negligible redundancy.

[28] proposed a selected mapping method for the reduction of PAPR of multi-carrier modulation systems, which is appropriate for a wide range of applications. [29] described a technique to estimate frequency offset using a repeated data symbol, and discussed the effects of frequency offset on the performance of OFDM. A new carrier frequency detector for OFDM was introduced in [30] and its performance was thoroughly analyzed in the presence of a multipath channel. Based on a data-aided frequency estimation algorithm, [31] presented and analyzed a technique for fast acquisition and accurate tracking of the carrier frequency in OFDM receivers.

2.2.1 Introduction of OFDM

All forms of frequency division multiplexing work by dividing up the information bits to be transmitted into a number of different bit streams (at a lower bit rate), then using these streams to modulate a number of sub-carriers (or sub-channels) which are a set of closely spaced carriers that are orthogonal to each other. The resultant modulated sub-carriers are then added together.

Unlike the original FDM technique, in which frequency channels are separated from each other, the sub-carriers in an OFDM system can overlap adjacent carriers with no interference between them because they are orthogonal. In fact if the sub-channels were spaced equal to the symbol rate on each sub-carrier, then the modulated signals will be orthogonal, and can be easily separated by a normal matched filter. In this way, OFDM can have higher spectral efficiency. Fig. 2.5 below shows the basic idea.

OFDM can achieve the same data rate as a single carrier system, by using a conventional modulation scheme on each sub-carrier at low speed rather than the high speed required in a single carrier system, which means each sub-carrier in the OFDM system only occupies a narrow bandwidth. Together with all those sub-carriers, a frequency selective fading channel can be turned into a group of frequency flat fading channels, which leads to much simpler channel equalization methods. Furthermore, OFDM has the ability to cope with different fading across frequency, by making use of these sub-carriers. More complex coding and modulation schemes can be used to deal

with the fading in the seriously faded sub-channels, and coding across the frequencies can also be used to achieve the frequency diversity.

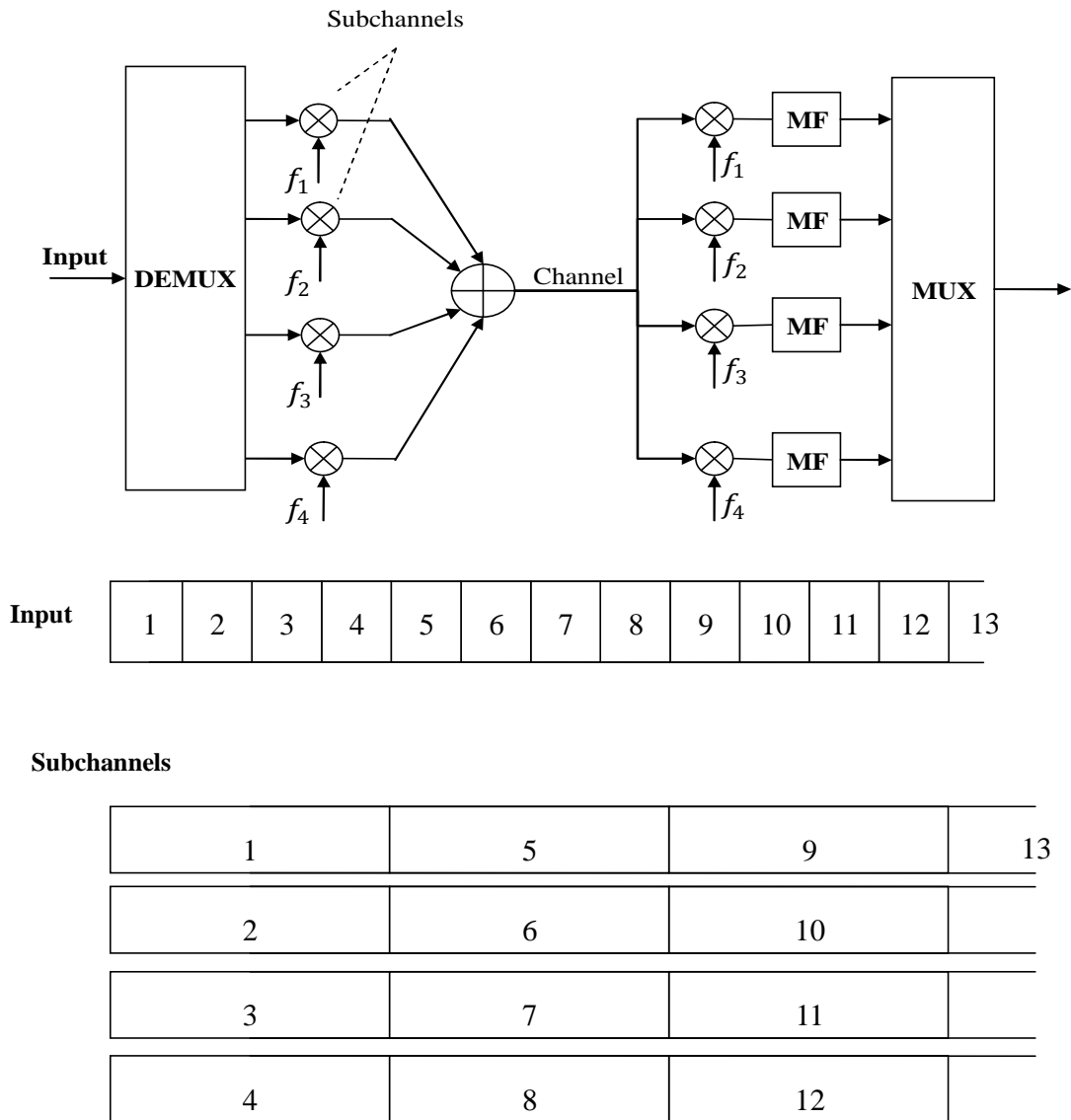


Figure 2.5 Principle of OFDM [32]

In practice, however, modern OFDM systems are not implemented with separate modulators, filters and demodulators, because the complexity and the cost of the hardware implementation in that way would be too high. Actually, using an *inverse discrete Fourier transform* (IDFT) and DFT respectively, the modulation and demodulation can be performed jointly. In fact, because the IDFT/DFT (or *inverse fast Fourier transform/fast Fourier transform* (IFFT/FFT)) transformation can be performed easily and rapidly by digital means, OFDM has become so popular recently.

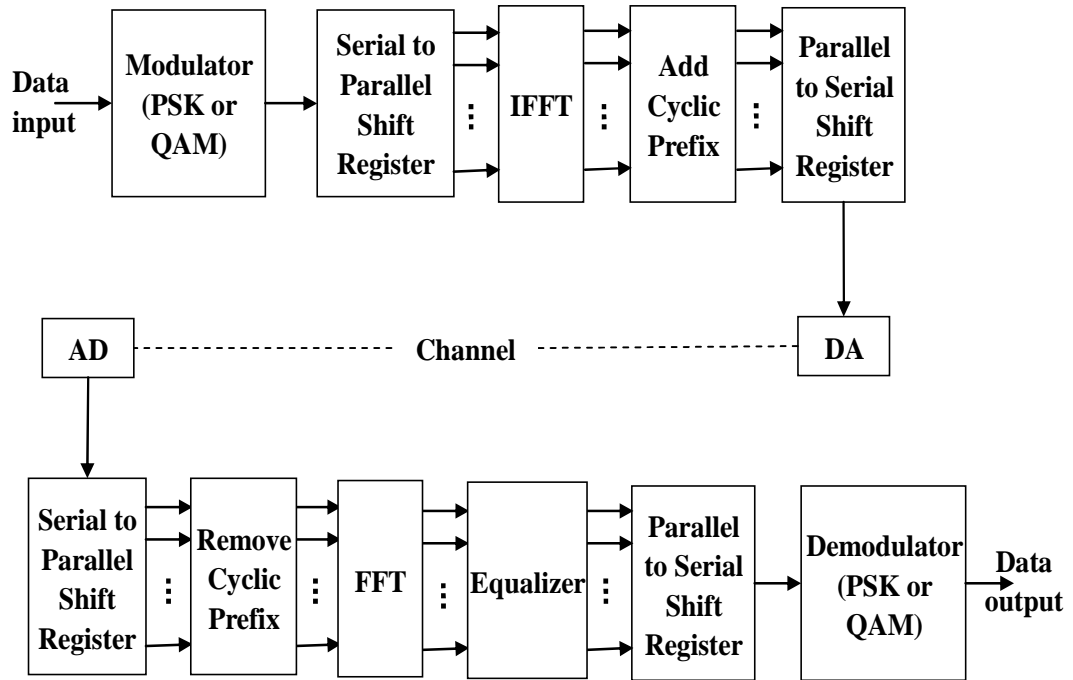


Figure 2.6 OFDM system block diagrams

Fig. 2.6 shows a basic OFDM system structure. At the transmitter, the data is first mapped to *phase-shift keying* (PSK) or *quadrature amplitude modulation* (QAM) symbols, and then some reference signals (also called Pilots) are inserted for the purpose of channel estimation. After that, the data is multiplexed and fed to the IFFT to modulate onto the orthogonal carrier set, and a CP is added here in order to cancel some ISI and ICI. Finally the data symbols are demultiplexed, and sent out through the antenna.

The receiver is more or less an inverse process. The equalization is actually quite simple for OFDM. As discussed before, the OFDM system could turn a frequency selective fading channel into a set of frequency flat fading sub-channels, which means the equalization just provides a set of single tap equalizer for the corresponding subchannels, so that greatly reduces complexity and processing delay. The pilots are removed after the demultiplexing.

OFDM requires very accurate frequency synchronization between the receiver and the transmitter, in order to maintain the sub-carriers' orthogonality. If frequency deviation occurs, the sub-carriers will no longer be orthogonal, causing ICI, i.e. cross-talk between the sub-carriers. Frequency offsets are typically caused by mismatched transmitter and receiver oscillators, or by Doppler shift due to movement. In order to avoid OFDM symbols overlapping each other due to frequency selective fading, a CP is

designed. Therefore, the insertion of the CP is a very important part of the OFDM system. As shown in Fig. 2.7, adding the CP involves taking last few samples of an OFDM symbol and adding them at the start of it.

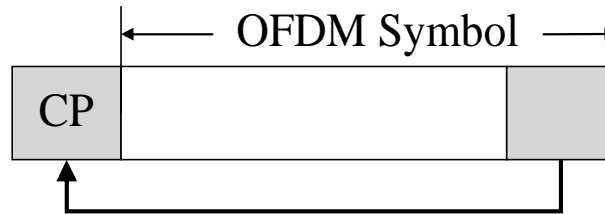


Figure 2.7 CP insertion

As shown in Fig. 2.8, the sudden phase change between OFDM symbols due to the delayed version of the received signal now falls into the CP period of the non-delayed version, thus a guard time period is provided. By removing the CP part of the symbol, the large harmonic effect caused by the sudden change can be now simply avoided, which is not included in the FFT integration period.

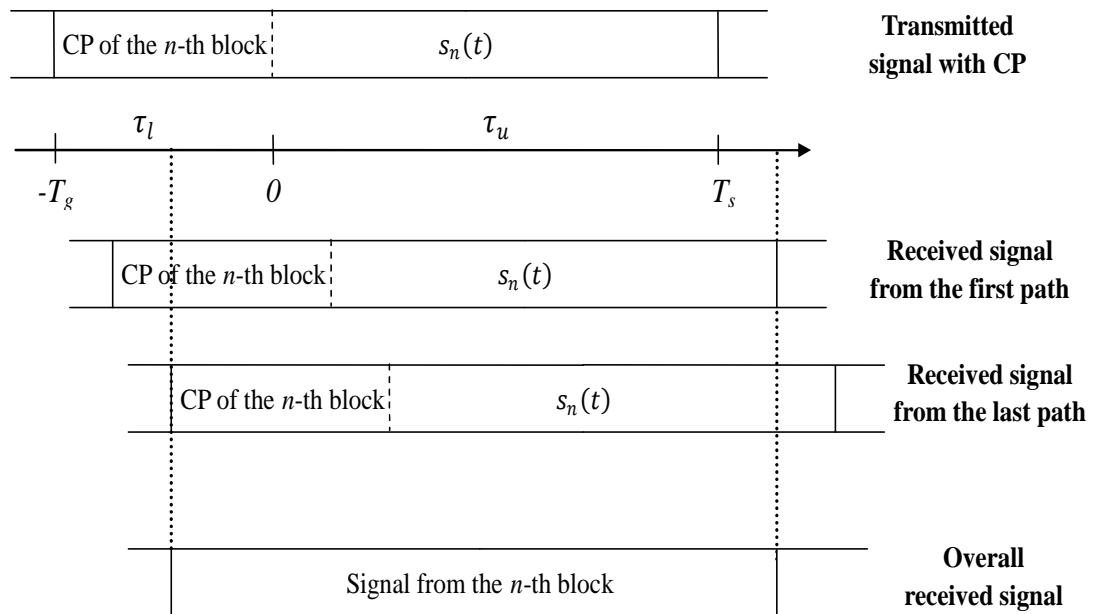


Figure 2.8 Function of CP

In wireless communication, ISI is also a serious problem. Because the multipath causes multiple delays in the received signal, the previous OFDM symbol would have an effect on the current symbol, which could be regarded as noise when integrating through the whole OFDM symbol. Those OFDM symbols can mostly be terminated before the new

integration period starts, by adding an appropriate length of CP which may be treated as guard time.

Fig. 2.9 shows the *bit error rate* (BER) performances of OFDM system without both CP and linear equalization, without CP and with equalization, with CP and without equalization, and with both CP and equalization are compared. Assume the channel is block fading, where the channel fading coefficients keep constant during a data frame. Rayleigh fading channel model is used, with 4 taps multipath ([1 0.9 0.7 0.5]). A SISO OFDM system is considered. The data length is 10000, OFDM subcarrier number 128, and the length of CP is 10. As shown in the figure, the performance with CP is much better than that without CP, which is because the CP can mitigate the ISI and ICI. Equalization at the receiver can also provide some gain.

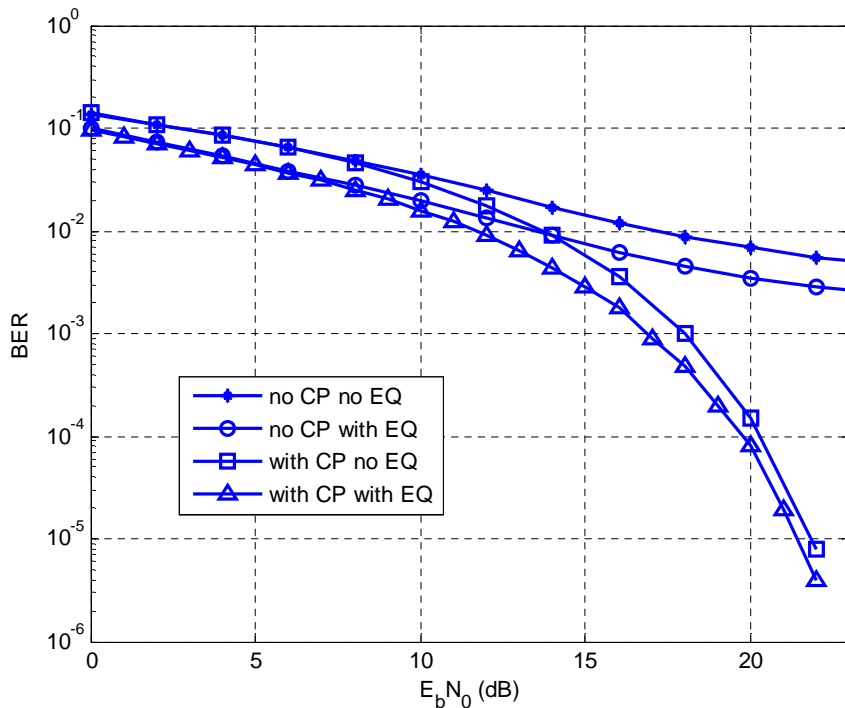


Figure 2.9 BER performances of OFDM system with/out CP and with/out equalization (the channel is perfect known at the receiver, with 4 taps multipath block fading channel (channel coefficients [1 0.9 0.7 0.5]), data length 10000, 128 subcarriers, and CP length 10)

2.2.2 OFDM System Model

Let $\{s_{n,k}\}_{k=0}^{N-1}$ with $E|s_{n,k}|^2 = \sigma_s^2$ be the complex symbols to be transmitted at the n -th OFDM block, then the OFDM-modulated signal can be represented by [14]

$$s_n(t) = \sum_{k=0}^{N-1} s_{n,k} e^{j2\pi k \Delta f t}, \quad 0 \leq t \leq T_s \quad (2.1)$$

where T_s , Δf , and N are the symbol duration, the subchannel separation, and the number of subchannels of OFDM signals, respectively. For the receiver to demodulate the OFDM signal, the symbol duration should be long enough, which is also called the orthogonality condition since it makes $e^{j2\pi k \Delta f t}$ orthogonal to each other for different k . With the orthogonal condition, the transmitted symbols $s_{n,k}$ can be detected at the receiver by

$$s_{n,k} = \frac{1}{T_s} \int_0^{T_s} s_n(t) e^{-j2\pi k \Delta f t} dt, \quad (2.2)$$

$$T_s \Delta f = 1,$$

if there is no channel distortion.

The sampled version of the baseband OFDM signal $s(t)$ in Eq. (2.1) can be expressed as

$$s\left(m \frac{T_s}{N}\right) = \sum_{k=0}^{N-1} s_{n,k} e^{j2\pi k \Delta f m \frac{T_s}{N}}$$

$$= \sum_{k=0}^{N-1} s_{n,k} e^{j \frac{2\pi k m}{N}}, \quad (2.3)$$

which is actually the IDFT of the transmitted symbols $\{s_{n,k}\}_{k=0}^{N-1}$ and can efficiently be calculated by FFT. It can easily be seen that demodulation at the receiver can be performed using the DFT instead of the integral in Eq. (2.2).

Fig. 2.8 shows the function of the CP. Without the CP, the length of the OFDM symbol is T_s , as shown in Eq. (2.1). With the CP, the transmitted signal is extended to $T = T_g + T_s$ and can be expressed as

$$\tilde{s}_n(t) = \sum_{k=0}^{N-1} s_{n,k} e^{j2\pi k \Delta f t}, \quad -T_g \leq t \leq T_s$$

It is obvious that $\tilde{s}_n(t) = s_n(t + T_s)$ for $-T_g \leq t \leq 0$, which is why it is called the CP.

The impulse response of a wireless channel can be expressed by [33]

$$h(t) = \sum_i \gamma_i \delta(t - \tau_i), \quad (2.4)$$

where τ_i and γ_i are the delay and the complex amplitude of the i -th path, respectively. Then, the received signal can be expressed as

$$x_n(t) = \sum_i \gamma_i \tilde{s}_n(t - \tau_i) + n(t),$$

where $n(t)$ represents the *additive white Gaussian noise* (AWGN) at the receiver. As demonstrated in Fig. 2.8, $x_n(t)$ consists of only the signal component from the n -th OFDM block when $\tau_l \leq t \leq \tau_u$, where $\tau_l = -T_g + \tau_M$, $\tau_u = T_s + \tau_m$, $\tau_M = \max_i\{\tau_i\}$, and $\tau_m = \min_i\{\tau_i\}$; otherwise, the received signal consists of signals from different OFDM blocks.

If $\tau_l \leq 0$ and $\tau_u \geq T_s$, then

$$\begin{aligned} x_{n,k} &= \frac{1}{T_s} \int_0^{T_s} x_n(t) e^{-j2\pi f_k t} dt \\ &= \frac{1}{T_s} \int_0^{T_s} \left\{ \sum_i \gamma_i \tilde{s}_n(t - \tau_i) + n(t) \right\} e^{-j2\pi f_k t} dt \\ &= H_k s_{n,k} + n_k, \end{aligned} \quad (2.5)$$

for $0 \leq k \leq N - 1$ and all n , where H_k denotes the frequency response of the wireless channel at the k -th subchannel and is defined as

$$H_k = \sum_i \gamma_i e^{-j2\pi k \Delta f \tau_i}$$

and n_k is the impact of AWGN and is defined as

$$n_k = \frac{1}{T_s} \int_0^{T_s} n(t) e^{-j2\pi f_k t} dt.$$

It can be proved that n_k are independent identically distributed complex circular Gaussian random variables with zero mean and variance σ_n^2 . With H_k , transmitted symbols can be estimated. For single carrier systems, the received signal is the convolution of the transmitted sequences or symbols and the impulse response of the wireless channel in addition to AWGN, whereas the impact of the channel is only a

multiplicative distortion at each subchannel for OFDM systems, which makes signal detection in OFDM systems very simple and is also one of the reasons why OFDM is very popular nowadays.

2.3 MIMO OFDM Systems

In mobile communications, using MIMO techniques in frequency selective fading environments, leads to a very complex equalization problem. In order to reduce the complexity, [34] combined the MIMO with OFDM, which can convert frequency selective fading channels to flat fading ones. Since then, in order to improve system performance, much research has been done on MIMO-OFDM.

[35] developed a MIMO-OFDM system using two independent space-time codes for two sets of two transmit antennas. At the receiver, the independent space-time codes were decoded using pre-whitening followed by ML decoding based on successive interference cancellation. A full rate coding strategy was proposed for MIMO-OFDM systems that exploited full spatial (transmit and receive) diversity, as well as frequency and time diversity, through the combination of binary codes and linear precoding [36]. [37] pointed out that an optimum code for MIMO-OFDM would code across all antennas and sub-carriers (as well as time) simultaneously. Since this can become very complex, a method was proposed for grouping antennas and codes in such a way that the inherent diversity is retained, so that the complexity is greatly reduced [37]. For the MIMO-OFDM systems, in recent years, system capacity, space/time/frequency coding, PAPR control, channel estimation, and receiver design have attracted substantial research efforts. The overviews of MIMO OFDM communications can be found in [38]-[40].

A multicarrier system can be efficiently implemented in discrete time using an IFFT to act as a modulator and an FFT to act as a demodulator. The transmitted data are the “frequency” domain coefficients and the samples at the output of the IFFT stage are “time” domain samples of the transmitted waveform. Fig. 2.10 shows a typical MIMO-OFDM implementation.

A MIMO channel with N_T transmitters and N_R receivers can be expressed as

$$\mathbf{r} = \mathbf{H}\mathbf{s} + \mathbf{n}, \quad (2.6)$$

where the vector \mathbf{r} ($N_R \times 1$), the vector \mathbf{s} ($N_T \times 1$) and the vector \mathbf{n} ($N_R \times 1$) are the received, transmitted and noise signals, respectively. Specifically, the vectors \mathbf{r} , \mathbf{s} , and \mathbf{n} are given by

$$\begin{aligned}\mathbf{r} &= [r_1, r_2, \dots, r_{N_R}]^T, \\ \mathbf{s} &= [s_1, s_2, \dots, s_{N_T}]^T, \\ \mathbf{n} &= [n_1, n_2, \dots, n_{N_R}]^T,\end{aligned}\quad (2.7)$$

where $(\cdot)^T$ denotes transpose, \mathbf{s} represents the OFDM signal, and \mathbf{n} represents the AWGN with zero mean and variance σ_n^2 .

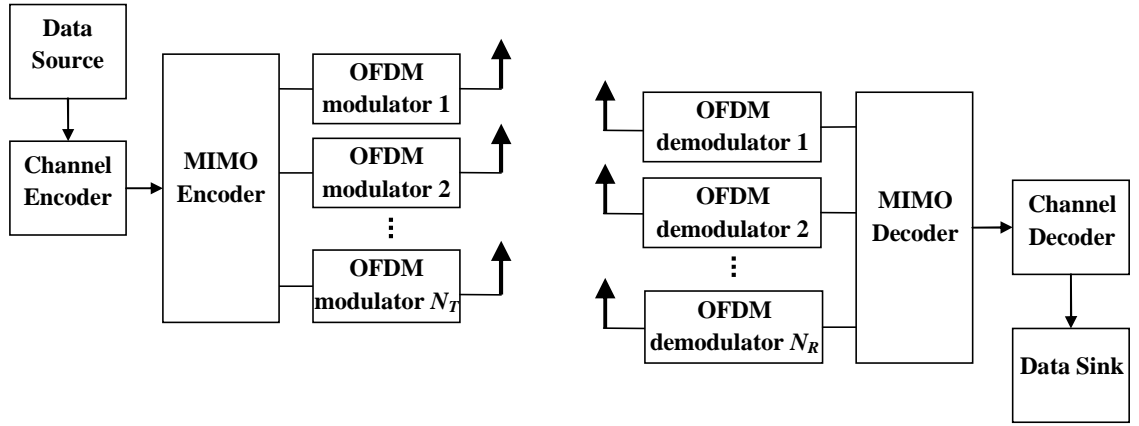


Figure 2.10 $N_T \times N_R$ MIMO-OFDM system

The $(N_R \times N_T)$ -dimensional frequency domain channel matrix \mathbf{H} , where each of the coefficients $[\mathbf{H}]_{i,j}$ represents the transfer function from the j -th transmitter to the i -th receiver, is given by

$$\mathbf{H} = \begin{bmatrix} h_{11} & h_{12} & \cdots & h_{1N_T} \\ h_{21} & h_{22} & \cdots & h_{2N_T} \\ \vdots & \vdots & \ddots & \vdots \\ h_{N_R1} & h_{N_R2} & \cdots & h_{N_RN_T} \end{bmatrix}.\quad (2.8)$$

2.4 Multiuser Detection

Multiuser system is a multiple access communication system, which is used for a system that uses a communication channel to enable several transmitters to send information at the same time. Multiple access communication is used widely in different communication systems, especially in mobile and satellite communications. The signal

sources in a multiple access channel are referred to as users. The multiple access communication scenario is depicted in Fig. 2.11.

The simplest approach for detection called the conventional detector, also known as the single-user matched filter detector, does not take into account any other users in the system or channel dynamics, and therefore is not robust to asynchronism, and fading channels. *Multiple access interference* (MAI) significantly limits the performance and capacity of transmission systems. *Multiuser detection* (MUD) reduces the interference. The optimal multiuser detector, ML multiuser detector, is proposed to provide detection performance close to that of single user detection but the complexity is exponentially proportional to the number of users [41]. This optimal detector often serves as a baseline of comparison for sub-optimal multiuser detectors.

Those sub-optimal detectors can be divided into two groups: linear detectors and *interference cancellation* (IC) detectors. The linear detectors mainly include the decorrelating detector and the *Minimum Mean Square Error* (MMSE) detector. The decorrelating detector multiplies the output of the conventional matched filter with the inverse of the correlation matrix, and therefore fully decouples the multiuser signal. It eliminates the MAI but enhances the noise power, and it needs a matrix inversion [42]. The MMSE detector, regarded as an improved decorrelating detector, can solve the problem of noise enhancement in low *signal to noise ratio* (SNR). It has better performance than the decorrelating detector but it requires the estimation of amplitudes and also a matrix inversion [41].

The IC detector, also called the *Decision-Feedback* (DF) detector, is one of the most popular methods because of the simplicity and good performance, which includes two classes: *successive interference cancellation* (SIC) and *parallel interference cancellation* (PIC) [41]. They invoke an iterative processing technique that combines detection and demodulation, which are based on the principle of removing the effects of the interfering users during each detection stage. However, during the consecutive detection stages, if the signals of the previous stages are detected erroneously, error propagation may occur.

There are also some sub-optimal approaches based the simplified optimal scheme, such as *Semi-definite relaxation* (SDR) [43], *Sphere Decoding* (SD) and *branch and bound* (BB) detectors [44]. They can achieve near optimal performance, however, their worst

case computational complexity is still too high. A comparison of these advanced MUD techniques is discussed in [44].

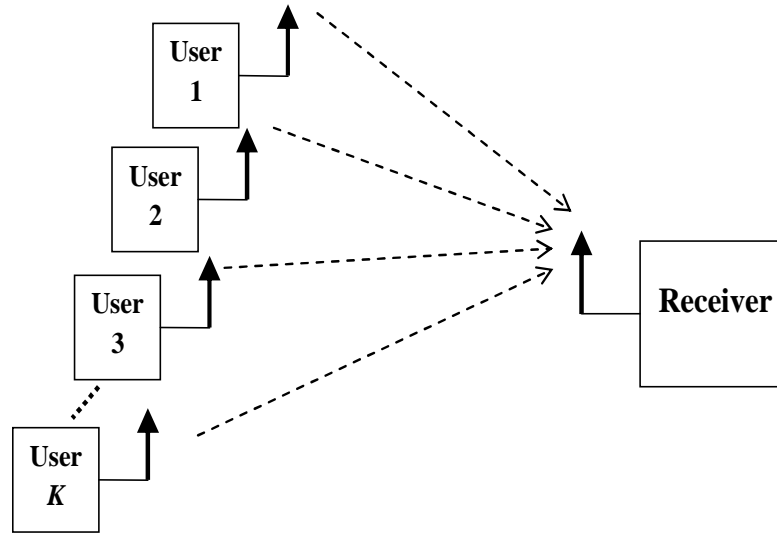


Figure 2.11 Multiple access communication system with K users

2.4.1 Matched Filter Detector

The matched filter detector is simply obtained by correlating the received signal with a known signal or template (i.e. the desired user's time reversed spreading waveform), and samples the output at the bit rate. The output of the matched filter can be expressed as

$$\tilde{\mathbf{r}} = \mathbf{H}^H(\mathbf{H}\mathbf{s} + \mathbf{n}). \quad (2.9)$$

This method of detection comes straight from the single user designs, which can also be used for MIMO systems. For *code division multiple access* (CDMA), this emphasizes the need for low cross-correlation between the spreading codes, otherwise the MAI term will dominate the correlator output. For MIMO systems, a bank of matched filters can be used to demodulate each independent user. In order to do this, we can either synchronize each matched filter to the bit epochs of its corresponding transmitter or oversample the received signal and use an asynchronous detector architecture.

MAI can cause high BER and poor system capacity: it increases with the number of users active in the system and the strength of interfering user(s) and is very sensitive to power variation among users.

For single-user system, the matched filter detector is the optimal linear filter for maximizing the SNR in the presence of additive stochastic noise, and will perform

optimally in a synchronous system with no channel ISI, and no neighbouring cell interference. However, the matched filter will result in poor detection performance when the number of users increases [41]. The desirable property of the matched filter is its very low computational complexity.

2.4.2 ZF Detector

The conventional detector does not use any information about the other users in the system and therefore cannot combat MAI. The decorrelating detector essentially applies the inverse of the correlation matrix of user signal to the output of the conventional detector. *Zero-forcing* (ZF) detection, which is a natural progression of the decorrelating detector, is a simple and effective technique for retrieving multiple transmitted data streams at the receiver. The received signal vector is shown in Eq. (2.10), the ZF estimate of the transmitted symbol vector can be written as

$$\begin{aligned}\tilde{\mathbf{r}} &= \mathbf{G}_{ZF}(\mathbf{H}\mathbf{s} + \mathbf{n}) \\ &= \mathbf{s} + \mathbf{G}_{ZF}\mathbf{n},\end{aligned}\tag{2.10}$$

where $\mathbf{G}_{ZF} = (\mathbf{H}^H\mathbf{H})^{-1}\mathbf{H}^H$. The ZF receiver eliminates the MAI, thereby significantly reducing receiver complexity. Noise is enhanced, however, which in general results in significant performance degradation. The diversity order equals $(N_R - N_T + 1)$ [2].

2.4.3 MMSE Detector

In order to improve performance in the presence of noise, the MMSE detector is introduced. The MMSE receiver balances MAI mitigation with noise enhancement and is given by

$$\mathbf{G}_{MMSE} = (\mathbf{H}^H\mathbf{H} + \sigma_n^2\mathbf{I})^{-1}\mathbf{H}^H.\tag{2.11}$$

If the SNR is lower, it approaches the matched filter given by

$$\mathbf{G}_{MMSE} \rightarrow \frac{\mathbf{H}^H}{\sigma_n^2}.$$

At high SNR, σ_n^2 tends to zero, so

$$\mathbf{G}_{MMSE} \rightarrow \mathbf{G}_{ZF}.$$

The MMSE receiver also achieves $(N_R - N_T + 1)$ th-order diversity.

2.4.4 ML Detector

The ML detector performs vector decoding and is optimal in the sense of minimizing the error probability. Assuming equally likely, the ML receiver tries to find $\tilde{\mathbf{s}}_{ML}$, according to

$$\tilde{\mathbf{s}}_{ML} = \arg \min_{\hat{\mathbf{s}} \in \Omega} \{\|\mathbf{r} - \mathbf{H}\hat{\mathbf{s}}\|^2\}, \quad (2.12)$$

where Ω is all the possible transmit vector symbols. The ML receiver realizes N_R th-order diversity for HE and full $(N_R N_T)$ diversity for VE.

The ML approach is more complicated than linear receivers (the above two schemes). For BPSK with two transmit antennas, Ω has $2^2 = 4$ combinations, while for four transmit antennas, Ω has $2^4 = 16$ combinations. If a higher order constellation like 64QAM is used for four transmit antennas, then the receiver needs to find the minimum from $64^4 = 1677216$ combinations, this requires much higher level of computational complexity which is impossible for real system design. In such scenarios, SD techniques may help to reduce the computational complexity [45].

2.4.5 Parallel Interference Cancellation

In addition to the optimal detection schemes, other nonlinear detectors have also been proposed, which use the interferers' data to detect that of the desired user. In order to reconstruct the interference, temporary data estimates are employed by IC detectors, and then subtract it from the received signal.

According to the received power, the SIC detector [46-48] can first detect the strongest user using conventional matched filtering, and then the signal of this strongest user is recreated and subtracted from the received signal. The resulting signal contains one fewer user if the interference is relatively accurately subtracted. Then the receiver will repeat the same process of recreating and subtracting the strongest signal among the remaining users, until the last user has been detected.

As shown in [49], however, interference cancellation of this class of detectors can be performed most reliably when there is a significant power difference between each of the users' signals. When power levels of each user are nearly the same, however its performance is poor. Meanwhile, the signals should be sorted by power correctly, and need to be reordered whenever the power profile changes. In a high capacity system

with widely variable power levels, this will be a particular risk. Finally, by this one by one serial processing, a relatively long processing delay will be result in.

PIC detection [50-53] removes the interference produced by the remaining users from each user simultaneously. For PIC detector, each user in the system receives equal treatment in the attempt to cancel its MAI. Compared with the SIC, the delay required to complete the process is dramatically reduced, since the IC is performed in parallel for all users. Moreover, in contrast to the SIC, the PIC performs the estimation for all users' signals separately at first, and then the signal decisions are used to reconstruct the MAI for subtraction. It is obvious that the parallel cancellation process can be divided into at least two stages, so PIC is also called multistage IC. The first stage of the multistage cancellation can be provided by linear detectors (ZF or MMSE detector).

By replacing the linear detector outputs with the increasingly reliable temporary decisions of the interfering users which is made by the PIC detector in the last iteration, the PIC approach can be further iterated, and the iteration can be performed as many times as needed. In general, as the number of iterations increases, the performance of the detector should continuously improve.

For each iteration, PIC detection can avoid the long delay derived from the serial processing in the SIC, and do not need to order the users by power. In order to achieve the best performance, the iterative PIC can be performed for many iterations. Therefore, PIC detection has been regarded as one of the most promising MUD techniques [54-56].

However, the risk of error propagation still exists. If the temporary decision is correct, the PIC can fully remove the MAI. If the temporary decision is wrong, however, the error will be doubled after the PIC. Hence the performance of the PIC based on hard decisions in each iteration may become worse with increasing number of iterations, especially in the early stages of the iterative processing. Accordingly in order to guarantee the convergence of the PIC, some schemes have been developed [57-59].

A straightforward approach is to use a soft decision rather than a hard decision in each iteration for cancellation. The amplitude of a symbol estimate may represent its reliability, if an appropriate algorithm is used. The potential error may be corrected by giving relatively small amplitudes to an unreliable symbol. This approach is called soft-in soft-out PIC. [57-59] also propose a similar soft decision-based approach, called partial PIC. Another enhancement can be made to try to improve the performance in the

first iteration, which is the weakest link. The matched filter and MMSE detector are both considered to serve as the first stage.

Finally using channel decoding following the PIC detection for each iteration is also a desirable approach. The temporary data estimates can be substantially improved by a powerful channel decoder, and more accurate interference reconstruction and subtraction can be achieved.

2.4.6 Performance Comparison between MUD Schemes

The above detections are compared for MIMO OFDM system, as shown in Fig. 2.12. Two transmit and two receive antennas are considered. A Rayleigh channel is assumed with uncorrelated fading between all transmit and receive antennas, with a memory of one symbol period, described by a 2-tap delay line model, where the second tap's average power is assumed to be weaker than the first. The channel coefficients of CIRs for the users are generated randomly and independently, and known by the receiver perfectly.

In this simulation, the CIR is $[1 \ 0.7]$. A block fading channel model is used. Each transmit antenna employed 10000 frames with 1024 bits per frame, *binary phase-shift keying* (BPSK) modulation, and OFDM modulation with 32 subcarriers and CP length 6. The BERs plotted are averages over all users.

As shown in Fig. 2.12, ZF, ZF-based PIC, ZF-based SIC, MMSE, MMSE-based PIC, and MMSE-based SIC all achieve the same diversity order, which is first order diversity in this case. However the matched filter and matched filter-based approach result error floors, due to the high MAI. Moreover, if the PIC is perfect (using the original signals from other users as the reconstructed interference), after the detection the interference will be removed perfectly, and the matched filter detector can achieve the optimal performance, slightly better than the ML detector: both are second order diversity.

This is because perfect PIC can remove all the interference due to the other users, and lead to optimal single user detection. In this case, the BER performance will be better than the multiuser ML detector, which does not have the benefit of perfect knowledge of the interferers.

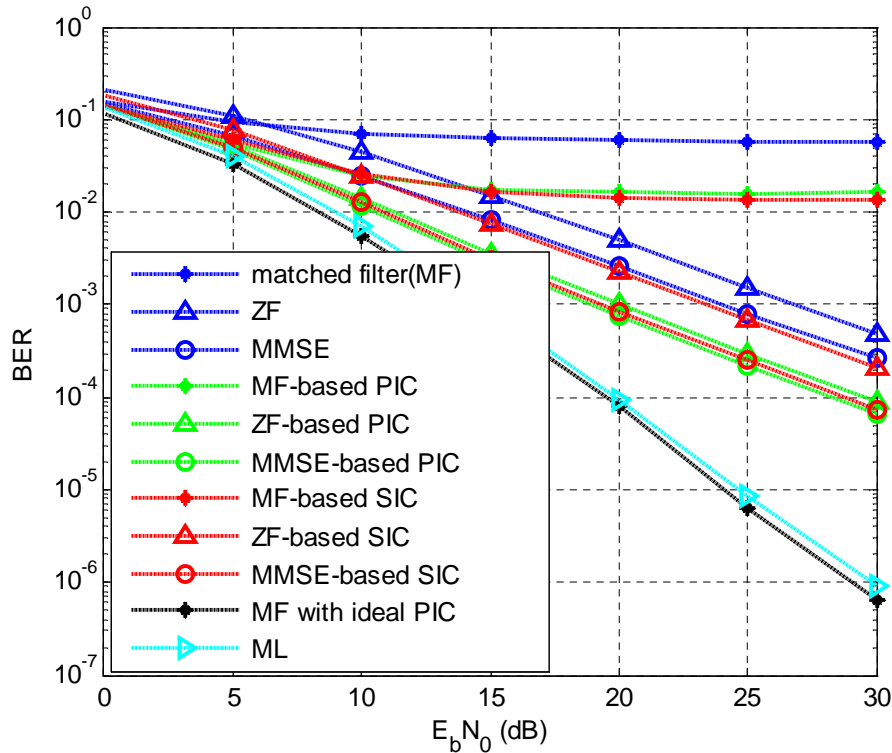


Figure 2.12 Comparison of linear and non-linear detections for MIMO (2-by-2) OFDM system

2.5 Convolutional Code

Coding allows bit errors introduced by transmission of a modulated signal through a wireless channel to be either detected or corrected by a decoder in the receiver. Coding can be considered as the embedding of signal constellation points in a higher-dimensional signaling space than is needed for communications. By going to a higher-dimensional space, the distance between points can be increased, which provides for better error correction and detection.

The main reason to apply error correction coding in a wireless system is to reduce the probability of bit or block error. The amount of error reduction provided by a given code is typically characterized by its coding gain in AWGN and its diversity gain in fading.

The coding gain in AWGN is generally a function of the minimum Euclidean distance of the code, which equals the minimum distance in signal space between codewords or error events. Thus, codes designed for AWGN channels maximize their Euclidean distance for good performance.

Codes design for AWGN channels do not generally work well in fading owing to bursts of errors that cannot be corrected for. However, good performance in fading can be obtained by combining AWGN channel codes with interleaving and by designing the code to optimize its inherent diversity. The interleaver spreads out bursts of errors over time, so it provides a form of time diversity. This diversity is exploited by the inherent diversity in the code. In fact, codes designed in this manner exhibit performance similar to *maximum ratio combining* (MRC) diversity, with diversity order equal to the minimum Hamming distance of the code. Hamming distance is the number of coded symbols that differ between different codewords or error events. Thus, coding and interleaving designed for fading channels maximize their Hamming distance for good performance.

The convolutional code, which was first introduced by [60] in 1955, is one of the most widely used *forward error correction* (FEC) codes. It adds dependence between successive blocks instead of treating them separately, which means the current output coded data depends on not only the current input data block but also some previous input. The code stream cannot be separated into several code words. The data could be encoded continuously until it is terminated. However in practice, the longer the code word is the more delay in the decoding process and the more complex the decoder structure.

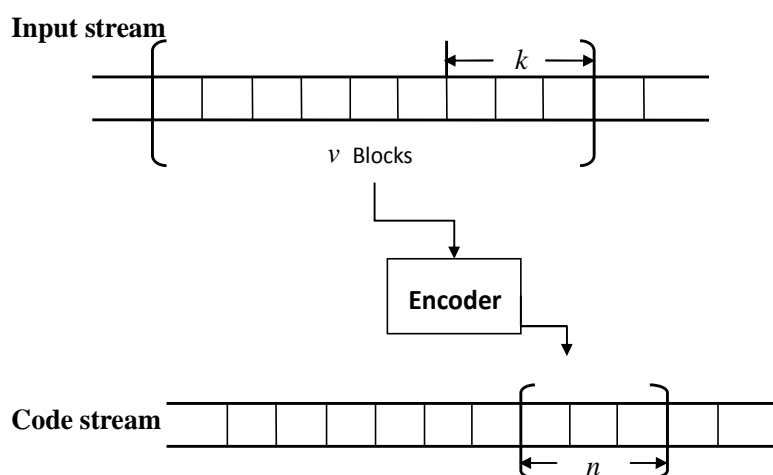


Figure 2.13. Code structure of general convolutional code

In Fig. 2.13, the code structure is illustrated briefly. The sliding window moved block by block along the input stream, can determine the output of the encoder. Each block contains k symbols. The n output symbols are not only generated from the current block

but also the previous $v - 1$ blocks. The v which is known as the constraint length of this code, is actually one plus the length of the longest shift register delay line in the encoder. The convolutional code here could be described as a (n, k, v) code.

The shift register lines which contain $v - 1$ steps of registers, work like a buffer and keep the previous input data effective. There are k shift register lines altogether, so each data block contains k symbols of data. In one output codeword, the number of symbols is the number of combinations of the modulo- M (for binary codes $M=2$) adders generated from the shift register lines, which is n . Therefore, there are n output symbols from the encoder for each input data block.

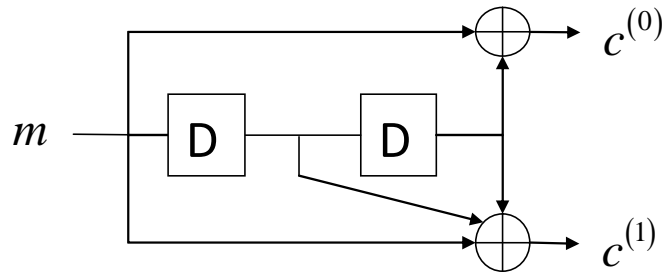
All the registers should set to be zero, before the encoder starts to encode, and then the data is fed to the input block by block. Each time when a new data block arrives, the current data block moves from one register to the next. All the registers should be reset to zero again when a code word is terminated, by feeding the input with zeros.

2.5.1 Convolutional Encoding

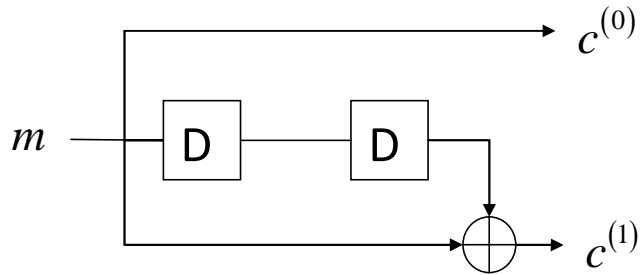
A rate $R = k/n$ convolutional encoder with memory order m , which is a discrete linear time-invariant system, can be realized as a k input, n output linear sequential circuit with input memory m , that is, inputs remain in the encoder for an additional m time units after entering. It performs a convolution of the input stream with the encoder's impulse responses.

Every output of an encoder can be described by its own transfer function, which is closely related to a generator polynomial. The transfer function is the ratio of the output signal to input signal.

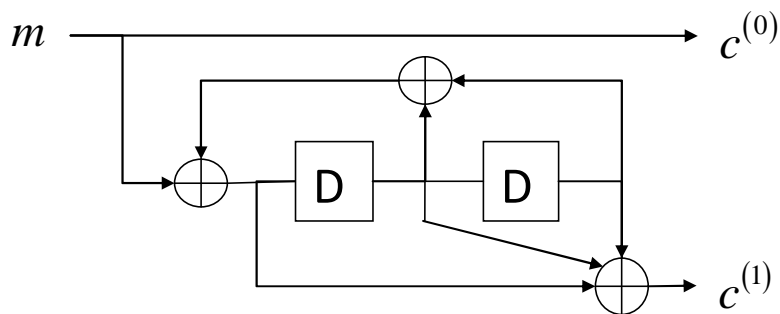
There are several kinds of encoder, systematic or non-systematic and recursive or non-recursive, which are shown in Fig. 2.14 (the structural properties of a convolutional encoder can be illustrated by using a code tree, trellis and state diagrams [60]). Systematic encoders yield codes where the message appears directly. Recursive encoders are related to *infinite impulse response* (IIR) (feedback) filters, whereas non-recursive ones are implemented as *finite impulse response* (FIR) (feedforward) filters.



(a) A binary non-systematic feedforward convolutional encoder



(b) A binary systematic feedforward convolutional encoder



(c) A binary systematic feedback convolutional encoder

Figure 2.14 Structures of convolutional encoder

A convolutional code can be uniquely described by three parameters: the generator polynomials, the code rate and the constraint length. The structure in the generator matrix g of convolutional codes is such that the encoding operation is equivalent to a convolution operation. For an input sequence $m = [m_0, m_1, \dots, m_L]$, the output sequence $c = [c_0, c_1, \dots, c_{L+M}]$ can be written as

$$c^{(j)} = m * g^{(j)}, \quad (2.13)$$

where $*$ denotes discrete-time convolution, $g^{(j)} = [g_0^{(j)}, g_1^{(j)}, \dots, g_M^{(j)}]$, and j means the j -th path.

For example, Fig. 2.14(a) depicts a convolutional encoder that has one input, two outputs, and two shift registers. The constraint length, which indicates the number of bits stored in each shift register including the current input bits, is three in this example. According to the connection status between the two outputs and the shift registers, the binary numbers corresponding to the upper and lower adders in Fig. 2.14(a) are [1 0 1] and [1 1 1], respectively.

Thus the generator polynomial matrix is given by

$$g = [1 + D^2, 1 + D + D^2].$$

These binary numbers are equivalent to the octal numbers 5 and 7 respectively, therefore the generator polynomial can be written as [5 7], and is frequently used for the following simulations in this thesis.

2.5.2 Convolutional Decoding

Decoding is the most difficult and computationally complex aspect of the implementation of convolutional codes, because there are no distinct codewords, only potentially infinite code sequences, which means that the decoder has to wait an unlimited time before it is able to decide between two possible code sequences.

Consider a message vector $m = [m_0, m_1, \dots, m_{k-1}]$ and the corresponding code vector $c = [c_0, c_1, \dots, c_{n-1}]$ obtained at the output of the convolutional encoder. Let $p(r|c)$ denote the conditional probability of receiving r , given that the code vector c was sent, where $r = [r_0, r_1, \dots, r_{n-1}]$ may differ from the code vector c due to channel noise. The maximum likelihood decoder is the one that chooses \hat{c} for which the log-likelihood function $\log(p(r|c))$ is maximum, as described by

$$\hat{c} = \arg \max \log(p(r|c)).$$

In fact the ML decoder is a minimum distance decoder that minimizes the Hamming distance between c and r . It compares each possible transmitted c and r , and chooses the possible c which is closest to r . For convolutional coding, the Hamming distance is used for hard-decision decoding, and the Euclidean distance is adopted for soft-decision decoding.

ML decoding or minimum distance decoding can be implemented via the Viterbi algorithm, which was introduced by Viterbi in 1967 [61]. It decodes a convolutional

code by choosing a path in the trellis whose c differs from r in the fewest number of entries. The Viterbi algorithm goes through the trellis, computes an appropriate metric and makes the decision on the path based on the computed metric. This metric for hard-decision is the Hamming distance between c and r . For each state in the trellis, the Viterbi algorithm compares the two paths entering the state. The path with the lower metric (called the survivor path) is retained and the other is discarded.

Summary of the Viterbi algorithm:

1. Initialization: Set the all-zero state at level 0, computation step $j + 1$ (let $j = 0, 1, 2, \dots$).
2. Compute the path metrics for all paths entering a state of the trellis by adding the path metric of each survivor path from level j .
3. Identify the survivor path with lowest metric and store it.
4. Repeat until complete.

For a convolutional code of constraint length K , no more than 2^{K-1} survivor paths and associated metrics will be stored, as the 2^{K-1} are guaranteed to contain the ML choice.

Hard decision assumes that the demodulator has made hard decisions on the received symbols, and then the decoder has only a received word to work on. In soft decision decoding information on the reliability of the decisions is passed from demodulator to the decoder [32]. It can improve the efficiency of decoding.

Convolutional codes are most easily implemented for the case $k = 1$, which leads to a code rate of $1/n$. If higher rate codes are required, both encoder and trellis diagram become much more complex. Puncturing provides an alternative method to achieve high rate convolutional codes. The principle is simply to delete some of the code symbols, so that fewer code symbols are transmitted per data symbol. Symbols are punctured according to a regular pattern, for example, the rate $1/2$ code is punctured every fourth code bit to provide a rate $2/3$ code.

2.6 Turbo Code

Shannon's noisy channel coding theorem implies that arbitrarily low decoding error probabilities can be achieved at any transmission rate less than the channel capacity by using sufficiently long block lengths [62]. The major problem of traditional codes is that

in order to achieve the Shannon's bound (which is described by Shannon in 1948 [63]), the code word length of a block code or the constraint length of a convolutional code need to be increased. These approaches result in exponential complexity of ML decoding, making them impractical. So a large amount of research was conducted into the construction of specific codes with good error-correcting capabilities and the development of efficient decoding algorithms for these codes. In 1993, Turbo codes were introduced by Berrou, Glavieux, and Thitimajshima in their paper [64]. The innovation of Turbo codes lies on the use of concatenated codes with interleavers and an iterative *maximum a posteriori probability* (MAP) decoding procedure. Turbo codes with iterative decoding can achieve BERs as low as 10^{-5} at SNRs within 1dB of the Shannon limit, that is, the value of E_b/N_0 for which the code rate equals channel capacity. So Turbo codes became a main focus of coding research and development, and soon there was a lot of implementation in practice.

2.6.1 Turbo Encoding

The Turbo code encoder is actually a concatenated encoder using two *recursive systematic convolutional* (RSC) codes. The principle of concatenated coding is to feed the output of one encoder (the outer encoder) to the input of another encoder. The final encoder before the channel is known as the inner encoder. In parallel concatenation, the same data is applied to two encoders in parallel with an interleaver π between them as shown in Fig. 2.15.

The codes used for the two encoders are recursive systematic convolutional codes. They can be very conveniently encoded using a structure consisting of a shift register, a set of *exclusive-OR* (XOR) gates, and a multiplexer [65].

Typical examples of a convolutional encoder are shown in Fig. 2.14. The code of Fig. 2.14(a) is not systematic because the code sequence does not contain the data sequence. It could be made systematic by driving one of the inputs to the multiplexer directly from the data input. The structure of Fig. 2.14(c) is used for the Turbo encoder, so that one copy of the data stream and the parity streams from two recursive encoders are multiplexed into the code stream, which will result in a code rate of 1/3.

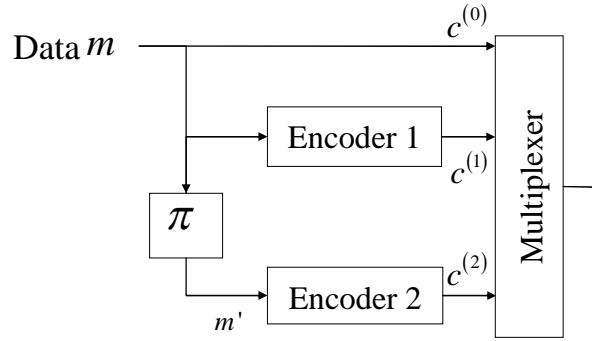


Figure 2.15 The basic Turbo encoding structure

As shown in Fig. 2.15, the systematic bits $c^{(0)}$ and the two sets of parity-check bits ($c^{(1)}$ and $c^{(2)}$) generated by the two encoders constitute the output of the Turbo encoder, so the final transmitted sequence (codeword) is given by the vector

$$c = [c_0^{(0)} c_0^{(1)} c_0^{(2)}, c_1^{(0)} c_1^{(1)} c_1^{(2)}, \dots, c_{K-1}^{(0)} c_{K-1}^{(1)} c_{K-1}^{(2)}].$$

Different code rates are achieved by puncturing the parity bit sequences. Puncturing the data bit sequence leads to a severe degradation in Turbo code performance. A simple puncturing process is punctured the two sets of parity bits, which will change the final sequence as

$$c = [c_0^{(0)} c_0^{(1)}, c_1^{(0)} c_1^{(2)}, \dots, c_{K-2}^{(0)} c_{K-2}^{(1)}, c_{K-1}^{(0)} c_{K-1}^{(2)}].$$

Generally, the encoder is initialized to the all-zero state and then starts to encode the data. After encoding a certain number of data bits a number of tail bits are added so as to make the encoder return to the all-zero state at the end of each block, thereafter the cycle is repeated.

There are two termination approaches of Turbo codes. One is to terminate the first RSC code in the encoder and leave the second one unterminated. A drawback of this approach is that the bits at the end of the block due to the second RSC code are more vulnerable to noise than the other bits. The other way is to terminate both constituent codes in the encoder in a symmetric manner. Through the combined use of a good interleaver and dual termination, the error floor can be reduced by an order of magnitude compared to the simple termination approach.

2.6.2 Interleaver

In the encoder schematic, the input data stream is applied directly to first encoder and the reordered version of the same data stream is applied to second encoder. An interleaver is an input-output mapping device that permutes the ordering of a sequence in a completely deterministic manner. Interleavers are effective in dealing with bursts of errors because, by shuffling the symbols at the receiver a burst of errors appearing in close proximity may be broken up and spread around, thereby creating an effective random channel [66] [67].

There are two main characteristics which determine the performance of an interleaver: the s -parameter and randomness [67] [68]. We know that the larger the minimum Hamming distance, the more powerful the code. For most codes, the minimum Hamming distance is in fact equal to the minimum number of '1's in the code sequence. If a sequence contains at least two '1's and brings the encoder back to the zero state, it is called a terminating sequence. A non-terminating sequence, or one that terminates only after a long period results in a large Hamming distance. In the parallel-concatenated code the same data sequence is applied to the first encoder, and then it is interleaved and applied to a second encoder. If the given sequence terminates the first encoder quickly, it is likely that it will not terminate the second encoder after interleaver [68]. This is why the design of the interleaver is important.

For a given interleaver with size N , the input to output mapping can be expressed by a function $\pi(i), i = 0, 1, \dots, N$. The output of this function is the position in the output sequence of the bit in position i at the input. If the output distance between two output of the function from the interleaver

$$|\pi(i) - \pi(j)| > t,$$

provided the distance between any two input symbols

$$|i - j| \leq s,$$

then the interleaver has spreading factors (s, t) . For a reasonable interleaver, the inequality $s \leq t$ should be maintained. And for better performance, s should be maximized (equal to t) if the other conditions are the same.

Combined all the different pairs of distance $(|i - j|, |\pi(i) - \pi(j)|)$ into a set D , the number of elements in D is called the dispersion of the interleaver. The dispersion of an

interleaver is a measure of the randomizing that it realizes. A high dispersion leads to low multiplicities in distance spectrum, and therefore to a better performance of the error rate.

The data sequence is not likely to terminate both RSC encoders at the same time, if the interleaver has large s -parameter and dispersion. Therefore it guarantees large Hamming distances between code sequences, and thus good BER performance.

One of the simplest interleavers is the Block Interleaver [66]. In this kind of interleaver, data is written row by row into a rectangular matrix, and read out column by column. Block interleavers are simple to construct and exhibit very high s -parameters (high spreading capability) and very low dispersions (low randomness).

The Random interleaver [68] uses a randomly generated mapping between input and output positions. The advantage of random interleavers is that they are easy to generate. The disadvantage is that the minimum spreading properties cannot be guaranteed. Therefore it is not possible to guarantee the BER performance of the interleaver. Random interleavers are conceptually the ‘opposite’ of a block interleaver because they tend to have very low s -parameters (low spreading capability) and very high dispersions (high randomness).

Semi-random interleavers were designed for Turbo codes in 1995 [69], which guarantee high s -parameter and dispersion, namely the S-Random interleaver. Because of that, compared to the block interleaver, the s -random interleaver has better ability to break down the self-terminating sequences. It then became a good reference for the design of Turbo interleavers. Improved S-Random interleavers have been proposed by several authors. Examples include Improved interleaver [70], Code Matched interleaver [71], the interleaver proposed for the UMTS Turbo code implementation [72], and the *Quadratic Permutation Polynomial* (QPP) interleavers [73].

In general, generating a length N s -random interleaver is a random process. The output position $\pi(i)$ is chosen at random, for each successive input data symbol i . For the previous symbol j , as discussed above, if the distance between data symbol i and j is less than s , $|\pi(i) - \pi(j)|$ must be not less than s . If not, then $\pi(i)$ is rejected and chosen again. Repeat this process until all the N positions are chosen. The interleaver might not be found in one search loop, so it needs a number of trials. In order to produce a solution within reasonable time, choose $s < \sqrt{N/2}$ [74].

$$L^{(1)}(x_l) = \log \left(\frac{p(x_l = +1 | r^{(0)}, r^{(1)}, L_e^2(x))}{p(x_l = -1 | r^{(0)}, r^{(1)}, L_e^2(x))} \right), \quad (2.14)$$

$$= L_c r_l^{(0)} + L_a^{(1)}(x_l), \quad (2.15)$$

where $r^{(0)}$ is the set of noisy systematic bits, $r^{(1)}$ is the set of noisy parity-check bits generated by encoder1, $L_c = 4E_s/N_0$ is the channel reliability factor, $L_a^{(1)}(x_l)$ is the a priori value for the first decoder, and $L_e^2(x)$ is the extrinsic information about the set of the message bits x derived from the second decoding stage and fed back to the first stage. (In order to initiate the Turbo decoding algorithm, set $L_e^2(x) = 0$ on the first iteration of the algorithm.)

The extrinsic information about the message bits derived from the first decoding stage is [62]

$$L_e^{(1)}(x_l) = L^{(1)}(x_l) - [L_c r_l^{(0)} + L_e^{(2)}(x_l)], \quad (2.16)$$

which, after interleaving, is passed to the input of second decoder as the a priori value $L_a^{(2)}(x_l)$. By using the BCJR algorithm, with the noisy parity-check bits $r^{(2)}$, the second decoding stage produces a more refined soft estimate

$$L^{(2)}(x_l) = L_c r_l^{(0)} + L_a^{(2)}(x_l). \quad (2.17)$$

The extrinsic information of this stage is

$$L_e^{(2)}(x_l) = L^{(2)}(x_l) - [L_c r_l^{(0)} + L_e^{(1)}(x_l)], \quad (2.18)$$

after deinterleaving, which is passed back to the input of first decoder as the a priori value $L_a^{(1)}(x_l)$. Through the application of $L_e^{(2)}(x_l)$ to the first stage, the feedback loop around the pair of decoding stages is thereby closed. After several iterations, an estimate of the message bits m is computed by hard-limiting the LLR $L^{(2)}(x)$ at the output of the second stage

$$\hat{m} = \text{sgn}(L^{(2)}(x)). \quad (2.19)$$

Feeding extrinsic information from one stage to the next in the Turbo decoder is to maintain as much statistical independence between the bits as possible from one iteration to the next. In this way, it can be shown that the estimate \hat{m} approaches the MAP solution as the number of iterations approaches infinity. Therefore it is called

MAP decoding. The details and derivation of this algorithm can be found in [32] [77] [78] [79].

The MAP algorithm involves a large number of multiplications and exponentiation, and it also works with actual probabilities and likelihood ratios which have a large range, therefore it is not usually implemented for reasons of computational complexity and difficulties in computer storage. To simplify the implementation, it is better to convert all likelihoods into logarithmic values rather than work with actual probabilities. This is known as the Log-MAP algorithm which is proposed by Robertson [77], which can provide computational simplicity and without loss of optimality.

Unfortunately, it makes the computation of sums of likelihoods much more complex. If we use a very simple approximation through the Log-MAP algorithm as:

$$l = \ln(e^{l_1} + e^{l_2}) \approx \max(l_1, l_2), \quad (2.20)$$

this approximation leads to the Max-Log-MAP algorithm. The Max-Log-MAP algorithm can drastically reduce the complexity of the MAP algorithm, but produces less accurate soft output. The details of these algorithms can also be found in [32] [77] and [78].

A compromise method can partly compensate for the loss [32]. We can introduce a correction factor,

$$\begin{aligned} \ln(e^{l_1} + e^{l_2}) &= \max(l_1, l_2) + \ln(1 + e^{-|l_2 - l_1|}) \\ &= \max(l_1, l_2) + f_c(|l_2 - l_1|), \end{aligned} \quad (2.21)$$

which results in the sub-optimal Log-MAP algorithm.

2.7 EXIT Chart

The Turbo decoding (or “Turbo principle”) is a general principle in decoding and detection. For an iterative Turbo decoder, the two decoders accept and deliver soft values to each other, where the extrinsic part of the soft-output of one decoder is passed on to the other to be used as a priori input. It is not easy to analyze and describe this iterative process with an information transfer between the two decoders. Because iterative decoding is the main point for the next chapter, it is necessary to learn its convergence behavior. One very useful tool, the *extrinsic information transfer* (EXIT) chart introduced by Stephan ten Brink [76], is considered in this part. It can be used to

better understand the convergence behavior of iterative decoding schemes, and the decoding trajectory can directly witness the exchange of extrinsic information, so that the Turbo ‘cliff’ position and BER can be predicted after an arbitrary number of iterations.

As shown in Fig. 2.17, the first decoder takes the intrinsic information X_1 , which include the systematic bits S_0 and the parity bits P_1 from first encoder, and the a priori input A_1 . Then it generates the soft output D_1 . The extrinsic information of the first decoder $E_1 = D_1 - A_1 - X_1$ is passed through the bit interleaver to become the a priori input A_2 of the second decoder. The extrinsic information for the second decoder $E_2 = D_2 - A_2 - X_2$ is passed through a deinterleaver to become the a priori knowledge A_1 of the first decoder.

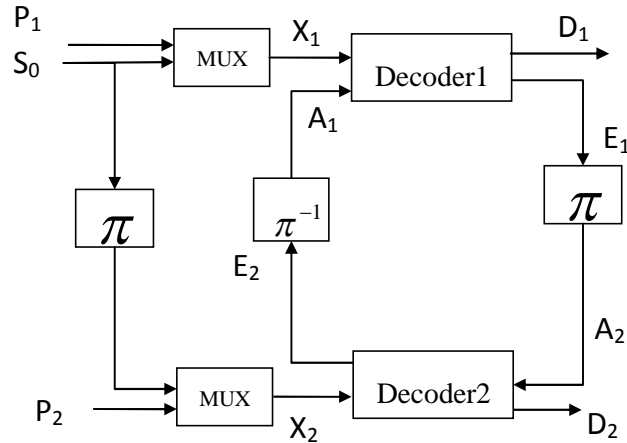


Figure 2.17 Iterative decoder for parallel concatenated codes

The detail of the calculation process for the EXIT chart can be found in [76]. The received signal from the AWGN channel is:

$$\mathbf{r} = \mathbf{x} + \mathbf{n}, \quad (2.22)$$

where \mathbf{x} is the vector of transmission signal, and \mathbf{r} is the vector of received signal. \mathbf{n} is Gaussian distributed noise vector with mean zero and variance $\sigma_n^2 = N_0/2$.

Then the conditional *probability density function* (PDF) can be calculated as

$$p(r|X = x) = \frac{e^{-((r-x)^2/2\sigma_n^2)}}{\sqrt{2\pi}\sigma_n}, \quad (2.23)$$

where X denotes the transmitted bits with realizations $x \in \pm 1$. The corresponding LLR can be calculated as

$$\begin{aligned} R &= \ln \frac{p(r|x = +1)}{p(r|x = -1)} \\ &= \frac{2}{\sigma_n^2} (\mathbf{x} + \mathbf{n}) = \mu_R \mathbf{x} + \mathbf{n}_R. \end{aligned}$$

Then the mean value and variance of R is

$$\begin{aligned} \mu_R &= \frac{2}{\sigma_n^2}, \\ \sigma_R^2 &= \left(\left(\frac{2}{\sigma_n^2} \right) \cdot \sigma_n \right)^2 = \frac{4}{\sigma_n^2}. \end{aligned}$$

Therefore the mean and variance can be connected as

$$\mu_R = \frac{\sigma_R^2}{2}. \quad (2.24)$$

For large interleavers the a priori values remain fairly uncorrelated from the respective channel observations over many iterations. This is because the extrinsic information E_k of the bit at time instance k is not influenced by the channel observations Z_k or a priori knowledge A_k , by looking at the decoder output $D = Z + A + E$ [76]. Moreover a large interleaver makes further contributions which reduces correlations and gets a better ‘separation’ of both decoders.

Also as illustrated in [80] the PDF of the extrinsic output values (a priori values for the next decoder respectively) approaches a Gaussian-like distribution with increasing numbers of iterations. The reason for this may be a Gaussian channel model is used. Meanwhile, in the L -value calculation of E , sums over many values are involved, which typically leads to Gaussian-like distributions [76].

Therefore [76] suggest that in order to predict the behaviour of the iterative decoder, the above two observations should be considered. So the a priori input A to the constituent decoder is suggested to be modeled by applying an independent Gaussian random variable n_A with variance σ_A^2 and mean zero in conjunction with the known transmitted systematic bits x .

$$A = \mu_A \mathbf{x} + \mathbf{n}_A.$$

The mean value μ_A must fulfill

$$\mu_A = \frac{\sigma_A^2}{2}.$$

The mutual information I_A is used to measure the information contents of the a priori input,

$$I_A = 1 - \int_{-\infty}^{\infty} \frac{e^{-((x-\sigma_A^2/2)^2/2\sigma_A^2)}}{\sqrt{2\pi}\sigma_A} \cdot \log_2[1 + e^{-x}]dX, \quad 0 \leq I_A \leq 1. \quad (2.25)$$

By appropriately choosing the parameter σ_A , a certain value of I_A is obtained. The mutual information of the extrinsic output I_E can be viewed as a function of I_A and E_b/N_0 , defined as $I_E = T(I_A, E_b/N_0)$ and $I_E = T(I_A)$ for fixed E_b/N_0 . For the desired I_A , I_E can be computed by Monte Carlo simulation.

Using I_A and I_E , we can draw the EXIT chart, which can show the behaviour of the iterative decoding intuitively. The EXIT chart can also be used to analysis the iterative process between detection and decoding. In the following chapters, it will be used to help us to understand the joint detection and decoding better.

2.8 Interleave-Division Multiple Access (IDMA)

Interference limits the performance of MAI [92] and multiple transmit antenna systems (*cross antenna interference* (CAI)) [96]. Iterative multiuser detection is used to enhance the performance of CDMA systems. However, the complexity of CDMA multiuser detection increases rapidly with the number of users. For well-known MMSE-based approach in [96], the complexity per user increases quadratically.

A characteristic feature for a conventional CDMA system is the use of signature sequences for user separation. Between FEC coding and spreading, interleaver is usually placed to combat fading effect. [92] briefly mentioned the possibility of employing interleaver for user separation in CDMA systems. In a CDMA system, different interleavers which are assigned to different users can improve the system performance [124] [125]. [126] investigated multiuser detection in narrowband applications with a small number of users. User-specific can be made in a bandwidth-efficient trellis coded-modulation system by selecting a unique combination of trellis code structure, interleaver and modulation constellation.

Inspired by these results, [107] presented a simple approach, called *interleave-division multiple access* (IDMA), to deal with both MAI and CAI. In an IDMA scheme, users can be distinguished by different chip-level interleaving methods instead of by different signatures as in a conventional CDMA system. The structure of the IDMA scheme is shown in Fig. 2.18.

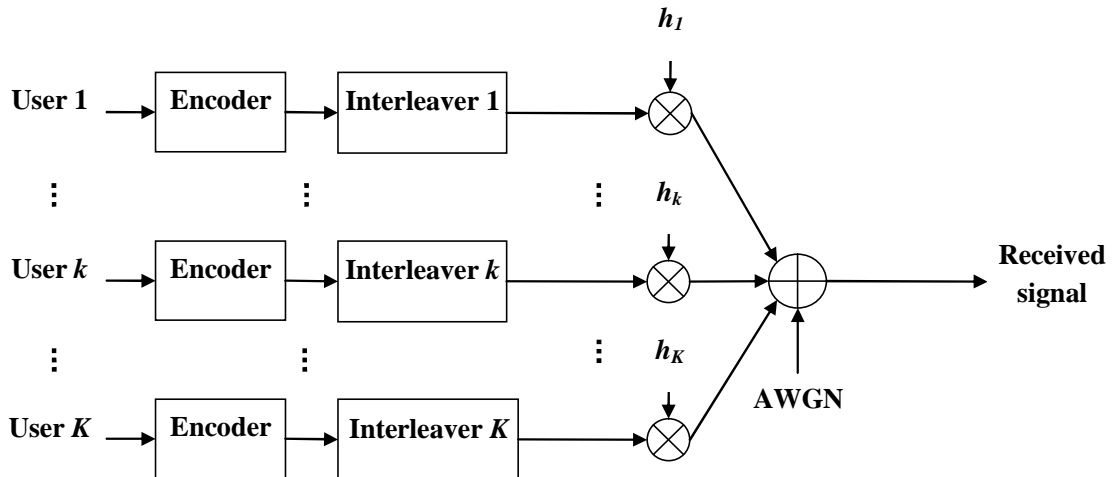


Figure 2.18. Structure of the IDMA system

The data of user k ($k = 1, \dots, K$) is first encoded by a conventional FEC encoder or a spreader or both, followed by a chip interleaver k , and then is transmitted. Unlike conventional CDMA, interleaver here is applied at the final stage of the transmitter. The key principle of IDMA is that the interleaver should be different for different users. The use of independent interleavers can ensure that the signals from different users are separable even when using the same spreading sequence for all the users. In this case, spreading can be replaced by repetition coding or by other low-rate coding. Then, interleaving remains the only means to distinguish users.

The IDMA will be used in chapter 5, which is combined with multiuser MIMO OFDM system to improve the system performance.

2.9 Simulations

A SISO system with/without convolutional code (generator [5 7], 1/2 rate) through AWGN, block fading and fast fading channel is considered, and Viterbi hard-decision decoding is used, as shown in Fig. 2.19. For block fading channel (or called slow fading

channel), the channel coefficients remain unchanged during one data frame (frame length 1000, 1000 frames), the BER performances are poor whether it is coded or not.

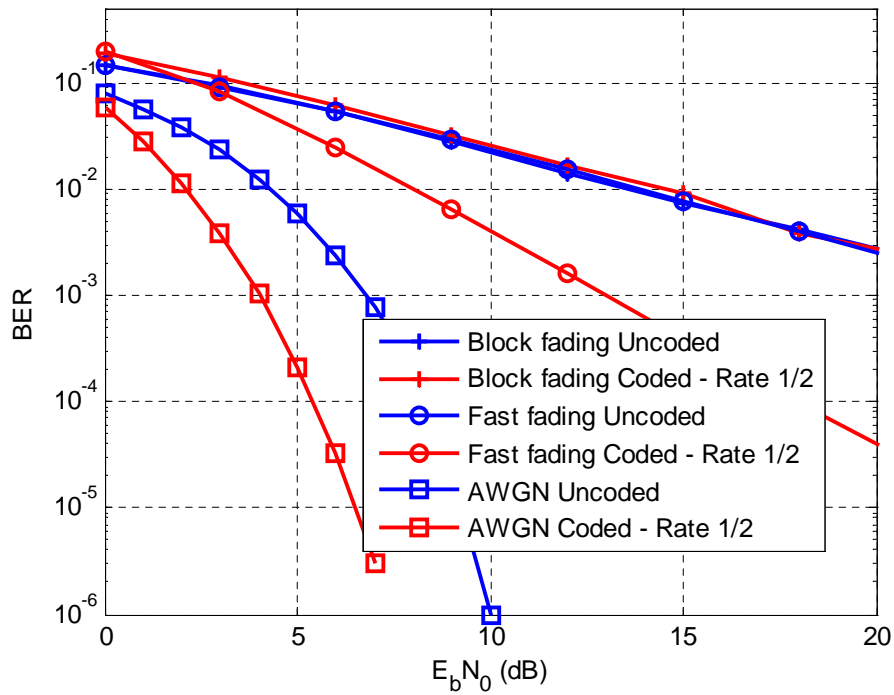


Figure 2.19. SISO system of AWGN, block fading and fast fading channel with/out convolutional code (1/2 rate)

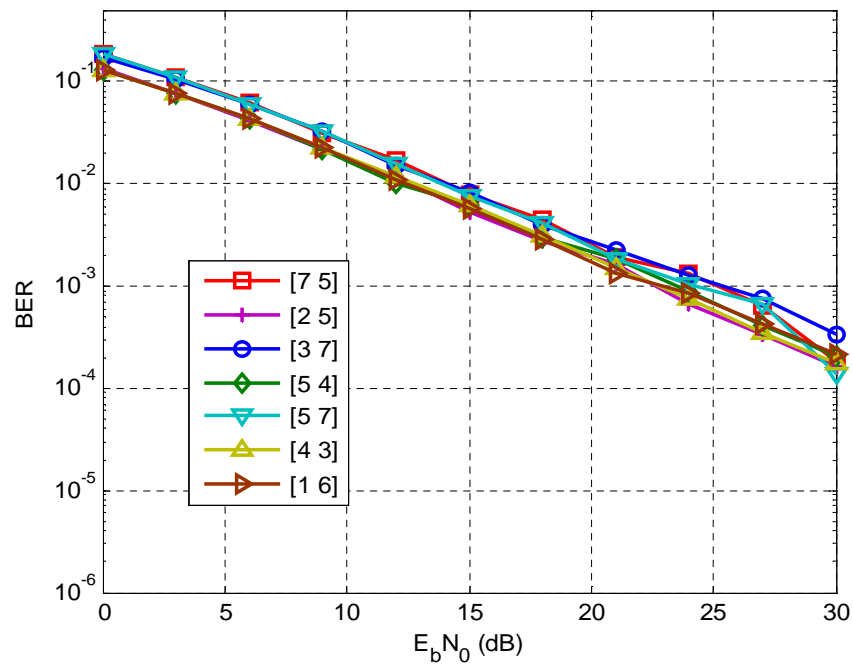


Figure 2.20. Comparison of BER performance for SISO system using convolutional code with different generator polynomials (with the same code rate 1/2) in a block fading channel

However, for AWGN and fast fading channel (the channel coefficients change bit by bit), the BER performance of the coded system is much better than that of uncoded system. It can be seen that the fast fading channel gain can be obtained by the coded system.

For code rate 1/2, different generator polynomials are compared for a SISO system with convolutional code through a block fading channel, and the hard-decision decoding is still used. As shown in Fig. 2.20, it can be seen that the difference between different generator polynomials for convolutional code in block fading channel is not much.

Fig. 2.21 shows the difference of a 2-by-2 system using a convolutional code (with generator [5 7]) with and without interleaving under fast fading channel. S-Random interleaver is employed here. Using an interleaver can spread out bursts of errors over time, so it can get some time diversity. Therefore an interleaver is often used in encoding.

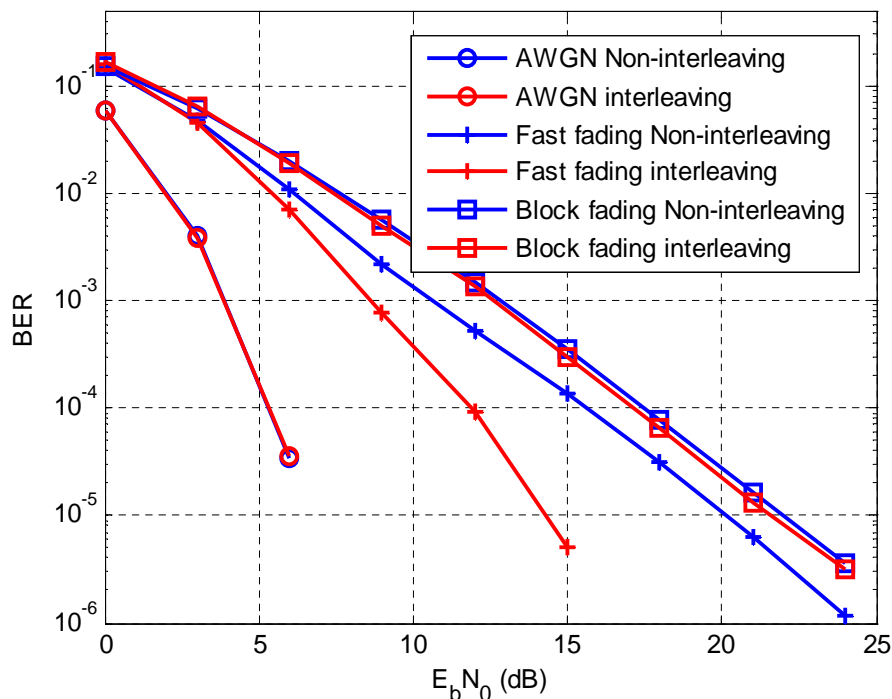


Figure 2.21. 2-by-2 system of fading channel using convolutional code (1/2 rate) with/out interleaver, hard decision decoding is considered.

As shown in Fig.2.21, the BER performance does not change under the AWGN channel whether an interleaver is used or not. For block fading channel, the BER performance of using an interleaver is a litter better than that without interleaving. Moreover for fast fading channel, it's obvious that the BER performance with interleaving is much better

than that without interleaving. This is because the fast fading channel can easily cause the burst errors. Using an interleaver in this case can obtain the channel gain.

Hard-decision decoding is simpler than soft-decision decoding, but it gives worse performance, as shown in Fig. 2.22. A 2-by-2 system with convolutional code ([5 7]) under fast fading channel using ML hard decision and MAP soft decision is considered. Using MAP soft decision as the input of the decoder, the BER performance is better than that of using ML hard decision.

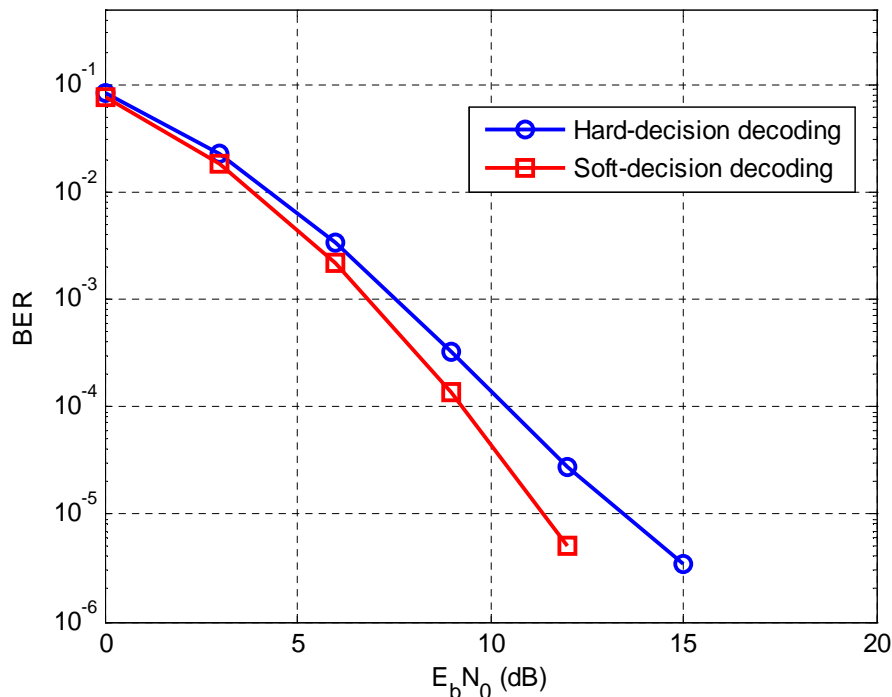


Figure 2.22. BER performance of ML hard decision and MAP soft decision of 2-by-2 system with fast fading channel using convolutional code (1/2 rate)

Fig. 2.23 shows the BER performance gain of using Turbo code (two convolutional concatenated encoder with generator [5 7]) compared with using convolutional code. The two sets of parity bits of Turbo code are punctured, so the total code rate is also 1/2. Through comparing three different channels (AWGN, block fading, and fast fading), this SISO system using Turbo code shows larger performance gain for AWGN and fast fading channel.

The above simulations of coding only show the performance of the data bits. For the next chapter, the parity bits are also needed. Therefore, Fig. 2.24 and Fig. 2.25 show the performance of both the data bits and the parity bits for convolutional code and Turbo code, respectively. A SISO system is considered, and three different channels as well.

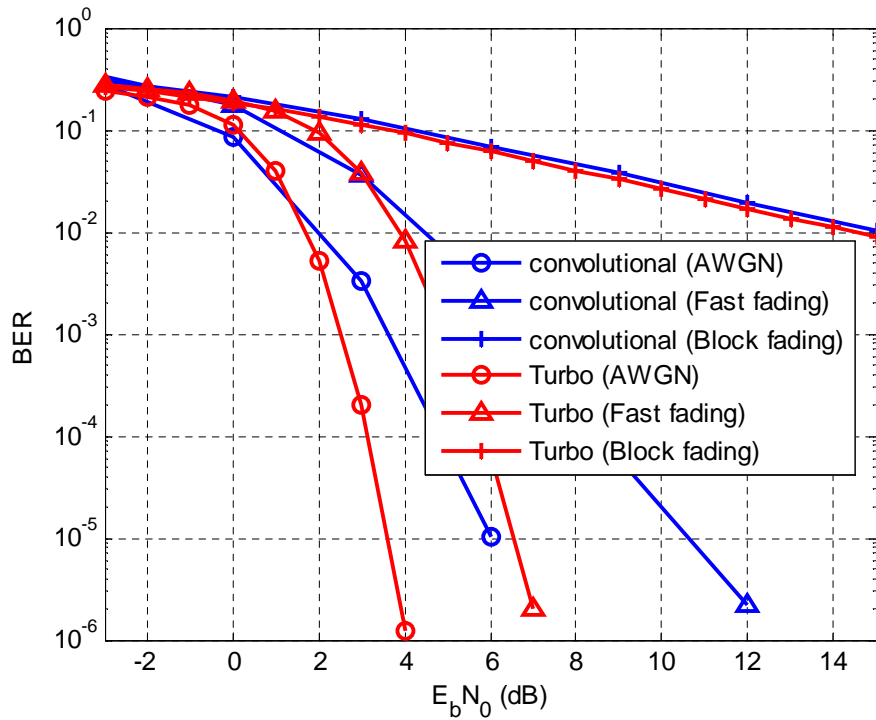


Figure 2.23. BER performance of SISO system of AWGN, block fading and fast fading channel using convolutional code (1/2 rate) and Turbo code (1/2 rate)

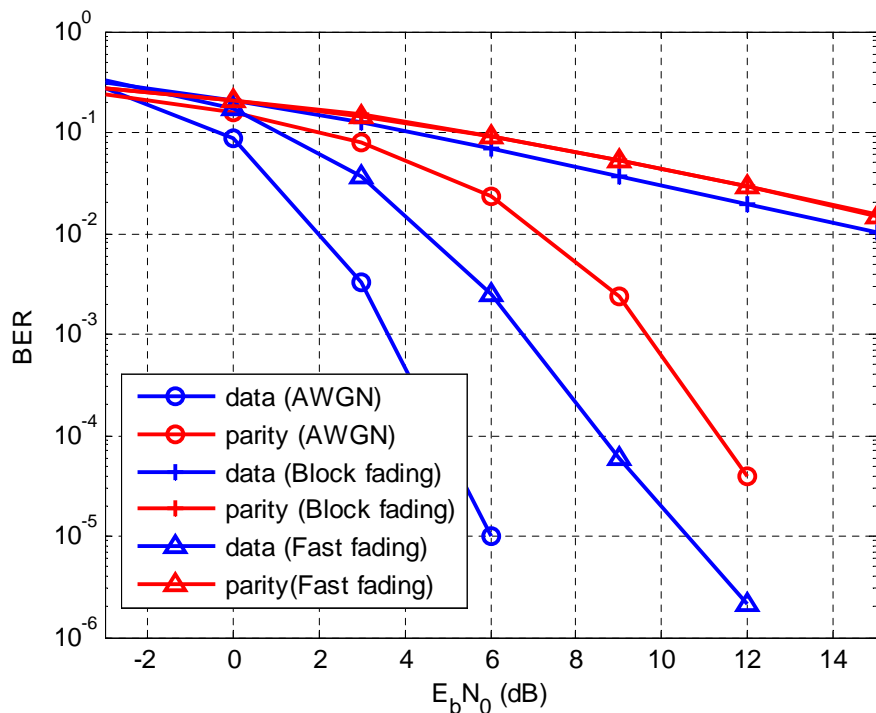


Figure 2.24. BER performance of data bits and parity bits of SISO system of AWGN, block fading and fast fading channel using convolutional code (1/2 rate)

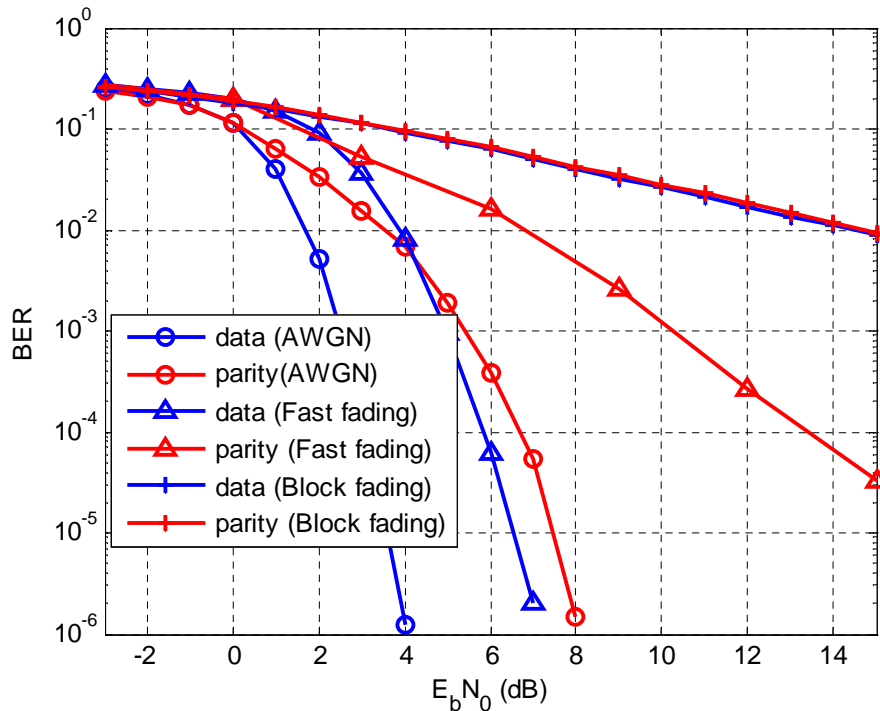


Figure 2.25. BER performance of data bits and parity bits of SISO system of AWGN, block fading and fast fading channel using Turbo code (symmetric PCC rate 1/2 rate)

Both figures show that the performance of data bits is better than that of parity bits. This is due to the extrinsic information transfer between the two decoders of Turbo decoder in the decoding of data bits, while decoding the parity bits has no such information. The decoder itself is not designed for the parity data. So it is understandable that the BER of the parity data is higher.

The EXIT chart is shown in Fig. 2.26, Fig. 2.27, Fig. 2.28 and Fig. 2.29. To illustrate the iterative nature of the decoder, both decoder characteristics are plotted into a single diagram. The axes are swapped for the second decoder. This is the EXIT chart for one of the decoders of rate 1/2 code.

A SISO system is considered. The interleaver size is 1024, the code polynomials are [5 7]. The channel used in the simulation is the AWGN channel, where different E_b/N_0 , 0.5dB, 0.8dB, 1.2dB and 3dB, are considered.

From these figures it can be seen that I_E is monotonically increasing with I_A . Increasing I_A means that more and more bits become known at the decoder, and there will be a growing conditioning of the mutual information I_E .

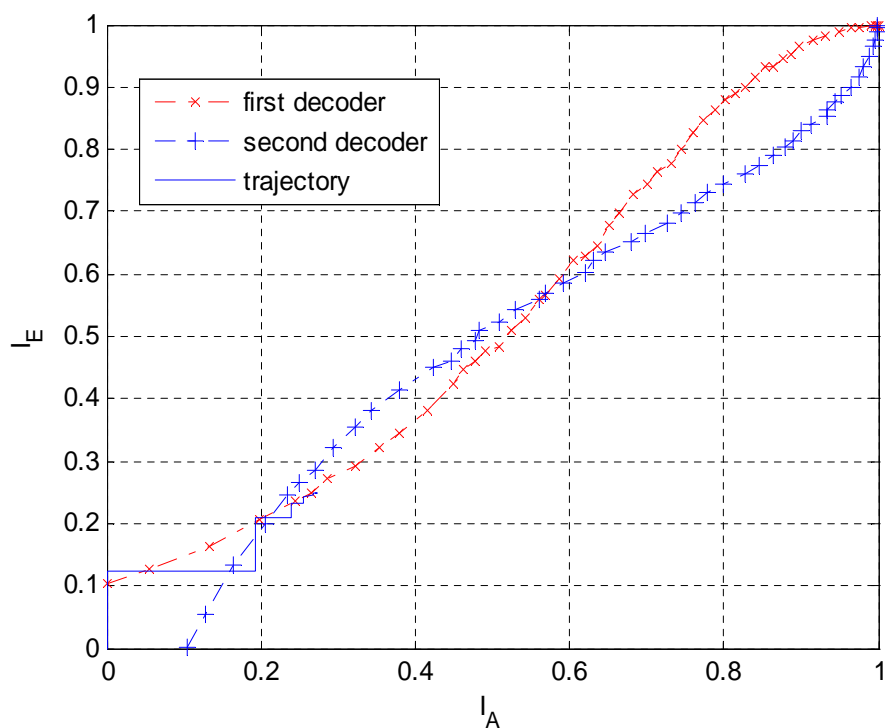


Figure 2.26. Extrinsic information transfer characteristics of soft in/soft out decoder for rate 1/2 convolutional code and simulated trajectory of iterative decoding at 0.5dB

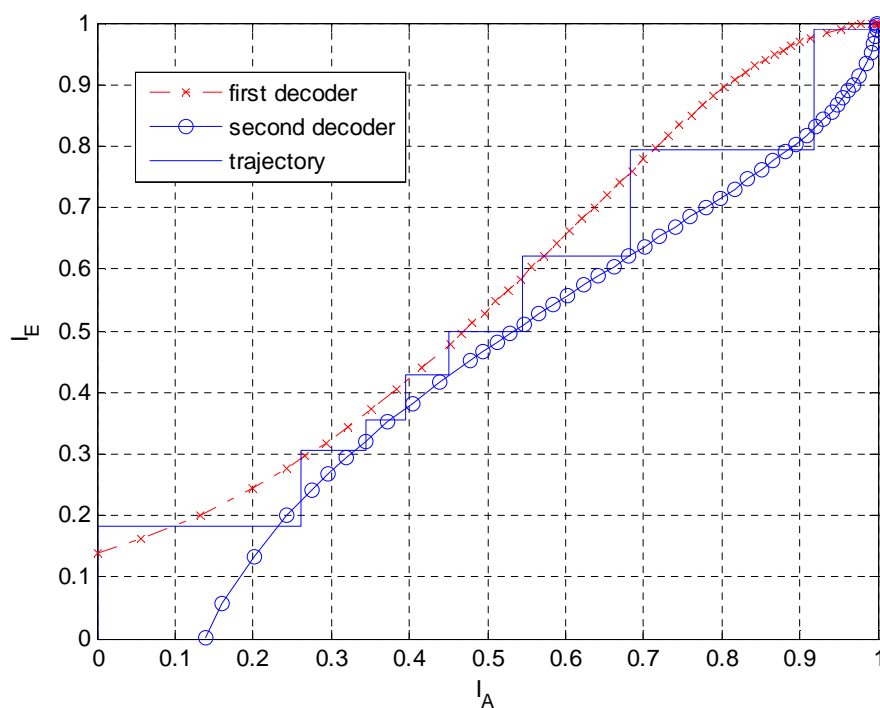


Figure 2.27. Extrinsic information transfer characteristics of soft in/soft out decoder for rate 1/2 convolutional code and simulated trajectory of iterative decoding at 0.8dB

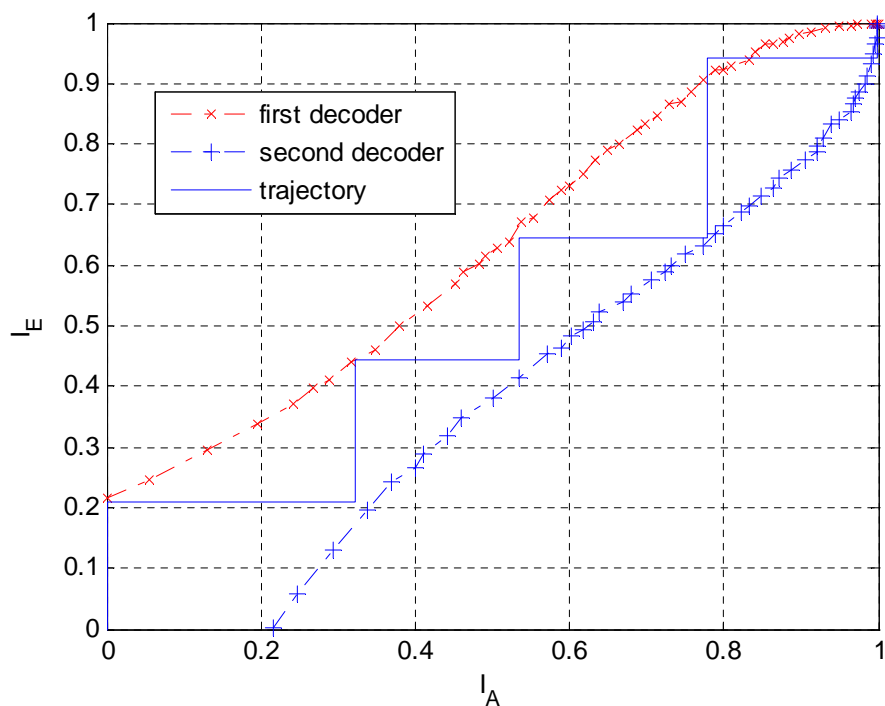


Figure 2.28. Extrinsic information transfer characteristics of soft in/soft out decoder for rate 1/2 convolutional code and simulated trajectory of iterative decoding at 1.2dB

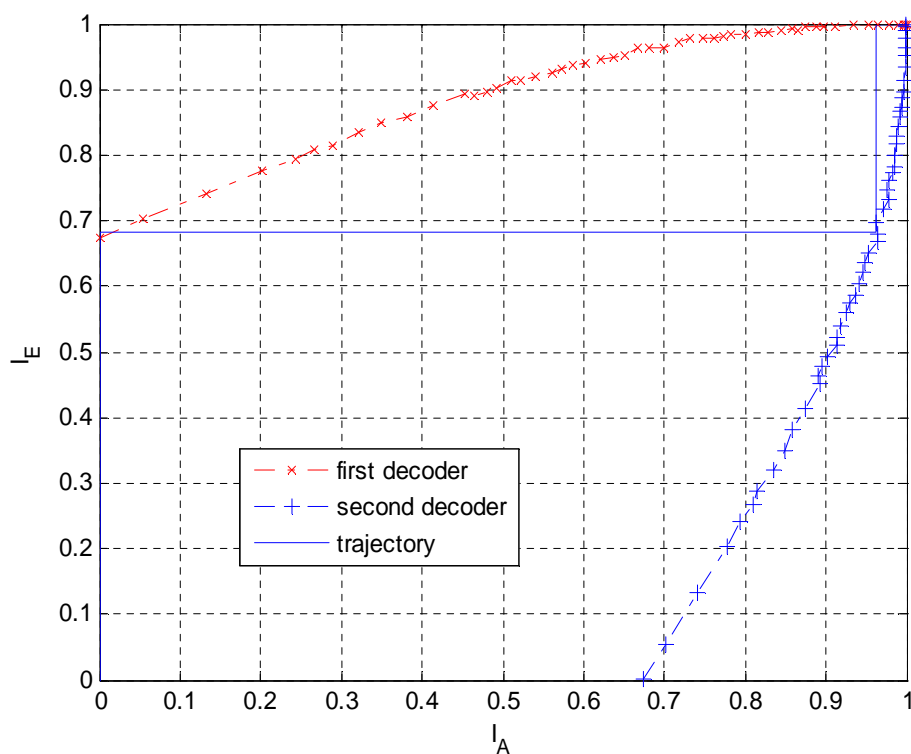


Figure 2.29 Extrinsic information transfer characteristics of soft in/soft out decoder for rate 1/2 convolutional code and simulated trajectory of iterative decoding at 3dB

The exchange of extrinsic information can be visualized as a decoding trajectory on these diagrams. When the E_b/N_0 is fixed, let i be the iteration index. When $i = 0$ the iteration starts with zero a priori knowledge $I_{A_1,0} = 0$. At i th iteration, the extrinsic output of the first decoder is $I_{E_1,i} = T(I_{A_1,i})$.

Then $I_{E_1,i}$ is forward to the second decoder as a priori knowledge $I_{A_2,i} = I_{E_1,i}$. The extrinsic output of the second decoder is $I_{E_2,i} = T(I_{A_2,i})$, and it is fed back to the first decoder to become $I_{A_1,i+1} = I_{E_2,i}$ of next iteration. The iteration stops if $I_{E_2,i+1} = I_{E_2,i}$, which corresponds to an intersection of both characteristics in the EXIT chart.

At 0.5dB, the trajectory gets stuck after two iterations. For 0.8dB, the trajectory has just managed to sneak through the bottleneck, and it needs several iterations to decoding. For 1.2dB, it only needs five iterations, while only two iterations are needed for 3dB. This means that the higher SNR is, the less number of iterations are needed, and the better performance is.

2.10 Conclusions

In this chapter, some fundamental techniques used in the following chapters, MIMO, OFDM, MUD, FEC code, and IDMA are introduced. This introduction mainly focuses on the approaches employed in this thesis. MIMO OFDM system is the basic system model of this thesis. The introduction to MUD focuses on the most original schemes: ZF and MMSE are the linear approach, which have low complexity but also low performance; the optimal ML has the perfect performance but high complexity. However, the matched filter can provide the optimal BER performance if the interference is perfectly cancelled. Based on the PIC, the matched filter will be employed in chapter 3.

IDMA inherits many advantages from CDMA. The key advantage is IDMA allows the use of a low complexity iterative multiuser detection technique. Therefore it will be considered as an effective complement of the proposed detection scheme in chapter 5.

Chapter 3

Low Complexity Iterative Detection for Overloaded Multiuser MIMO OFDM Systems

Contents

3.1 Introduction	56
3.2 Turbo Multiuser Detection.....	57
3.3 System Model.....	59
3.4 Multiuser Receiver for AWGN Channels.....	60
3.5 Multiuser Receiver for Flat Fading Channels	70
3.6 Multiuser Receiver for Frequency Selective Channels	72
3.7 Iterative Interference Cancellation (IIC) Receiver	76
3.8 Performance of IIC MUD.....	88
3.9 Conclusions.....	96

In this chapter an *Iterative Interference Cancellation* (IIC) multiuser receiver structure will be introduced employing MRC detection as its first stage.

3.1 Introduction

As mentioned previously, MIMO systems have two categories: underloaded and overloaded systems. Since the computational complexity of the optimal MUD increases exponentially with the number of simultaneous users, it is unrealistic for the optimal receiver to work for large numbers of users. Consequently, many suboptimal detection schemes have been proposed for MUD, possessing low computational load, but also having poorer detection performance compared to the optimal detector. Especially in the overloaded system, linear MUD schemes fail to show good BER performance, due to the rank-deficient channel covariance matrix.

In chapter 2, we have discussed linear MUD schemes such as ZF and MMSE. The performances of both are better than that of the matched filter, but worse than ML. The non-linear MUD schemes SIC and PIC, can remove the interference gradually as the iteration number increases. The BER performance shows that if the interference can be eliminated perfectly, the matched filter can achieve the optimal performance, and can obtain better diversity (compared to ZF and MMSE).

For CDMA systems, the performance can be severely degraded by interference, including both ISI and the interference between users. In [81], Goldsmith proposed an iterative weighted interference cancellation for CDMA system with RAKE reception, where an initial hard estimate of the data bits obtained by a RAKE was used to regenerate and subtract out the ISI and co-channel interference after weighting, in order to get a better estimate of the bits. Subsequently, it repeated the regeneration and weighted subtraction process using these estimates and continued this process over multiple stages.

Partial PIC and convolutional coding was employed in [82], in which a soft cancellation factor was considered to weight the interference estimates. The best choice of the soft cancellation factor can be found to optimize the combined performance of interference cancellation and coding.

An iterative adaptive soft parallel interference canceller was proposed for Turbo coded MIMO multiplexing [83], which was applied to transform a MIMO channel into *single-input multiple-output* (SIMO) channels for MRC. The replicas of the interference from different transmit antennas are generated and subtracted from the received signals.

At the first iteration, *maximum likelihood detection* (MLD) was used to generate the log-likelihood ratio sequence. An adaptive soft cancellation weight was introduced to avoid the increasing of the interference when MLD is incorrect.

An iterative interference cancellation scheme was proposed for STBC multirate multiuser systems, which was based on MMSE and ML detection [84]. For STBC-OFDM system, [85] shows an iterative interference cancellation scheme to reduce both *co-channel interference* (CCI) and ICI jointly. A list-SIC algorithm was presented to obtain a candidate list to obtain soft information used in the CCI cancellation. [86] uses a simple iterative interference cancellation scheme for OFDM signals with blanking nonlinearity in impulsive noise channels.

Several iterative interference cancellation schemes proposed in [87]-[91], also studied linear (MMSE, MRC) plus non-linear (SIC, PIC) detection schemes. It is noticed that another class of detection schemes are also proposed frequently, the optimal multiuser detector [92]-[95], which are based on the iterative ML detector combining with the FEC code. However this class of iterative receiver still has too high a computational complexity for feasible applications, even though they have much reduced complexity by using Sphere Detection. It is obvious that in order to construct a suitable iterative receiver with lower complexity, the combination of the matched filter and PIC is a reasonable solution.

The rest of this chapter is organized as follows: In Section 3.2, Turbo multiuser detection is introduced. Then we describe the system model in Section 3.3. Multiuser receivers for the AWGN channel, flat fading channel, and frequency selective channel are detailed in section 3.4, 3.5 and 3.6. In section 3.7, we propose a new iterative interference cancellation receiver. In Section 3.8, we offer our simulation results, and conclude in Section 3.9.

3.2 Turbo Multiuser Detection

The PIC approach is regarded as one of the most promising among various MUD schemes, because of the adoption of the “iterative structure”. The remarkable performance of the powerful “Turbo Codes” shows that when the temporary results generated in the current iteration are fed back to the input of the next iteration, it is likely to bring some benefits. Since the introduction of Turbo codes, the iterative

structure is then called the “Turbo Principle”, and is employed by the multiuser detection scheme called “Turbo Multiuser Detection”. However, a Turbo multiuser receiver does not necessarily involve a Turbo decoder: a convolutional decoder is also suitable.

PIC detection can improve the receiver’s performance continuously with increasing number of iterations. But sometimes the PIC receiver gives a worse result in the current iteration than in the previous one. This oscillatory behaviour, which is caused by the error propagation, can result in failure of convergence.

In a PIC receiver, the MAI which is subtracted from the received signal in the next iteration, is reconstructed by using the temporary decisions of the users’ data detected in the current iteration. This is the reason why PIC detection performs well. However the potential problem is also located here. If some of the decisions for the users’ data are erroneous, a wrong decision of a bit will result in a wrong interference reconstruction, and a wrong value of interference is subtracted from the multiuser signal, so that MAI can potentially be strengthened, instead of cancelled. The error is therefore propagated to the corresponding bits of other users’ signals. If this is a serious error, it is possible to lead the decision of the data into the wrong direction in the next iteration.

There are two measures that can be taken to avoid this problem. One is employing soft PIC detection rather than hard detection. This can be implemented using two approaches:

- 1) The temporary estimates can be provided by a *soft-in soft-out* (SISO) detection or decoding process whose outputs represent the data as well as their reliability. Then the soft outputs, rather than the hard decisions, can be fed to the PIC detector directly, after normalization if needed. Thus we can subtract the interference generated from the reliable bits and restrict the influence of the unreliable ones.
- 2) Employ partial PIC. It uses a weight factor to scale the MAI estimates obtained from past hard decisions before subtracting them from the received signal, thus reducing the sensitivity to errors in the estimated MAI.

In this thesis, the former approach is adopted. Another measure is tried to improve the quality of the data estimated before they are used to reconstruct the interference. In this

scheme, FEC decoders, such as convolutional or Turbo decoders, are involved for each iteration.

Based on the above considerations, the convolutional decoder is selected to be involved in the iterations. On the one hand, the convolutional decoder has nice error correction ability with low complexity, and PIC detection can benefit from it. On the other hand, a convolutional decoder can return the LLR that can be used to judge the reliability of the data. This structure is also called Turbo Multiuser Detection, although it does not employ the Turbo decoder.

It is noticed that a Turbo decoder is also can be used. However, it utilizes the MAP algorithm to obtain the LLR, which is much more complicated, not only the algorithm, but also the Turbo code itself. There is no doubt that a Turbo decoder has remarkable error correction ability, however if a convolutional decoder is sufficient, we can just use the convolutional decoder.

Hence, an iterative matched filter-based PIC detector for convolutional-coded MIMO OFDM is derived.

3.3 System Model

An uplink MU MIMO system with M users is considered. For simplicity, it is assumed that the signals of the multiple users are time aligned at the receiver front end. M users with a total of N_T transmit antennas simultaneously transmit data signals to the base station with N_R receive antennas. Much research has assumed or based on the assumption that the number of receive antennas is equal to or greater than the transmitters ($N_R \geq N_T$), this is the *underloaded* system. On the contrary, we focus on the *overloaded* system, where receive antennas are fewer than the transmitters ($N_R < N_T$). We assume that users are uncorrelated and each user has only one antenna, that is $M = N_T$.

Fig. 3.1 illustrates the structure of the system model. The data of each user is encoded by the convolutional encoder first, and then passed through the interleaver which is used to avoid burst errors. In order to make the interleaver work well, the length L of the data frame should be sufficient. Finally, after BPSK modulation, the data is transmitted.

The received signal for one symbol through the channel can be expressed as

$$\mathbf{r} = \mathbf{H}\mathbf{s} + \mathbf{n}, \quad (3.1)$$

where the received signal \mathbf{r} , channel matrix \mathbf{H} , transmitted signal \mathbf{s} , and AWGN \mathbf{n} with zero mean and variance σ_n^2 are respectively expressed in discrete-time form as:

$$\mathbf{r} = [r[1], r[2], \dots, r[N_R]]^T, \quad (3.2)$$

$$\mathbf{s} = [s[1], s[2], \dots, s[N_T]]^T, \quad (3.3)$$

$$\mathbf{n} = [n[1], n[2], \dots, n[N_R]]^T, \quad (3.4)$$

$$\mathbf{H} = \begin{bmatrix} h_{11} & h_{12} & \dots & h_{1N_T} \\ h_{21} & h_{22} & \dots & h_{2N_T} \\ \vdots & \vdots & \ddots & \vdots \\ h_{N_R1} & h_{N_R2} & \dots & h_{N_RN_T} \end{bmatrix}. \quad (3.5)$$

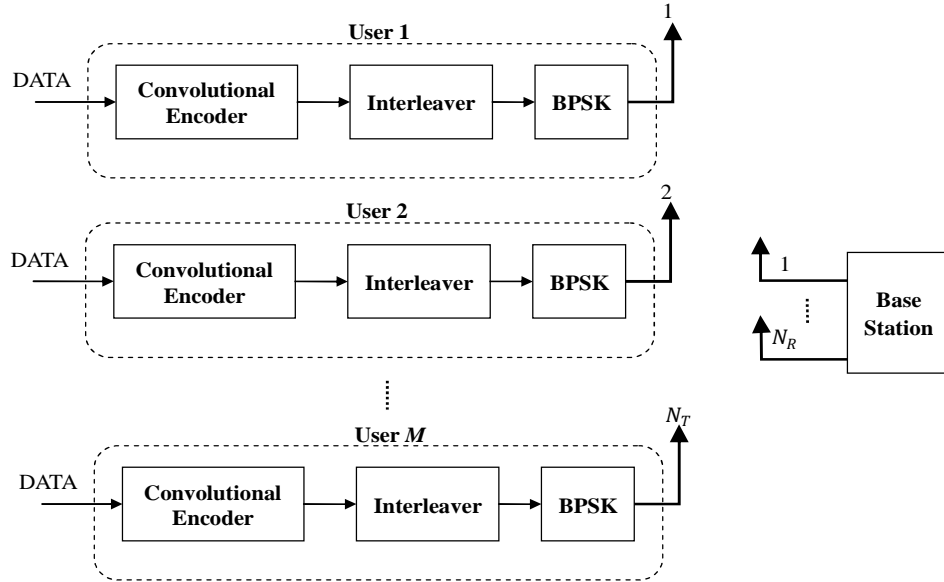


Figure 3.1 The structure of overloaded multiuser MIMO system

3.4 Multiuser Receiver for AWGN Channel

In order to obtain a suitable detection algorithm, we first consider the AWGN channel, assuming there is no fading at all. The received signal in Eq. (3.1) can be rewritten as

$$\mathbf{r} = \mathbf{H}_{AWGN}\mathbf{s} + \mathbf{n}, \quad (3.6)$$

where the channel matrix \mathbf{H}_{AWGN} can be expressed as a matrix of constant one

$$\mathbf{H}_{AWGN} = \mathbf{1}_{N_RN_T}. \quad (3.7)$$

A matched filter using MRC is employed in the iterative receiver. The structure of the matched filter receiver is depicted in Fig. 3.2.

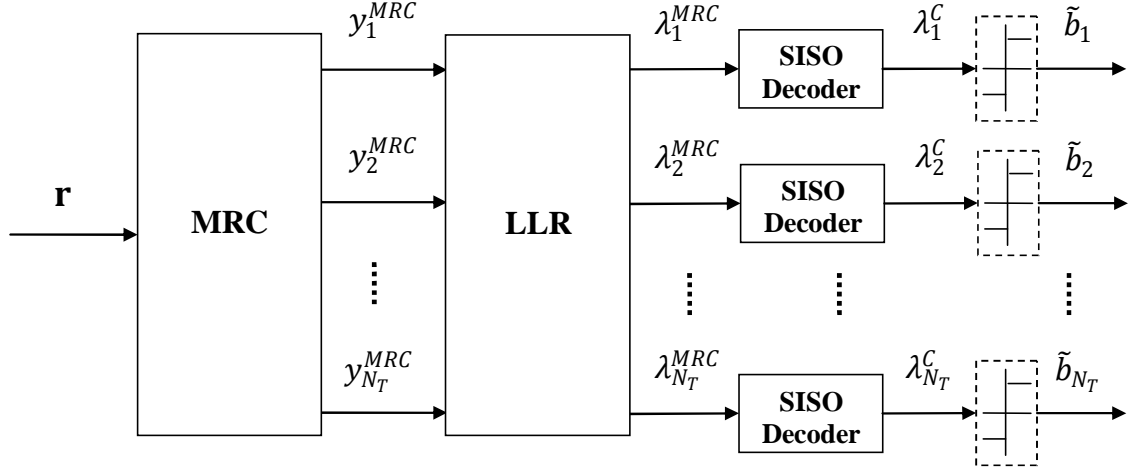


Figure 3.2 Matched filter multiuser receiver for overloaded MIMO system

The received signal is first maximum ratio combined by the matched filter,

$$\mathbf{y}_{MRC} = \mathbf{H}_{AWGN}^H \mathbf{r}, \quad (3.8)$$

$$= \mathbf{H}_{AWGN}^H \mathbf{H}_{AWGN} \mathbf{s} + \mathbf{H}_{AWGN}^H \mathbf{n}, \quad (3.9)$$

$$= \mathbf{R}_{AWGN} \mathbf{s} + \mathbf{W}, \quad (3.10)$$

where \mathbf{R}_{AWGN} is the channel covariance matrix with constant elements, and \mathbf{W} is the AWGN noise multiplied by the Hermitian of channel matrix.

Then the outputs of the filter are converted into LLR values, which are used for the SISO decoder. For one symbol b , the LLR of the m th user corresponding to the n_t th transmitter is given by:

$$\lambda_{n_t}^{MRC} = \log \left(\frac{P[b = +1]}{P[b = -1]} \right). \quad (3.11)$$

The noise \mathbf{W} is still Gaussian distribution, with zero mean and variance σ_n^2 , its probability density function is

$$P_w = \frac{1}{\sqrt{2\pi}\sigma_n} \exp \left(-\frac{w^2}{2\sigma_n^2} \right). \quad (3.12)$$

Together with Eq. (3.10) and (3.12), Eq. (3.11) can be written as

$$\begin{aligned}
 \lambda_{n_t}^{MRC} &= \log \left(\frac{\frac{1}{\sqrt{2\pi}\sigma_n} \exp\left(-\frac{(y_{n_t}^{MRC} - 1)^2}{2\sigma_n^2}\right)}{\frac{1}{\sqrt{2\pi}\sigma_n} \exp\left(-\frac{(y_{n_t}^{MRC} + 1)^2}{2\sigma_n^2}\right)} \right), \\
 &= \log \left(\exp\left(-\frac{(y_{n_t}^{MRC} - 1)^2}{2\sigma_n^2}\right) \right) - \log \left(\exp\left(-\frac{(y_{n_t}^{MRC} + 1)^2}{2\sigma_n^2}\right) \right), \\
 &= \frac{(y_{n_t}^{MRC} + 1)^2}{2\sigma_n^2} - \frac{(y_{n_t}^{MRC} - 1)^2}{2\sigma_n^2}, \\
 &= \frac{2}{\sigma_n^2} \cdot y_{n_t}^{MRC}. \tag{3.13}
 \end{aligned}$$

When the SNR is low, such as 0dB, the converted LLR values are small. When the SNR is high, the converted LLR values are much larger. The LLR values are linearly increasing with the SNR.

Feeding the soft value to the SISO decoder, the LLR of decoder output λ_c is obtained. Before they are used to reconstruct the MAI, the LLRs should be converted to the soft values of the data. In conventional methods, a hard decision is taken. Any LLR above 0 will be converted to +1 and any LLR below 0 will be converted to -1 for BPSK. Considering the uncertainty of the data, this is clearly not the optimum approach. In this case, a wrong decision will lead to an erroneous value. As expressed in Section 3.2, this will result in severe error propagation. The LLR of a bit given by the SISO decoder involves its reliability information as well as its value. The hard decision definitely discards this valuable information.

Instead of hard decisions, some soft approaches have been employed to estimate the data, such as in [96]. Soft values between +1 and -1 are given. A relatively reliable data leads to a value approaching +1 and -1, while an unreliable bit will lead to a value close to 0.

Obviously, giving a value close to 0 to an unreliable bit is more helpful for its potential correction, and to reduce the error propagation caused by an error. We can derive the threshold as follows. The LLR of the m th user corresponding to the n_t th transmitter is given by:

$$\lambda_{n_t}^c = \log \left(\frac{P[b_{n_t} = +1]}{P[b_{n_t} = -1]} \right), \quad (3.14)$$

where

$$P[b_{n_t} = +1] + P[b_{n_t} = -1] = 1. \quad (3.15)$$

Combining Eq. (3.14) and (3.15), we can obtain

$$P[b_{n_t} = +1] = \frac{\exp(\lambda_{n_t}^c)}{1 + \exp(\lambda_{n_t}^c)}, \quad (3.16)$$

$$P[b_{n_t} = -1] = \frac{1}{1 + \exp(\lambda_{n_t}^c)} = \frac{\exp(-\lambda_{n_t}^c)}{1 + \exp(-\lambda_{n_t}^c)}. \quad (3.17)$$

Assuming $\hat{b} \in \{+1, -1\}$, we can have

$$\begin{aligned} P[b_{n_t} = \hat{b}] &= \frac{\exp(\hat{b}\lambda_{n_t}^c)}{1 + \exp(\hat{b}\lambda_{n_t}^c)} \\ &= \frac{\exp(\hat{b}\lambda_{n_t}^c/2)}{\exp(-\hat{b}\lambda_{n_t}^c/2) + \exp(\hat{b}\lambda_{n_t}^c/2)} \\ &= \frac{\cosh(\hat{b}\lambda_{n_t}^c/2) (1 + \hat{b}\tanh(\hat{b}\lambda_{n_t}^c/2))}{2\cosh(\hat{b}\lambda_{n_t}^c/2)} \\ &= \frac{1}{2} (1 + \hat{b}\tanh(\hat{b}\lambda_{n_t}^c/2)). \end{aligned} \quad (3.18)$$

Then the soft estimates of the symbol b_{n_t} can be given as [96]:

$$\begin{aligned} \tilde{b}_{n_t} &= \sum_{\hat{b} \in \{+1, -1\}} \hat{b} P[b_{n_t}] \\ &= \sum_{\hat{b} \in \{+1, -1\}} \frac{\hat{b}}{2} (1 + \hat{b}\tanh(\lambda_{n_t}^c/2)) \\ &= \tanh\left(\frac{\lambda_{n_t}^c}{2}\right). \end{aligned} \quad (3.19)$$

This threshold is depicted in Fig. 3.3. We find $\tilde{b}_{n_t} \in [-1, +1]$, and hence the normalization is naturally achieved.

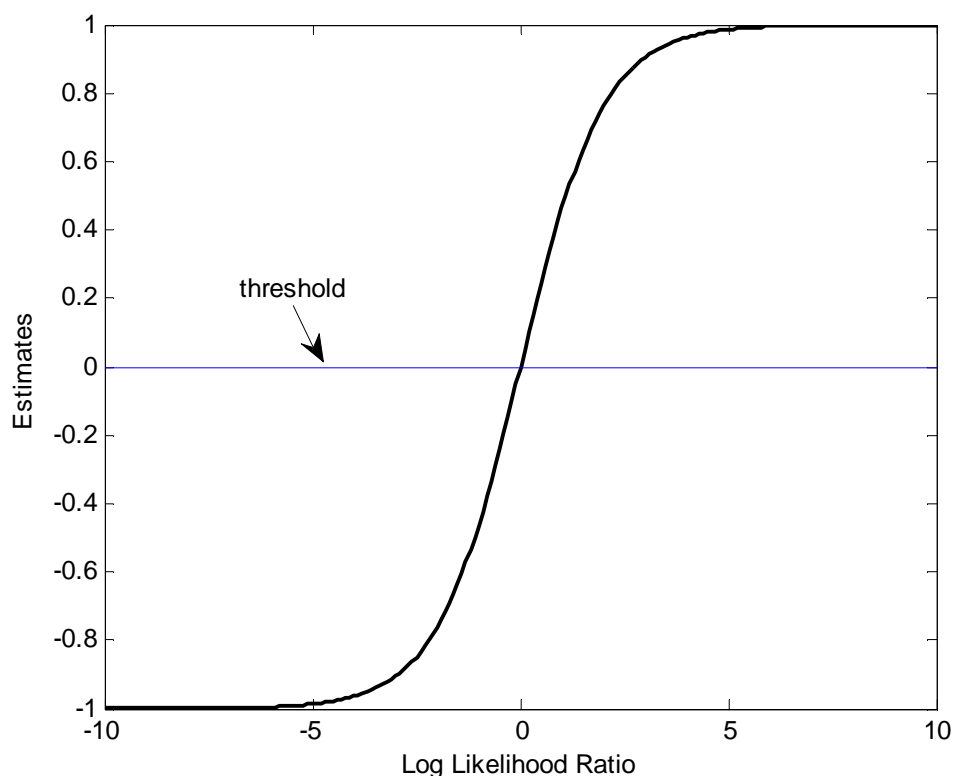


Figure 3.3 Threshold used to convert LLR to soft estimate

3.4.1 Iterative PIC Receiver

The outline of the matched filter PIC multiuser receiver is shown in Fig. 3.4. First the matched filter receiver introduced above is employed to combine the received signal. After converting the detection output to a soft value, the LLRs are fed to the SISO decoder. The SISO decoder can yield the LLR of both the information bits and the parity bits. Then the LLR values are converted to the normalized soft estimates employing the threshold given in Fig. 3.3, and finally are used to reconstruct the MAI between users. The first stage of the detection is then complete, and in later iterations a different structure is adopted.

The essence of the interference reconstruction is to repeat what happened in the channel and at the front end of the receiver. The data estimates are regarded as the original data transmitted from the users. If the data estimates are accurate enough, the MAI can also be reproduced correctly. Of course, nothing can be done to reconstruct the noise because it is completely random. After the MAI is subtracted from the matched filter output, it is supposed that the refreshed signal of PIC output has been improved. Then

after feeding it into the LLR calculator, the output is inputted to the SISO decoder again. The better the signal source provided to the decoder, the more accurate the decoded data.

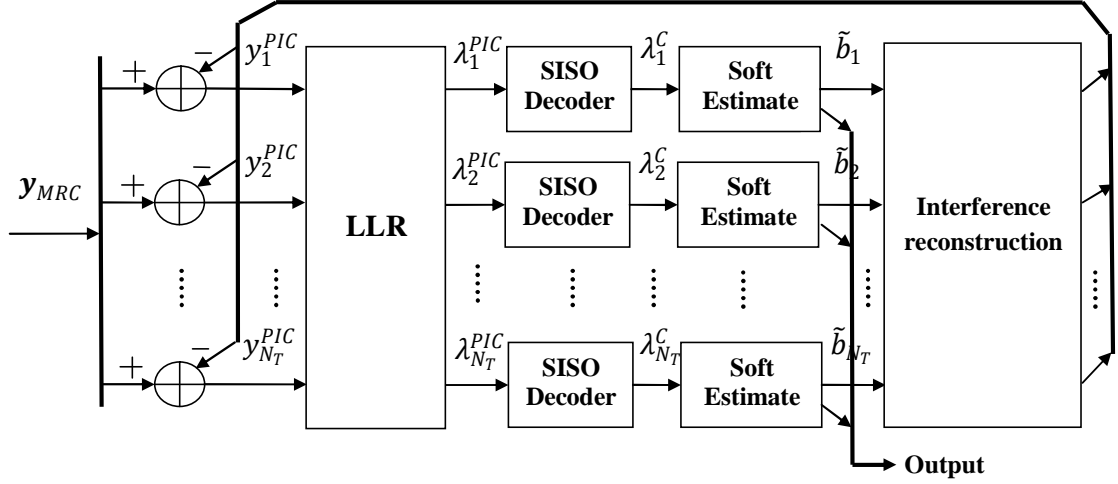


Figure 3.4 Structure diagram of the iterative PIC receiver

Then the improved decoder outputs will be converted to more accurate data estimates that can be used to yield a more accurate interference construction. Hence it is reasonable to believe that the receiver will improve continuously with increasing number of iterations. The components included in the first stage of iterative reception have been introduced: matched filtering, hard to soft value conversion and SISO decoding. After the output of the SISO decoder, the LLR of the data are converted to their soft estimates, and will be used to reconstruct and cancel the interference. The output of PIC detection can be expressed as:

$$\mathbf{y}_{PIC} = \mathbf{y}_{MRC} - (\mathbf{R}_{AWGN} - \text{diag}(\mathbf{R}_{AWGN}))\tilde{\mathbf{b}}, \quad (3.20)$$

$$\text{diag}(\mathbf{R}_{AWGN}) = \begin{bmatrix} a_{11} & 0 & \cdots & 0 \\ 0 & a_{22} & \cdots & 0 \\ \vdots & \vdots & \ddots & \vdots \\ 0 & 0 & \cdots & a_{N_T N_T} \end{bmatrix}, \quad (3.21)$$

$$\tilde{\mathbf{b}} = [\tilde{b}_1, \tilde{b}_2, \dots, \tilde{b}_{N_T}]^T, \quad (3.22)$$

where a_{ii} is constant value.

In Table 3.1, the computational complexity of the iterative receiver in AWGN channel is estimated. This is a rough estimation, and the complexity in practice depends on different communications scenarios.

The computation complexity of the iterative PIC receiver is defined as the required number of operations for the signal processing (the number of multipliers) in the detector per data frame and per iteration. For each received antenna, matched filter requires $N_T L$ multipliers for the algorithm, which leads to the total $N_T N_R L$ multipliers for the whole receiver. At the interference cancellation part, $N_T^2 N_R$ multipliers are required for the calculation of correlation matrix, and $N_T^2 L$ multipliers are required for the PIC detection. The PIC detection needs repeat for every iteration.

Table 3.1: Complexities of Iterative PIC Receiver in AWGN channel

Matched Filter	$O(N_T N_R L)$
Calculation of Correlation Matrix	$O(N_T^2 N_R)$
PIC Detection	$O(N_T^2 L)$ per iteration

L = length of data frame, N_T = number of transmit antennas,
 N_R = number of receiver antennas

3.4.2 Performance of Iterative PIC Receiver in AWGN Channels

In this section, the performance of joint the matched filter based PIC detection and decoding approach is illustrated by some simulation examples. An uplink MIMO system is under investigation. All users are assumed to employ 1024-bit, 1/2 code rate with generator [5 7], and BPSK modulation.

Fig. 3.5, 3.6 and 3.7 show the bit error rate (BER) performances of the iterative PIC receiver for two users, three users and four users, where the number of receivers is the same as the total number of transmitters.

The results show that the iterative PIC receiver can work very well for the underloaded system. As the number of users increases, the receiver needs more numbers of iterations to converge. As the figures shown, two users only need two iterations, three users need four iterations, and four users need six iterations. The perfect PIC curve is obtained by using the original data as the estimated data for cancellation. We can see that after several iterations, the BER performance of iterative PIC receiver is very close to that of perfect PIC for the underloaded system.

Fig. 3.8 shows the BER performance of the overloaded system with two users and one receiver. We can see that after eight iterations, there is still an error floor. It seems that the iterative PIC receiver cannot work for the overloaded system. However, the black curve shows that if the PIC can provide a perfect interference cancellation, this receiver can achieve an ideal performance. Fig. 3.9 shows that if we set the two users with different transmit power amplitudes, such as 1 and 0.5, the receiver also can converge well.

For BPSK, the transmitted signal is '+1' and '-1' for the two user system. With the equal power, after the AWGN channel, the received signal will be '-2', '0' and '+2', added with noise. The receiver cannot work well, the main reason for which is that nearly half the values are '0'.

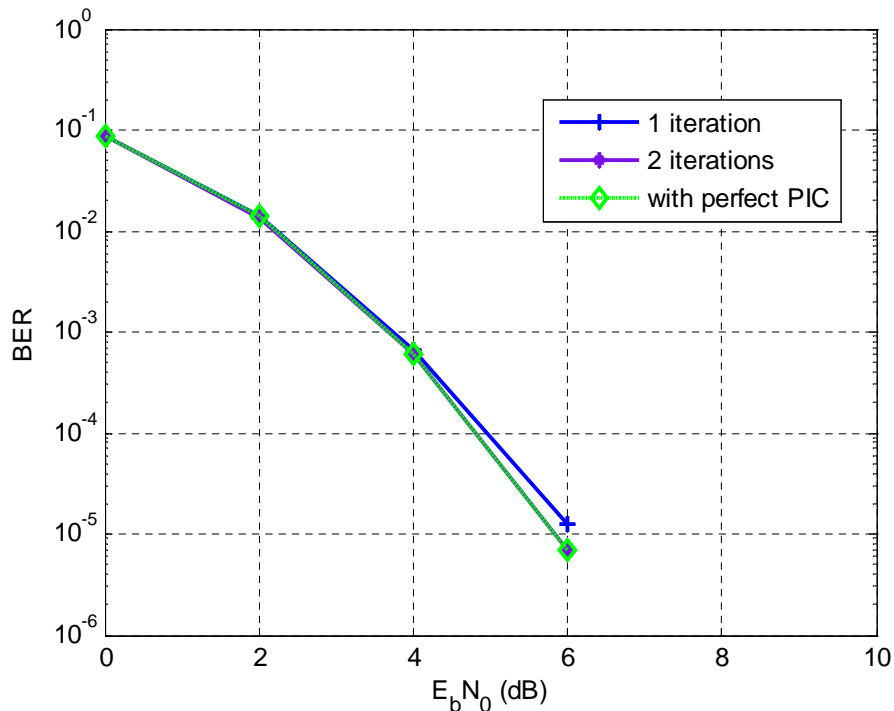


Figure 3.5 BER performance of iterative PIC receiver for the two user (one transmitter for each user) two receiver system in AWGN channel

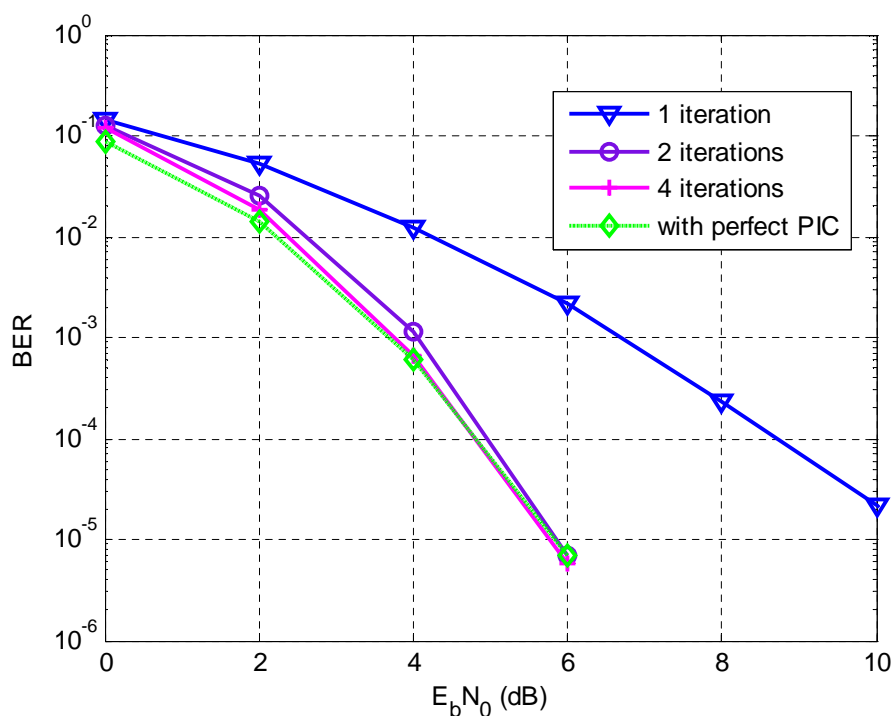


Figure 3.6 BER performance of iterative PIC receiver for the three user (one transmitter for each user) three receiver system in AWGN channel

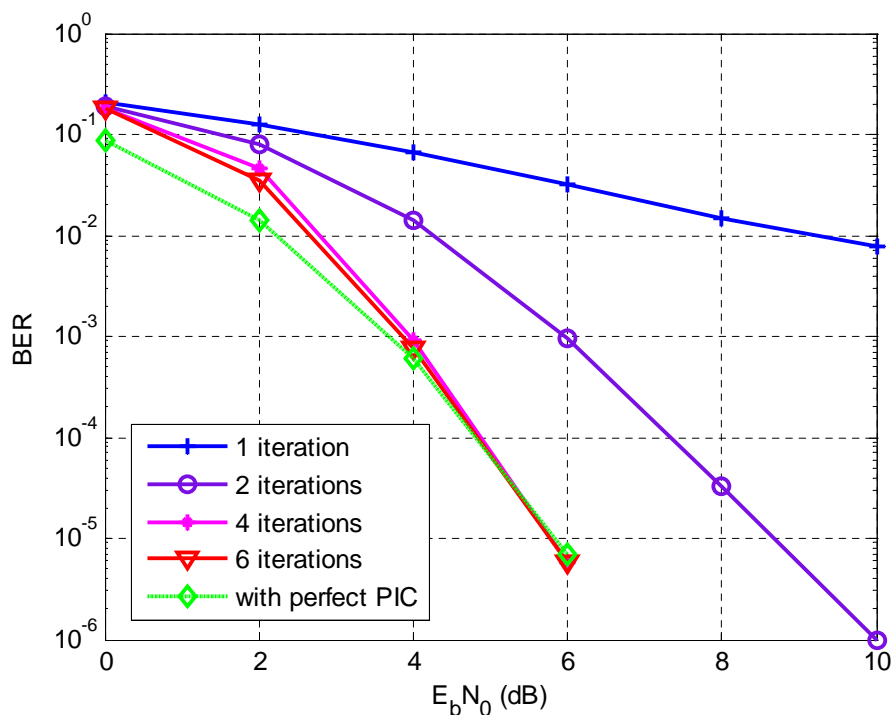


Figure 3.7 BER performance of iterative PIC receiver for the four user (one transmitter for each user) four receiver system in AWGN channel

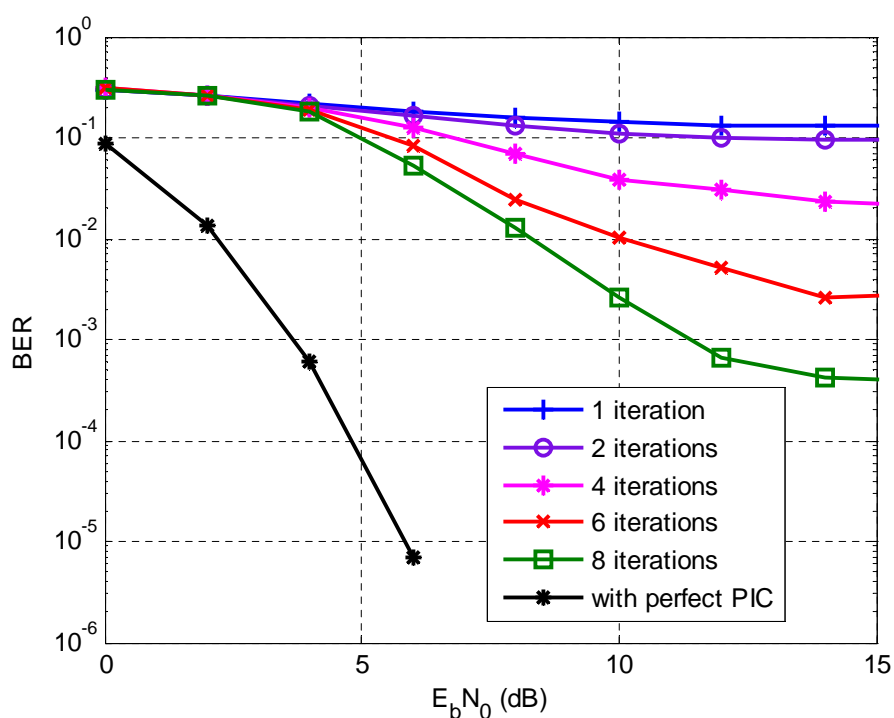


Figure 3.8 BER performance of iterative PIC receiver for the two user (one transmitter for each user) one receiver system in AWGN channel

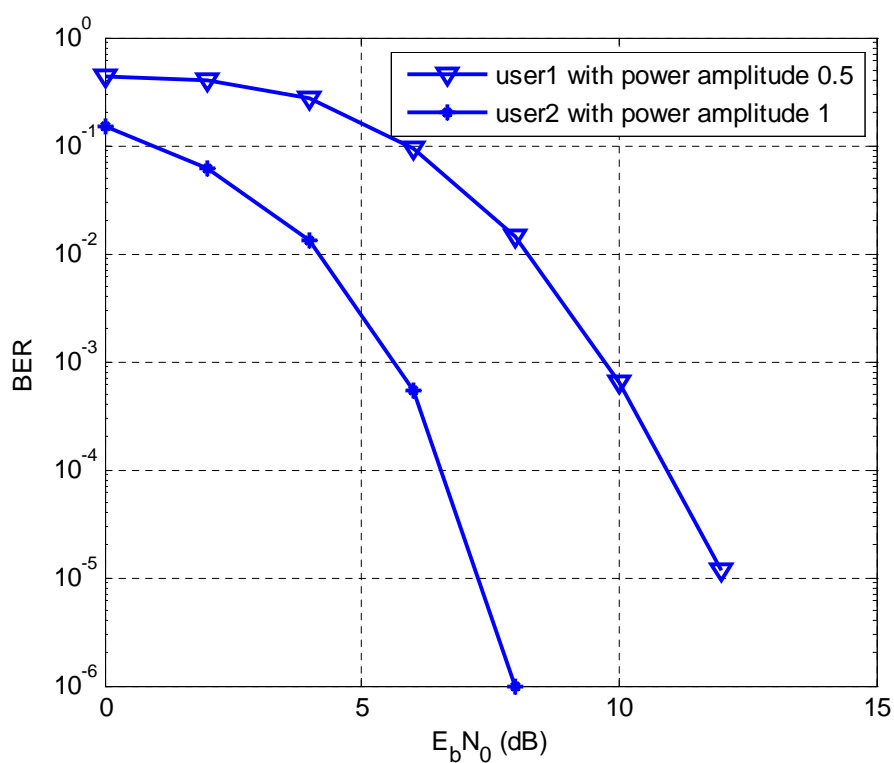


Figure 3.9 BER performance of iterative PIC receiver for the two user (one transmitter for each user) one receiver system in AWGN channel with unequal power (1, 0.5)

3.5 Multiuser Receiver for Flat Fading Channels

In the previous section, the basic principle of the Turbo multiuser receiver with a simple AWGN channel model has been introduced. The simulation results show that the iterative PIC receiver cannot work for the overloaded system, due to the zeros caused by the equal power. Now the receiver is modified for the flat fading channel to see if the receiver can distinguish the signals from the fading channel.

In wireless communications, fading is the variation of the attenuation affecting a signal over certain propagation media, which may vary with time, geographical position or radio frequency, and is often modelled as a random process. For wireless systems, fading may either be due to multipath propagation, referred to as multipath induced fading, or due to shadowing from obstacles affecting the wave propagation, referred to as shadow fading.

In this section, a frequency-flat fading channel with Rayleigh distribution is considered. This model describes the wireless channel without the presence of the line of sight, and assumes that signal components through multiple paths reach the receiver at the same time, with no relative delay between paths. The well-know block fading channel model is used [96]. This is a widely-used simplification of time-varying model, and it assumes that the channel responses remain stationary for the duration of one block of channel symbols, and then take up a new uncorrelated set of random values for the next block. Correspondingly, L will also denote the length of a fading block.

In the Rayleigh fading model, the fading factor of the n_r -th receiver n_t -th transmitter (or m -th user) is a complex Gaussian random value:

$$h_{n_r n_t} = h_{n_r n_t}^{Re} + j h_{n_r n_t}^{Im}, \quad (3.23)$$

and the noise at the n_r -th receiver is

$$n_{n_r} = n_{n_r}^{Re} + j n_{n_r}^{Im}, \quad (3.24)$$

where $h_{n_r n_t}^{Re}$, $h_{n_r n_t}^{Im}$, $n_{n_r}^{Re}$, $n_{n_r}^{Im}$, are independent Gaussian variables.

Using Eq. (3.23), the received signal can be expressed as

$$\mathbf{r} = \mathbf{H}_{Bfading} \mathbf{s} + \mathbf{n}, \quad (3.25)$$

where the block fading channel matrix $\mathbf{H}_{Bfading}$ is

$$\mathbf{H}_{Bfading} = \begin{bmatrix} h_{11} & h_{12} & \cdots & h_{1N_T} \\ h_{21} & h_{22} & \cdots & h_{2N_T} \\ \vdots & \vdots & \ddots & \vdots \\ h_{N_R1} & h_{N_R2} & \cdots & h_{N_RN_T} \end{bmatrix}. \quad (3.26)$$

As shown in Fig. 3.2, after the matched filter, the received signal is

$$\mathbf{y}_{MRC} = \mathbf{R}_{Bfading} \mathbf{s} + \mathbf{W}, \quad (3.27)$$

where $\mathbf{R}_{Bfading}$ is the block fading channel covariance matrix.

As discussed above, after the decoding and interference cancellation, the PIC output is

$$\mathbf{y}_{PIC} = \mathbf{y}_{MRC} - \left(\mathbf{R}_{Bfading} - \text{diag}(\mathbf{R}_{Bfading}) \right) \hat{\mathbf{b}}. \quad (3.28)$$

3.5.1 Performance of Iterative PIC Receiver in Block Fading Channels

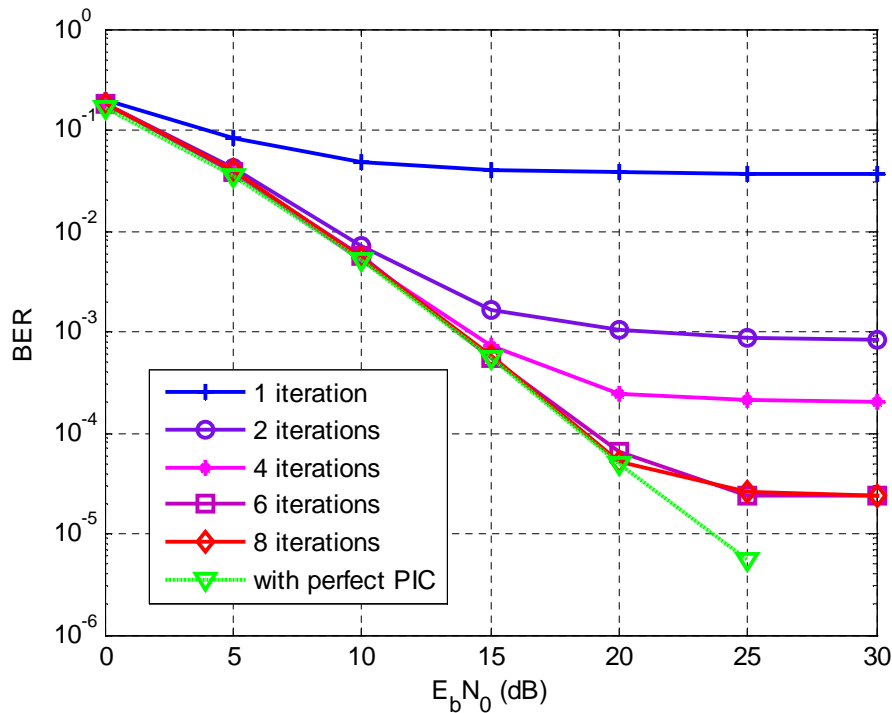


Figure 3.10 BER performance of iterative PIC receiver for the two user (one transmitter for each user) two receiver system in Rayleigh flat fading channel

In this section, the same system is considered, and the Rayleigh flat fading channel coefficients are generated randomly. Fig. 3.10 shows the BER performance of a two user two receiver system in a Rayleigh flat fading channel. After eight iterations, there is still an error floor at high SNR. Fig. 3.11 shows the case of a two user one receiver system in a Rayleigh flat fading channel. Although its BER performance also has an

error floor, after eight iterations, the BER performance is much closer to the performance with perfect PIC, compared to the system in AWGN channel. In this case, if we ignore the error floor, it is obvious that the system can work better in the fading channel.

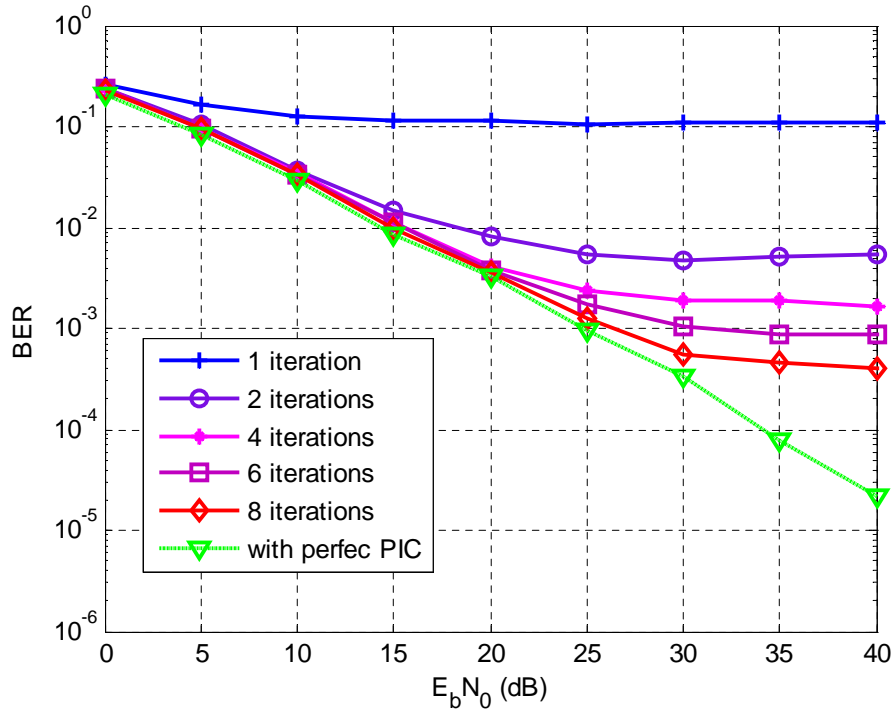


Figure 3.11 BER performance of iterative PIC receiver for the two user (one transmitter for each user) one receiver system in Rayleigh flat fading channel

3.6 Multiuser Receiver for Frequency Selective Channels

The flat fading channel model assumes that the components of one signal source through different paths reach the receiver simultaneously. However, in more practical channels, different paths will introduce distinct propagation delays. Thus the multipath signals are not aligned when they are received by the receiver. The received signal is actually a sum of shifted versions of the transmitted signal with different fading.

The multipath fading can be expressed using a delay line model, in which effect of the channel can be written as an impulse response. The *channel impulse response* (CIR) for the n_r -th receiver n_t -th user is given by

$$h_{n_r n_t}(t) = \sum_{d=0}^{D-1} h_{n_r n_t}[d] \delta(t - dT), \quad (3.29)$$

where $h_{n_r n_t}[d]$ is the complex fading factor of the n_r th receiver n_t th user's d th delay tap, and T is the symbol interval. In real life, the interval between each delay is completely random value. However, for simplicity, we assume the delay interval is integer multiple of symbol interval, which is the simplest case. $h_{n_r n_t}[d]$ is generated following the Rayleigh distribution, or $\text{Re}(h_{n_r n_t}[d]) \sim \mathcal{N}(0, \overline{\sigma[d]^2}/2)$, $\text{Im}(h_{n_r n_t}[d]) \sim \mathcal{N}(0, \overline{\sigma[d]^2}/2)$, where $\overline{\sigma[d]^2}$ is the variance of the d th delay tap amplitude, and satisfying the normalization:

$$\sum_{d=0}^{D-1} \overline{\sigma[d]^2} = 1. \quad (3.30)$$

The faded signal should be a convolution of the CIR and the transmitted signal.

As discussed in chapter 2, a frequency selective fading channel can be divided into a set of frequency flat fading channels by using OFDM, which can help to take advantage of frequency diversity and cope with severe channel conditions. Due to the robustness to ICI and ISI and its superiority to cope with the frequency selective fading channel, we employ OFDM for the frequency selective fading channel. The system is shown in Fig. 3.12 and Fig. 3.13.

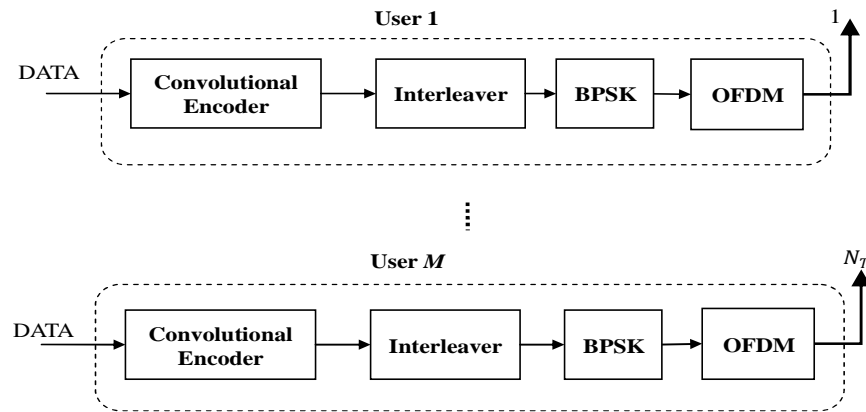


Figure 3.12 The transmitter structure of overloaded multiuser MIMO OFDM system

The data of each user is first encoded by the convolutional encoder, and then passed through the interleaver. After BPSK and OFDM modulation, the data is finally transmitted.

For one data frame, the transmitted data are grouped into N OFDM symbols, and each symbol has K subcarriers. For the k th subcarrier, the received signal can be expressed as

$$\mathbf{r}_k = \mathbf{H}_k \mathbf{s}_k + \mathbf{n}_k, \quad (3.31)$$

where $k = 1 \dots K$, $\mathbf{s}_k = [s_1^k, s_2^k, \dots, s_{N_T}^k]^T$ is a column vector containing the transmitted symbols, and the AWGN vector with zero mean and variance σ^2 is given by $\mathbf{n}_k = [n_1^k, n_2^k, \dots, n_{N_R}^k]^T$. The equivalent frequency domain channel submatrix \mathbf{H}_k can be expressed as

$$\mathbf{H}_k = \begin{bmatrix} h_{11} & h_{12} & \dots & h_{1N_T} \\ h_{21} & h_{22} & \dots & h_{2N_T} \\ \vdots & \vdots & \ddots & \vdots \\ h_{N_R1} & h_{N_R2} & \dots & h_{N_RN_T} \end{bmatrix}. \quad (3.32)$$

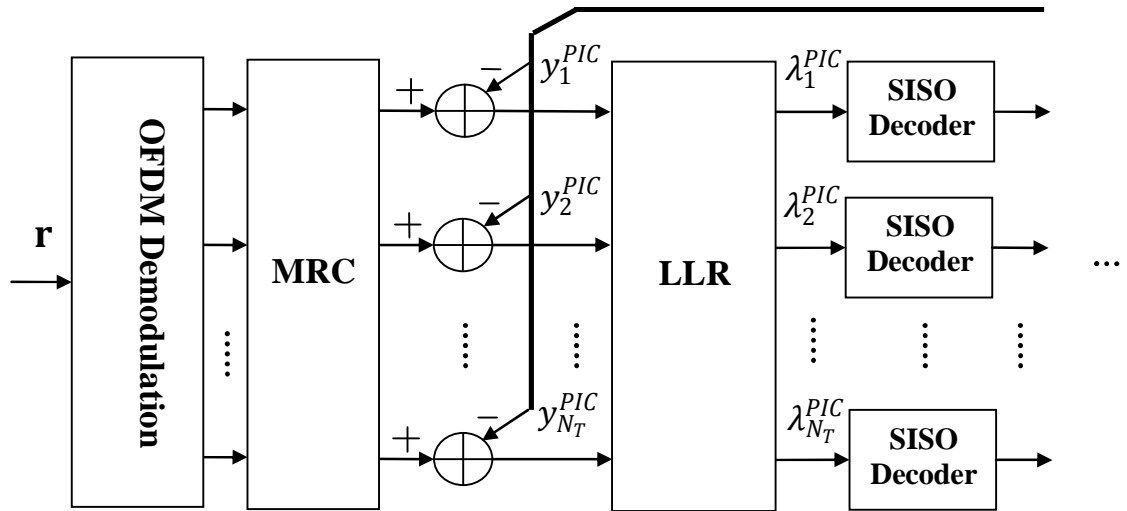


Figure 3.13 The receiver structure of overloaded multiuser MIMO OFDM system

As the Fig. 3.13 shown, after the matched filter, the received signal is

$$\mathbf{y}_{k,MRC} = \mathbf{R}_{k,Sfading} \mathbf{s}_k + \mathbf{W}_k, \quad (3.33)$$

where $\mathbf{R}_{k,Sfading}$ is the equivalent frequency domain channel covariance matrix for k th subcarrier.

As discussed above, after the decoding and interference cancelling, the PIC output is

$$\mathbf{y}_{k,PIC} = \mathbf{y}_{k,MRC} - \left(\mathbf{R}_{k,Sfading} - \text{diag}(\mathbf{R}_{k,Bfading}) \right) \tilde{\mathbf{b}}_k. \quad (3.34)$$

3.6.1 Performance of Iterative PIC Receiver in Frequency Selective Fading Channels

Fig. 3.14 and 3.15 show the BER performance of iterative PIC receiver in frequency selective fading when the numbers of receivers are two and one for the two user system. The simulation elements are almost the same as above, each user employs 1024-bit, $1/2$ code rate with generator [5 7], BPSK and 32 subcarriers for OFDM modulation. A Rayleigh channel is assumed with uncorrelated fading between all transmit and receive antennas, with a memory of one symbol period, described by a 2-tap delay line model. We assume the first tap is without any loss and fixed, and the second tap is random variable whose average power is less than the first tap's (here, the channel coefficients of two taps is [1 0.7]). The channel coefficients of CIRs for the users are generated randomly and independently. A block fading channel model is used.

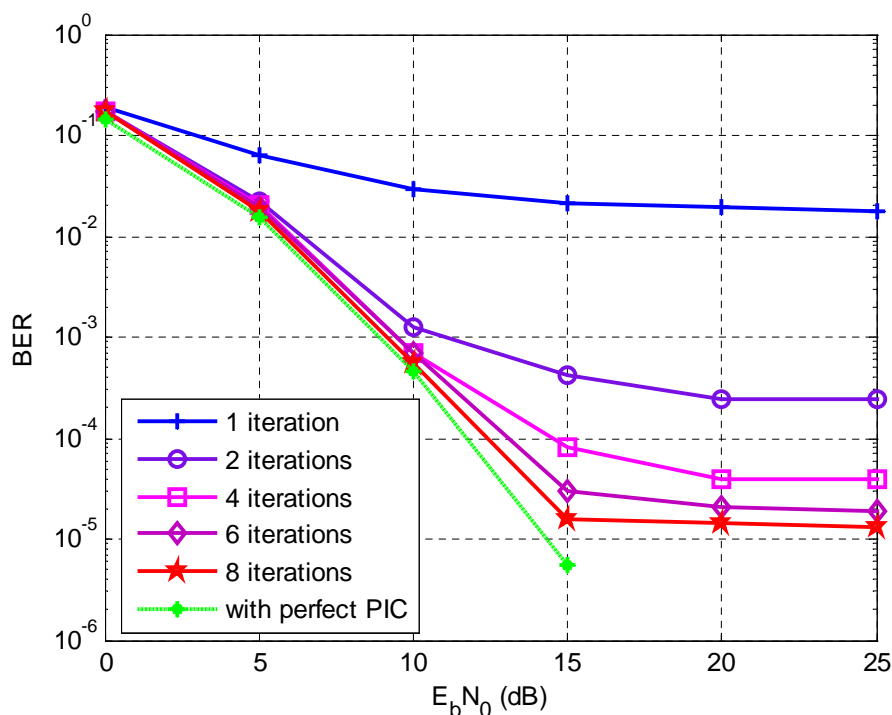


Figure 3.14 BER performance of iterative PIC receiver for the two user (one transmitter for each user) two receiver system in frequency selective fading channel

From Fig. 3.14, we can see that after eight iterations, the BER performance of the iterative PIC receiver is close to that with perfect PIC. However, it still has an error floor. Fig. 3.15 shows that the BER performances are very poor when the system is overloaded. However, like Fig. 3.11, after eight iterations, the BER performance is

closer to that with perfect PIC, which means the iterative PIC receiver can obtain some channel gain from the fading channel.

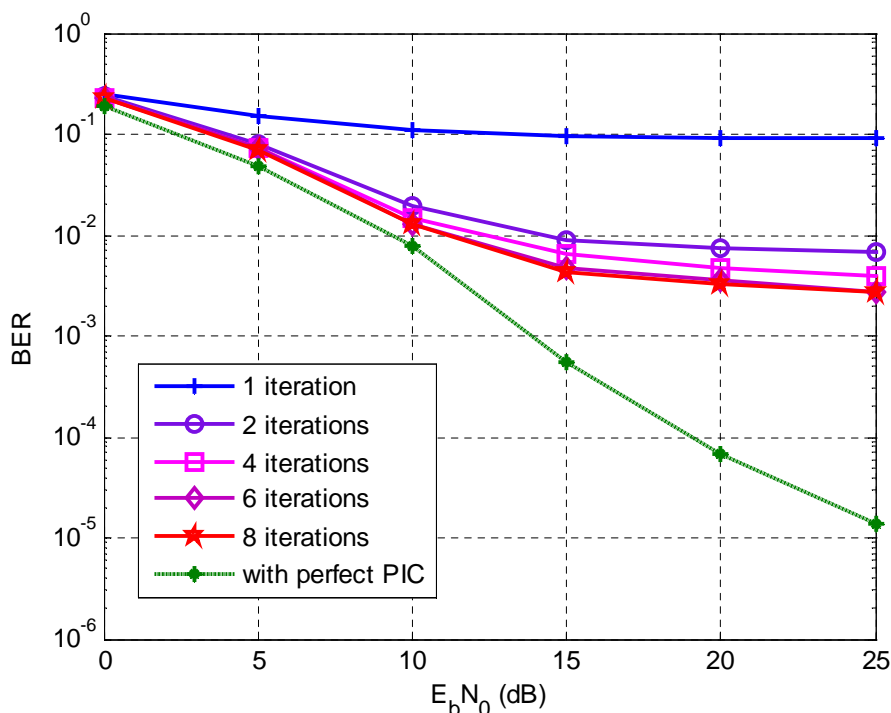


Figure 3.15 BER performance of iterative PIC receiver for the two user (one transmitter for each user) one receiver OFDM system in frequency selective fading channel

3.7 Iterative Interference Cancellation (IIC) Receiver

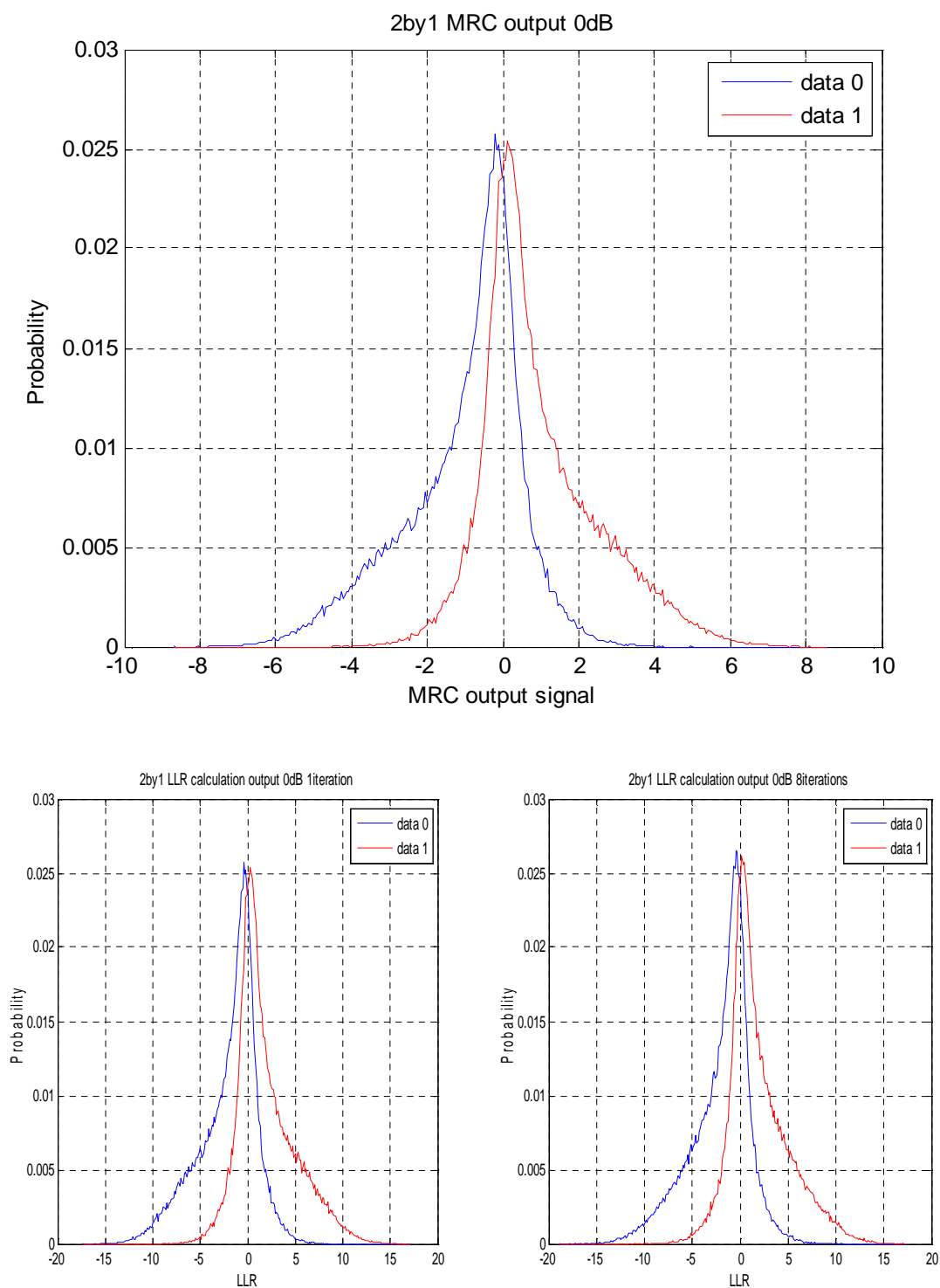
In sections 3.4, 3.5, and 3.6, we discussed the performance of iterative PIC receiver in AWGN, Rayleigh block fading, and frequency selective fading channel. From the simulation results, we can see that the receiver has poor performance for the overloaded system, and an error floor in the BER performance has appeared.

Why is there an error floor? For some deeply fading channels, the interference, whose power is much stronger than that of the desired signal and cannot perfectly be cancelled, will cause errors to remain in the detected signal no matter how high the SNR is. The case where BER cannot be reduced with a larger SNR is known as an error floor.

The problem occurs before the decoding. For the decoder, we assume that the inputs have a Gaussian-like distribution, but what if they do not?

Fig. 3.16 shows the PDF of the MRC outputs and LLR outputs for the two user one receiver system in a frequency selective fading channel. When SNR is 0dB, the received

signals are affected by the interference and noise, after the MRC, the PDFs of data ‘0’ and data ‘1’ are heavily overlapped. We can see that after the LLR calculation, the situation is not improved, whether the joint detecting and decoding run through one iteration or eight iterations.



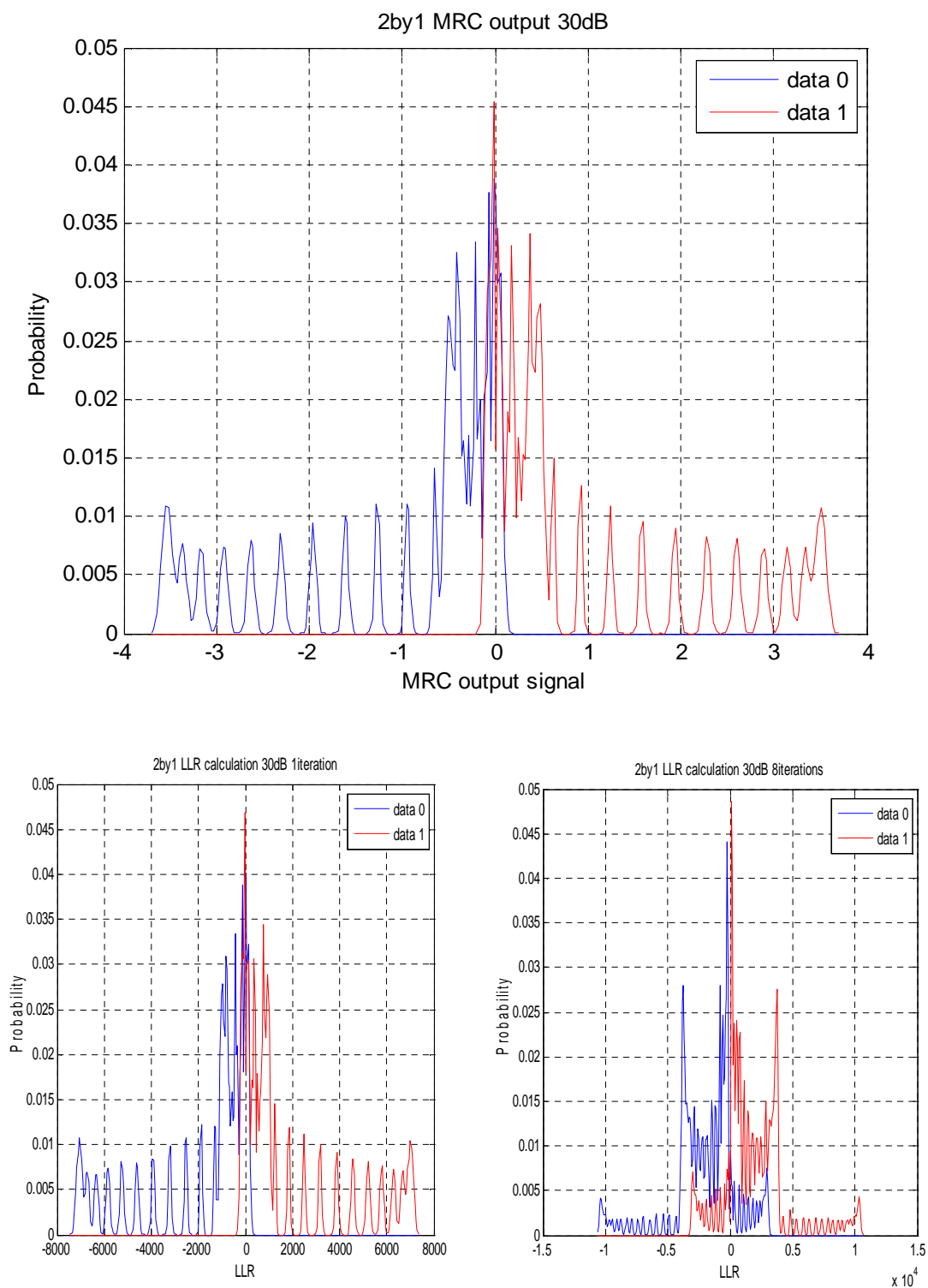


Figure 3.16 PDFs of the MRC output and LLR output for the two user one receiver system in frequency selective fading channel (2 taps delay model)

As the SNR increases, the interference gradually becomes the main effect. The figures at 30dB show that after eight iterations, the output of LLR calculation becomes even worse.

The inputs of the decoder are the outputs of the MRC multiplied by a factor, as shown in Eq. (3.13). From the figures, we can see that both the PDFs of the MRC output and the decoder input are far from the Gaussian distribution whether the SNR is high or not. The main problem is the LLR calculation cannot effectively distinguish and process the signals: enlarge the reliable values and reduce the unreliable values. When the data is overlapped too much, the decoder takes the wrong information, and makes an error in judgment. Therefore, the detector suffers an obvious error floor in its BER performance.

3.7.1 LLR Scaling Factor

For the SISO decoder, a valid LLR should be close to the Gaussian distribution. According to [76], the mean and variance of a valid LLR must fulfil

$$\mu_{LLR} = \sigma_{LLR}^2/2, \quad (3.35)$$

where μ_{LLR} and σ_{LLR}^2 are the mean value and variance of the LLRs, which are the soft decoder inputs. In order to satisfy Eq. (3.35), a new scaling factor β is applied to the MRC output, we call it LLR converter,

$$\mu_{LLR} = \mu_{MRC}\beta, \quad (3.36)$$

$$\sigma_{LLR}^2 = \sigma_{MRC}^2\beta^2, \quad (3.37)$$

where μ_{MRC} and σ_{MRC}^2 are the mean and variance of MRC output respectively. Combining Eq. (3.35), (3.36), and (3.37), we can obtain

$$\beta = \frac{2\mu_{MRC}}{\sigma_{MRC}^2}. \quad (3.38)$$

For BPSK, the transmitted signal $\mathbf{s}_k = \pm 1$. From Eq. (3.33), the mean value of MRC output μ_{MRC} is influenced by the channel covariance matrix $\mathbf{R}_{k,Sfading}$, and the variance σ_{MRC}^2 is the sum of the variances from the channel and noise.

The channel covariance matrix for the k th subcarrier can be written as

$$\mathbf{R}_{k,Sfading} = \mathbf{H}_k^H \mathbf{H}_k = \begin{bmatrix} R_{11} & \cdots & R_{1N_T} \\ \vdots & \ddots & \vdots \\ R_{N_T1} & \cdots & R_{N_TN_T} \end{bmatrix}. \quad (3.39)$$

From Eq. (3.33) and (3.39), since $\mathbf{s}_k = \pm 1$, it is obvious that the mean value

$$\mu_{MRC,k} = [\text{diag}(\mathbf{R}_{k,Sfading})]^T$$

$$= [R_{11}, R_{22}, \dots, R_{N_T N_T}]^T. \quad (3.40)$$

Denote

$$\mathbf{G}_k = \mathbf{R}_{k, \text{sfading}} - \text{diag}(\text{diag}(\mathbf{R}_{k, \text{sfading}}))$$

$$= \begin{bmatrix} 0 & \mathbf{g}_{12} & \cdots & \mathbf{g}_{1N_T} \\ \mathbf{g}_{21} & 0 & \cdots & \mathbf{g}_{2N_T} \\ \vdots & \vdots & \ddots & \vdots \\ \mathbf{g}_{N_T1} & \mathbf{g}_{N_T2} & \cdots & 0 \end{bmatrix}, \quad (3.41)$$

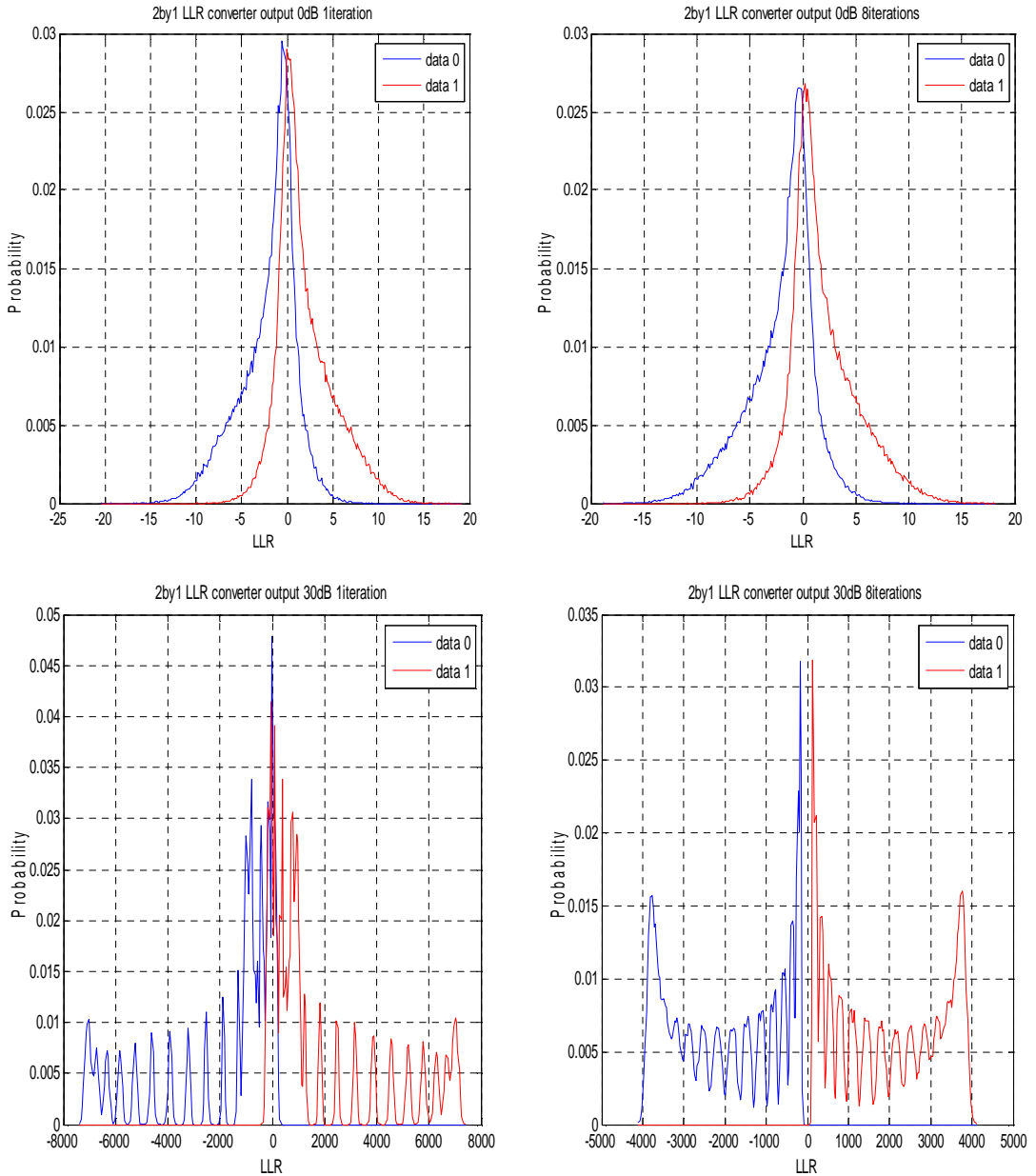


Figure 3.17 PDFs of the LLR converter output for the two user one receiver system in frequency selective fading channel (2 taps delay model)

the variance

$$\sigma_{MRC,k,i}^2 = \sum_{j=1}^{N_T} \text{Re}\{g_{ij}^k\}^2 + \sum_{l=1}^{N_R} \text{Re}\{h_{li}^k\}^2 \cdot \sigma_n^2, \quad (3.42)$$

of which the first term is due to interference and the latter is from noise, $i = 1 \dots N_T$, and σ_n^2 is the variance of AWGN, g_{ij}^k and h_{li}^k are the element of \mathbf{G}_k and \mathbf{H}_k respectively.

Assuming everything works well, as the number of iterations increases, the interference will largely be cancelled. So after several iterations, the received signal is only affected by the noise, and the variance in Eq. (3.42) now can be expressed as

$$\sigma_{MRC,k,i}^2 = \sum_{l=1}^{N_R} \text{Re}\{h_{li}^k\}^2 \cdot \sigma_n^2. \quad (3.43)$$

Fig. 3.17 shows the PDFs of LLR converter output, the channel used here is the same as Fig. 3.16. At 30dB, after eight iterations, the LLR converter can totally separate the data ‘0’ and data ‘1’. Compared to Eq. (3.33), the new proposed scaling factor (Eq. (3.38), (3.40), (3.42), and (3.43)) is clearly more appropriate from PDF point of view. Using this scaling factor can result more reliable soft values for the SISO decoder: the reliable soft values will be enlarged by multiplying a large scaling factor, while the unreliable soft values will be reduced by multiplying a small one. This method has been published in [105].

3.7.2 Iterative Interference Cancellation MUD

Combining the above sections, we now build up an *iterative interference cancellation* (IIC) receiver. The MRC detector is first employed, which shows the reconstruction of the interference for each user, and its use for cancelling this estimated interference in the next iteration. (We also refer to the MRC as “RAKE” detection, by analogy in the spatial domain with the operation in the time domain of the Rake detector in a CDMA system). A LLR converter is used after the MRC detector, which rescales the MRC output in a proper way. The outputs of LLR converter are decoded by the SISO decoders, and their outputs, the LLR values, are converted to the soft estimates.

Next the data estimates are fed to the PIC detector. The PIC reconstructs the interference with the correlation matrix and the data estimates, and then subtracts it from the MRC receiver output. After the PIC, the improved signals are passed to the LLR converter again, and more reliable LLRs are obtained. After the SISO decoders, the new data estimates are generated, and used to replace the old ones, the interference can be updated in the reconstruction. It is reasonable to expect that the wanted data will improve continuously with increasing number of iterations.

The receiver structure is shown in Fig. 3.18, we assume the CIRs are known to the receiver perfectly. In order to improve the IIC performance from the very beginning, we find the user data stream giving the largest soft *estimate to interference ratio* (EIR):

$$EIR_i = \frac{\sum_{j=1}^{N_K} llr_{ij}}{\max(\mathbf{I}_{MAX,i})}, \quad (3.44)$$

where llr_{ij} is the (i, j) -th element of LLR converter output matrix, and the maximum estimate interference

$$\mathbf{I}_{MAX,i}^k = \max_{s_i^k = \pm 1} \left\{ \sum_{i,j} g_{ij}^k s_i^k \right\} = \sum_{j=1}^{N_T} |g_{ij}^k|, \quad (3.45)$$

where g_{ij}^k is the (i, j) th element of \mathbf{G}_k , and $i = 1 \dots N_T$. Using the EIR, we choose the data stream only to reconstruct the interference, which is called the SIC-based approach.

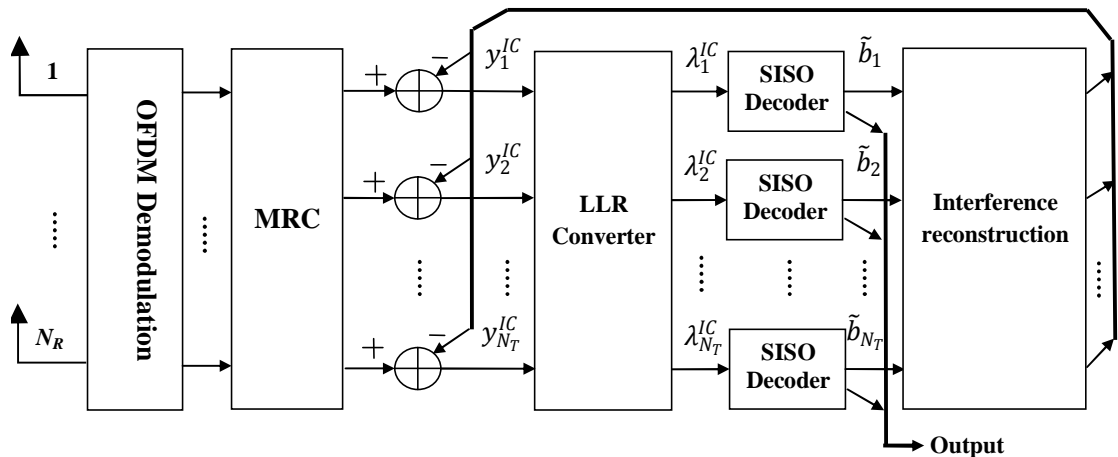


Figure 3.18 The structure of IIC-MUD scheme

The resulting estimate of MAI can then be subtracted from the MRC output

$$\mathbf{y}_{IC,k} = \mathbf{y}_{MRC,k} - (\mathbf{R}_k - \text{diag}(\mathbf{R}_k))\tilde{\mathbf{b}}_k. \quad (3.46)$$

Note that this SIC-based approach is used only on the first iteration. For subsequent iterations, the improved signals $\mathbf{y}_{IC,k}$ are passed to the LLR converter again. Then feeding the rescaled LLR values to the decoders, new soft estimates can be obtained. Now full PIC is used to reconstruct the interference, in which the interference estimate is based on the decoded data streams from all users.

As the iteration number increases, the interference is cancelled substantially. After several iterations (for simulation, we simply choose half of the total number of iterations), the scaling factor is updated due to the change of variance, so that the LLR values become more and more reliable. With the better data estimates, the PIC can be continuously improved.

Table 3.2: Complexities of IIC Receiver in frequency selective fading channel

MRC Receiver	$O(N_T N_R N K)$ per frame
CIR Correlation Matrix	$O(N_T^2 N_R K)$ per frame
LLR Converter for first half iterations	$O(N_T^3 K) + O(N_R^2 N_T K) + O(N_T K)$ per frame
LLR converter for last half iterations	$O(N_R^2 N_T K) + O(N_T K)$ per frame
SIC Detection	$O(N_T N K)$ per frame
PIC Detection	$O(N_T^2 N K)$ per frame per iteration, except first iteration

K = number of OFDM subcarriers, N = number of OFDM symbols,
 N_T = number of transmit antennas, N_R = number of receiver antennas

In Table 3.2, the computational complexities of the IIC-MUD receiver are estimated. This is a rough estimation and the complexity in practice depends on different communications scenarios. The computation complexity of the IIC receiver is defined as the required number of operations for the signal processing (the number of multipliers) in the detector per data frame and per iteration.

For $N_R \times N_T$ system, the MRC receiver requires $N_T N_R N K$ multipliers for each frame. For the LLR converter and interference reconstruction, in order to calculate the channel

correlation matrix, $N_T^2 N_R K$ multipliers are needed for each frame. We assume the channel is flat during a data frame, so the channel correlation matrix only needs to be calculated once.

The scaling factor for LLR converter, needs to be calculated twice for each frame. First, the effect of both the interference and noise is considered, so it requires $N_T^3 K + N_R^2 N_T K + N_T K$ multipliers. For the second, only the effect of noise is considered, which leads to $N_R^2 N_T K + N_T K$ multipliers. The SIC detection has $N_T N K$ multipliers, need to be calculated only once for each frame. Finally, the PIC detection is used from the second iterations to the end, which requires $N_T^2 N K$ multipliers per iteration per frame.

3.7.3 Iterative MAP MUD

Whether the system is underloaded or overloaded, MAP is the optimal solution. In this section, we discuss the iterative MAP receiver for performance comparison. The receiver structure is shown in Fig. 3.19.

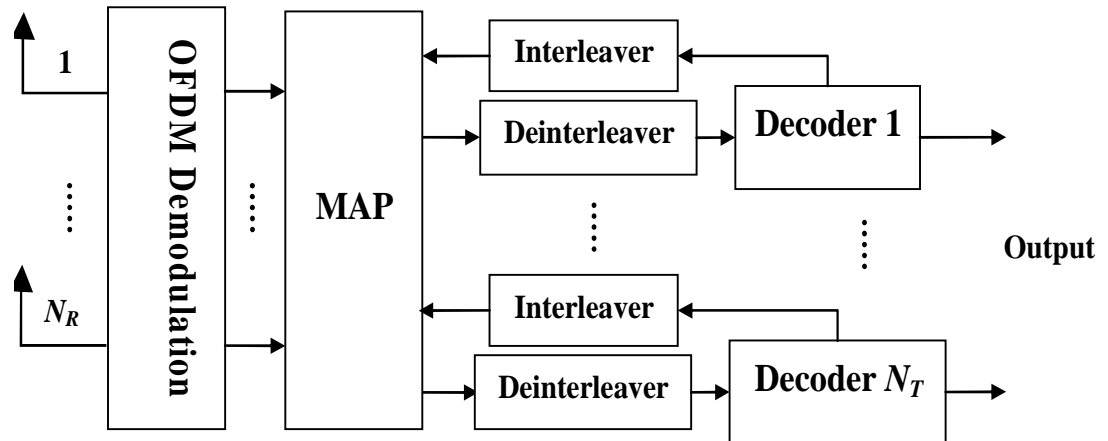


Figure 3.19 Structure of iterative MAP receiver

As mentioned in chapter 2, the computational complexity of MAP detector grows exponentially as the number of users increases. So here, we will only show the two user case, which has four combinations of all the possible transmit vector symbols, as shown in Fig. 3.20.

$$\Omega = [11 \ 10 \ 00 \ 01]. \quad (3.47)$$

The probability for each combination is

$$P_{\Omega} = \exp\left(\frac{-d_{\Omega}^2}{2\sigma^2}\right), \quad (3.48)$$

where σ^2 is the variance of AWGN, d_{Ω}^2 is the Euclidean distance

$$d_{\Omega}^2 = |\mathbf{r}_k - \mathbf{H}_k \tilde{\mathbf{s}}_k|^2, \quad (3.49)$$

and $\tilde{\mathbf{s}}_k$ is one combination of Ω . We assume the CIRs are known to the receiver perfectly.

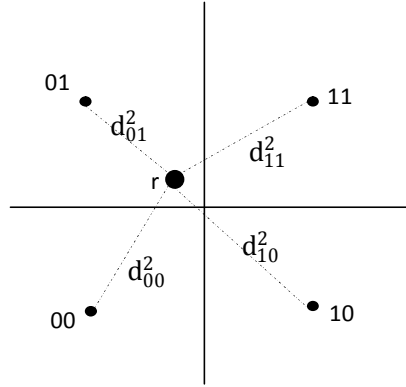


Figure 3.20 Four combinations of all the possible transmit vector symbols for the two user case. For hard decision, we only need to calculate four d_{Ω}^2 values, and then take the maximum one. For soft decision, the log-likelihood ratio (LLR) should be calculated. For bit 1:

$$L_1 = \log\left(\frac{P(b_1 = 1|r)}{P(b_1 = 0|r)}\right). \quad (3.50)$$

Using Bayes' theorem,

$$P(b_1 = 1|r) = \frac{P(r|b_1 = 1)P(b_1 = 1)}{P(r)}, \quad (3.51)$$

where $P(r)$ denotes the PDF of received signal, and

$$P(r|b_1 = 1) = P(r|10)P(b_2 = 0) + P(r|11)P(b_2 = 1). \quad (3.52)$$

Combining Eq. (3.51) and (3.52), we can get

$$P(b_1 = 1|r) = \frac{P(b_1 = 1)}{P(r)} (P(r|10)P(b_2 = 0) + P(r|11)P(b_2 = 1)). \quad (3.53)$$

Similarly,

$$P(b_1 = 0|r) = \frac{P(b_1 = 0)}{P(r)} (P(r|00)P(b_2 = 0) + P(r|01)P(b_2 = 1)). \quad (3.54)$$

Using Eq. (3.53) and (3.54), Eq. (3.50) becomes

$$L_1 = \log\left(\frac{P(b_1 = 1)}{P(b_1 = 0)}\right) + \log\left(\frac{P(r|10)P(b_2 = 0) + P(r|11)P(b_2 = 1)}{P(r|00)P(b_2 = 0) + P(r|01)P(b_2 = 1)}\right), \quad (3.55)$$

where the first term is the a priori LLR L_{a1} of bit 1 which come from the decoder, and the second term is the extrinsic LLR L_{e1} of bit 1. Considering Eq. (3.48),

$$L_{e1} = \log\left(\frac{\exp\left(\frac{-d_{10}^2}{2\sigma^2}\right) + \exp\left(\frac{-d_{11}^2}{2\sigma^2}\right)\exp(L_{a2})}{\exp\left(\frac{-d_{00}^2}{2\sigma^2}\right) + \exp\left(\frac{-d_{01}^2}{2\sigma^2}\right)\exp(L_{a2})}\right), \quad (3.56)$$

where L_{a2} is the a priori LLR of bit 2,

$$L_{a2} = \log\left(\frac{P(b_2 = 1)}{P(b_2 = 0)}\right). \quad (3.57)$$

Using the simplification:

$$\log(e^a + e^b) = \max(a, b) + \log(1 + \exp(-|a - b|)), \quad (3.58)$$

Eq. (3.56) can be simplified as

$$L_{e1} = \max\left(\frac{-d_{10}^2}{2\sigma^2}, \frac{-d_{11}^2}{2\sigma^2} + L_{a2}\right) + \log\left(1 + \exp\left(-\left|\frac{-d_{11}^2}{2\sigma^2} + L_{a2} + \frac{d_{10}^2}{2\sigma^2}\right|\right)\right) \\ - \max\left(\frac{-d_{00}^2}{2\sigma^2}, \frac{-d_{01}^2}{2\sigma^2} + L_{a2}\right) - \log\left(1 + \exp\left(-\left|\frac{-d_{01}^2}{2\sigma^2} + L_{a2} + \frac{d_{00}^2}{2\sigma^2}\right|\right)\right). \quad (3.59)$$

For bit 2, the LLR can be easily obtained by doing the same calculation, where it also needs the a priori LLR L_{a1} of bit 1.

For the first iteration, we assume ‘1’ and ‘0’ are of equal probability, so both L_{a1} and L_{a2} are 0.5. In the following iterations, they are updated to the LLRs of each bit from the previous iteration.

This method can be extended to the four user case, which causes sixteen combinations at the receiver, where four bits need to be considered at the same time. It is obvious that this method becomes very complicated as the number of users increases. So for more users’ case, the optimal MUD cannot be implemented easily.

3.7.4 Performance Comparison between Iterative MAP MUD and IIC MUD

In order to compare the performance of the iterative interference cancellation multiuser detection (IIC-MUD), the performance of iterative MAP MUD is also given. Fig. 3.21 shows the BER performance of the overloaded OFDM system in frequency selective fading channel, which has two users and one receiver. A Rayleigh channel is assumed with uncorrelated fading between all transmit and receive antennas, with a memory of one symbol period, described by a 2-tap delay line model, where the second tap's average power is assumed to be weaker than the first. The channel coefficients of CIRs for the users are generated randomly and independently, and known by the receiver perfectly. A block fading channel model is used. Each user employs 1024-bit, 1/2 code rate with generator [5 7], BPSK and 32subcarrier for OFDM modulation, and CP length 6. The BERs plotted are averages over all users.

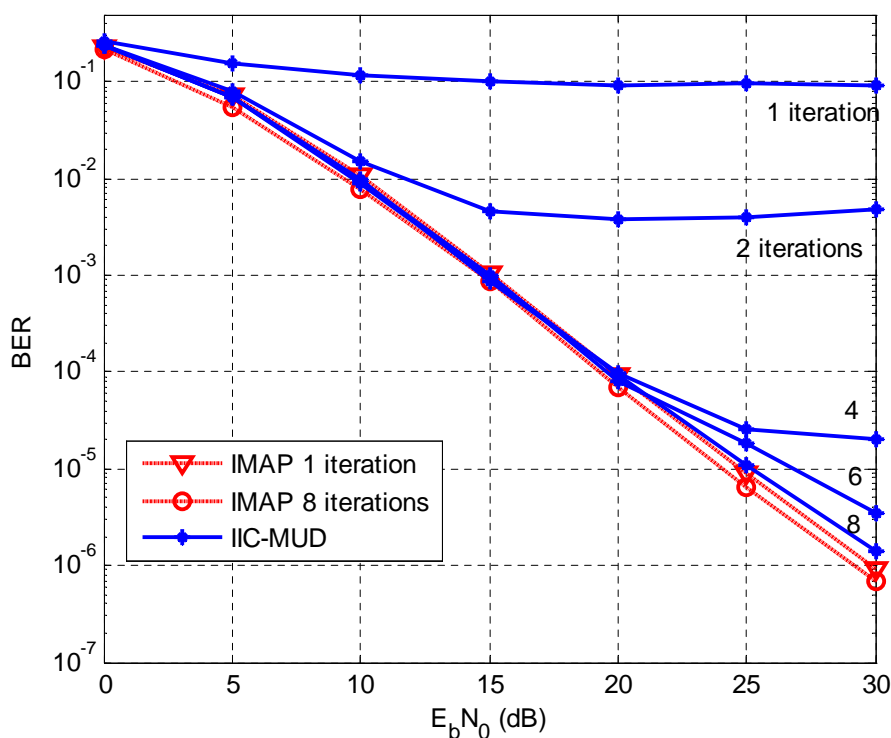


Figure 3.21 BER performance of IIC MUD for 2×1 OFDM system

Fig. 3.21 illustrates the BER performance of the IIC-MUD for different numbers of iterations. For comparison, the performances of the iterative MAP detector for one iteration and eight iterations are also given. We can see that the BER performance of IIC-MUD are converged after eight iterations, which is better than that of MAP with one

iteration and very close to that of MAP with eight iterations. The results suggest that the IIC detector can effectively detect the data by suppressing the MAI. It achieves a BER of 10^{-5} at a 25dB within eight iterations, only 1dB worse than that of MAP with eight iterations.

3.8 Performance of IIC MUD

Fig. 3.22 shows the BER performance of the 2-by-1 OFDM system with IIC-MUD using a Turbo code and a convolutional code. Here, the Turbo code is punctured to 1/2 code rate with the same generator [5 7] as the convolutional code.

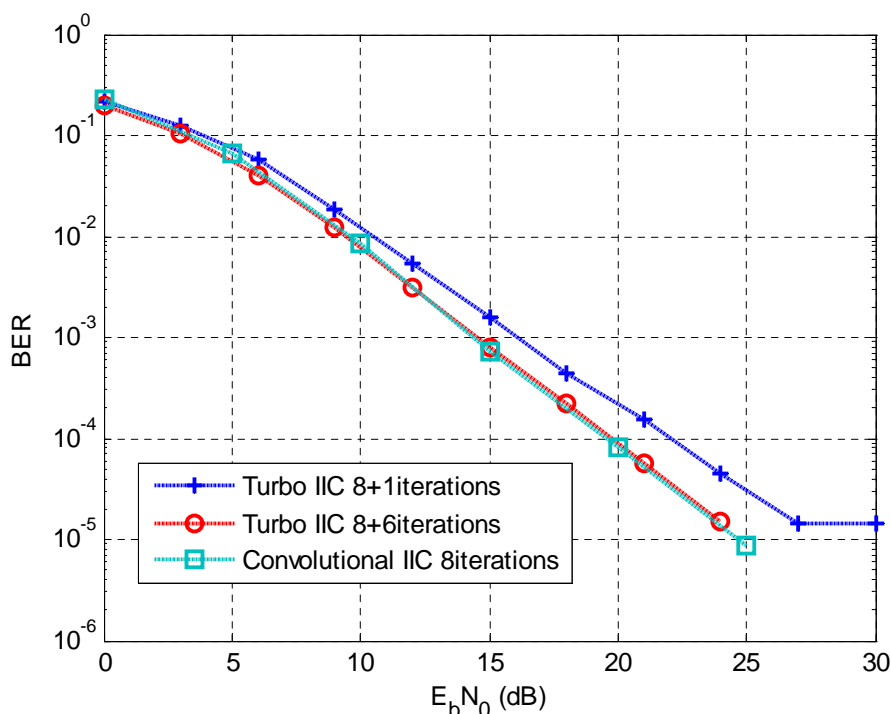


Figure 3.22 BER performances of IIC MUD for 2×1 OFDM system using Turbo code ([5 7], 1/2 code rate) and convolutional code ([5 7], 1/2 code rate)

As shown in Fig. 3.22, the BER performance for IIC using Turbo code with eight outer iterations detection and decoding, and one inner iteration between two concatenated decoder is presented, which is worse than that for IIC using the convolutional code with eight iterations. Moreover the BER performance for IIC using Turbo code with eight outer iterations and six inner iterations is almost the same as that for IIC using the convolutional code. This result shows that the Turbo code cannot obtain extra gain for the overloaded system. The behaviour of the convolutional code has been very good for our IIC MUD.

Fig. 3.23 shows the IIC MUD can work well in Rayleigh Block fading channel for two users with one receiver or two receivers. The BER performances of IIC MUD after eight iterations are compared to that of IIC MUD with perfect PIC.

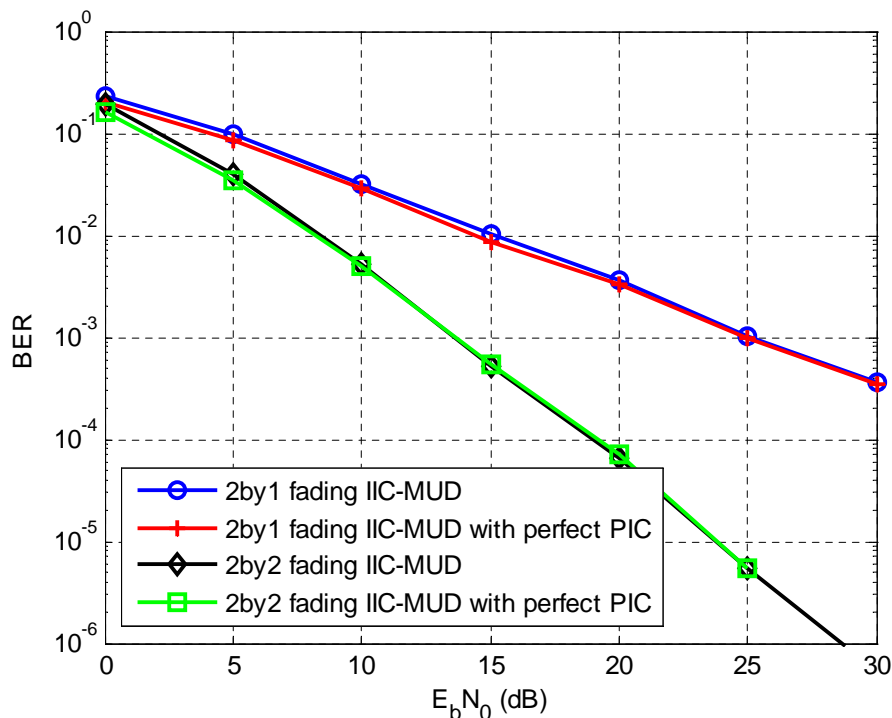
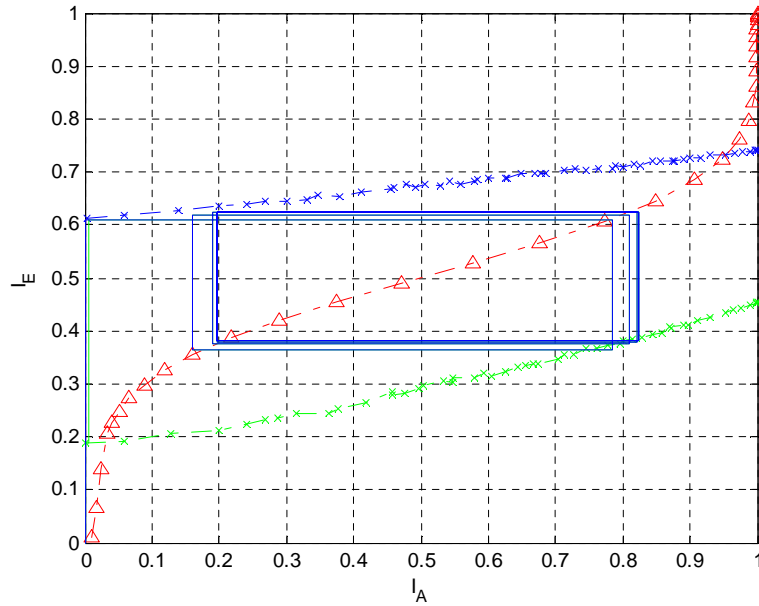


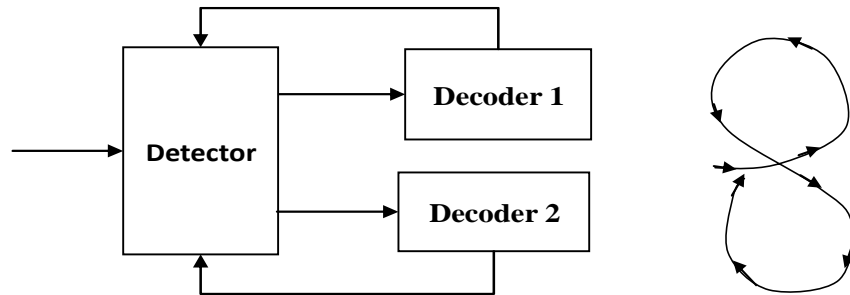
Figure 3.23 BER performances of IIC MUD for 2×1 and 2×2 OFDM system

For iterative methods, one most effective test methods is the EXIT chart. Fig. 3.24 shows two situations of the detection process of the two user case. The trajectories show the changes between the detector and decoder. By using the SIC-based approach, the detector can choose the powerful user's data to reconstruct the interference and subtract it from the receiver output. For one specific channel, at 10dB, between the two detector's curves, we can see that both curves intersect with the decoder's curve. The more powerful user, such as user one is chosen first, after the feedback of decoder one, the detection proceeds to user two, and then goes back to decoder two, and so on. The whole iterative process is like a figure of eight.

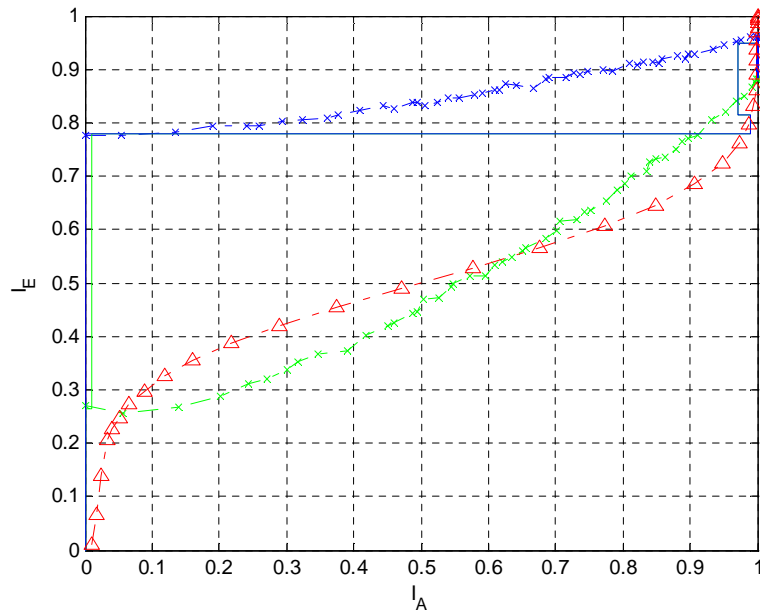
Comparing Fig. 3.24 (a) and (c), we can see that, by using the SIC-based approach at the first iteration, if the two users are both in a deeply fading channel, then the detection will fall into an infinite loop, and the performance cannot converge. However, as long as one user is in a good environment, the performance can converge perfectly.



(a) EXIT chart for a specific bad channel, when SNR is 10dB



(b) The whole iterative process: for one iteration, it starts from detector, and then goes to the decoder 1, back to detector and goes to decoder 2, and finally back to detector again; for the next iteration, repeat this process.



(c) EXIT chart for a specific good channel, when SNR is 10dB

Figure 3.24 EXIT charts for two specific cases: (a) bad channel and (c) good channel, while (b) shows the whole iterative process which is like a figure of eight

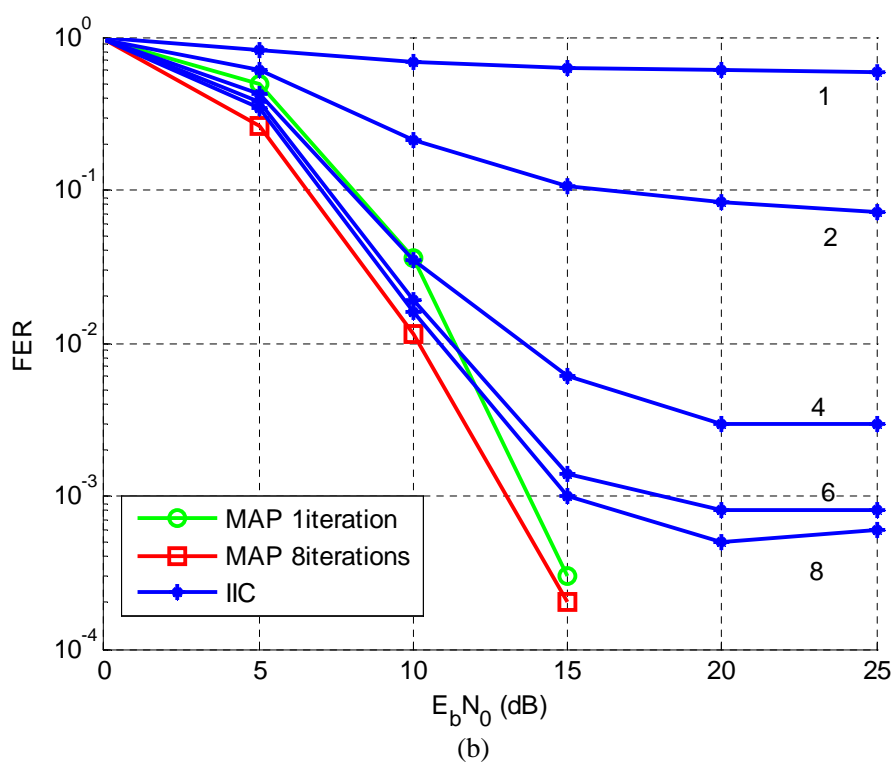
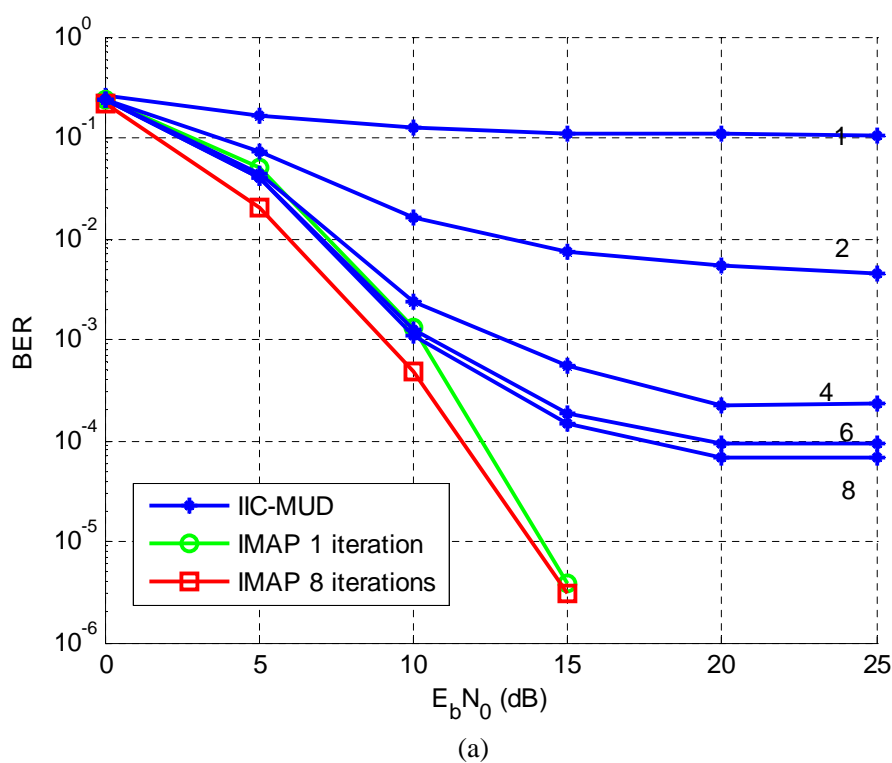


Figure 3.25 BER performance (a) and FER performance (b) for 4×2 OFDM system, compared with the optimal approach (IMAP)

Fig. 3.25 shows the four users case, where the base station has two receive antennas. From the figures, we can see that the IIC MUD can achieve almost the optimum

performance for both the BER and frame error rate (FER) performance at low SNR. However, for high SNR (above 10dB shown in the figures), both the BER and FER of the IIC MUD will have an error floor.

The error floor which occurs may be due to some fading channels where the signals are deeply faded so that we cannot tell the difference between the desired signal and interference. From the FER performance, we can see that there is almost only one bad channel among 1000 channels, which is quite rare. In practice, this FER corresponds to an quite low outage probability, which is good enough for mobile users.

Fig. 3.26 shows that the error floor for the 4-by-2 system is caused by the detector not the encoder. However, the BER performance using a Turbo code is worse than that of using a convolutional code.

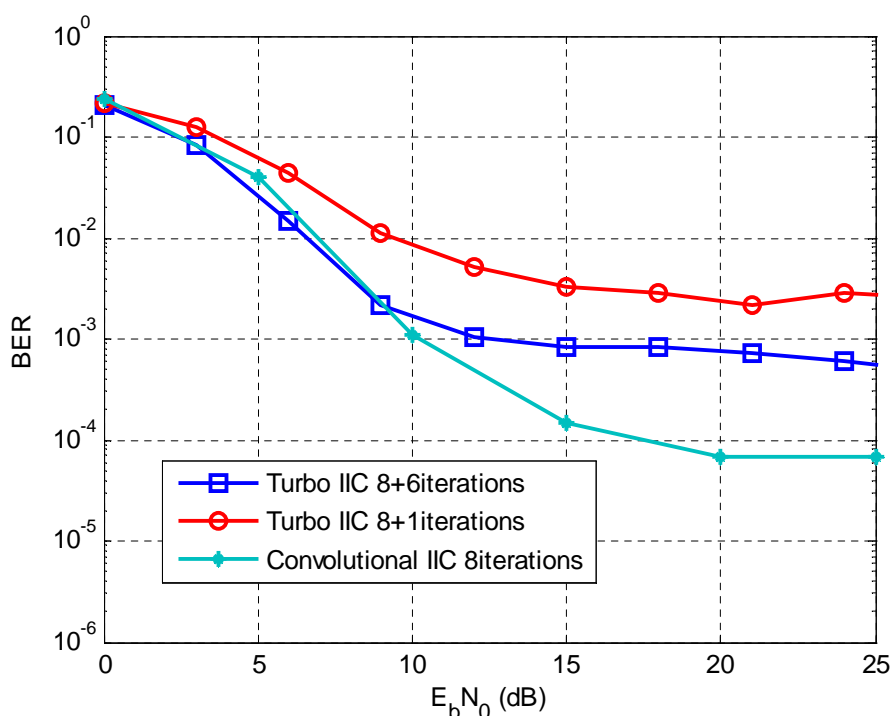


Figure 3.26 BER performances of IIC MUD for 4×2 OFDM system using Turbo code ([5 7], 1/2 code rate) and convolutional code ([5 7], 1/2 code rate)

Fig. 3.27 shows that a channel which cannot work for a convolutional code ([5 7], 1/2 code rate) definitely cannot work for a Turbo code ([5 7], 1/2 code rate). At the left side of the EXIT chart, the EXIT curve of the Turbo decoder is higher than that of the convolutional decoder, so that a detector EXIT curve which intersects with that of the convolutional decoder will always intersect with that of the Turbo decoder. On the other

hand a detector EXIT curve which intersects with that of the Turbo decoder may not intersect with that of the convolutional decoder. So a channel that can work for a Turbo code must work for a convolutional code as well. However, the channel which can work for convolutional code cannot necessarily work for the Turbo code. The EXIT curve of the Turbo decoder may intersect with the detector's, while for the convolutional decoder the tunnel is open.

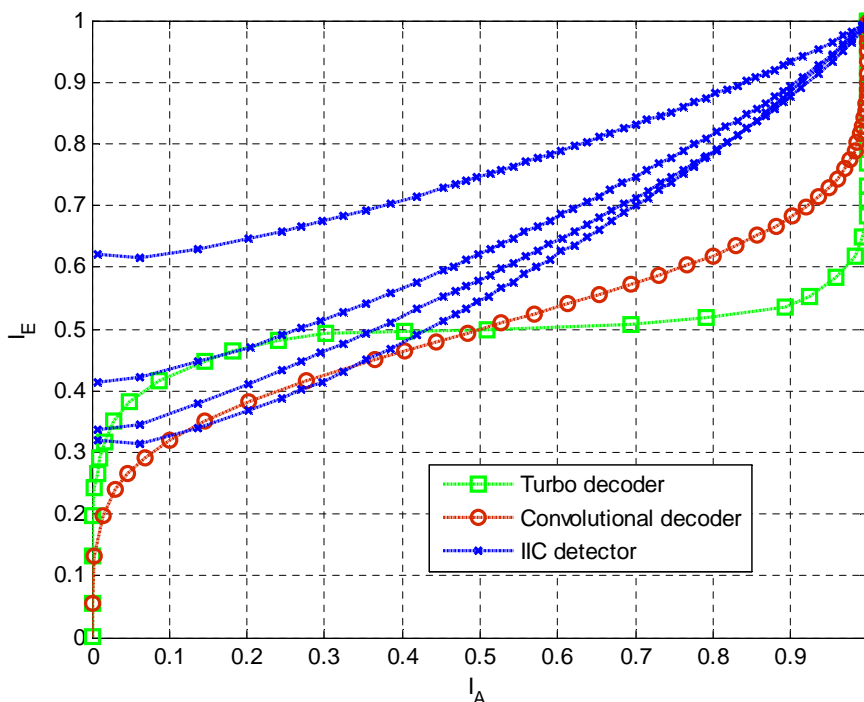


Figure 3.27 EXIT chart of IIC MUD for 4×2 OFDM system using Turbo code ($[5, 7]$, $1/2$ code rate) and convolutional code ($[5, 7]$, $1/2$ code rate)

However Fig. 3.28 shows the result if the four users have different transmit powers, the error floor then disappears. The same parameters are used, except that the four users have two different powers. Here, 0dB , 0dB , -3dB , and -3dB are used for each user separately.

The use of a lower code rate is also a solution to solve the error floor. Here, we define the *overloading factor* (OLF), which is equal to the number of transmit antennas divided by the number of receive antennas. For 4-by-2 system, the OLF is 2. For 10-by-2 system, the OLF is 5. Fig. 3.29 illustrates the BER performances of IIC MUD for fixed channel multipath (2 taps) under different OLFs using $1/3$ code rate. It can be seen that using $1/3$ code rate, the IIC can work well for the four users system. As the OLF increases, the

BER performance becomes worse, due to the increasing number of users and the increasing interference.

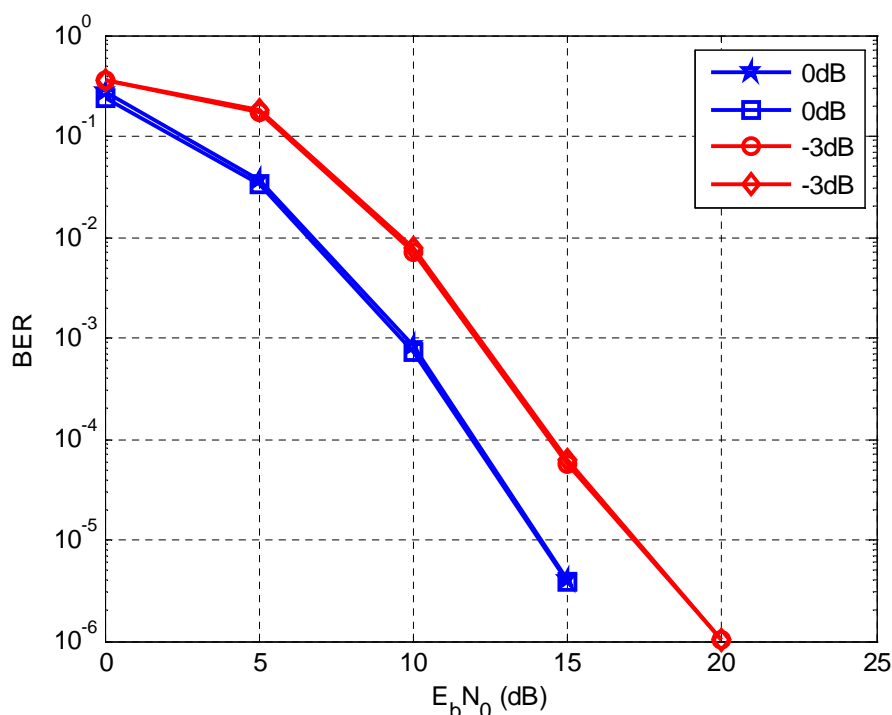


Figure 3.28 BER performance for the four user two receiver system with different transmit power (0, 0,-3 and -3dB)

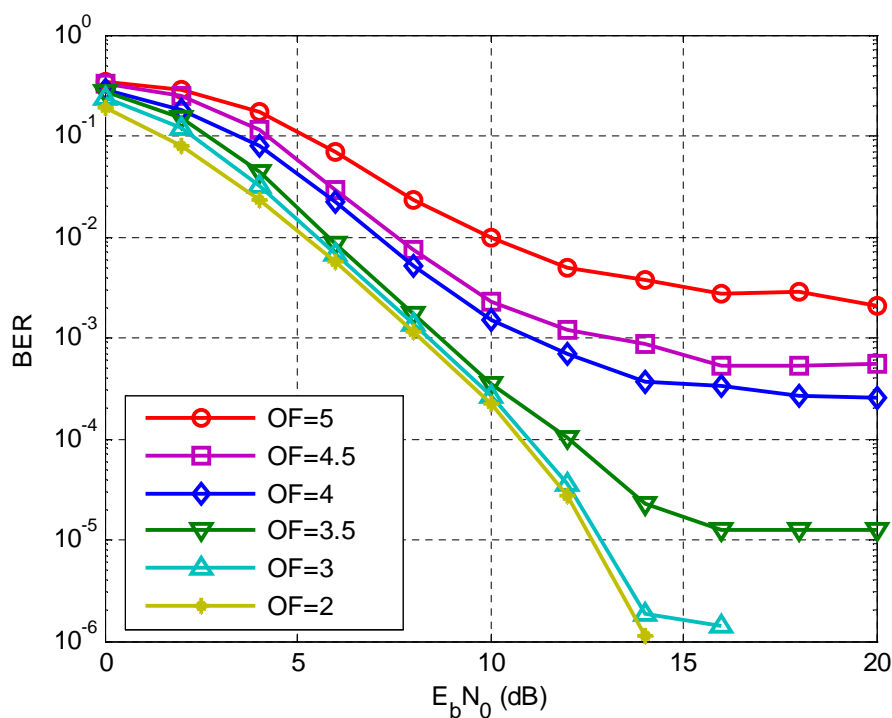


Figure 3.29 BER performance of IIC MUD for fixed channel multipath (2 taps) under different OLFs using 1/3 code rate

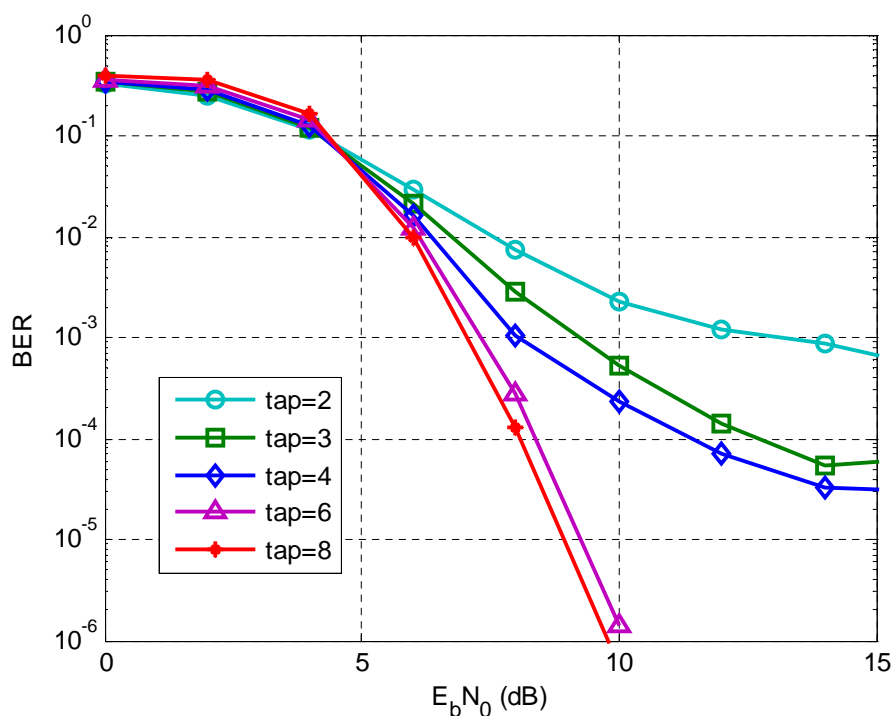


Figure 3.30 BER performance of IIC MUD for fixed code rate (1/3) and OLF (4.5) under different channel taps

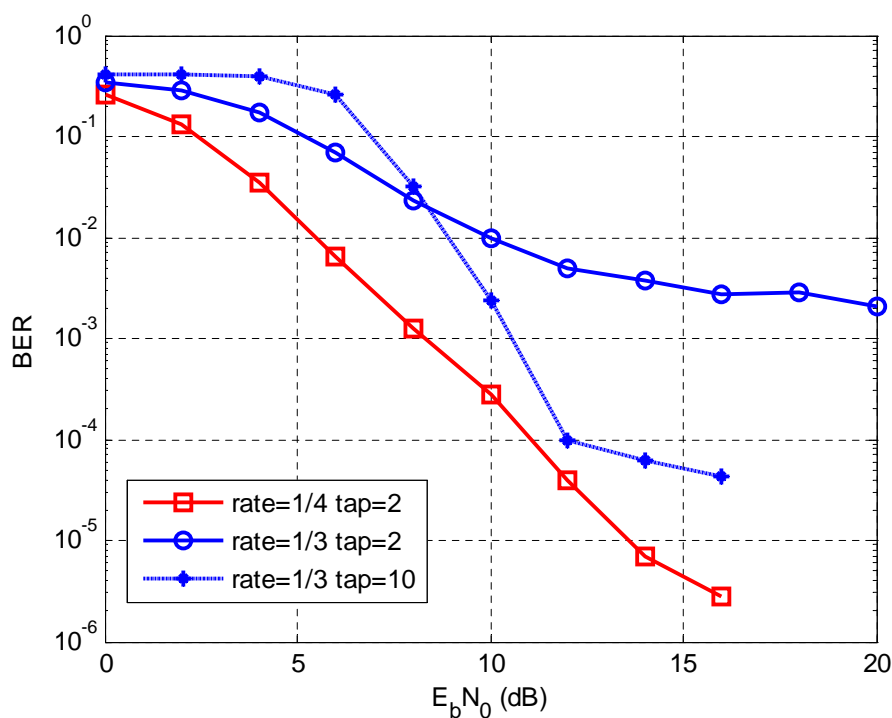


Figure 3.31 BER performance of IIC MUD for fixed OLF (5) under different channel taps and code rates

Fig 3.30 shows the BER performance of IIC MUD for fixed code rate (1/3) and OLF (4.5, i.e. nine transmitters and two receivers) under different channel taps. As the number of

taps increases, the BER performance becomes better. At low SNR, the BER for a channel with more taps is worse than that for fewer taps, due to the high noise. At high SNR, the IIC can easily remove the interference under more taps channel. The more channel taps there are, the more information the IIC receiver can get. For the overloaded system, as the OLF increases, a lower code rate is required. As shown in Fig. 3.31, the 10-by-2 system (OLF=5) cannot work for 1/3 code rate even with a 10 tap channel. In this case, 1/4 code rate is applied, and the result shows that IIC can work with a 2 tap channel.

3.9 Conclusions

In this chapter, the iterative PIC MUD is discussed, which has a fairly low computational complexity, and works well for underloaded systems in AWGN channel. However, for fading channel and overloaded system, this detector cannot work. From the distribution of the input of the SISO decoder, we propose a new LLR conversion method. A new scaling factor is calculated from the channel directly, which can make the LLRs more reliable. Then combining the LLR converter with the iterative PIC receiver, a low complexity iterative interference cancellation multiuser detection (IIC-MUD) method is proposed. This scheme requires a low complexity, and can achieve high BER performance which is very close to that of the optimal approach (MAP detection).

The iterative MAP receiver for two users' case is introduced, which is applied for the performance comparison. The simulation results show the proposed technique can effectively suppress the MAI, and can achieve near-optimum BER performance for the 2-by-1 system. For the 4-by-2 system, it still can work quite well at low SNR. Although it has an error floor at high SNR, the FER performance which corresponds to an outage probability is sufficiently high for mobile users.

If we use different powers for each user, the error floor for the four user system can be reduced. For more users, or heavily overloaded system, a lower code rate is required. The results show that our IIC is influenced by the number of channel taps, the value of OLF, and the code rate.

Chapter 4

Channel Selection for Iterative Interference Cancellation Multiuser Detection

Contents

4.1 Introduction	98
4.2 Channel Selection Criterion	99
4.3 Adaptive Transmissions	105
4.4 System Model for Different Channels using Different Code Rates	106
4.5 System Model for Multiple Transmissions	108
4.6 Simulation Results.....	110
4.7 Conclusions	116

In this chapter, in order to avoid the drawback of the *Iterative Interference Cancellation* (IIC) multiuser receiver, a channel selection scheme based on the EXIT chart will be introduced.

4.1 Introduction

In last chapter, we have introduced a new low-complexity iterative interference cancellation multiuser detection (IIC-MUD) scheme for the overloaded MIMO OFDM systems. This technique can effectively suppress the MAI, and can achieve near-optimum BER performance for the overloaded system with two users. With four users, however, for certain channels this detector will not converge to low BER at high SNR, resulting in a significant outage probability.

Under ideal conditions, the desired signal is mainly affected by both the interference and noise at low SNR, and only by interference at high SNR. The error floor which occurs at high SNR shows that for some fading channels, the IIC MUD cannot separate the interference and desired signal(s). After several iterations, for those deeply fading channels, the PDF of the IIC output will be very similar to the Fig. 3.17 shown. The simulation results show that the number of bad channels is quite rare. We can completely filter out these unwanted channels, which leads to the channel selection scheme.

Generally, channel selection is used for cognitive radio networks in the *medium access control* (MAC) layer [97] [98]. Using the channel selection technique can alleviate data frame losses, reduce the transmission errors, and overcome some multichannel problems.

Wireless channels are time varying due to the multipath fading phenomenon. Traditionally, channel fading is viewed as a destructive factor that reduces communication reliability. An effective way for the physical layer to combat fading is to obtain multiple independent replicas of the transmitted signal at the receiver by means of diversity. In a wireless network, independent paths between a base station and individual users form a new type of diversity. Many studies show that the communication system capacity can be maximized by picking the user with the best channel to transmit, which is called multiuser selection diversity [99]. Although these are based on the “best channel” criterion, they are scheduling schemes of the system resources across users.

In this chapter, we directly choose the channel which is good for convergence performance by considering the EXIT chart. From the EXIT chart point of view, for those specific channels, the EXIT chart of the detector and decoder intersect on the left of the diagram, so that the ‘tunnel’ is closed at the very beginning. Even if the SNR is very high, it still cannot converge.

The IIC MUD scheme is based on the LLR scaling factor, which is calculated directly from the channel covariance matrix. In order to easily filter out those bad channels, we find the connection between the mutual information and the channel information, and then make the channel selection criterion straightforward.

Then based on the selection criterion, we enhance the detector by applying, at the first iteration, a channel analyzer and selector which passes only those channels which are likely to converge. Moreover the channel analyzer calculates the scaling factor used in the LLR converter directly from channel.

This chapter is organized as follows: Section 4.2 introduces the system model. Section 4.3 shows the channel selection criterion. Simulation results are shown in section 4.4. Finally the chapter concludes in section 4.5.

4.2 Channel Selection Criterion

In this chapter, a channel selection criterion is derived for an IIC multiuser receiver, which is to select the suitable channel that can converge, based on an EXIT chart where the tunnel of the detector and decoder is open. We consider the same system model with more users, which has been discussed in previous chapter, as shown in Fig. 3.1.

In this section, we discuss the channel selection scheme for the IIC multiuser receiver. We employ a channel analyzer and selector at the receiver, rejecting all those ‘specific’ channels for which the detector cannot converge. Then for the remaining feasible channels, the received data will be processed through a MRC detector. We assume the CIRs are perfectly known to the receiver. Fig. 4.1 shows the IIC receiver with channel analyzer and selector.

At the first stage, the CIRs are first analyzed by the channel analyzer, which determines whether a channel is good or not, and then the channel selector selects the good ones.

From the EXIT chart point of view, Fig. 4.2 shows the different performance of a bad channel and a good channel. As shown in Fig. 4.2, in the first half of the iterations (such as the first four of eight iterations), the desired signal is affected by both the interference and noise, so Eq. (3.38) (3.40) and (3.42) are used for the scaling factor calculation. In the last half of the iterations (such as last four of eight iterations), the desired signal is affected mainly by the noise, so Eq. (3.38) (3.40) and (3.43) are used.

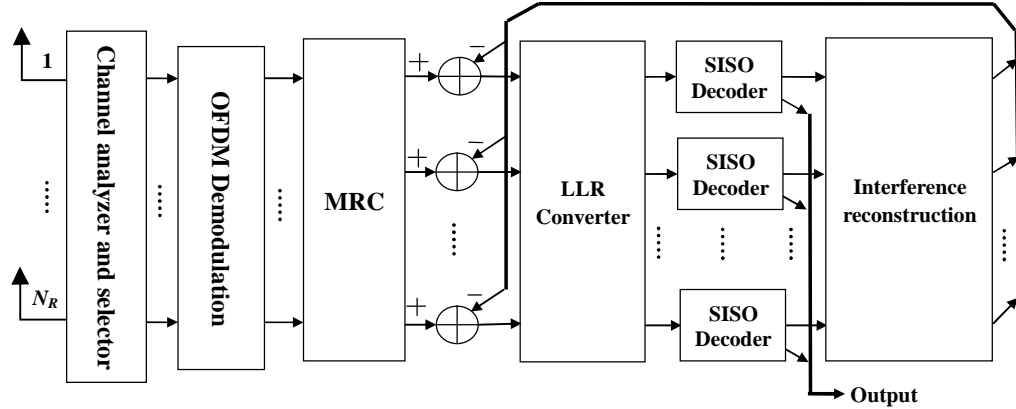


Figure 4.1 The structure of IIC MUD with channel analyzer and selector

For a bad channel, the EXIT curves of the detector and decoder are stuck at the very beginning. The trajectory shows that the IIC MUD is blocked at the first iteration, while the good channel can make the tunnel open and also ensure the convergence of the IIC MUD. We evaluate the performance at 50dB to ensure that the performance is affected only by the nature of channels. It is obvious that if the tunnel is closed at high SNR, then it is surely closed at lower SNR.

It is reasonable to assume that if the mutual information on the left of the EXIT chart, i.e. mutual information of input signal without a priori, is higher than some threshold, then the tunnel of the exit chart will certainly be open at high SNR, so that the trajectory could converge.

The input of the decoder is the output of the LLR convertor, which is the detector output multiplied by a scaling factor, so the mutual information of the detector and decoder are unchanged. After the LLR convertor, for k th subcarrier, valid a priori input LLR values are obtained:

$$\begin{aligned}\lambda_k &= \beta_k \cdot y_{k,MRC} \\ &= \beta_k \mathbf{H}_k^H \mathbf{r}_k\end{aligned}$$

$$= \boldsymbol{\beta}_k \mathbf{R}_{k,Sfading} \mathbf{s}_k + \boldsymbol{\beta}_k \mathbf{H}_k^H \mathbf{n}_k, \quad (4.1)$$

where $\mathbf{s}_k = [s_1, s_2, \dots, s_{N_T}]^T$ is the known transmitted systematic bits (for BPSK, $\mathbf{s}_k \in \{-1, +1\}$), \mathbf{H}_k^H is the Hermitian of channel matrix in frequency domain, the channel covariance matrix is

$$\mathbf{R}_{k,Sfading} = \mathbf{H}_k^H \mathbf{H}_k = \begin{bmatrix} R_{11} & \cdots & R_{1N_T} \\ \vdots & \ddots & \vdots \\ R_{N_T1} & \cdots & R_{N_T N_T} \end{bmatrix}, \quad (4.2)$$

and the scaling factor can be expressed as

$$\begin{aligned} \boldsymbol{\beta}_k &= [\beta_1, \beta_2, \dots, \beta_{N_T}]^T, \\ \beta_{i, 1 \leq i \leq N_T} &= \frac{2\mu_{i,MRC}}{\sigma_{i,MRC}^2} \\ &= \frac{2R_{ii}}{\sum_{j=1}^{N_T} Re\{R_{ij}\}^2 + \sum_{l=1}^{N_R} Re\{h_{li}\}^2 \cdot \sigma_n^2}, \end{aligned} \quad (4.3)$$

where h_{li} is the (l, i) -th element of matrix \mathbf{H}_k . So the vector of mean value and variance of the valid LLR $\boldsymbol{\lambda}$ are

$$\begin{aligned} \boldsymbol{\mu}_{k,LLR} &= [\mu_1, \mu_2, \dots, \mu_{N_T}]^T, \\ \mu_{i, 1 \leq i \leq N_T} &= \mu_{i,MRC} \beta_i \\ &= \frac{2R_{ii}^2}{\sum_{j=1}^{N_T} Re\{R_{ij}^k\}^2 + \sum_{l=1}^{N_R} Re\{h_{li}^k\}^2 \cdot \sigma_n^2}, \end{aligned} \quad (4.4)$$

$$\boldsymbol{\sigma}_{k,LLR}^2 = 2\boldsymbol{\mu}_{k,LLR}. \quad (4.5)$$

With Eq. (4.4) and (4.5), for all data frame, Eq. (4.1) can be rewritten as:

$$\boldsymbol{\lambda}_k = \boldsymbol{\mu}_{k,LLR} \cdot \mathbf{s}_k + \mathbf{n}_{k,LLR}, \quad (4.6)$$

where \mathbf{n}_{LLR} has a Gaussian-like distribution, with mean zero and variance $\boldsymbol{\sigma}_{LLR}^2$.

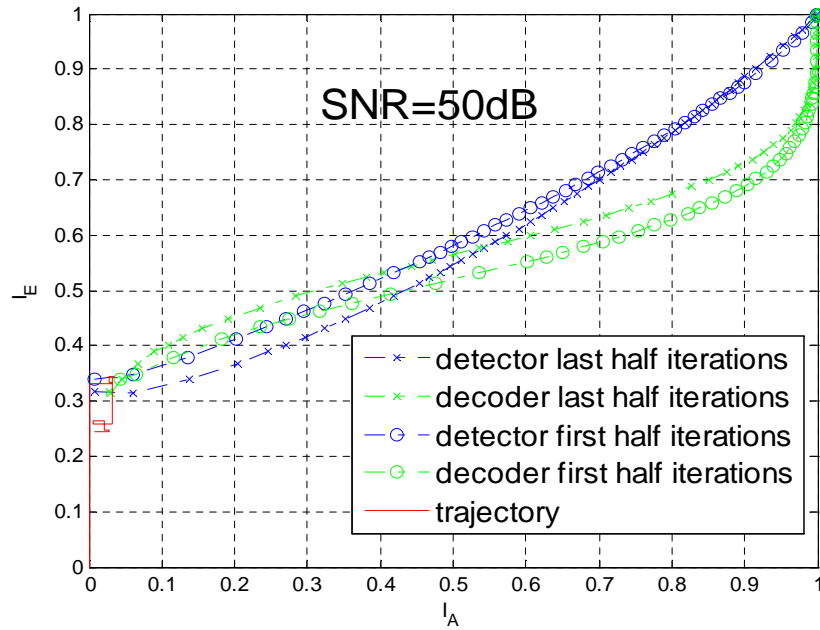
The mutual information between $\boldsymbol{\lambda}$ and \mathbf{s} is defined as

$$\begin{aligned} I(\mathbf{s}; \boldsymbol{\lambda}) &= \iint f(s, \lambda) \log \frac{f(s, \lambda)}{f(s) \cdot f(\lambda)} ds d\lambda \\ &= \iint f(s) \cdot f(\lambda|s) \log \frac{f(s) \cdot f(\lambda|s)}{f(s) \cdot f(\lambda)} ds d\lambda \end{aligned}$$

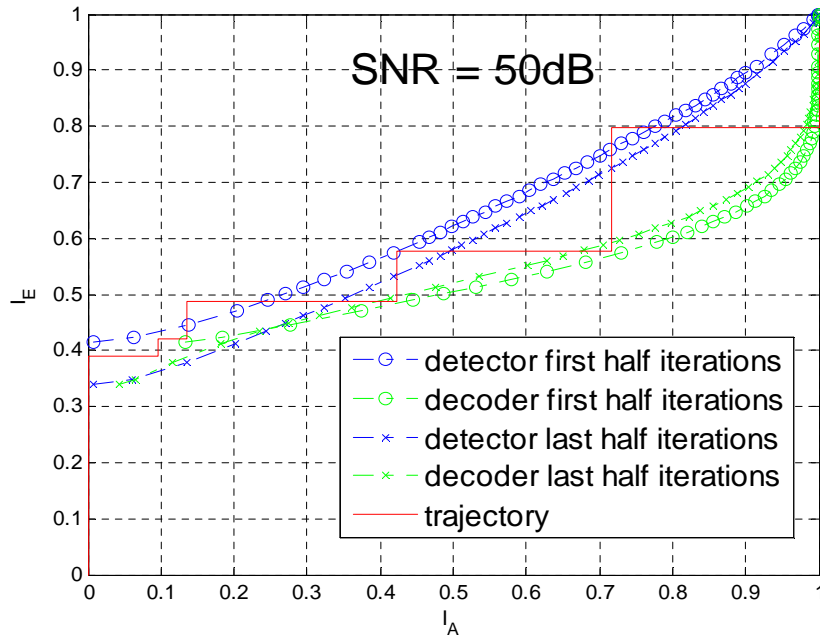
$$= \int f(\lambda|s)P(s) \log \frac{f(\lambda|s)}{f(\lambda)} d\lambda, \quad (4.7)$$

with

$$f(\lambda) = f(s = +1) \cdot f(\lambda|s = +1) + f(s = -1) \cdot f(\lambda|s = -1). \quad (4.8)$$



(a)



(b)

Figure 4.2 EXIT chart for a bad channel (a) and a good channel (b)

Assuming the probabilities of ‘+1’ and ‘−1’ are equal, Eq. (4.7) can be expressed as

$$I(\mathbf{s}; \boldsymbol{\lambda}) = \frac{1}{2} \sum_{s=\pm 1} \int_{-\infty}^{+\infty} f(\lambda|s) \log \frac{f(\lambda|s)}{\frac{1}{2}(f(\lambda|s=+1) + f(\lambda|s=-1))} d\lambda. \quad (4.9)$$

The conditional probability density function of $\boldsymbol{\lambda}$ is

$$f(\lambda|s) = \frac{1}{\sqrt{2\pi}\sigma_{LLR}} \exp\left(-\frac{(\lambda - \mu_{LLR}s)^2}{2\sigma_{LLR}^2}\right), \quad (4.10)$$

where μ_{LLR} and σ_{LLR}^2 are the element of $\boldsymbol{\mu}_{k,LLR}$ and $\boldsymbol{\sigma}_{k,LLR}^2$ respectively. With (4.5),

$$f(\lambda|s) = \frac{1}{\sqrt{4\pi\mu_{LLR}}} \exp\left(-\frac{(\lambda - \mu_{LLR}s)^2}{4\mu_{LLR}}\right), \quad (4.11)$$

$$\begin{aligned} f(-\lambda|s) &= \frac{1}{\sqrt{4\pi\mu_{LLR}}} \exp\left(-\frac{(\lambda + \mu_{LLR}s)^2}{4\mu_{LLR}}\right) \\ &= f(\lambda|s)\exp(-\lambda s), \end{aligned} \quad (4.12)$$

so Eq. (4.9) becomes

$$\begin{aligned} I(\mu_{LLR}) &= \frac{1}{2} \left(\int_{-\infty}^{+\infty} f(\lambda|s=+1) \log \frac{2f(\lambda|s=+1)}{(f(\lambda|s=+1) + f(\lambda|s=-1))} d\lambda \right. \\ &\quad \left. + \int_{-\infty}^{+\infty} f(\lambda|s=-1) \log \frac{2f(\lambda|s=-1)}{(f(\lambda|s=+1) + f(\lambda|s=-1))} d\lambda \right) \\ &= \frac{1}{2} \left(\int_{-\infty}^{+\infty} f(\lambda|s=+1) \log \frac{2}{(1 + \exp(-\lambda))} d\lambda \right. \\ &\quad \left. + \int_{-\infty}^{+\infty} f(\lambda|s=-1) \log \frac{2}{(1 + \exp(\lambda))} d\lambda \right) \\ &= 1 - \int_{-\infty}^{+\infty} \frac{\exp\left(-\frac{(\lambda - \mu_{LLR})^2}{4\mu_{LLR}}\right)}{\sqrt{4\pi\mu_{LLR}}} \log_2(1 + \exp(-\lambda)) d\lambda. \end{aligned} \quad (4.13)$$

Since μ_{LLR} is the diagonal value of channel covariance matrix $\mathbf{R}_{k,Sfading}$, so

$$\mu_{LLR} > 0,$$

and [76]

$$\begin{aligned} \lim_{\mu_{LLR} \rightarrow 0} I(\mu_{LLR}) &= 0, \\ \lim_{\mu_{LLR} \rightarrow \infty} I(\mu_{LLR}) &= 1. \end{aligned} \quad (4.14)$$

Now using Eq. (4.4), we can analyze the channel and obtain the mean value μ_{LLR} directly from the channel, and then Eq. (4.13) is used to select convergent channels, by calculating the mutual information at the LLR converter output, without interference cancellation. For mutual information below a given threshold we identify the channel as ‘bad’, and reject it.

If the channel is good, then the received signal will be passed to MRC detection as its first stage, as shown in Fig.4.1, which shows the reconstruction of the interference for each user, and its use for cancelling this estimated interference in the next iteration. Then the detecting and decoding process is the same as we discussed in chapter 3. After several iterations, the scaling factor is recalculated as

$$\beta_{i,1 \leq i \leq N_T} = \frac{2R_{ii}}{\sum_{l=1}^{N_R} Re\{h_{li}^k\}^2 \cdot \sigma_n^2}. \quad (4.15)$$

Table 4.1: Look-up table for mean value vs mutual information

Mean value	Mutual information
1.5	0.3972
1.6	0.4162
1.7	0.4346
1.8	0.4523
1.9	0.4694
2.0	0.4859
2.1	0.5019
2.2	0.5173
2.3	0.5321
2.4	0.5465

Table 4.1 shows the look-up value for the mutual information, according to the mean value from the channel. In this case, it is easy to obtain the mutual information, which reduces the computational complexity significantly. In the simulation part, we choose

mutual information equal to 0.48 as the threshold, which is around 2.0 for the mean value. So according to the channel information, we can easily distinguish the channel whether it is good or not, and select the good one.

4.3 Adaptive Transmissions

In the previous section, a selection criterion for the channels is introduced to filter out those bad channels which cannot converge. The selection scheme is based on the mutual information of the output of the detector, which can be directly calculated from the channel matrix. If the mutual information is higher than a threshold, then we determine that channel to be a good channel. Otherwise, the channel is determined to be bad, and rejected, the user's data will need to be transmitted again.

From the simulation results, we can see that a small proportion of channels is deeply faded and cannot converge, resulting in a non-zero outage probability, even at high SNR. As shown in chapter 3, the FER performance corresponds to an very low outage probability. However, the results in Fig.4.7 show that the rejected channel rate is larger than the FER, which means that some good channels are rejected. Although the ratio is very small, it is a waste.

In order to make full use of all the CIRs, in this section, we propose two schemes to deal with those bad channels. We choose the specific threshold, which is selected according to Fig. 4.7. If the mutual information is lower than the threshold, the channel is bad, so that we will change the transmission scheme:

- 1) Change the code rate. A lower code rate can be used for the bad channels. The EXIT chart shows that the tunnel between the detector and decoder is closed for the bad channels. Using a lower code rate will make the whole EXIT curve of the decoder move down, which will directly make the tunnel open.
- 2) Using multiple transmissions. For the bad channels, the users' data can be divided into N_{OLF} groups, and then transmitted N_{OLF} times, where OLF is the overloading factor (equals to the number of transmit antennas divide by the number of receive antenna). In this case, the channel matrix is full rank, so that the matched filter can provide more reliable LLRs at the first iteration.

Basically, the above two schemes both can be classified as adaptive transmission. A lot of adaptive schemes have been proposed for wireless communications, such as adaptive modelling, adaptive beamforming, adaptive channel estimation, adaptive detection, adaptive synchronization, adaptive transmission, etc. [100] proposed several schemes based on the rank or conditional number of the channel and received SINR. [101] introduced a transmission parameter called the number of transmission substreams. The adaptive scheme adjusts the number of transmission substreams according to channel conditions, which can obtain both efficiency and reliability under channel fading. [102]-[104] show various adaptive transmission schemes based on channel quality estimations. The transmitter needs channel state information (CSI) for the upcoming transmission frame. Most of the adaptive transmission schemes are based on a channel prediction, and switch the transmission schemes according to the CSI.

Adaptive transmission, which can greatly improve the performance of a communication link under fading environment, adjusts optimally transmit power level, precoding matrix, modulation and coding schemes at the cost of requiring perfect CSI. In most communication systems using adaptive transmission, the CSI is estimated at the receiver and fed back to the transmitter. The transmitter cannot obtain the CSI on time. If the channel is fast fading, the CSI will be quickly outdated, and no longer accurate at the transmitter.

However, for our system, we use the block fading channel model, which means the channel coefficients keep constant for one data frame. The two schemes we proposed, only need simple feedback (the channel is good or bad), which requires only one bit. If the channel is good, the transmitter keeps transmitting, otherwise adjust the transmission scheme. The transmitter in our system does not need the actual CSI.

4.4 System Model for Different Channels using Different Code Rates

In the previous section, we analyzed the channel performance by using Eq. (4.4), based on the channel information. Then Eq. (4.13) is used to select convergent channels, by calculating the mutual information at the LLR converter output, without interference cancellation. For mutual information below the given threshold we identify the channel as 'bad'. These 'bad' channels, however, can be distinguished using the EXIT chart,

based on the mutual information. Fig.4.2 shows the difference between the EXIT chart of a ‘good’ channel and a ‘bad’ channel.

At the receiver, if one channel is identified to be a bad channel, then a message is fed back to the transmitter and used to adjust the transmission scheme, as shown in Fig.4.3.

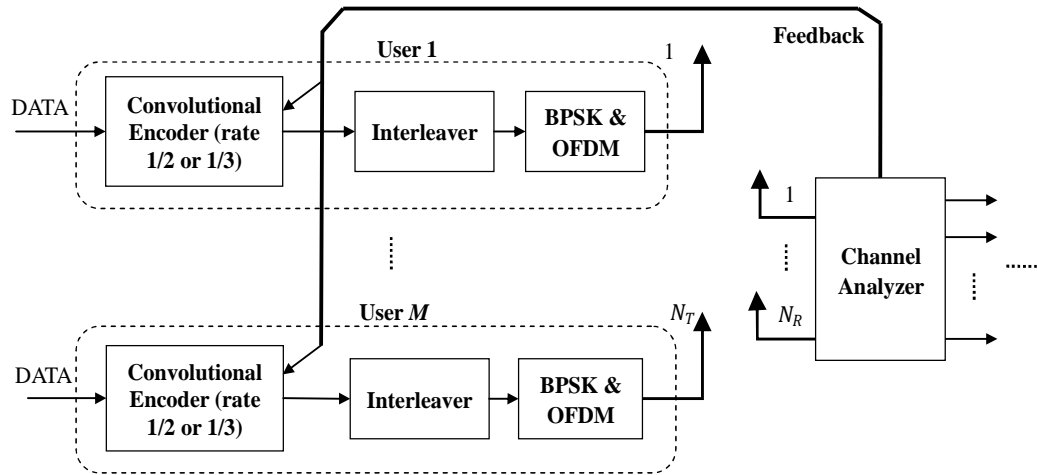


Figure 4.3 The structure of adaptive system for different channels using different code rates

Because bad channels are rare, the users’ data is first encoded by the rate 1/2 convolutional encoder, and then transmitted after BPSK and OFDM modulation. We assume the CIRs are perfectly known by the receiver. At the receiver, only if the channel analyzer identifies a channel to be bad, then the transmitter will get the feedback and adjust the encoder to using rate 1/3 (code generator [7 3 5]). Otherwise, the encoder will use rate 1/2 ([5 7]) all the time.

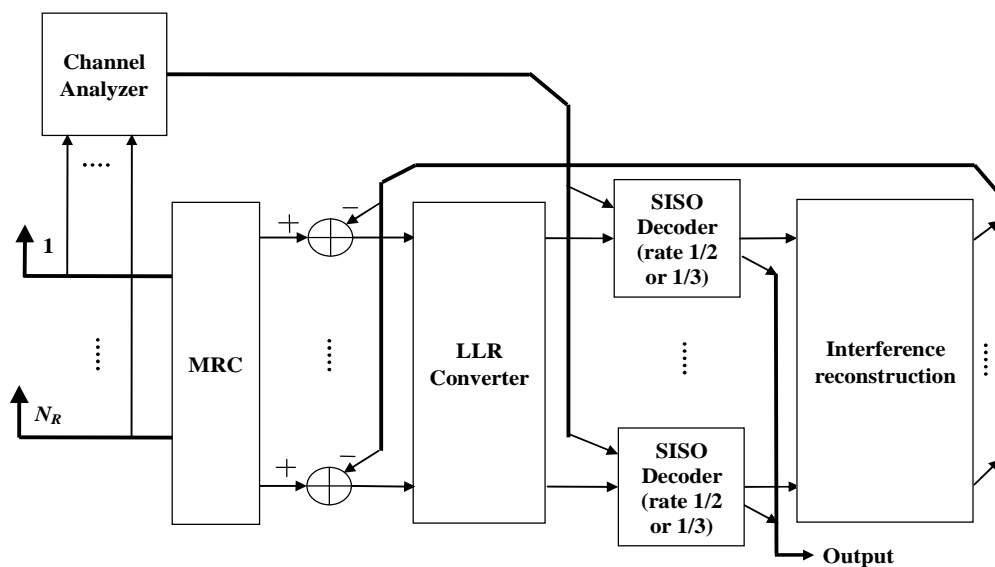


Figure 4.4 The adaptive receiver structure for different channels using different code rates

The adaptive receiver employs IIC for the detecting and decoding, as shown in Fig.4.4. The receiver processing is the same as we discussed in previous section. Only when a channel is identified as a bad channel, the channel analyzer will send a message to the decoder, adjusting the code rate.

4.5 System Model for Multiple Transmissions

For the non-convergent channels, another transmission scheme is introduced in this section. The system model is given by

$$\mathbf{r}_k = \mathbf{H}_k^1 \mathbf{s}_k^1 + \mathbf{H}_k^2 \mathbf{s}_k^2 + \dots + \mathbf{H}_k^{N_{OLF}} \mathbf{s}_k^{N_{OLF}} + \mathbf{n}_k, \quad (4.16)$$

$$N_{OLF} = N_T / N_R. \quad (4.17)$$

We divide the users into N_{OLF} groups, each containing N_R users. The users' data is transmitted in N_{OLF} time slots. The system model is shown in Fig.4.5.

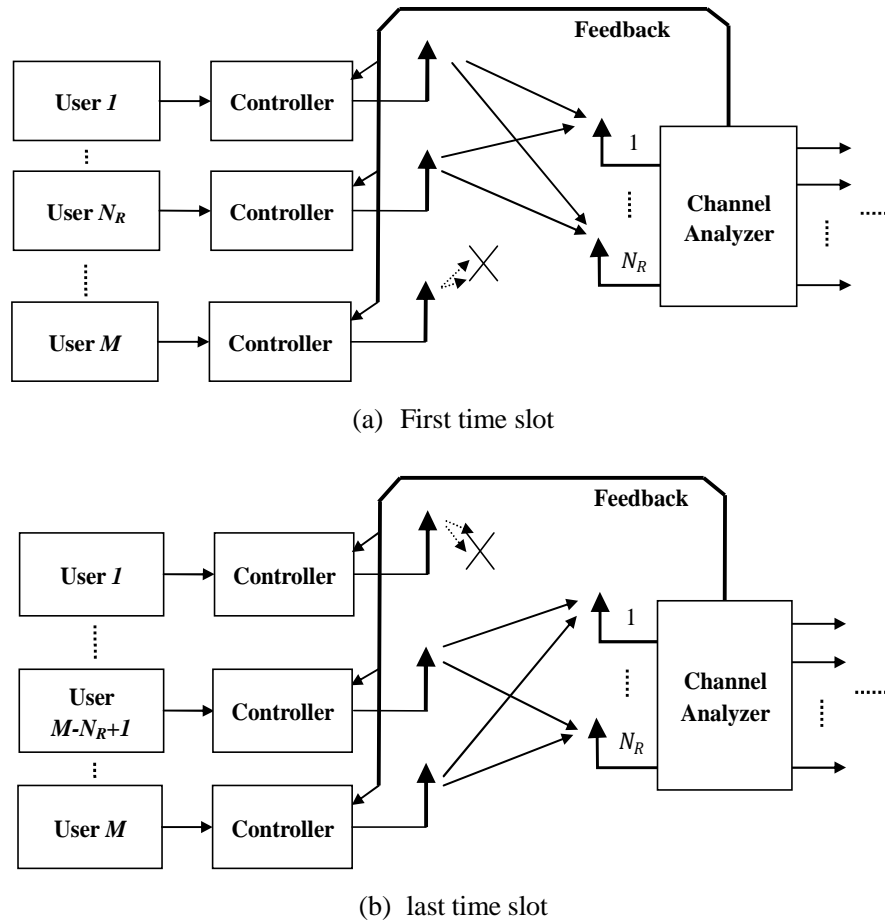


Figure 4.5 The structure of adaptive system for multiple transmissions

At the receiver, N_{OLF} full rank sub-channels are obtained, so that the matched filter can provide more reliable output at the first iteration. The adaptive receiver structure is shown in Fig.4.6.

At the receiver, the channel analyzer will also provide a message for each channel. If the channel is good, the original IIC will be used. Or it will switch to a set of IIC, which will detect and decode the signal successively.

The output of the matched filter is

$$\mathbf{y}_{MRC,k}^n = \mathbf{H}_k^{nH} \mathbf{H}_k^n \mathbf{r}_k, \quad (4.18)$$

where $n = 1, 2, \dots, N_{OLF}$. Then using Eq. (4.3), reliable LLRs are obtained. After the decoder, the soft outputs are used to calculate the soft estimate of the user data symbols. Through the interference reconstruction, the interference can be subtracted from the MRC output. The following process is the same as discussed above. After several iterations, Eq. (4.15) is used to update the scaling factor.

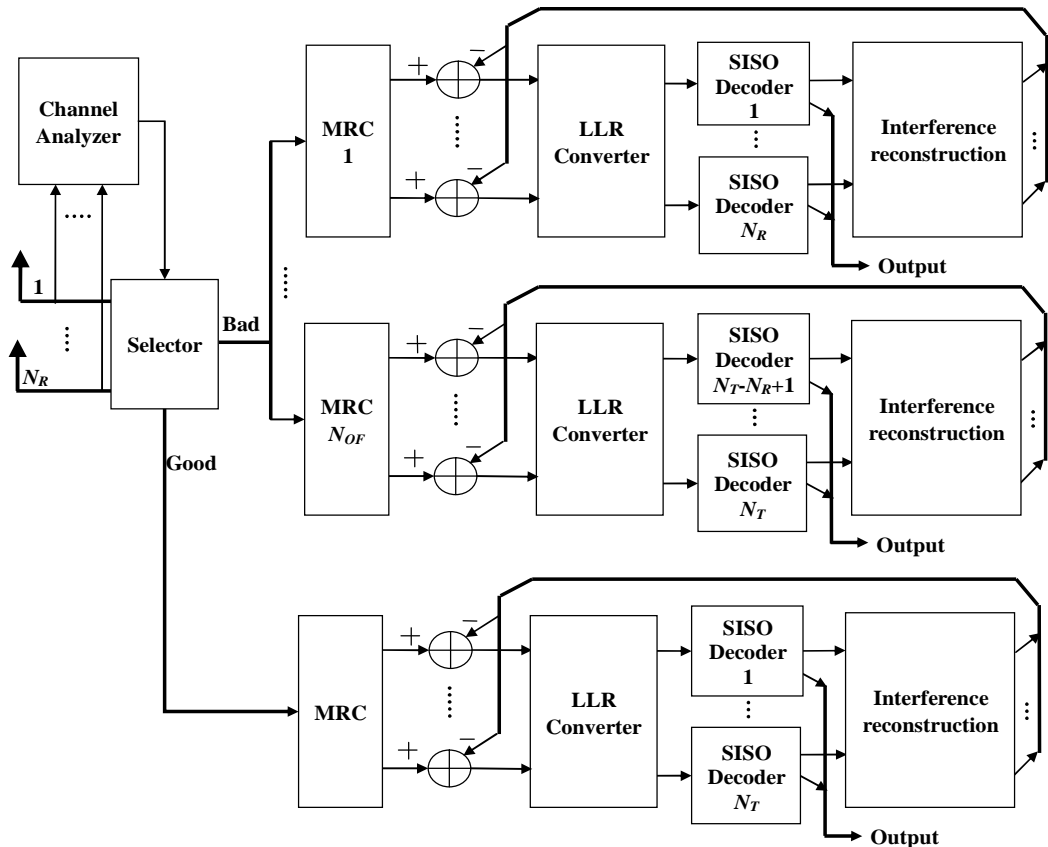


Figure 4.6 The adaptive receiver structure for multiple transmissions

4.6 Simulation Results

In this section, an uplink overloaded system with four users is considered. Each user employs 10000 frames, 1024-bits per frame with rate 1/2 convolutional codes (with generator [5, 7]), BPSK modulation, and 32 subcarriers for OFDM modulation. A Rayleigh channel is assumed with uncorrelated fading between all transmit and receive antennas, and a block fading channel model is used. The BERs plotted are averages over all users.

Fig. 3.26 illustrates the BER and FER performance of the IIC-MUD of the four user case, where the base station has two receive antennas. This simulation uses the same method for calculating scaling factor as Eq. (4.3) and (4.15), without channel selection. After eight iterations, the BER and FER performance of IIC-MUD is close to that of IMAP with eight iterations (better than that of IMAP with one iteration) when SNR is below 10dB, while it has an error floor when SNR is above 10dB. The FER performance shows that the number of bad channels is very rare.

These ‘bad’ channels, however, can be distinguished using the EXIT chart, based on the mutual information. Fig. 4.2 shows the difference between the EXIT chart of a ‘good’ channel and a ‘bad’ channel. From the figure, we can see that at the first iteration, at the left hand side, the mutual information of the detector is around 0.3~0.4, without any feedback. For 0.4, the EXIT tunnel is open, while for 0.3 it is closed. For the first half of total number of iterations, Eq. (4.3) is used to calculate the scaling factor, while for the other half iterations Eq. (4.15) is used.

In order to make the tunnel open, according to Eq. (4.13), if we find the threshold, then we can tell the difference between the bad and good channels from the mean value μ_{LLR} . Fig.4.7 shows the relationship among *rejected channel rate* (RCR), *errored channel rate* (ECR), and mutual information for 10000 accepted channels. RCR means the proportion of the total number of channels that are rejected, while ECR means the proportion of accepted channels that lead to frame errors, and hence is equivalent to FER.

As shown in Fig. 4.7, at 50dB, when the threshold of mutual information is 0.05, no channel is rejected, and the ECR is around 5×10^{-4} , which is almost the same as the FER in Fig. 3.26(b). When the threshold is larger than 0.35, some channels are rejected,

and the ECR decreases to zero gradually. As the threshold increases, the ECR is improved significantly.

We can see that when the threshold is around 0.48, the ECR is zero, and the RCR is 0.04, which means only 400 channels are rejected among 10400 channels, and this will cause the error floor to disappear. So setting the threshold equal to 0.48 is reasonable. Using 0.48 as the threshold of mutual information, the channel selector can filter out almost all of the bad channels, and pass the good channels. Fig.4.8 shows the BER and FER performance of the IIC-MUD, using these passing channels. These results have been published in [106].

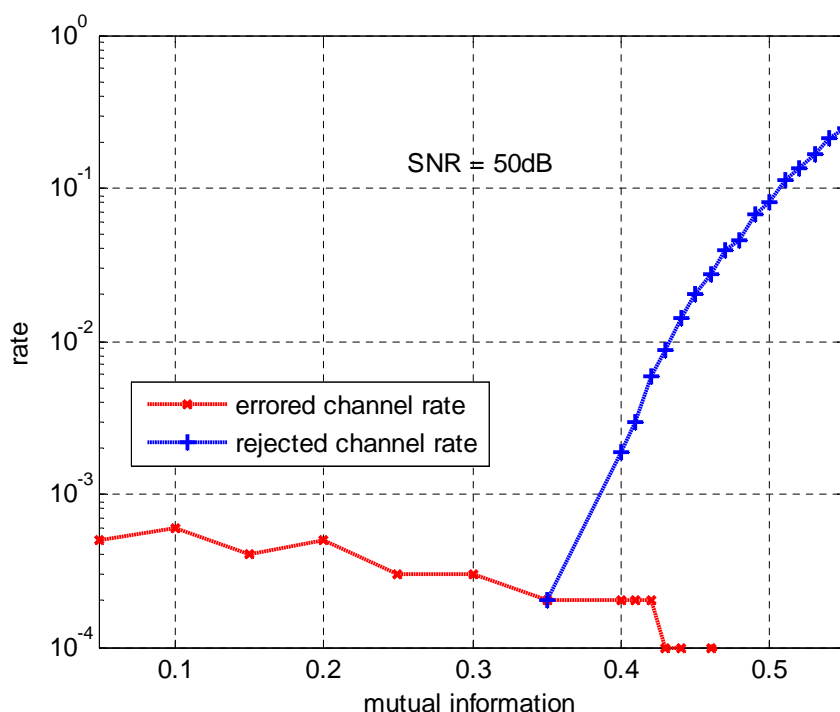


Figure 4.7 Rejected channel rate (RCR) and errored channel rate (ECR)

As shown in Fig.4.8, both the BER and FER performance of IIC-MUD with selection converges after eight iterations: this is better than for MAP with one iteration, and very close to the performance of MAP with eight iterations. After eight iterations, the FER performance is almost the same as that of MAP with eight iterations. The results suggest that the new IIC detector can avoid the bad channels and detect the data effectively. It achieves a BER of 10^{-6} , and a FER of 10^{-4} within 20dB within eight iterations.

Fig. 4.9 illustrates the BER performance of the IIC-MUD with channel selection of the eight users' case, where the base station has four receive antennas. The threshold of

mutual information is also 0.48. For different channel taps, the IIC-MUD can work well.

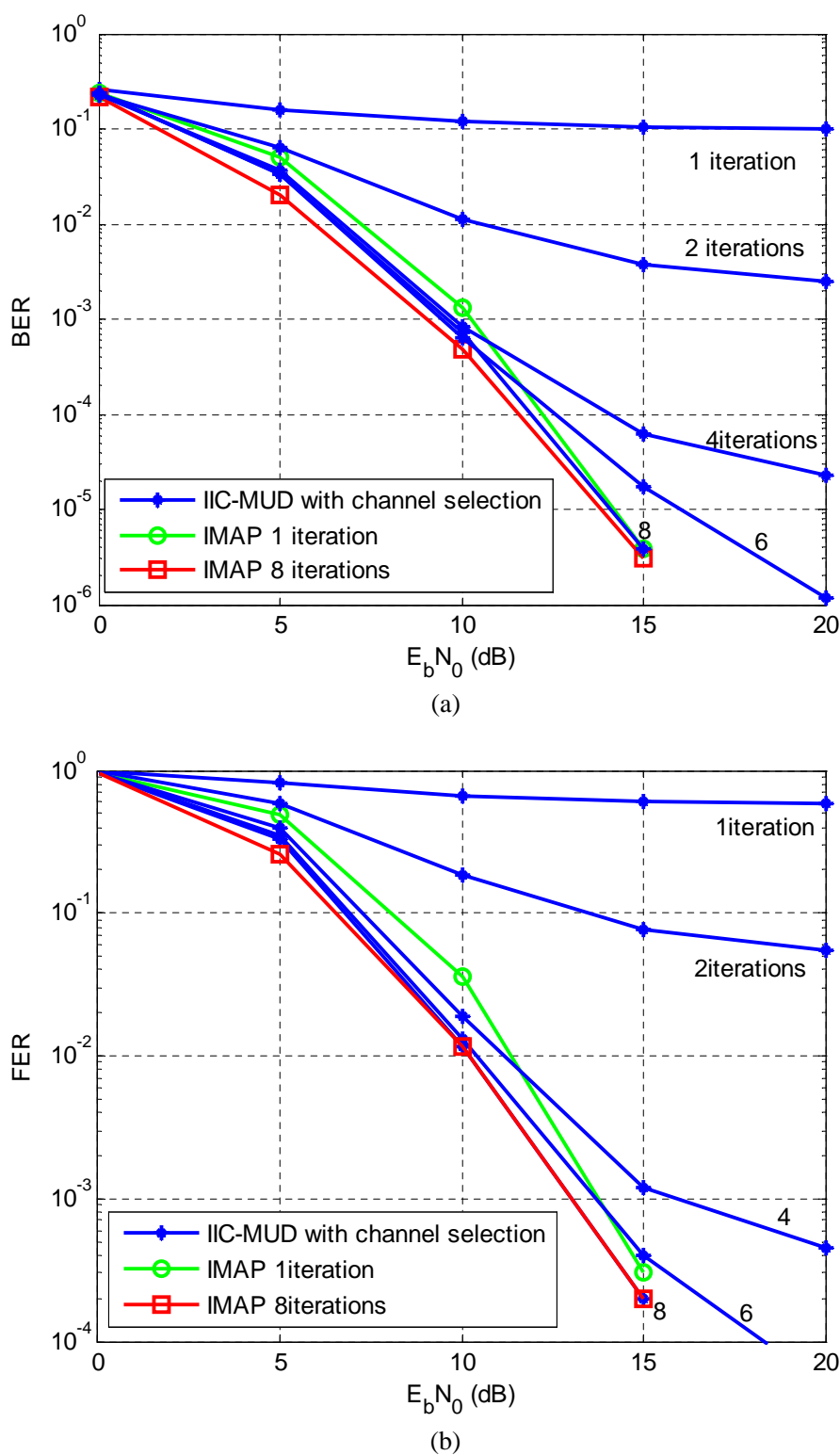


Figure 4.8 BER (a) and FER (b) performance for the four user two receiver system using IIC-MUD with channel selection

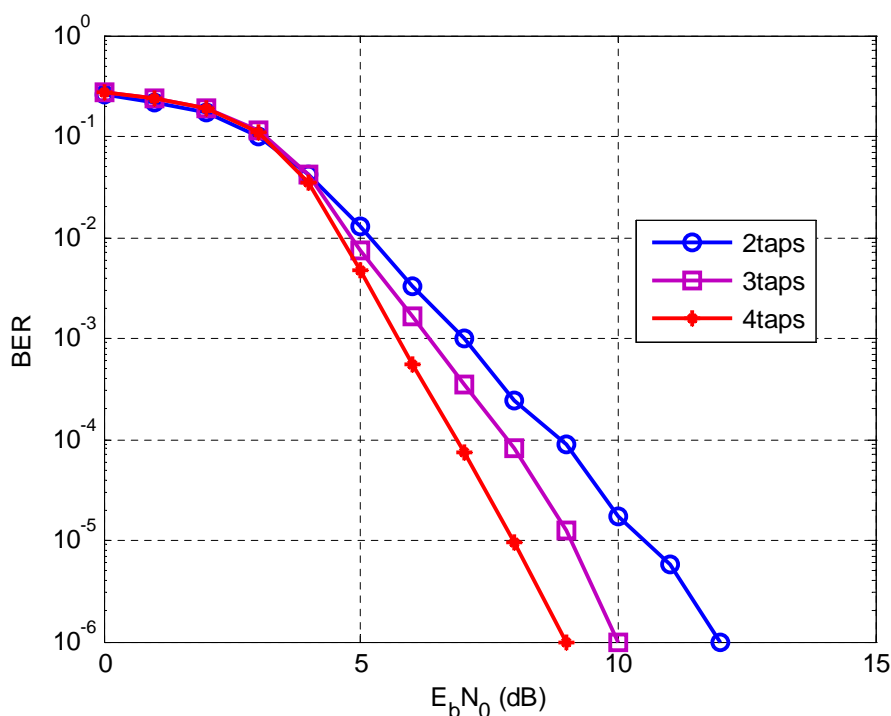


Figure 4.9 BER performance for the eight user four receiver system using IIC-MUD with channel selection under different channel taps (2, 3, 4 taps)

The variation of throughput (in bits per symbol) with SNR is shown in Fig.4.10. The maximum throughput is 0.5, due to the maximum rate of the code. The figure shows that the throughput for both schemes (one is using different code rates for different channels, and the other is multiple transmission) approaches this value as the SNR increases, but does not reach it because of the bad channels which still occur at high SNR. At around 8dB, the throughput for both schemes reach 0.45, 90% of the maximum throughput, which means the bad channels do not greatly influence the throughput. However the lower code rate approach consistently achieves a higher throughput.

Fig.4.11 shows the BER and FER performance for the two proposed schemes for bad channels, compared to the IIC with and without channel selection. One uses the rate 1/3 convolutional code (with 768-bit per frame and generator [7, 3, 5]) for the bad channels, while 1152-bit per frame and rate 1/2 ([5, 7]) convolutional code is used for good channels.

The other uses multiple transmissions when the channel is bad. For the four user case, we divide the four users into two groups, then transmit the data in two time slots, receive and process the data sequentially. For good channels, original IIC-MUD is still used. (Both are use code rate 1/2.)

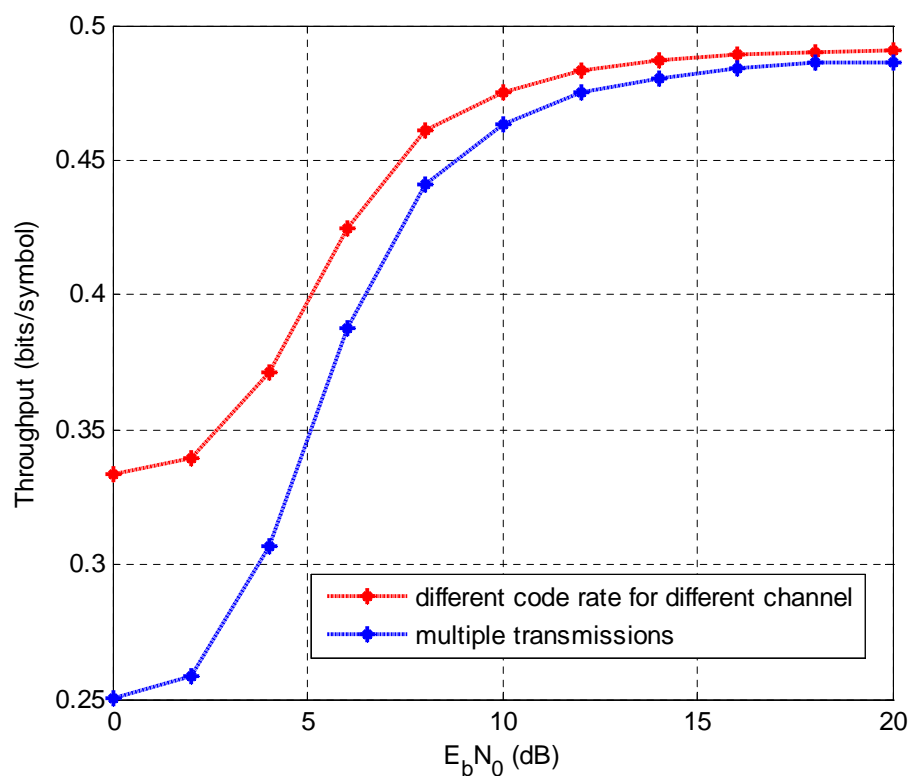


Figure 4.10 Throughput vs SNR for two adaptive schemes

After 8 iterations, we can see that both schemes successfully remove the error floor compared to the IIC without channel selection, and make full use of the channels, compared to the IIC with channel selection. The lower code rate approach also gives a lower error rate (shown in Fig. 4.11), as well as higher throughput (shown in Fig. 4.10).

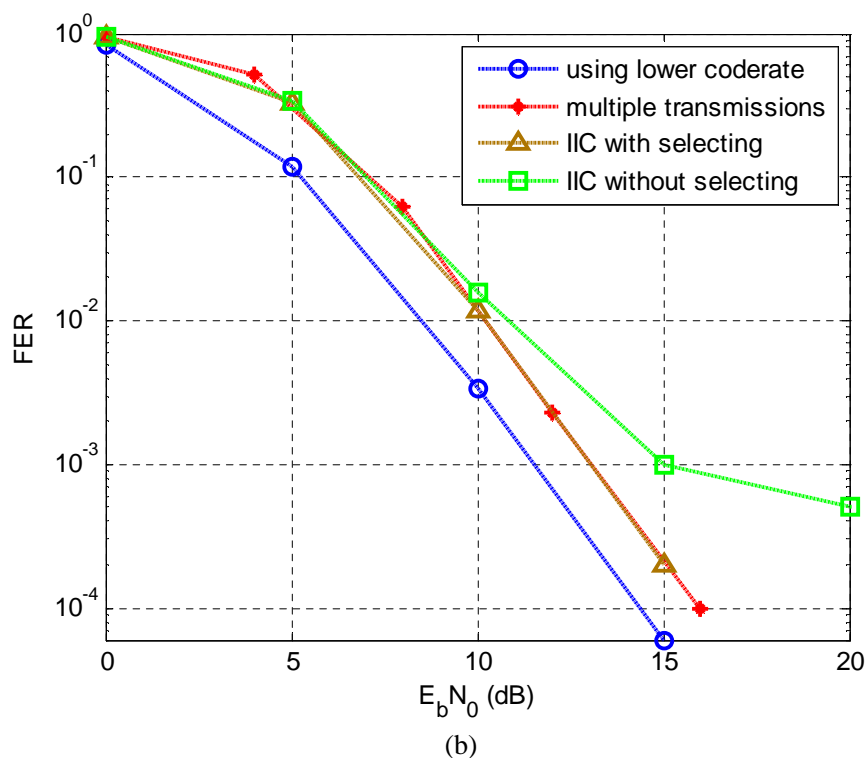
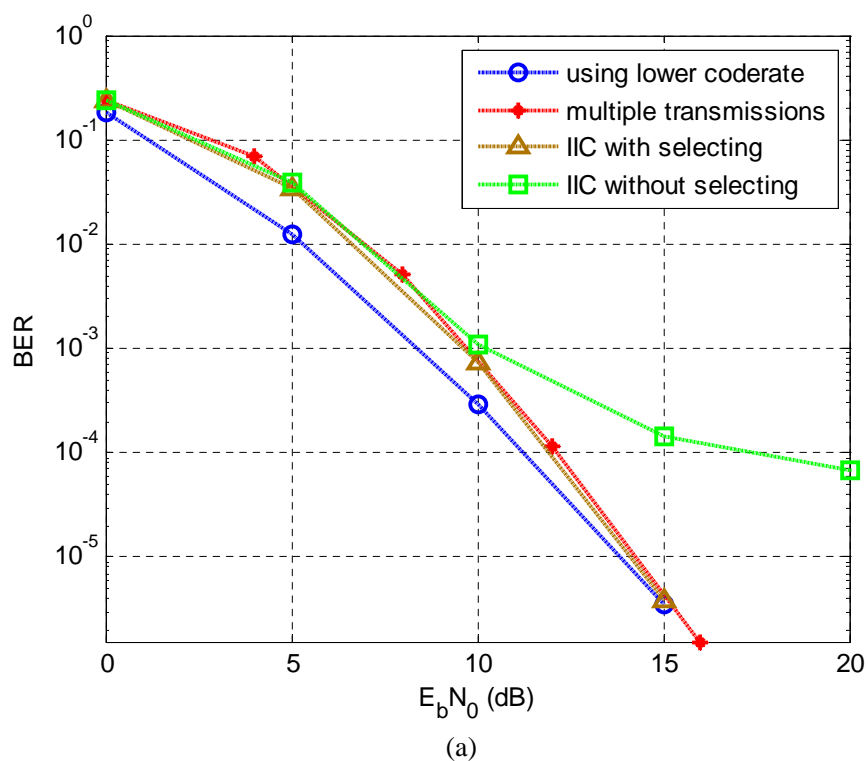


Figure 4.11 BER (a) and FER (b) performance for the four user two receiver system using lower code rate ([7,3,5], rate1/3) and adaptive transmission for bad channels compared to the IIC with and without channel selection

4.7 Conclusions

In this chapter, in order to solve the problem of the error floor, we introduce a channel selection scheme for the IIC MUD, which is based on the EXIT chart point of view. We first study the EXIT chart of IIC MUD, and then distinguish the performance of a ‘good’ channel and a ‘bad’ channel. For the good channel, the tunnel between the detector and decoder is open, so that the trajectory can converge. However, the bad channel will cause the tunnel to close, and the trajectory will be blocked at the very beginning.

From the EXIT chart, we know that if the mutual information of the detector is higher than a certain level, then the tunnel will definitely be open. Based on this situation, we design a channel selection scheme to distinguish the channels by choosing a threshold of the mutual information. We find the relationship between the channel information and the mutual information, so that we can determine the channel either good or bad directly from the channel information.

This technique can effectively suppress the MAI, and can achieve near-optimum BER performance for the overloaded system. This technique removes the error floor perfectly. The BER performance is almost the same as that of MAP, with only 4% rejections.

For the rejected channels, two adaptive transmission schemes are proposed. One is adaptive encoding for the encoder at the transmitter, and a low feedback from the receiver is used for the rate switching. Another is adaptive multiple transmissions, and the feedback from the receiver is also used for the transmission control.

Both of them work well for the deeply fading channels, and remove the error floor perfectly. The exchange rate of the two schemes between the good and bad channel is only 4%, which is the same as the ECR.

Chapter 5

Iterative Interference Cancellation for IDMA Systems

Contents

5.1 Introduction.....	118
5.2 The IDMA System Model.....	120
5.3 The Elementary Signal Estimator (ESE).....	121
5.4 Simulation Results	125
5.5 Conclusions.....	130

In this chapter, the *interleave-division multiple access* (IDMA) [107] is used for the overloaded multiuser MIMO OFDM system. Moreover the *Iterative Interference Cancellation* (IIC) multiuser receiver is used for detection. The simulation results show the IIC MUD can work well in this scenario.

5.1 Introduction

In chapter 3, we have discussed a new low-complexity iterative interference cancellation multiuser detection (IIC-MUD) technique for the overloaded MIMO OFDM system, which can suppress the MAI effectively and can achieve near-optimum BER performance for the two user system. However, for the four user case, the BER performance cannot converge at high SNR when using this technique.

In chapter 4, we analyzed the error floor of the BER performance for the 4-by-2 system. There are some deeply fading channels, where the detector cannot distinguish ‘0’ and ‘1’ in the desired signal in the presence of interference. However, the simulation results show that the probability of these channels is very low. From the EXIT chart, we can see that these fading channels are bad channels, which make the tunnel between the detector and decoder close. Therefore, we designed a channel analyzer and selector to filter out those bad channels by setting a threshold based on the channel information. Although the simulation results show the BER performance is close to the optimum (MAP) performance, those bad channels are filtered out which is kind of wasted.

In light of this, chapter 4 proposed two adaptive schemes for those bad channels, one is using a lower code rate for these bad channels, and another is using multiple transmissions. Both methods can make good use of the bad channels, and achieve near-optimum BER performance. The methods proposed in chapter 4 can remove the error floor completely. Those methods, however, need to calculate the mutual information of the detector output for each channel, and the transmitter needs the feedback from the receiver. For the mutual information, we can directly find the value through the look-up table. For the feedback, however, this is a little troublesome.

Interleave-division multiple access (IDMA) was first proposed in 2002. It inherits many advantages from CDMA such as diversity against fading and mitigation of the worst-case other-cell user interference problem [107]. Combined with low-rate channel coding, user-specific interleavers are employed in IDMA for user separation. The attractive feature of IDMA is that it allows the use of a low-complexity iterative MUD technique.

However, the complexity of IDMA’s receiver still increases linearly with the number of channel paths, which can be overcome by combining with OFDM, called OFDM-IDMA

[108]. Moreover, the extension of OFDM-IDMA into the MIMO transmission has also been proposed in [109] [110], which combines most of the advantages of the multiple access schemes and avoids their individual disadvantages. With OFDM-IDMA, ISI is resolved by an OFDM layer and MAI is suppressed by an IDMA layer, both at low cost. The key advantage of OFDM-IDMA is that the complexity of MUD can be reduced significantly for each user independently of the channel length, and is significantly lower than that of other alternatives [108].

Many previous works on OFDM-IDMA are discussed in [107-113]. The major research areas are frequency synchronization, channel equalization, SNR evolution and so on. [111] combines IDMA and *single carrier frequency division multiple access* (SC-FDMA) and analyzes its sensitivity to *carrier frequency offsets* (CFOs).

[112] proposed a new scheme based on OFDM-IDMA system where the CFO correction is no longer necessary. A new channel estimator is proposed in [110] for the uplink MIMO-OFDM-IDMA system, which employs *soft decision-directed channel estimation* (SDCE) and *tap selection* (TS) to improve the accuracy of the channel estimation. By tracking the average symbol SNR at each iteration and providing a faster solution than brute-force simulations, the SNR evolution can predict the BER performance of the IDMA based systems.

[113] introduced a revised SNR updating formula for OFDM-IDMA systems, which provides a tighter lower bound of the expected SNR in the evolution procedure.

The above works are all based on the *elementary signal estimator* (ESE) receiver, for multipath channels, where the main idea of low complexity of ESE is applying a simple rake-type operation, which however cannot make use of CIRs effectively.

In this chapter, we extend IDMA to the MIMO OFDM system, and then use our IIC multiuser receiver. The simulation results show that the IIC MUD can work well for the IDMA system, whose BER performance is near optimum, without error floor, and much better than the ESE which is widely used for the IDMA system.

This chapter is organized as follows: Section 5.2 introduces the IDMA system model. Section 5.3 shows the details of the ESE. Simulation results are shown in section 5.4. Finally the chapter concludes in section 5.5.

5.2 The IDMA System Model

An uplink MIMO OFDM IDMA system is considered. The key principle of IDMA is that the interleavers should be different for different users. The structure of the system model is illustrated in Fig.5.1. The users' data are first encoded by using a low-rate channel code that is a concatenation of the convolutional and repetition codes. Then each coded bit sequence is interleaved by a user-specific interleaver. The interleavers are generated independently and randomly. Together with the user-specific interleaver, the repetition code performs a kind of spreading, somewhat similar to the spreading in a CDMA system.

Finally, the interleaved coded data is transmitted after the BPSK and OFDM modulation. To balance the +1 and -1, the repetition sequence should be $\{+1, -1, +1, -1, \dots\}$.

Each subcarrier can be occupied by several users, so users are solely distinguished by their interleavers. The received signal after OFDM demodulation can be expressed as

$$\mathbf{r}_k = \mathbf{H}_k \mathbf{s}_k + \mathbf{n}_k, \quad (5.1)$$

where \mathbf{H}_k is an $N_R \times N_T$ equivalent frequency domain channel matrix, $\mathbf{s}_k = [s_1, s_2, \dots, s_{N_T}]^T$ is the transmitted bits and \mathbf{n}_k is the AWGN vector which has zero mean and variance σ_n^2 , and $k = 1 \dots K$ is the subcarrier number. We assume multipath block fading channels are used: in this case the channel coefficients stay constant during one data frame.

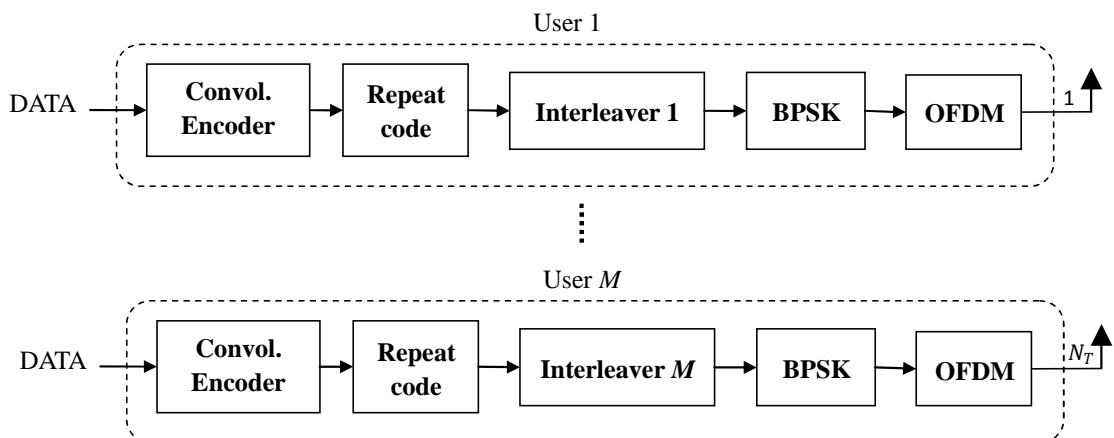


Figure 5.1 The structure of a MIMO-OFDM IDMA system

5.3 The Elementary Signal Estimator (ESE)

In this section, an ESE is introduced, which is used for performance comparison. The ESE, which is proposed for IDMA, is an iterative sub-optimal detection scheme [114]. The structure is shown in Fig.5.2.

As shown in Fig.5.1, the input data sequence of m -th user is encoded based on a low-rate code, generating a coded sequence. The coded bits are permuted by a specific interleaver, so that users are solely distinguished by their interleavers, hence the name IDMA.

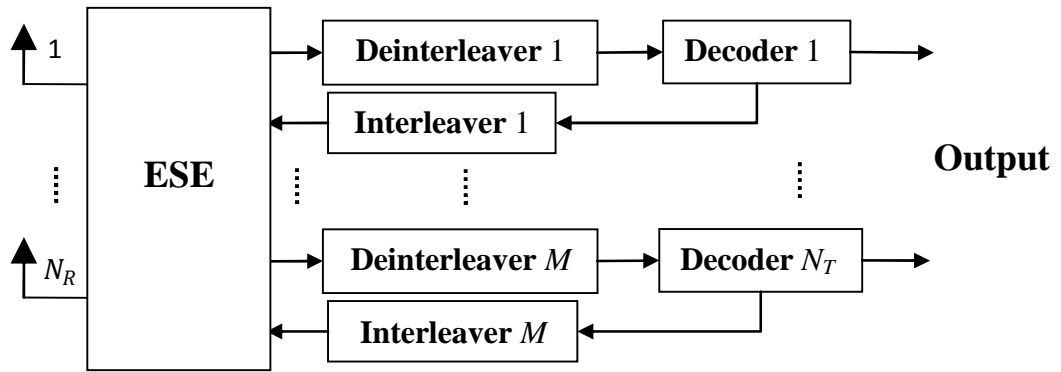


Figure 5.2 The structure of ESE receiver

The most critical point of IDMA is that the interleavers should be different for different users. These interleavers disperse the coded sequences so that the neighbouring code bits are approximately uncorrelated.

The receiver consists of an ESE and M (or N_T) SISO decoders. The multiple access and coding constraints are considered separately in the ESE and SISO decoders. The output of the ESE is extrinsic LLRs about transmitted signal $s_{n_t}(j)$ defined below:

$$\lambda_{ESE}(s_{n_t}(j)) = \log \left(\frac{f(s_{n_t}(j) = +1)}{f(s_{n_t}(j) = -1)} \right), \quad (5.2)$$

where $n_t = 1 \cdots N_T$ is the number of the transmit antennas, and $j = 1 \cdots J$ is the frame length.

Using random interleavers, the ESE operation can be carried out in a bit-by-bit manner, with only one sampler(j) used at a time. For the n_r -th receive antenna, Eq. (5.1) is rewritten as

$$\begin{aligned}
 r_{n_r}(j) &= \sum_{n_t} h_{n_r n_t} s_{n_t}(j) + n(j) \\
 &= h_{n_r n_t} s_{n_t}(j) + \varepsilon_{n_t}(j),
 \end{aligned} \tag{5.3}$$

where

$$\varepsilon_{n_t}(j) = \sum_{n_t' \neq n_t} h_{n_r n_t'} s_{n_t'}(j) + n(j), \tag{5.4}$$

is the interference and noise in $r_{n_r}(j)$ with respect to n_t -th user, and $h_{n_r n_t}$ is the element of equivalent frequency domain channel matrix \mathbf{H} .

From the central limit theorem, $\varepsilon_{n_t}(j)$ can be approximated as a Gaussian variable, and $r_{n_r}(j)$ can be characterized by a conditional Gaussian PDF,

$$\begin{aligned}
 f(r_{n_r}(j) | s_{n_t}(j) = \pm 1) &= \frac{1}{\sqrt{2\pi \text{Var}(\varepsilon_{n_t}(j))}} \cdot \\
 &\exp\left(-\frac{\left(r_{n_r}(j) - \left(\pm h_{n_r n_t} + \text{E}(\varepsilon_{n_t}(j))\right)\right)^2}{2\text{Var}(\varepsilon_{n_t}(j))}\right),
 \end{aligned} \tag{5.5}$$

where $\text{E}(\cdot)$ and $\text{Var}(\cdot)$ are the mean and variance functions respectively.

Using Eq. (5.5), Eq. (5.2) can be rewritten as

$$\begin{aligned}
 \lambda_{ESE}^{n_r}(s_{n_t}(j)) &= \log \left(\frac{\exp\left(-\frac{\left(r_{n_r}(j) - \left(h_{n_r n_t} + \text{E}(\varepsilon_{n_t}(j))\right)\right)^2}{2\text{Var}(\varepsilon_{n_t}(j))}\right)}{\exp\left(-\frac{\left(r_{n_r}(j) - \left(-h_{n_r n_t} + \text{E}(\varepsilon_{n_t}(j))\right)\right)^2}{2\text{Var}(\varepsilon_{n_t}(j))}\right)} \right) \\
 &= -\frac{\left(\left(r_{n_r}(j) - \text{E}(\varepsilon_{n_t}(j))\right) - h_{n_r n_t}\right)^2}{2\text{Var}(\varepsilon_{n_t}(j))} + \frac{\left(\left(r_{n_r}(j) - \text{E}(\varepsilon_{n_t}(j))\right) + h_{n_r n_t}\right)^2}{2\text{Var}(\varepsilon_{n_t}(j))} \\
 &= \frac{2h_{n_r n_t} \cdot \left(r_{n_r}(j) - \text{E}(\varepsilon_{n_t}(j))\right)}{\text{Var}(\varepsilon_{n_t}(j))},
 \end{aligned} \tag{5.6}$$

where

$$E(\varepsilon_{n_t}(j)) = E(r_{n_r}(j)) - h_{n_r n_t} E(s_{n_t}(j)), \quad (5.7)$$

$$\text{Var}(\varepsilon_{n_t}(j)) = \text{Var}(r_{n_r}(j)) - |h_{n_r n_t}|^2 \text{Var}(s_{n_t}(j)). \quad (5.8)$$

For the iterative detecting and decoding process, at the first iteration, we first set the extrinsic LLRs of the decoder $\lambda_C(s_{n_t}(j)) = 0$. According to Eq. (3.19), we can obtain

$$E(s_{n_t}(j)) = \tanh\left(\frac{\lambda_C(s_{n_t}(j))}{2}\right), \quad (5.9)$$

and then, we can calculate

$$\text{Var}(s_{n_t}(j)) = 1 - \left(E(s_{n_t}(j))\right)^2, \quad (5.10)$$

$$E(r_{n_r}(j)) = \sum_{n_t=1}^{N_T} h_{n_r n_t} E(s_{n_t}(j)), \quad (5.11)$$

$$\text{Var}(r_{n_r}(j)) = \sum_{n_t=1}^{N_T} |h_{n_r n_t}|^2 \text{Var}(s_{n_t}(j)) + \sigma_n^2. \quad (5.12)$$

The frequency selective fading channel coefficients are complex values, so the above terms -all take the real part only, due to the BPSK modulation. Using Eq. (5.9)-(5.12), Eq. (5.7) and (5.8) can be calculated, and finally obtained Eq. (5.6). For the multiple receive antennas, a RAKE-type operation is applied:

$$\lambda_{ESE}(s_{n_t}(j)) = \sum_{n_r=1}^{N_R} \lambda_{ESE}^{n_r}(s_{n_t}(j)). \quad (5.13)$$

In Table 5.1 and Table 5.2, the computational complexities of the ESE and IIC receiver are estimated. This is a rough estimation and the complexity in practice depends on different communications scenarios. The computation complexity of the receivers is defined as the required number of operations for the signal processing (the number of multipliers) in the detector per coded symbol and per iteration.

Considering a $N_R \times N_T$ system, for the IIC receiver, only PIC needs repeat the calculation for each iteration. The other operations only need calculate once. However, the ESE requires updating those equations (Eq. (5.6) ~ Eq. (5.12)) for each iteration. According to Table 5.1, the computational complexity of ESE is lower than that of IIC for one iteration, while for the whole iterative processing, the ESE is more complicated

than IIC. However, for 10-by-2 system, after eight iterations, the computational complexity of ESE is lower than that of IIC.

Table 5.1: Complexity comparison between IIC and ESE for 4-by-2 system using BPSK:
 $N_T = 4$, $N_R = 2$, iteration no.=8

MUD	Number of multiplications	
IIC	Matched filter	$O(N_T N_R)$
	Correlation matrix	$O(N_T^2 N_R)$
	LLR converter for first half iterations	$O(N_T^3) + O(N_R^2 N_T) + O(N_T)$
	LLR converter for last half iterations	$O(N_R^2 N_T) + O(N_T)$
	PIC	$O(N_T^2)$ per iteration
	Total	272
ESE	Eq. (5.9)	$O(N_T)$ per iteration
	Eq. (5.10)	$O(N_T)$ per iteration
	Eq. (5.11)	$O(N_R N_T)$ per iteration
	Eq. (5.12)	$O(N_R N_T) + O(N_R N_T)$ per iteration
	Eq. (5.7)	$O(N_R N_T)$ per iteration
	Eq. (5.8)	$O(N_R N_T) + O(N_R N_T)$ per iteration
	Eq. (5.6)	$O(N_R N_T) + O(N_R N_T)$ per iteration
	Total	$72*8=576$

Table 5.2: Complexity comparison between IIC and ESE for 10-by-2 system using BPSK: $N_T = 10$, $N_R = 2$, iteration no.=8

MUD	Number of multiplications
IIC	2120
ESE	$180 \times 8 = 1440$

5.4 Simulation Results

In the simulations, a 4×1 and a 4×2 OFDM IDMA systems are considered. Both users are assumed to employ 1024-bits per frame and 10000 frames with a rate 1/2 convolutional code (with generator [5, 7]) serially concatenated with a low rate repetition code, BPSK and 32 subcarriers for OFDM modulation, and CP length 10. A Rayleigh channel is assumed with uncorrelated fading between all transmit and receive antennas. A block fading channel is used, which means the channel coefficients stay constant for one frame period. 10 iterations are required for the ESE, MAP, and IIC-MUD which is proposed in chapter 3.

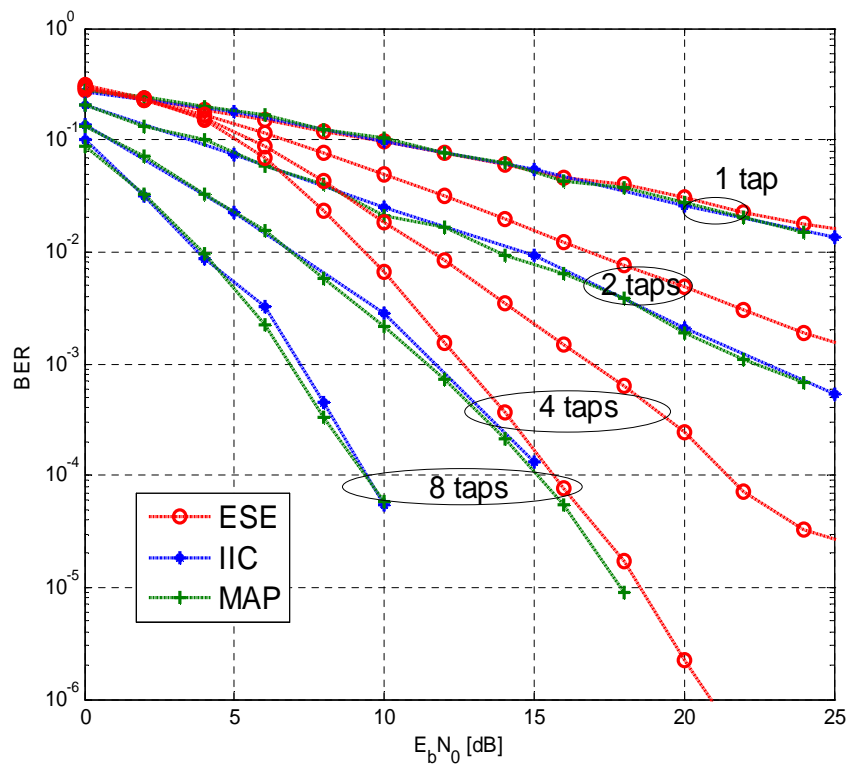


Figure 5.3 BER performance of the 4×1 OFDM-IDMA system with rate-1/4 repetition code (1/8 total rate), ESE, IIC, and MAP approaches are compared

For a comparison, the BER performance and FER performance of the 4×2 OFDM system using IIC are shown in Fig.3.26. Because of some deeply fading channels, the IIC-MUD cannot converge at high SNR, although in practice the FER performance corresponds to an outage probability of less than 1%, good enough for mobile users.

Fig.5.3 shows the BER performance of 4×1 OFDM-IDMA system with rate-1/4 repetition code (1/8 total rate). We consider the multipath with 1 tap (channel coefficient [1]), 2 taps ([1 0.8]), 4 taps ([1 0.8 0.6 0.3]), and 8 taps ([1 0.8 0.6 0.3 0.7 0.5 0.2 0.4]). From the figure, we can see that when channel multipath is more than 1 tap, the performance of IIC-MUD is much better than ESE MUD. After 10 iterations, the IIC-MUD can achieve almost the optimal (MAP) performance. Fig.5.4 shows the BER performance of 4×2 OFDM-IDMA system with rate-1/2 repetition code (1/4 total rate). Compared to Fig.3.26, the IIC-MUD now can work very well. The performance of the proposed IIC-MUD is still much better than that of ESE MUD. Especially for 2 taps channel, the BER performance of ESE MUD seems to have an error floor, which is the same as shown in Fig.3.26. These results have been published in [115].

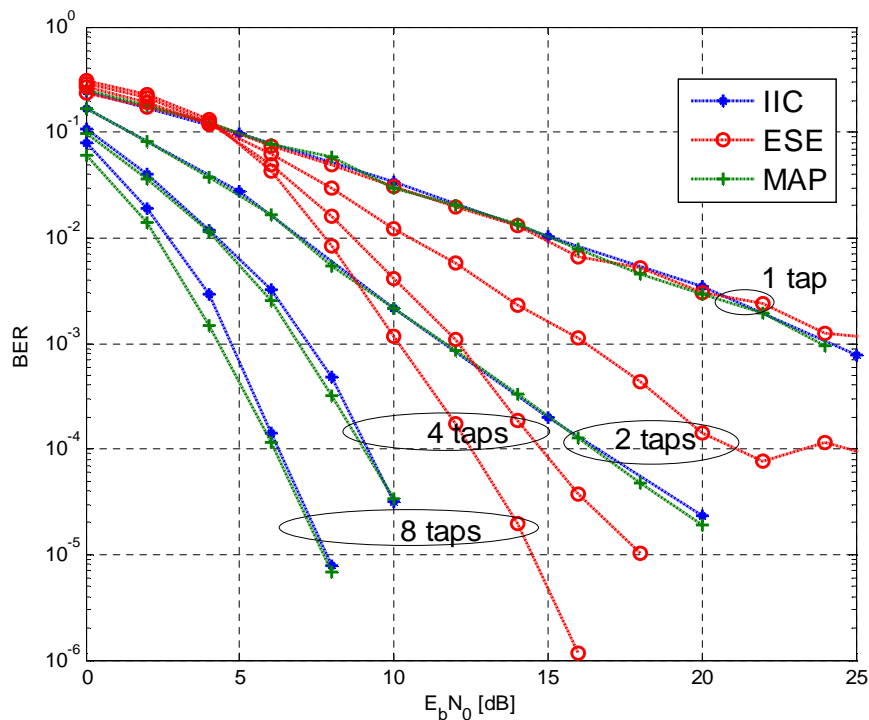


Figure 5.4 BER performance of the 4×2 OFDM-IDMA system with rate-1/2 repetition code (1/4 total rate), ESE, IIC, and MAP approaches are compared

From Fig. 5.3 and Fig. 5.4, we can see that employed the IDMA in transmitter, the IIC-MUD can make full use of CIRs and obtain channel gain, and achieve almost the optimal (MAP) performance. Fig. 5.5 illustrates the EXIT chart of the 4×2 OFDM-IDMA system with rate-1/2 repetition code (1/4 total rate) over 10000 channels, where the decoder with IDMA and without IDMA are compared. The EXIT curve of the decoder without IDMA intersects with the IIC detector EXIT curve at the right top corner, while the tunnel between the EXIT curve of decoder with IDMA and the detector EXIT curve is open all the time. This explains why IIC can work well for the 4×2 OFDM-IDMA system.

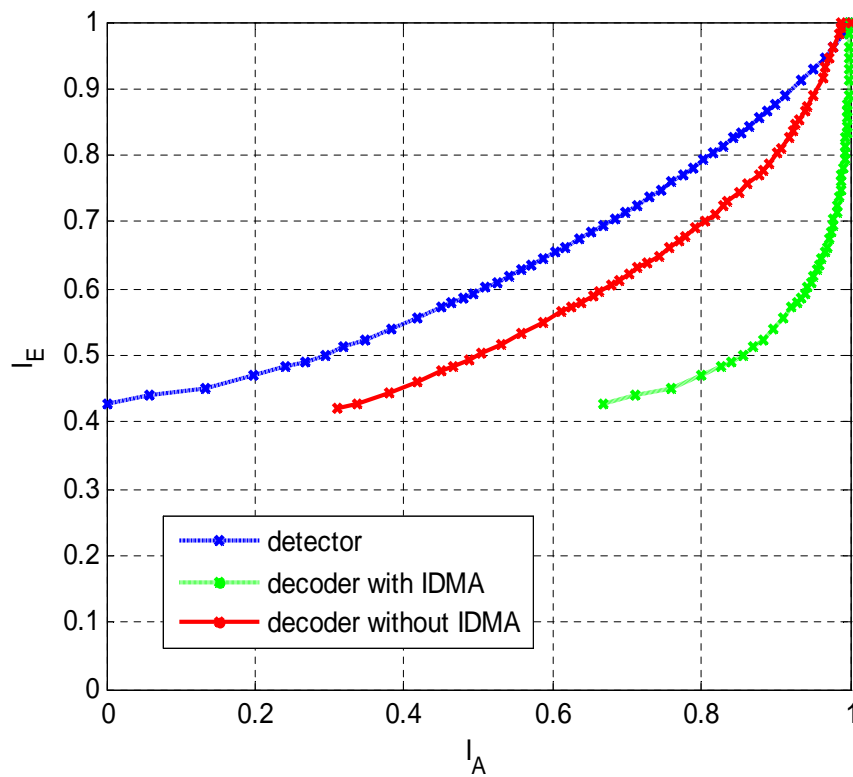
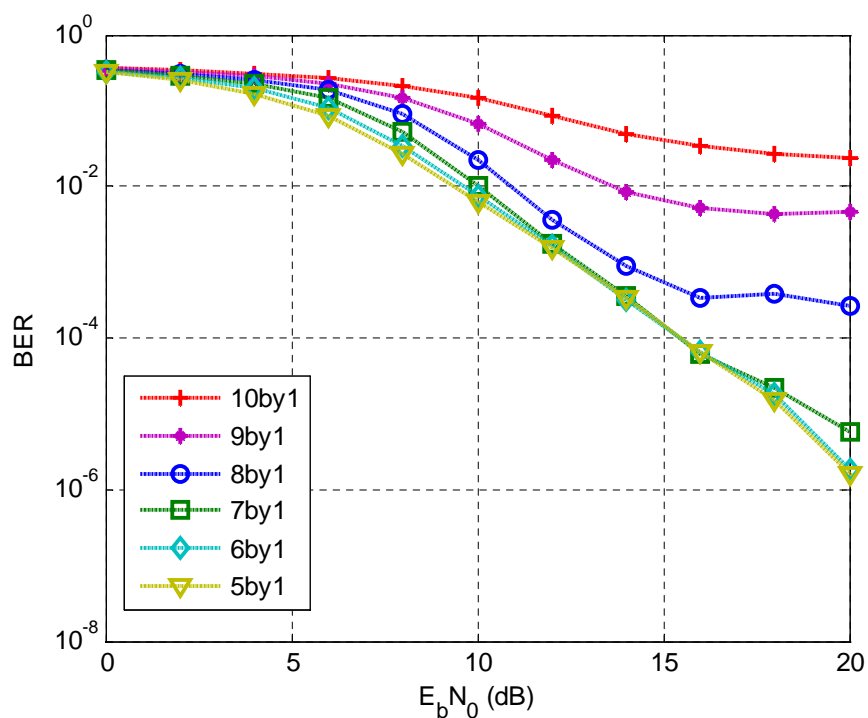
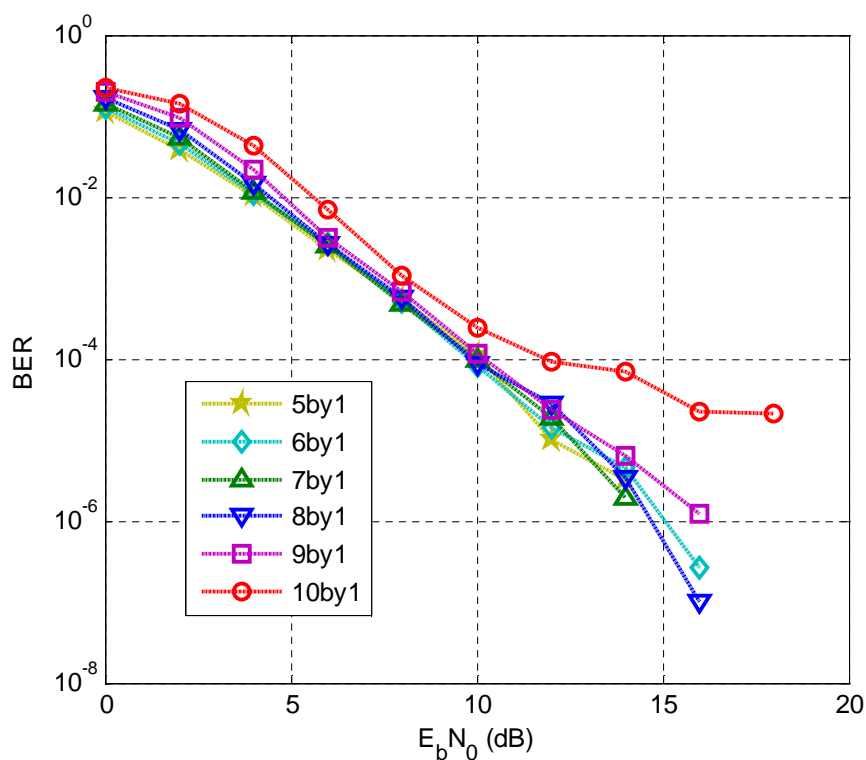


Figure 5.5 EXIT chart of the 4×2 OFDM-IDMA system with rate-1/2 repetition code (1/4 total rate); With IDMA and without IDMA are compared

Fig 5.6 and 5.7 present the comparison of BER performance between ESE and IIC under eight taps' multipath channel for different users, or different OLF. As shown in Fig. 5.6, the IIC can work for a nine user system by using a rate 1/4 repetition code where OLF is 9, while the ESE cannot work for the eight user system. Fig. 5.7 shows the IIC can work for the nine user system by using rate 1/2 repetition code where OLF is 4.5, while the ESE cannot work even for the six user case.

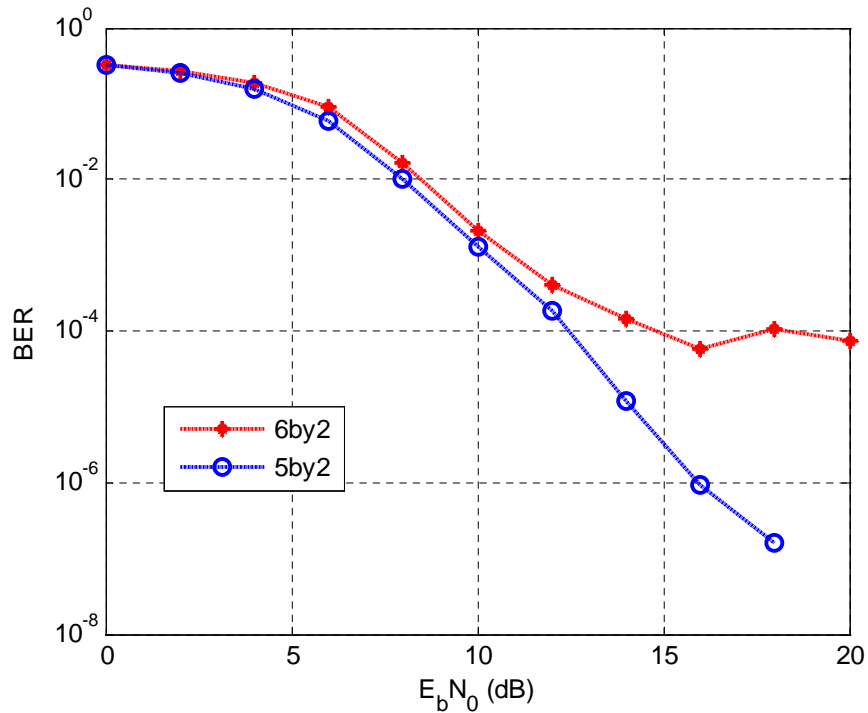


(a) ESE

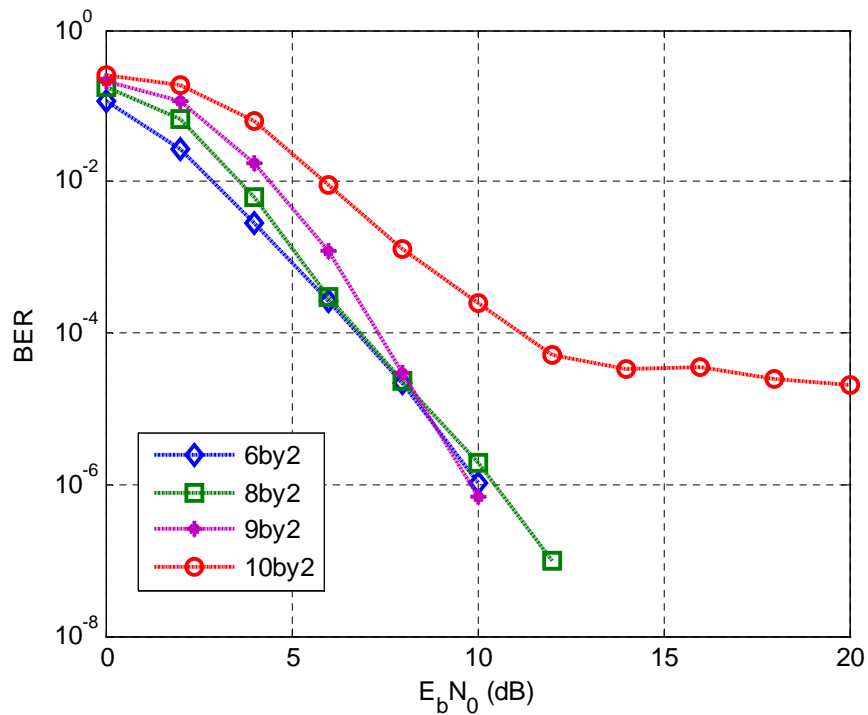


(b) IIC

Figure 5.6 BER performance of OFDM-IDMA system with rate-1/4 repetition code (1/8 total rate) for different users; With ESE (a) and with IIC (b) are compared



(a) ESE



(b) IIC

Figure 5.7 BER performance of OFDM-IDMA system with rate-1/2 repetition code (1/4 total rate) for different users; With ESE (a) and with IIC (b) are compared

In both cases, IIC cannot work for the ten user system, which is the same as shown in chapter 3 where a lower code rate is required for the ten user system. Here, a lower code rate of the repetition code is also required. Fig. 5.8 shows that using a lower

code rate of the repetition code can achieve better performance for the ten user system.

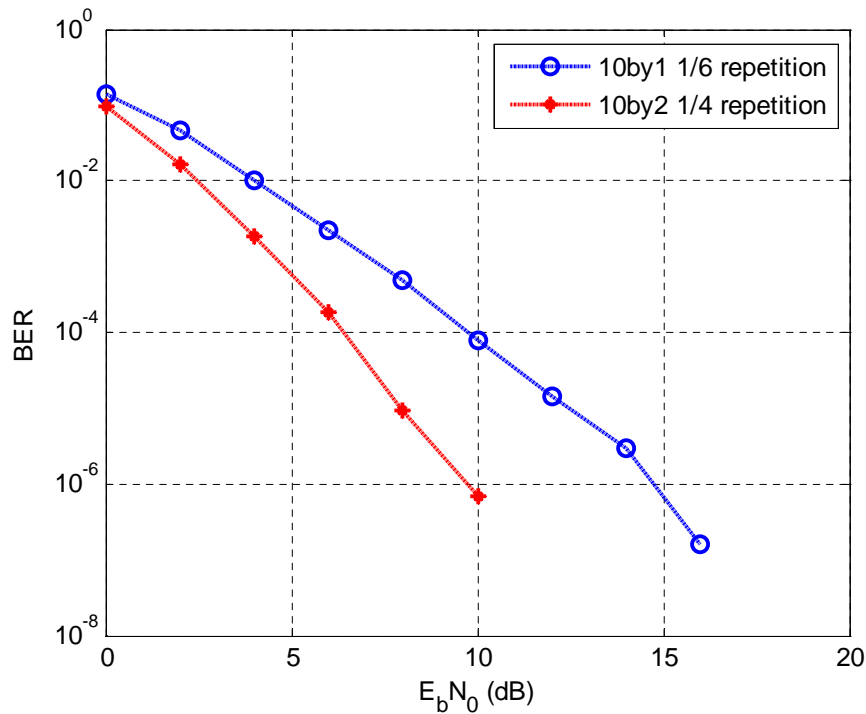


Figure 5.8 BER performance of OFDM-IDMA system for ten user case: 10-by-1 with rate-1/6 repetition code (1/12 total rate) and 10-by-2 with rate-1/4 repetition code (1/8 total rate)

5.5 Conclusions

The low complexity iterative interference cancellation (IIC) multiuser detection method, which is introduced in chapter 3, now is used for overloaded multiuser MIMO OFDM IDMA systems in this chapter.

The IDMA system is first discussed. Then for comparison, the ESE which is widely used for IDMA system is introduced. This technique is of a low complexity for a high number of user. However, the simulation results show that our IIC scheme performs much better than ESE. For a multipath channel, the more channel taps, the better the BER performance (compared to ESE).

The BER performance shows that the IIC can effectively suppress the MAI, make full use of channel information to obtain the channel gain, and can achieve almost optimal (MAP) BER performance for the overloaded system.

Chapter 6

Channel Estimation for Iterative Interference cancellation Multiuser Detection

Contents

6.1 Introduction.....	132
6.2 Wiener Filter	133
6.3 Iterative Channel Estimation by Wiener Filter.....	138
6.4 Iterative Channel Estimation for MIMO Systems.....	140
6.5 Simulation Results	142
6.6 Conclusions.....	149

In our previous work, it is assumed that perfect channel knowledge is known at the receiver. In practice, however, it is necessary to obtain the channel impulse response by means of channel estimation. In this chapter, Wiener filter based channel estimation is introduced, and our *Iterative Interference Cancellation* (IIC) multiuser receiver is tested under the estimated channel.

6.1 Introduction

In wireless communications, the availability of channel knowledge at the receiver is the key to achieve reliable coherent reception and the accuracy of channel estimation affects the system performance critically.

In previous chapters, we assumed the channel knowledge is perfectly known at the receiver. Our low-complexity iterative interference cancellation multiuser detection (IIC-MUD) scheme is based on the perfect channel knowledge (PCK), and achieves near-optimum BER performance for the two user system. For more users, the channel analyzer and selector are applied, which are also based on PCK.

What if the channel is not perfectly known at the receiver? How accurate must channel knowledge be not to affect the performance of our detection? These two issues will be answered in this chapter.

Considering the system model in chapter 3, the received signal can be expressed as

$$\mathbf{r} = \mathbf{H}\mathbf{s} + \mathbf{n}, \quad (6.1)$$

where \mathbf{H} is the channel matrix, \mathbf{s} is the transmitted data, and \mathbf{n} is White Gaussian noise with zero mean and variance σ_n^2 , respectively.

Assume the channel matrix is not perfectly known at the receiver,

$$\hat{\mathbf{H}} = \mathbf{H} + \mathbf{H}_{error}, \quad (6.2)$$

where \mathbf{H}_{error} is the random Gaussian variables with zero mean and variance σ_H^2 , which also can be considered as the *mean square error* (MSE).

We assume some fixed values of the MSE, and then generate \mathbf{H}_{error} randomly to obtain several different non-perfect channel matrices $\hat{\mathbf{H}}$. Using the IIC-MUD based on the two user system, Fig. 6.1 shows the BER performance of 2-by-1 OFDM system influenced by the accuracy of the channel knowledge.

From Fig. 6.1, we can see that the accuracy of the channel knowledge did affect the performance of IIC, where the BER error floor appears when the channel is badly estimated. As the MSE decreases, the BER is improved significantly. When the MSE is 0.0005, the performance of IIC is almost the same as with PCK.

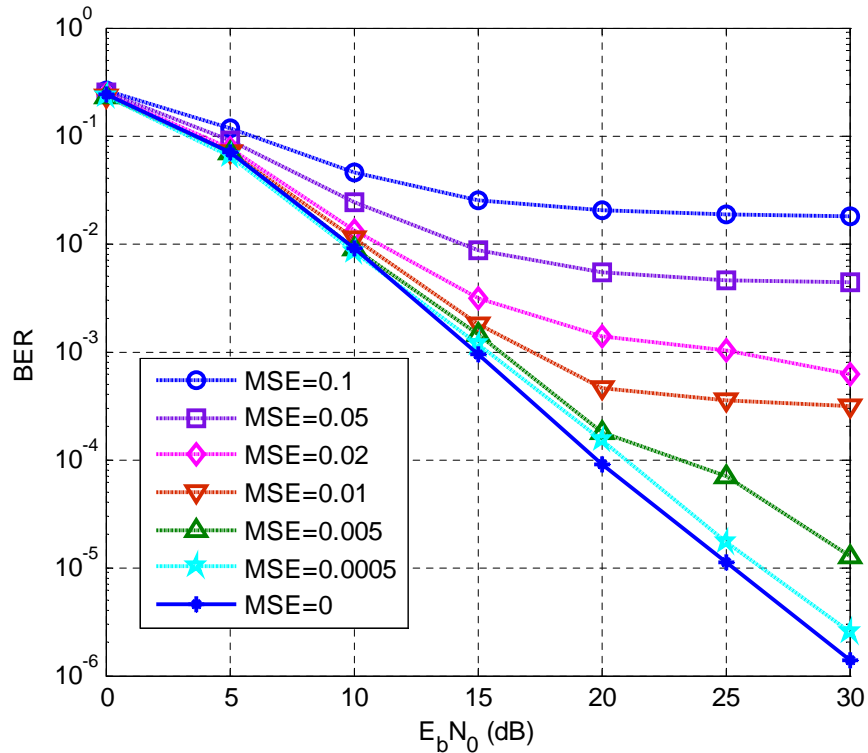


Figure 6.1 BER performance of IIC with imperfect channel knowledge

As shown in Fig. 6.1, as long as the MSE less than 0.0005, IIC can work very well. Considering our system, MIMO OFDM system, a pilot-based channel estimation scheme which can achieve lower MSE is employed. In this chapter, a Wiener filter based *linear minimum mean square error* (LMMSE) estimation approach [116] [117] is employed, which is simple and easy to implement for the OFDM system.

This chapter is organized as follows: Section 6.2 introduces the channel estimation by Wiener filtering. Section 6.3 shows the iterative channel estimation. Simulation results are shown in section 6.4. Finally the chapter concludes in section 6.5.

6.2 Wiener Filter

The basic principle of pilot-assisted channel estimation is to estimate the channel values at any time or frequency at the receiver, by inserting pilot symbols known by the receiver into transmitted data at different time or frequency. There are two types of pilot insertion: one is using one whole OFDM symbol to transmit the pilot, and the other is inserting N_p pilots to an OFDM symbol, where N_p should be larger than the number of delay taps, as shown in Fig. 6.2.

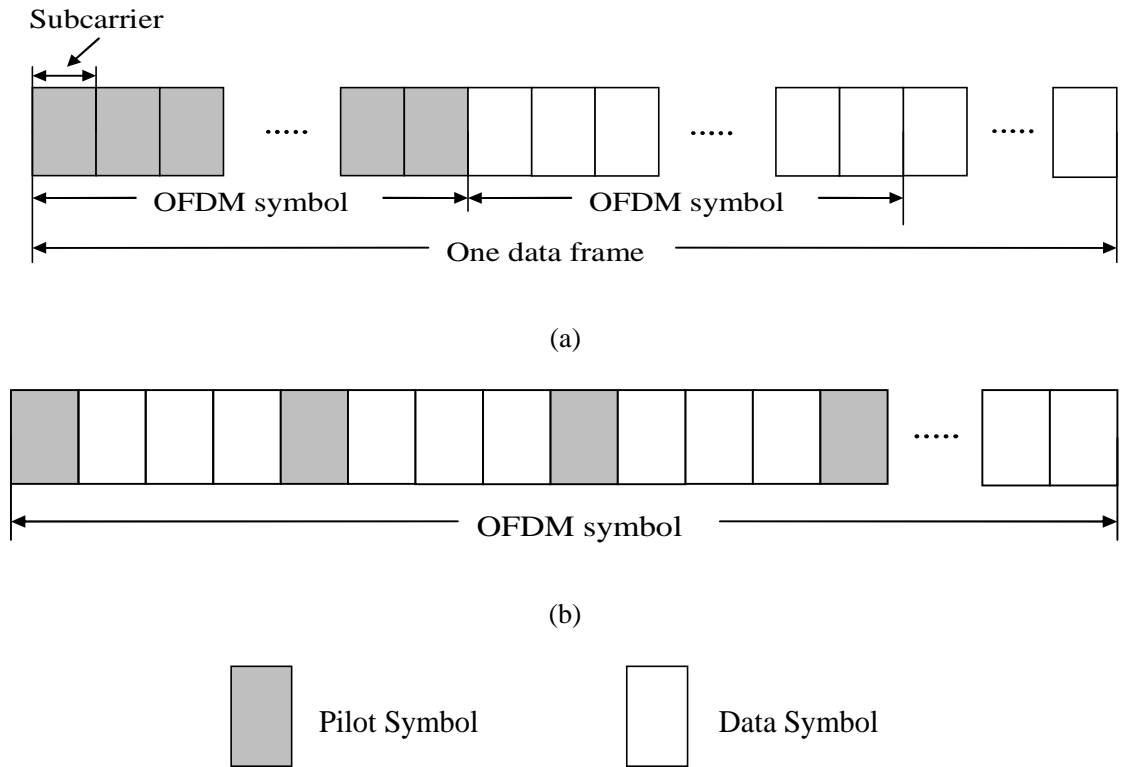


Figure 6.2 Pilot insertion structures: (a) using one whole OFDM symbol for transmitting pilots, and (b) using interpolation during one OFDM symbol

The Wiener filter (the LMMSE estimation approach) is capable of approaching a low accuracy bound [118]. The use of the Wiener filter for the channel estimation was used in [116-119]. Both pilot insertion structures shown in Fig. 6.2 are widely used, while, in this section, we will consider the structure in Fig. 6.2(a). An infinite length Wiener filter is optimal in the sense of minimum MSE. In practice, however, a finite length has to be used.

The problem of this estimator is to find the channel estimates as a linear combination of the pilot estimates and provide noise suppression as well. The corresponding structure of the channel estimator is shown in Fig. 6.3. For transmitting pilots, the received signal of Eq. (6.1) can be rewritten as

$$\mathbf{r}_p = \mathbf{s}_p \mathbf{h}_p + \mathbf{n}_p, \quad (6.3)$$

where \mathbf{r}_p is the $N_p \times 1$ received vector, \mathbf{s}_p is a $N_p \times N_p$ diagonal matrix containing pilots only, \mathbf{h}_p is a channel attenuation vector, and \mathbf{n}_p is the Gaussian noise. The noise \mathbf{n}_p is assumed to be uncorrelated with the channel \mathbf{h}_p .

The channel estimate vector can be obtained by the least square approach:

$$\hat{\mathbf{h}}_{LS} = \left[\frac{r_1}{s_1}, \frac{r_2}{s_2}, \dots, \frac{r_{N_P}}{s_{N_P}} \right]^T. \quad (6.4)$$

Note that $\hat{\mathbf{h}}_{LS}$ is rough estimate including the effect of noise, and the variance of that noise is also the variance of estimation errors.

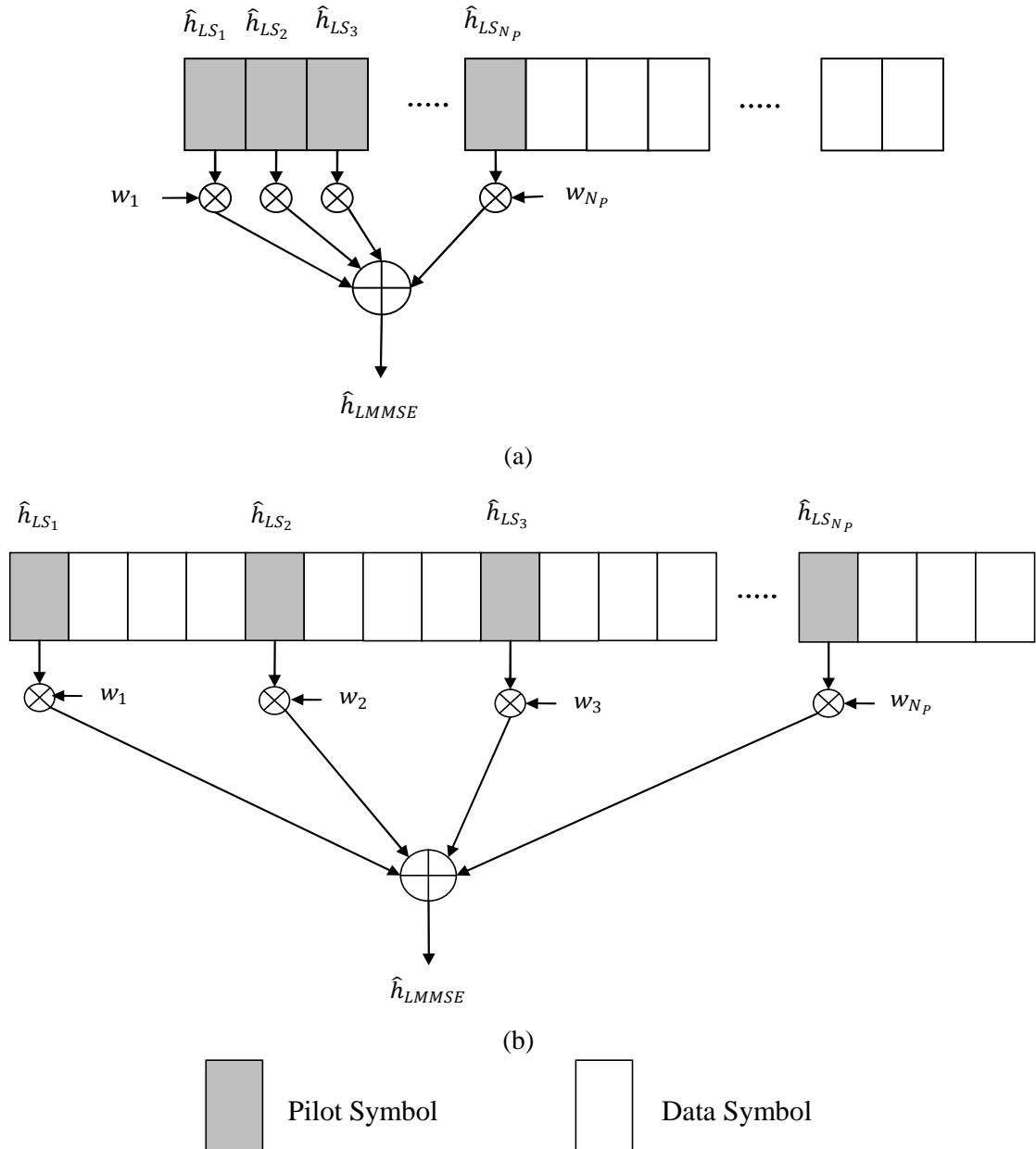


Figure 6.3 Two structures of Channel estimation by Wiener filtering: (a) using one whole OFDM symbol for transmitting pilots, and (b) using interpolation during one OFDM symbol

In the OFDM system, channel estimates are obtained across time or frequency by using channel time or frequency correlations respectively.

For a time fading signal, assuming Jakes' isotropic scattering model [119], the time correlation matrix \mathbf{R}_{hh}^t is given by [117]

$$\mathbf{R}_{hh}^t(m, n) = J_0(2\pi f_d T_s(m - n)), \quad (6.5)$$

where m and n are pilot or data positions over all transmitted OFDM symbols, J_0 is the 0-th order Bessel function of the first kind, f_d is the maximum Doppler frequency, and T_s is the OFDM symbol period including the guard time.

The frequency correlations are obtained differently depending on the power delay profile of the multipath channel:

- a) For a uniformly distributed power delay profile [116],

$$\mathbf{R}_{hh}^f(m, n) = \begin{cases} 1, & \text{if } m = n \\ \frac{1 - e^{-j2\pi L \frac{m-n}{N_s}}}{j2\pi L \frac{m-n}{N_s}}, & \text{if } m \neq n \end{cases} \quad (6.6)$$

- b) For an exponentially decay power delay profile [117],

$$\mathbf{R}_{hh}^f(m, n) = \frac{1}{1 + 2\pi j \tau_{rms} f_s (m - n)}, \quad (6.7)$$

where L is the order of the multipath channel, N_s is the FFT size or the number of subcarriers, τ_{rms} is the root-mean-square delay spread of the multipath channel, and f_s is the subcarrier spacing which is taken from the inverse of the useful OFDM symbol time excluding the guard time.

A MMSE estimator is designed to minimize the MSE between actual channel values and channel estimates, which is satisfied by [122]

$$\mathbf{W} = \mathbf{R}_{DP} \widehat{\mathbf{R}}_{PP}^{-1}, \quad (6.8)$$

where \mathbf{W} is the $N_D \times N_P$ Wiener filter interpolation matrix, N_D is the number of data symbols, \mathbf{R}_{DP} is a $N_D \times N_P$ matrix containing cross correlations between data symbols and pilot symbols, and $\widehat{\mathbf{R}}_{PP}$ is a $N_P \times N_P$ matrix containing autocorrelations between pilot symbols including noise smoothing [122],

$$\widehat{\mathbf{R}}_{PP} = \mathbf{R}_{PP} + \sigma_n^2 (\mathbf{s}_P \mathbf{s}_P^H)^{-1}, \quad (6.9)$$

where \mathbf{R}_{PP} is a $N_P \times N_P$ matrix containing autocorrelations between pilot symbols. The elements in \mathbf{R}_{DP} and \mathbf{R}_{PP} are all obtained from the channel correlation R_{hh} .

For \mathbf{R}_{DP} , $m(1 \leq m \leq N_D)$ is the order number in the data symbol sequence or subcarrier sequence, and $n(1 \leq n \leq N_p)$ is the order number in the pilot symbol sequence or subcarrier sequence. For \mathbf{R}_{PP} , $m, n(1 \leq m, n \leq N_p)$ denote the order number in the pilot symbol sequence or subcarrier sequence.

Using Wiener filtering, more accurate channel estimates are obtained [117]

$$\hat{\mathbf{h}}_{LMMSE} = \mathbf{W}\hat{\mathbf{h}}_{LS}. \quad (6.10)$$

Substituting Eq. (6.8) (6.9) into (6.10), the LMMSE estimate of the channel is expressed as

$$\hat{\mathbf{h}}_{LMMSE} = \mathbf{R}_{DP} \left(\mathbf{R}_{PP} + \sigma_n^2 (\mathbf{s}_P \mathbf{s}_P^H)^{-1} \right)^{-1} \hat{\mathbf{h}}_{LS}. \quad (6.11)$$

The complexity of the LMMSE estimator is that a matrix inversion is needed every time the data in \mathbf{s}_P changes. [116] reduce the complexity of this estimator by replacing the term $(\mathbf{s}_P \mathbf{s}_P^H)^{-1}$ in Eq. (6.11) with its expectation $E\{(\mathbf{s}_P \mathbf{s}_P^H)^{-1}\}$. So that the simplified estimator can be obtained [116]

$$\hat{\mathbf{h}}_{LMMSE} = \mathbf{R}_{DP} \left(\mathbf{R}_{PP} + \frac{\beta}{\text{SNR}_P} \mathbf{I} \right)^{-1} \hat{\mathbf{h}}_{LS}, \quad (6.12)$$

where

$$\beta = E\{|s|^2\}E\{1/|s|^2\}, \quad (6.13)$$

is a constant depending on the signal constellation, e.g., $\beta = 17/9$ for 16-QAM and $\beta = 1$ for BPSK;

$$\text{SNR}_P = \frac{E\{|s|^2\}}{\sigma_n^2}, \quad (6.14)$$

is the pilot symbol power to noise power ratio, and \mathbf{I} is a $N_p \times N_p$ identity matrix. This simplified estimator does not need to calculate the matrix inversion frequently. Moreover, if the channel model or certain property (such as power delay profile, delay spread, and so on) of the fading channel is given, \mathbf{R}_{DP} and \mathbf{R}_{PP} are known beforehand or are set to fixed nominal values, the inversion term in Eq. (6.12) needs to be calculated only when SNR_P changes.

6.3 Iterative Channel Estimation by Wiener Filter

The Wiener filter has been used for iterative channel estimation of fast flat fading channels and dramatic performance gains over non-iterative schemes are achieved [121][122]. In this section, the benefits of the outer coding and the iterative channel estimation are considered. The system model is shown in Fig. 6.4.

At the transmit end, the user's data is first encoded by a convolutional encoder, then the output of the encoder is interleaved to break up the correlated fading channel for avoiding burst errors. After BPSK modulation, pilot symbols are then inserted into the interleaved coded symbols. Then OFDM modulation is applied, it passes through the fading channel (noise is added here), and the modulated signal is received at the receiver.

After OFDM demodulation, the channel estimates are first obtained from the Wiener filter based on the pilots known at the receiver, using Eq. (6.4) and (6.12). Such channel estimates are often not accurate as the number of pilots is small. The estimation can be refined by treating soft decision of the coded symbol as a pilot symbol at the next iteration. Since the soft value $\tilde{\mathbf{s}}$ which contains not only the data value but also the corresponding probability, is used, Eq. (6.4) is written as

$$\hat{\mathbf{h}}_{LS}^i = \mathbf{r}\tilde{\mathbf{s}}^*, \quad (6.15)$$

where i is the iteration number, and $\tilde{\mathbf{s}}^*$ is the conjugate of the soft values. And Eq. (6.12) is written as

$$\hat{\mathbf{h}}_{LMMSE}^i = \mathbf{R}_{hh} \left(\mathbf{R}_{hh} + \frac{\beta}{\text{SNR}} \mathbf{I} \right)^{-1} \hat{\mathbf{h}}_{LS}^i, \quad (6.16)$$

where \mathbf{R}_{hh} is a $N_{P+D} \times N_{P+D}$ matrix containing autocorrelations between pilot and data symbols, N_{P+D} is the total length of data and pilot symbols, and SNR is the signal (including data and pilots) to noise ratio. We use the whole \mathbf{R}_{hh} here, because we take the whole data plus pilots as known pilots.

For each iteration, the estimator uses the improved soft data bits as known pilots to obtain more accurate estimates. The estimator and the decoder work in an iterative manner and the overall performance is expected to improve as the number of iterations increases.

The MSE of the above LMMSE channel estimation is calculated by

$$\text{MSE}_{\text{simulated}} = E \left\{ \left| \mathbf{h} - \hat{\mathbf{h}}_{\text{LMMSE}} \right|^2 \right\}, \quad (6.17)$$

where \mathbf{h} is the actual channel matrix, and $\hat{\mathbf{h}}_{\text{LMMSE}}$ is the estimated channel matrix.

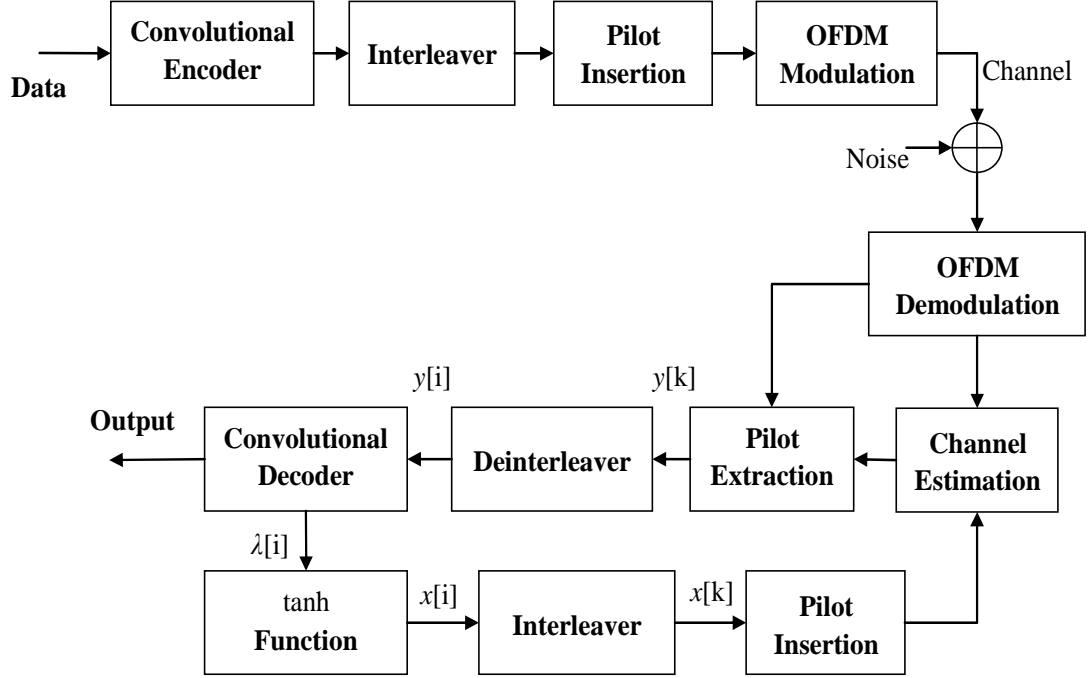


Figure 6.4 System structure of iterative channel estimation and signal detection

In order to compare the accuracy of the estimation, the MSE reference is given by [123]

$$\text{MSE}_{\text{reference}} = \frac{1}{N_D} \sum_{i=1}^{N_D} \Phi(i, i), \quad (6.18)$$

where the reference matrix

$$\Phi = \mathbf{I} - \mathbf{R}_{\text{DP}} \left(\mathbf{R}_{\text{PP}} + \frac{\beta}{\text{SNR}} \mathbf{I} \right)^{-1} \mathbf{R}_{\text{DP}}^{\text{H}}. \quad (6.19)$$

For the iterative case, the LMMSE estimator is changed after the first iteration :

$$\hat{\mathbf{h}}_{\text{LMMSE}} = \mathbf{R}_{\text{hh}} \left(\mathbf{R}_{\text{hh}} + \frac{\beta}{\text{SNR}} \mathbf{I} \right)^{-1} \hat{\mathbf{h}}_{\text{LS}}^{\text{iter}}, \quad (6.20)$$

and the MSE reference matrix also becomes

$$\Phi = \mathbf{I} - \mathbf{R}_{\text{hh}} \left(\mathbf{R}_{\text{hh}} + \frac{\beta}{\text{SNR}} \mathbf{I} \right)^{-1} \mathbf{R}_{\text{hh}}^{\text{H}}. \quad (6.21)$$

6.4 Iterative Channel Estimation for MIMO Systems

For the MIMO system, the system model is different from the SISO system. For the transmitter, the main difference between the MIMO and the SISO system is the pilot insertion. We insert the pilots for the different users separately, which means for the N_T user case we use N_T OFDM symbol to insert pilots (first symbol for first user, second symbol for second user, and so on), as shown in Fig. 6.5.

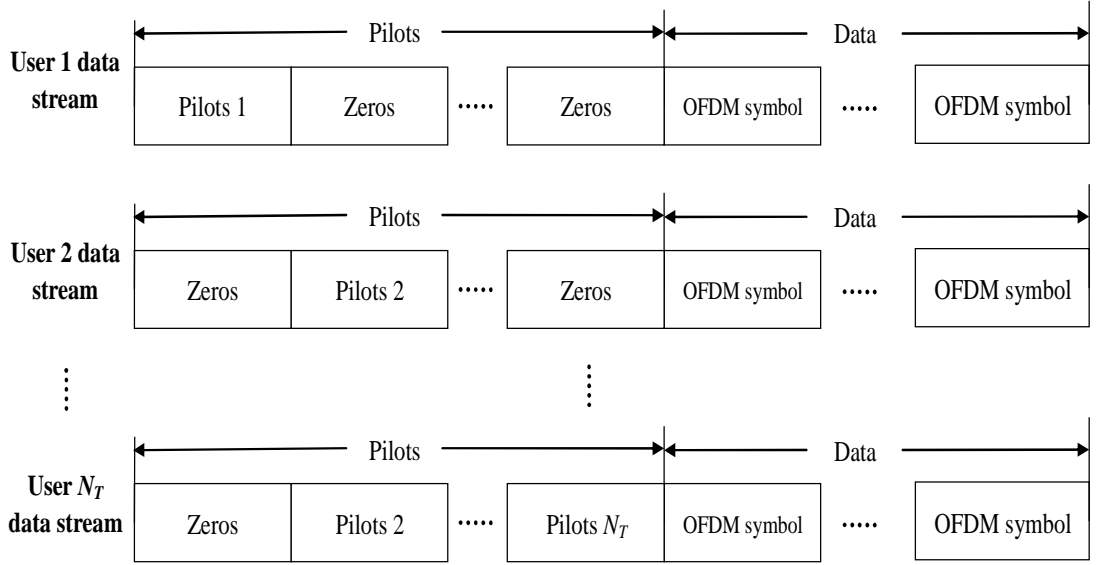


Figure 6.5 Pilots insertion for MIMO system

The receiver structure is shown in Fig. 6.6. As shown in Fig. 6.5, we can see that the interference is zero for the desired users' pilots. Therefore, Eq. (6.4) and (6.12) can be directly used for the first iteration. For the following iterations, however, we need to consider the interference cancellation for the channel estimation, because the whole data frame is taken as known pilots.

Eq. (6.15) can be rewritten as

$$\hat{\mathbf{h}}_{LS}^i = [\hat{h}_{LS}^1, \hat{h}_{LS}^2, \dots, \hat{h}_{LS}^K], \quad (6.22)$$

$$\hat{h}_{LS}^k = \left(\mathbf{r} - \begin{bmatrix} 0 & \hat{h}_{12} & \dots & \hat{h}_{1N_T} \\ \hat{h}_{21} & 0 & \dots & \hat{h}_{2N_T} \\ \vdots & \vdots & \ddots & \vdots \\ \hat{h}_{N_R1} & \hat{h}_{N_R2} & \dots & 0 \end{bmatrix} \tilde{\mathbf{s}}^* \right) .* \tilde{\mathbf{s}}^*, \quad (6.23)$$

where \hat{h}_{n_r, n_t} is the (n_r, n_t) -th channel estimate from the previous iteration.

There is another way to obtain \hat{h}_{LS}^k by using the pseudo-inverse method. In this case, we do not need the interference cancellation during the channel estimation.

$$\hat{h}_{LS}^k = \mathbf{r}_k \mathbf{S}_k^H (\mathbf{S}_k \mathbf{S}_k^H)^{-1}, \quad (6.24)$$

where $k = 1, 2, \dots, K$ is the subcarrier number.

And then Eq. (6.16) is used to obtain more accurate estimates $\hat{\mathbf{h}}_{LMMSE}^i$. The channel estimator, the detector and the decoder work like iterative cycle. For each iteration, the updated channel estimates will improve the results of the detector, which are used for the decoder, and then generate more reliable outputs. As the iteration number increases, the decoder will perform better and better.

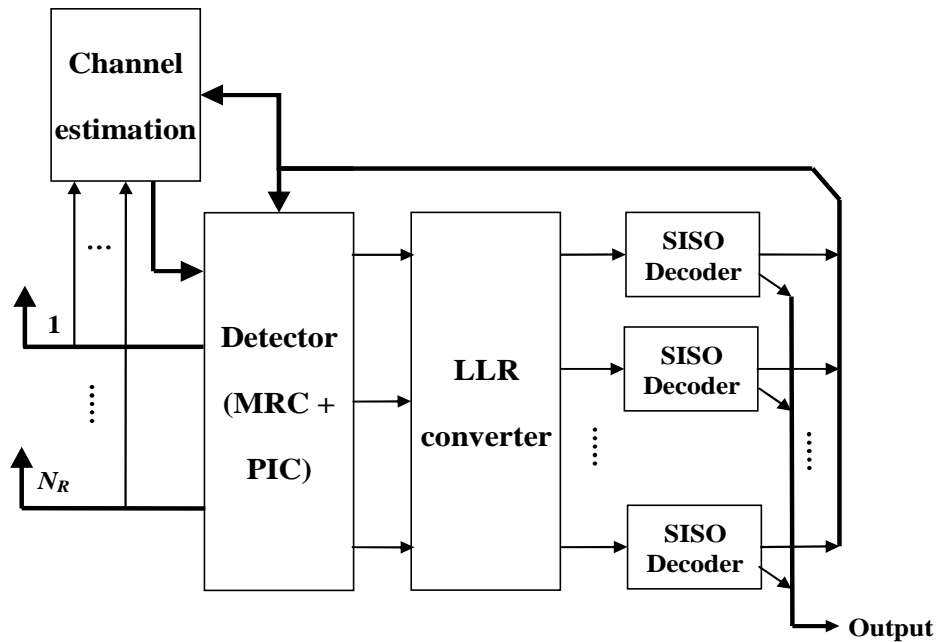


Figure 6.6 Receiver structure of channel estimation for MIMO system

The computational complexity comparison between interference cancellation and the pseudo-inverse method for iterative channel estimation is estimated below. This is a rough estimation and the complexity in practice depends on different communications scenarios. The computation complexity of the receivers is defined as the required number of operations for the signal processing (the number of multipliers) in the detector per data frame and per iteration.

For the iterative channel estimation, both the pilots and soft data in previous iteration are considered as the known pilots in the next iteration. Hence the interference cancellation method has the complexity of $O(N_T N_R N K) + O(N_T N K)$, where N is the length of

OFDM symbol, K is the subcarrier number. The pseudo-inverse method need a matrix inversion, so it has the complexity of $(N_T^2 N_R K) + O(N_R N_T K N) + O(N_T^2 N_R K N)$. Both methods need to be repeated for each iteration. Table 6.1 shows the specific case of the complexity comparison between these two methods

Table 6.1: Complexities comparison between interference cancellation and pseudo-inverse method for channel estimation

Interference cancellation	26112 per iteration
Pseudo-inverse method	88064 per iteration

no. of transmitter $N_T = 4$, no. of receiver $N_R = 2$,
 no. of OFDM symbols $N = 68$ (64 data symbols and 4 pilot symbols),
 no. of subcarriers $K = 32$

6.5 Simulation Results

In this section, a SISO OFDM system is first considered. The transmitter employs 128-bit/frame and 10000 frames with a rate 1/2 convolutional code (with generator [5, 7]), BPSK modulation, and OFDM modulation with 16 subcarriers. A Rayleigh channel is assumed with uncorrelated fading between all transmit and receive antennas. A block fading two tap channel is used, which means the channel coefficients stay constant for one frame period, with uniformly distributed power delay profile.

The MSE performance of SISO OFDM system is presented in Fig. 6.7, where channel estimation by Wiener filter based on pilots is considered. The MSE reference with only pilot length (one OFDM symbol, *i.e.* 16 bits here) is also presented. As shown in Fig. 6.7, we can see that the MSE can achieve less than 10^{-3} at 30dB, even just based on pilots (with only one iteration), which is good enough for our IIC detector.

Fig. 6.8 shows the MSE performance of overloaded 2-by-1 OFDM system. Here, the pilots are transmitted through one OFDM symbol period, and only one iteration channel estimation is considered. At 30dB, the MSE is 0.0007, which is small enough to make sure the BER converge. The BER performance of this case is presented in Fig. 6.9, compared to the IIC with PCK, IIC works well under the estimated channel, after eight iterations.

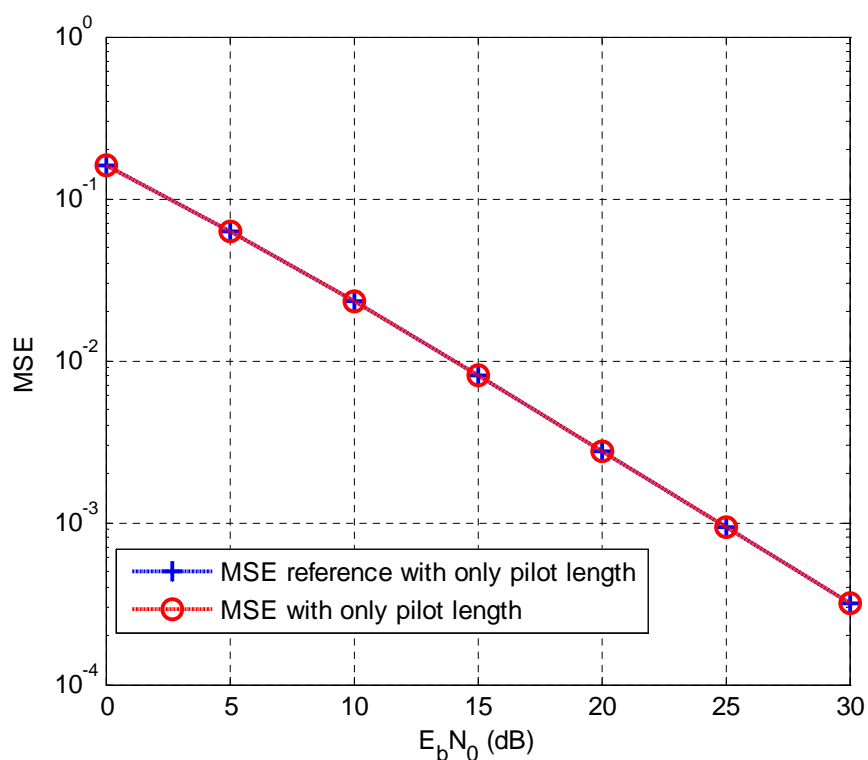


Figure 6.7 MSE performance for SISO OFDM system by Wiener filter

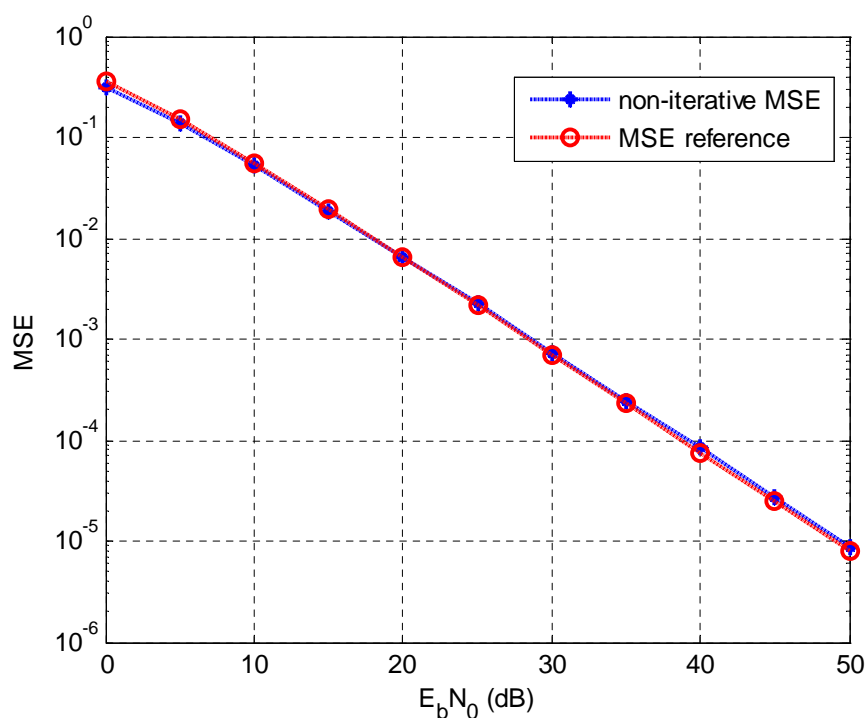


Figure 6.8 MSE performance for 2-by-1 OFDM system by Wiener filter, with only one iteration

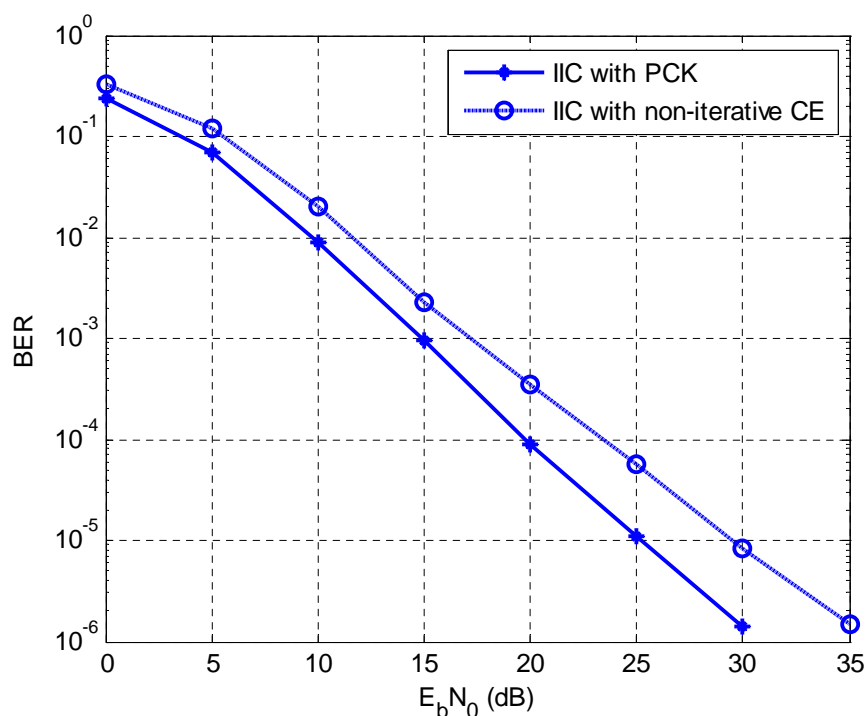


Figure 6.9 BER performance of 2-by-1 OFDM system with only one iteration channel estimation

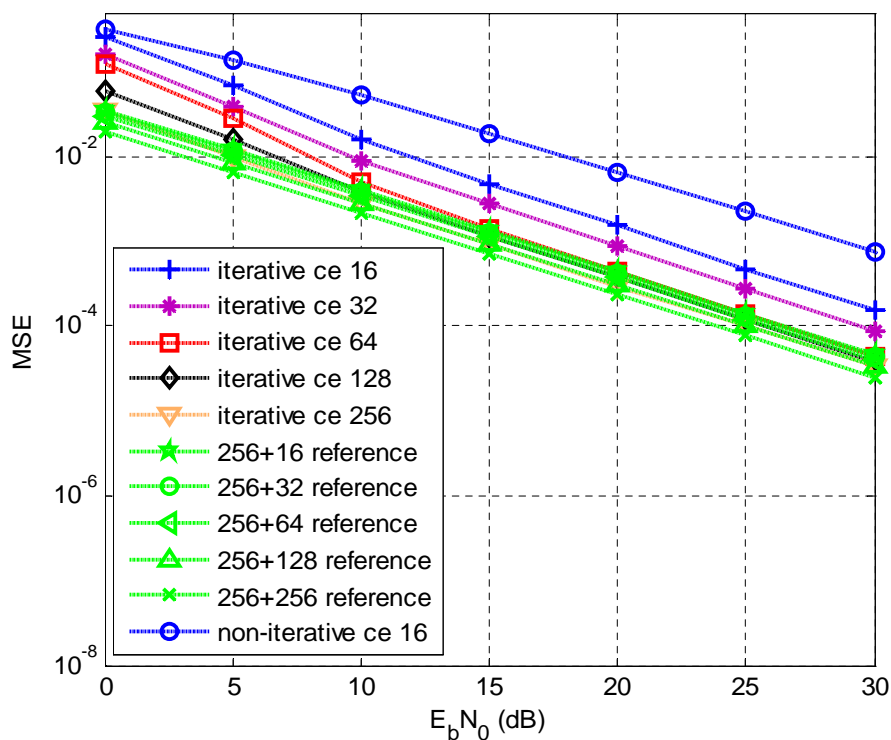


Figure 6.10 MSE performance of iterative channel estimation (ce) for 2-by-1 OFDM system by Wiener filter, using different length of pilots (16, 32, 64, 128, 256), compared with different MSE references (data length 256 + pilot length)

Fig. 6.10 shows the MSE performance of iterative channel estimation for 2-by-1 system. The interference cancellation method is considered during the iterative channel estimation. Different estimation results with different length of pilots (16, 32, 64, 128 and 256) for the first iteration are presented, the FFT length is the same as that of pilots. From the figure, we can see that the MSE performance is greatly improved by using the iterative channel estimation with 16-bit pilots, compared to the non-iterative channel estimation. Although the simulation result cannot match the theoretical curve, the figure shows the longer the pilot length, the closer the practical curve and the theoretical curve are.

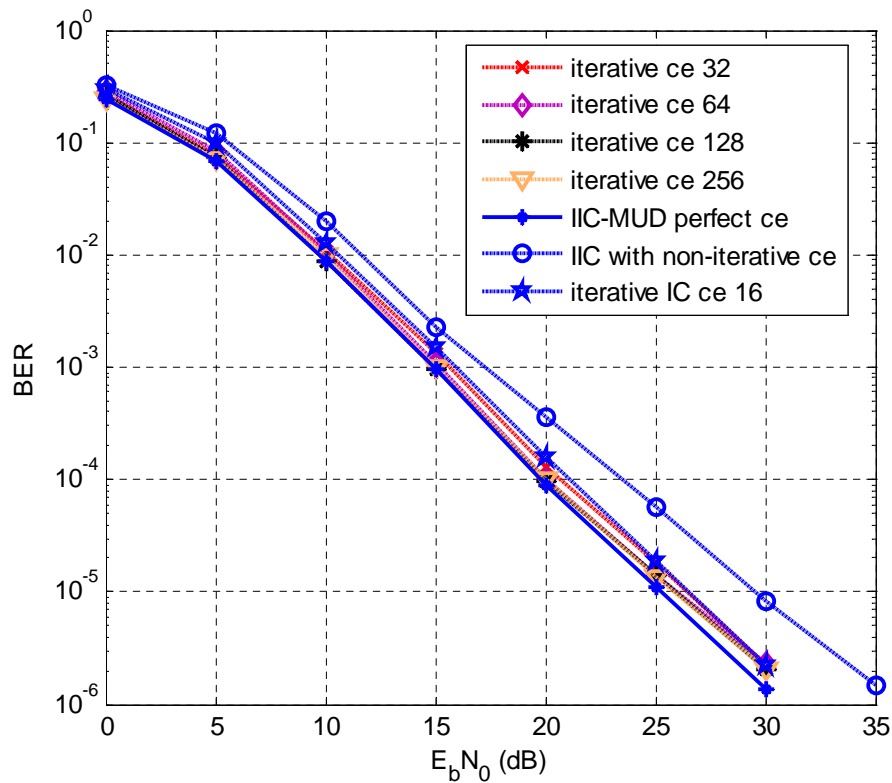


Figure 6.11 BER performance of iterative channel estimation (ce) for 2-by-1 OFDM system by Wiener filter

Fig. 6.11 illustrates the BER performance of iterative channel estimation for the 2-by-1 system. Using the iterative channel estimation can dramatically improve the BER performance. The MSE performance is influenced by the length of pilots, however, the BER performance does not. It seems that no matter how long the length of pilots, the BER performance is nearly the same.

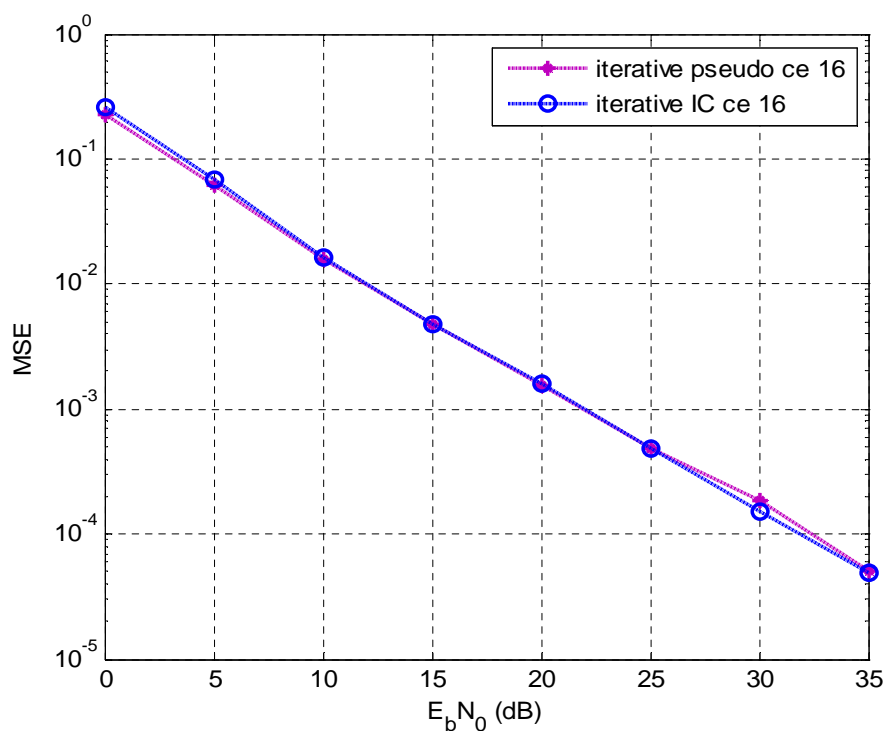


Figure 6.12 MSE performance of iterative channel estimation with interference cancellation method and pseudo-inverse method for 2-by-1 OFDM system by Wiener filter

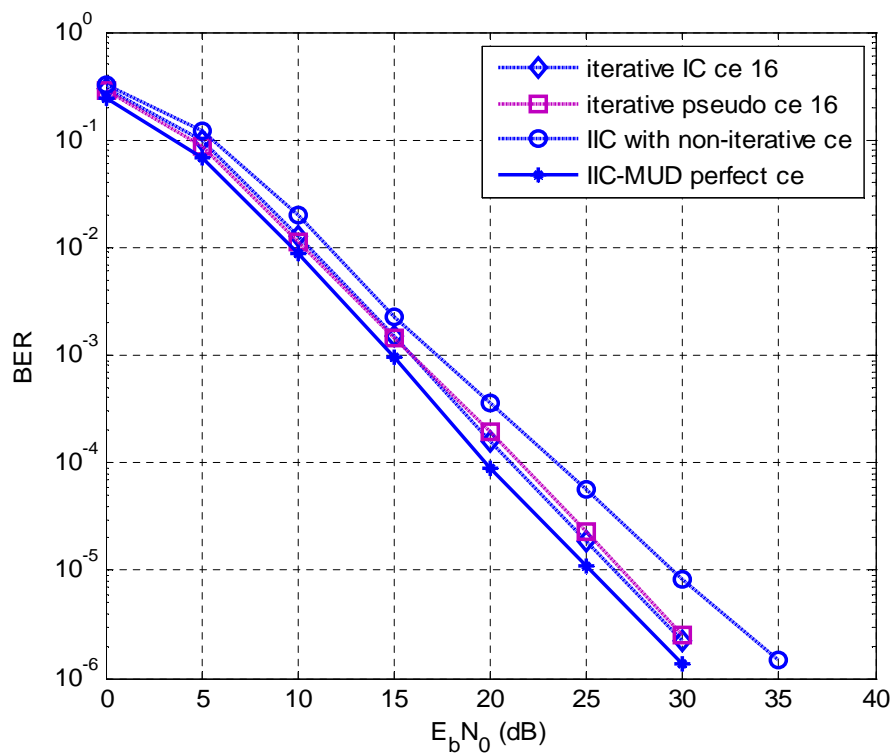


Figure 6.13 BER performance of iterative channel estimation (ce) with interference cancellation method and pseudo-inverse method for 2-by-1 OFDM system by Wiener filter

Fig. 6.12 and 6.13 show the MSE and BER performance comparison between interference cancellation method and pseudo-inverse method for iterative channel estimation. The results show that both methods have almost the same performance. However the complexity of the pseudo-inverse method is higher than that of the interference cancellation method, therefore we prefer the interference cancellation method.

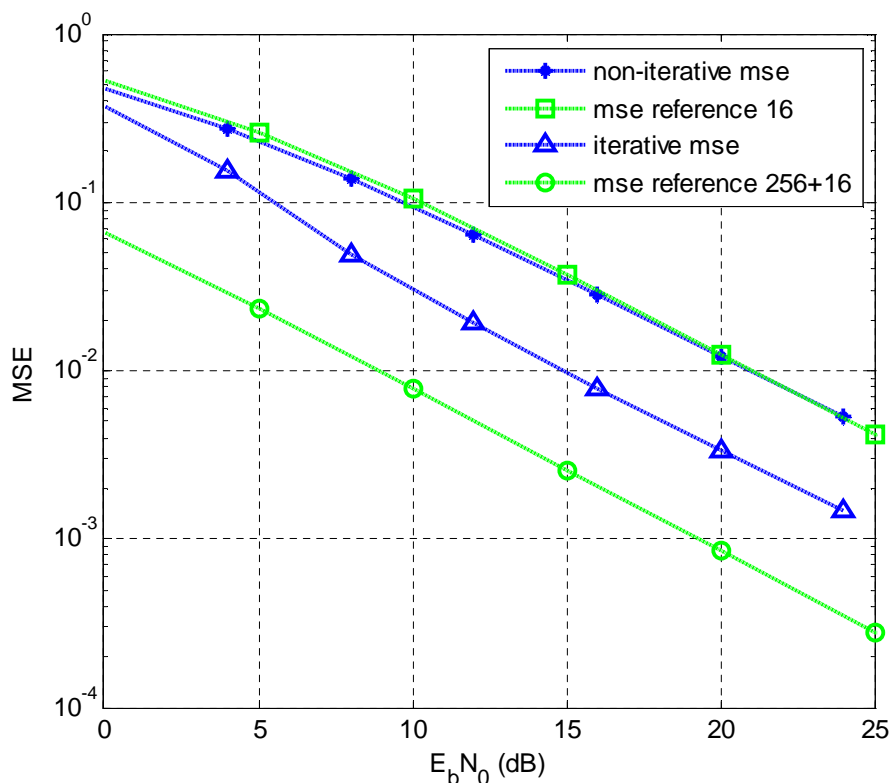


Figure 6.14 MSE performance of non-iterative (pilots length 16) vs iterative channel estimation (pilots length 256+16) for 4-by-2 OFDM system by Wiener filter, without channel selection

Considering the four user case, the interference cancellation based iterative channel estimation is used. For 4-by-2 system, due to the error floor, IIC without channel selection and with channel selection are considered. The non-iterative and iterative MSE performance without channel selection are shown in Fig. 6.14. Fig. 6.15 shows the BER performance of this system without channel selection. From the figure, we can see that the iterative channel estimation also can obtain more gain for the four user case.

Fig. 6.16 shows the MSE performance of non-iterative and iterative channel estimation with channel selection, which is almost the same compared with that without channel selection. This means the channel selection or not cannot affect the channel estimation.

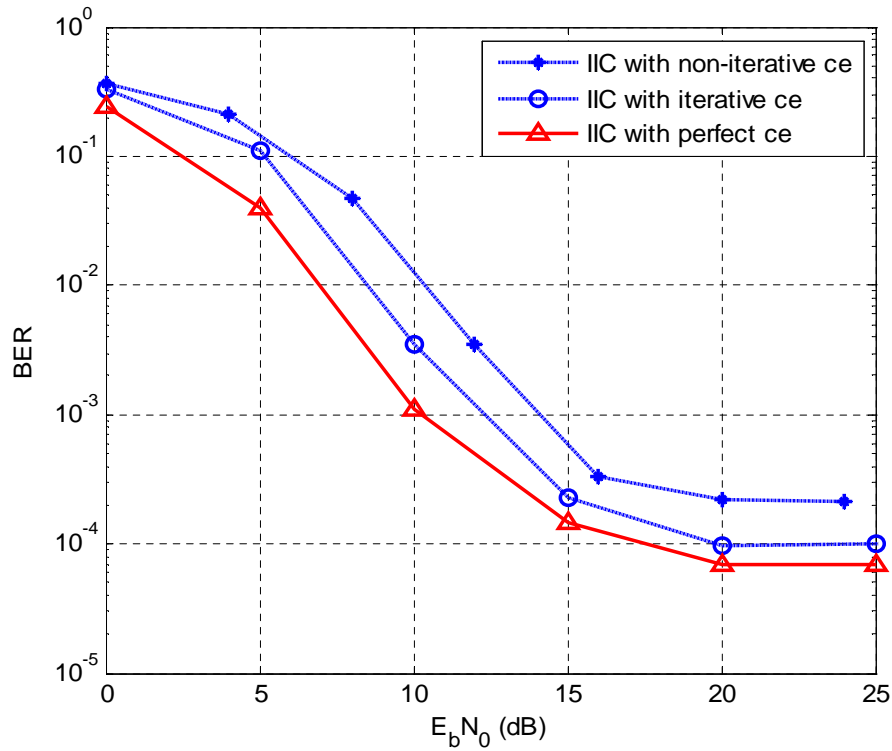


Figure 6.15 BER performance of 4-by-2 OFDM system with non-iterative vs iterative channel estimation by Wiener filter, without channel selection

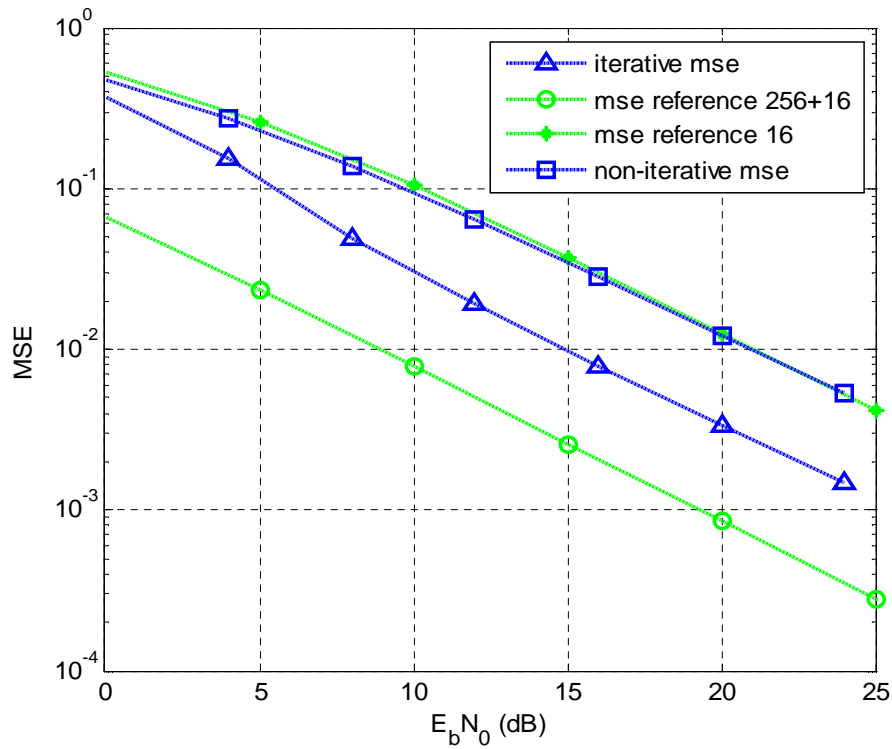


Figure 6.16 MSE performance of non-iterative vs iterative channel estimation for 4-by-2 OFDM system by Wiener filter, with channel selection

Fig. 6.17 shows the BER performance of non-iterative and iterative channel estimation with channel selection. The iterative channel estimation still gets more gain, 2dB less than the BER with perfect channel knowledge. The gap is larger than that of 2-by-1 system. This may be because the channel selection which is calculated based on the channel estimation is used here.

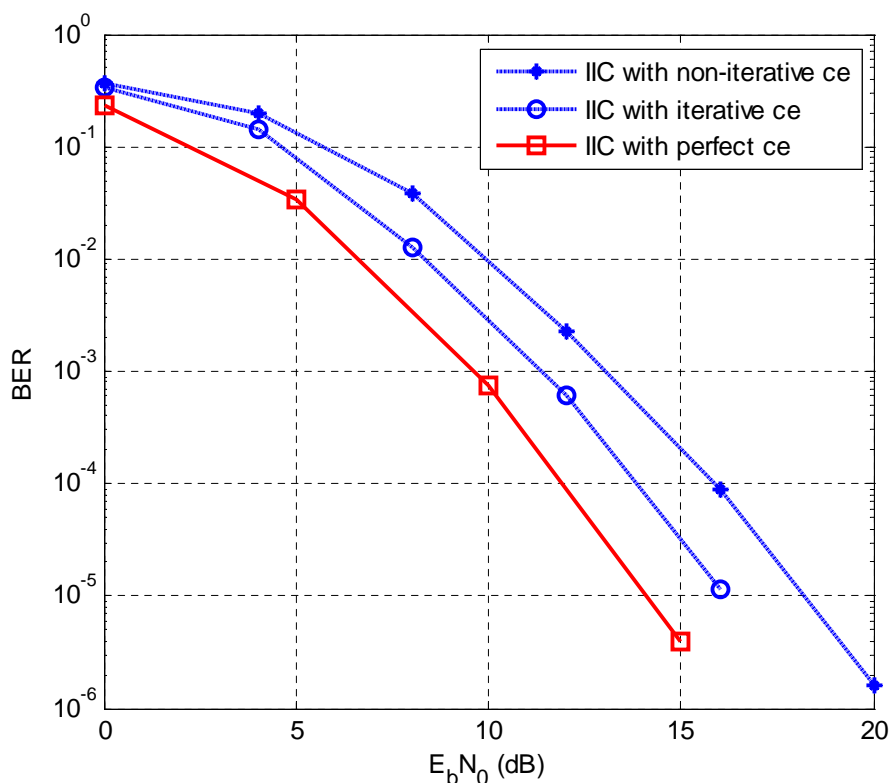


Figure 6.17 BER performance of 4-by-2 OFDM system with iterative vs non-iterative channel estimation by Wiener filter, with channel selection

6.6 Conclusions

In this chapter, the non-perfect channel knowledge is first introduced to the IIC detector. The simulation result shows our IIC detector is sensitive to the channel knowledge.

Then pilot-based channel estimation by the Wiener filter is introduced, which is the ideal channel estimation of the OFDM system. The iterative channel estimation technique is also applied.

For iterative channel estimation, we introduce two methods. One is based on the interference cancellation, and the other is based on the pseudo-inverse method. The simulation results show that both methods have almost the same MSE and BER

performance, while the latter has more complexity. In this case, we prefer the former for the iterative channel estimation.

Although the iterative channel estimation can obtain more gains, it requires more computational complexity. Moreover, the simulation results show that with only one iteration or non-iterative channel estimation, our IIC detector can work well, which reduces the complexity significantly.

The 2-by-1 and 4-by-2 systems are considered in the simulation section, which show that the accuracy of the channel estimation does influence the performance of the IIC detector, but not much.

Chapter 7

Conclusions and Future Work

Contents

7.1 Summary of Work	152
7.2 List of Contributions	153
7.3 Future Work.....	154

The main content of this thesis is summarized in this chapter. In section 7.1, we draw on the important results from previous chapters. The novel contributions are reviewed in section 7.2. Finally, a selection of possible future work is proposed in section 7.3.

7.1 Summary of Work

This thesis deals with multiuser detection for overloaded MIMO OFDM systems. The multiuser receiver is designed based on the ‘Turbo principle’, which means the MUD and the decoding are combined in an iterative structure. In each iteration, the soft information is exchanged between these two components, so that both components can be continuously improved, and therefore can achieve a substantial performance gain.

Considering the unavailability of linear MUD and optimal MUD, an iterative multiuser detection scheme is proposed for overloaded multiuser MIMO OFDM system. Based on the iterative principle, joint detection and decoding with simple matched filter and convolutional code is used. The main idea of this combination is simple and low complexity. However, the matched filter has very poor performance. In this case, PIC is employed to reduce the interference. For the overloaded case, the number of receive antennas is fewer than that of the transmit antennas, the received signal contain too much interference, so that the LLR is unreliable and causes problems in decoding. In order to obtain reliable LLR, we design a LLR convertor where a scaling factor which is calculated directly from CHANNEL INFORMATION is applied. In addition to the calculation of the channel covariance, this method is almost linear, the complexity is therefore very low, and for the two user system, the BER performance is close to the optimal approach.

For the case of more users, a channel selection scheme is proposed to solve the error floor of the BER performance, which is obtained from the EXIT chart point of view. The mutual information is used to distinguish whether a channel is good or not. The mutual information is also calculated directly from the CHANNEL INFORMATION, and can be predicted in a look-up table which greatly reduces the complexity. For those so-called bad channels, we have two methods to process them. One is simply throwing them away. Without the influence of bad channels, the BER performance of proposed method is close to the optimal approach. Another is using adaptive methods.

We propose two adaptive methods to solve them. One is using lower code rate for bad channels. The other is dividing the transmitters into several groups for transmission at the non-convergent channels, which can reduce the interferences fundamentally. Simulation results show that both schemes can work well.

IDMA allows the use of a low complexity iterative multiuser detection technique so that it is an effective complement of the IIC MUD. Combined with IDMA, our proposed IIC

can achieve almost the optimal performance without any channel selection. Compared to the ESE, our IIC can make full use of CIR, and hence achieve much better performance with nearly the same level of complexity.

We assume the CIR is perfectly known at the receiver all the time. The scaling factor and channel selection both are based on this assumption. So the influence of channel accuracy is considered. By using the Wiener filter, both non-iterative and iterative channel estimation are obtained. The simulation results show the non-iterative channel estimation is good enough for the IIC, but the iterative channel estimation can achieve more gain, and obtain much closer BER performance of IIC compared with perfect channel knowledge.

7.2 List of Contributions

The contributions of this thesis are listed below.

1. In chapter 3, a low complexity *iterative interference cancellation* (IIC) multiuser detection scheme is proposed for the overloaded multiuser MIMO OFDM system, which combines the matched filter, convolutional codes, and PIC. A scaling factor is introduced to provide reliable LLRs, which is based on the channel matrix and is used to make the output of the matched filter close to Gaussian-like distribution, so that the decoder can obtain the information from the LLRs effectively. The BER performance of this IIC MUD is close to the optimal approach, but with much less complexity.
2. In chapter 4, a channel selection scheme is proposed to avoid the influence of some bad channels. From the EXIT chart point of view, we set a threshold to the mutual information. Above it, the tunnel between the detector and decoder is open. Below it, the tunnel is closed. The former is the good channel, while the latter is the bad channel. The mutual information is calculated directly from the channel information. Without the influence of bad channels, the BER performance of proposed method is close to that of the optimal detector (MAP).
3. In chapter 4, for channel selection scheme, we proposed two adaptive methods to process the so-called bad channels. One is using lower code rate for bad channels. The other is dividing the transmitters into several groups for transmission at the non-convergent channels, due to the OLF, which can reduce

the interference fundamentally. Both methods require low feedback, and the simulation results show that both can work well.

4. In chapter 5, IDMA is employed to separate users by engaging user-specific interleavers. By taking advantage of IDMA, our proposed IIC can achieve almost the optimal performance for more users or much more overloaded systems, without any BER error floor. Moreover, compared to ESE, our IIC has nearly the same level of complexities, but achieve much better performance.
5. In chapter 6, channel estimation is considered. By using the Wiener filter, we can provide both non-iterative and iterative channel estimation. The simulation results show both estimations are affected by the length of pilots. The long the length of pilots, the better the MSE performance of both schemes. However, the BER performance is still the same, little affected by the channel accuracy.

7.3 Future Work

Some suggestions for future work based on this thesis are given below:

1. The block fading channel is assumed through most of the thesis. However, extreme cases need to be studied in which frequency selective channels that remain static during one OFDM symbol period should be considered. Moreover, channels may also vary fast even within a symbol, which is called a doubly-selective fading channel. In these cases, the interference cancelation is more difficult, and the scaling factor for LLRs becomes much more challenging.
2. The proposed IIC detector in this thesis is focused on the BPSK modulation. However, it can be easily extended to higher order modulation, such as QPSK or 16QAM. Allowing high order modulations can yield more potential performance gain. Using different modulation schemes, the soft estimates of decoder output are different. The proposed IIC can handle these schemes with minor modifications.

Glossary

AWGN	Additive White Gaussian Noise
BB	Branch and Bound
BCJR	Bahl Cocke Jelinek and Raviv
BER	Bit Error Rate
BPSK	Binary Phase Shift Keying
CAI	Cross Antenna Interference
CCI	Co-Channel Interference
CDMA	Code Division Multiple Access
CFO	Carrier Frequency Offset
CIR	Channel Impulse Response
CP	Cyclic Prefix
CSI	Channel State Information
DAB	Digital Audio Broadcasting
DF	Decision Feedback
DFT	Discrete Fourier Transform
DVB	Digital Video Broadcasting
ECR	Errored Channel Rate
EIR	Estimate to Interference Ratio
ESE	Elementary Signal Estimator
EXIT	EXtrinsic Information Transfer
FEC	Forward Error Control
FFT	Fast Fourier Transform
FIR	Finite Impulse Response
HE	Horizontal Encoding
IC	Interference Cancellation

ICI	Inter-Carrier Interference
IDMA	Interleave Division Multiple Access
IDFT	Inverse Discrete Fourier Transform
IFFT	Inverse Fast Fourier Transform
IIC	Iterative Interference Cancellation
IIR	Infinite Impulse Response
ISI	Inter-Symbol Interference
LLR	Log-Likelihood Ratio
LMMSE	Linear Minimum Mean Square Error
LST	Layered Space Time
LTE	Long Term Evolution
MAC	Media Access Control
MAI	Multiple Access Interference
MAP	Maximum a Posteriori
MC	Multi-Carrier
MIMO	Multiple Input Multiple Output
ML	Maximum Likelihood
MLD	Maximum Likelihood Detection
MMSE	Minimum Mean Square Error
MRC	Maximum Ratio Combining
MSE	Mean Square Error
MUD	Multi-User Detection
OFDM	Orthogonal Frequency Division Multiplexing
OLF	OverLoading Factor
O-QAM	Orthogonal Quadrature Amplitude Modulation
PAPR	Peak to Average Power Ratio
PDA	Probabilistic Data Association
PDF	Probability Density Function
PIC	Parallel Interference Cancellation

PSK	Phase Shift Keying
QAM	Quadrature Amplitude Modulation
QPP	Quadratic Permutation Polynomial
QPSK	Quadrature Phase Shift Keying
RCR	Rejected Channel Rate
RSC	Recursive Systematic Convolutional
SC-FDMA	Single Carrier Frequency Division Multiple Access
SD	Sphere Decoding
SDCE	Soft Decision-directed Channel Estimation
SDR	Semi-Definite Relaxation
SIC	Successive Interference Cancellation
SIMO	Single Input Multiple Output
SISO	Single Input Single Output (Soft Input Soft Output)
SNR	Signal to Noise Ratio
STBC	Space Time Block Codes
STTC	Space Time Trellis Codes
TS	Tap Selection
VBLAST	Vertical Bell Laboratories LST
VE	Vertical Encoding
WiMax	Worldwide Interoperability for Microwave Access
WLAN	Wireless Local Area Network
XOR	Exclusive-OR
ZF	Zero Forcing

Bibliography

- [1] B. Vucetic and J. Yuan, *Space-time coding*, John Wiley & Sons Ltd., Chichester, UK, 2003.
- [2] A. J. Paulraj, D. A. Gore, R. U. Nabar, and H. Bolcskei, "An overview of MIMO communications: A key to gigabit wireless," *Proceedings of IEEE*, vol. 92, no. 2, pp. 198-218, February 2004.
- [3] G. J. Foschini and M. J. Gans, "On limits of wireless communication in a fading environment when using multiple antennas," *Wireless Personal Communications*, vol. 6, no. 3, pp. 311-335, March 1998.
- [4] I. E. Telatar, "Capacity of multi-antenna Gaussian channels," *European Transactions on telecommunications*, vol. 10, pp. 585-595, November 1999.
- [5] A. G. Burr, "Space time codes and MIMO transmission," in A. Sibille, C. Oestages, and A. Zanella (Eds), *MIMO from Theory to Implementation*: Amsterdam, Elsevier, 2010.
- [6] A. Kaye and D. George, "Transmission of Multiplexed PAM Signals Over Multiple Channel and Diversity Systems", *IEEE Transactions on Communications Technology*, vol.18, no.5, pp. 520-526, October 1970.
- [7] W. van Etten, "Maximum Likelihood Receiver for Multiple Channel Transmission Systems", *IEEE Transactions on Communications Technology*, vol.24, no.2, pp. 276-283, February 1976.
- [8] V. Tarokh, N. Seshadri, and A. R. Calderbank, "Space-time codes for high data rate wireless communication: performance criterion and code construction," *IEEE Journal on Selected Areas in Communications*, vol.44, no.2, March 1998.

- [9] A. F. Naguib, V. Tarokh, N. Seshadri, and A. R. Calderbank, "A space-time coding modem for high-data-rate wireless communications," *IEEE Journal on Selected Areas in Communications*, vol.16, no.8, October 1998.
- [10] V. Tarokh, H. Jafarkhani, and A. R. Calderbank, "Space-time block codes from orthogonal designs", *IEEE Transactions on Information Theory*, vol.45, no.5, pp.1456-1467, July 1999.
- [11] G. J. Foschini, "Layered space-time architecture for wireless communication in a fading environment when using multi-element antennas," *Bell Labs Technical Journal*, October 1996.
- [12] P. W. Wolniansky, G. J. Foschini, G. D. Golden, and R. A. Valenzuela, "V-BLAST: an architecture for realizing very high data rates over the rich-scattering wireless channel," *Signals, Systems, and Electronics, ISSSE 98*, pp. 295-300, October 1998.
- [13] G. D. Golden, C. J. Foschini, R. A. Valenzuela and P. W. Wolniansky, "Detection algorithm and initial laboratory results using VBLAST space-time communication architecture," *Electronics Letter*, vol. 35, pp. 14-16, January 1999.
- [14] T. Hwang, Chenyang Yang, Gang Wu, Shaoqian Li and Geoffrey Ye Li, "OFDM and Its Wireless Applications: A Survey," *IEEE Transactions on Vehicular Technology*, vol. 58, no. 4, pp. 1673-1694, May 2009.
- [15] R. W. Chang, "Synthesis of band-limited orthogonal signals for multichannel data transmission," *Bell System Technical Journal*, vol. 45, pp. 1775-1796, December 1966.
- [16] B. R. Saltzberg, "Performance of an efficient parallel data transmission system," *IEEE Transactions on Communications*, vol. COM-15, no. 6, pp. 805-811, December 1967.
- [17] R.W. Chang, "Orthogonal frequency division multiplexing," U.S. Patent 3 488 445, filed November 14, 1966, issued January 6, 1970.
- [18] R.W. Chang and R. A. Gibby, "A theoretical study of performance of an orthogonal multiplexing data transmission scheme," *IEEE Transactions on Communications*, vol. COM-16, no. 4, pp. 529-540, August 1968.
- [19] S. Weinstein and P. Ebert, "Data transmission by frequency-division multiplexing

- using the discrete Fourier transform,” *IEEE Transactions on Communications*, vol. COM-19, no. 5, pp. 628-634, October 1971.
- [20] I. Kalet, “The multitone channel,” *IEEE Transactions on Communications*, vol. 37, no. 2, pp. 119-124, February 1989.
- [21] T. J. Willink and P. H. Wittke, “Optimization and performance evaluation of multicarrier transmission,” *IEEE Transactions on Information Theory*, vol. 43, no. 2, pp. 426-440, March 1997.
- [22] L. J. Cimini, “Analysis and simulation of a digital mobile channel using orthogonal frequency division multiplexing,” *IEEE Transactions on Communications*, vol. COM-33, no. 7, pp. 665-675, July 1985.
- [23] M. Alard and R. Lassalle, “Principles of modulation and channel coding for digital broadcasting for mobile receivers,” *EBU Technical Review*, pp. 168-190, August 1987.
- [24] J. A. C. Bingham, “Multicarrier modulation for data transmission: An idea whose time has come,” *IEEE Communications Magazine*, vol. 28, no. 5, pp. 5-14, May 1990.
- [25] R. Van Nee and R. Prasad, *OFDM for Wireless Multimedia Communications*. Artech, 1999.
- [26] A. E. Jones, T. A. Wilkinson, and S. K. Barton, “Block coding scheme for reduction of peak to mean envelope power ratio of multicarrier transmission schemes,” *Electronics Letters*, vol.30, no.25, pp.2098-2099, December 1994
- [27] P. Van Eetvelt, G. Wade, and M. Tomlinson, “Peak to average power reduction for OFDM schemes by selective scrambling,” *Electronics Letters*, vol.32, no.21, pp.1963-1964, October 1996.
- [28] R. W. Bauml, R. F. H. Fischer, and J. B. Huber, “Reducing the peak-to-average power ratio of multicarrier modulation by selected mapping,” *Electronics Letters*, vol.32, no.22, pp.2056-2057, October 1996.
- [29] P. H. Moose, “A technique for orthogonal frequency division multiplexing frequency offset correction,” *IEEE Transactions on Communications*, vol.42, no.10, pp.2908-2914, October 1994.

- [30] F. Daffara, and O. Adami, "A new frequency detector for orthogonal multicarrier transmission techniques," *1995 IEEE 45th Vehicular Technology Conference*, vol.2, pp.804-809 July 1995.
- [31] M. Luise, and R. Reggiannini, "Carrier frequency acquisition and tracking for OFDM systems," *IEEE Transactions on Communications*, vol.44, no.11, pp.1590-1598, November 1996.
- [32] A. G. Burr, *Advanced Modulation and Coding for Wireless Communications*, Prentice Hall, 2001.
- [33] R. Steele, *Mobile Radio Communications*, New York: IEEE Press, 1992.
- [34] G. G. Raleigh, and J. M. Cioffi, "Spatio-temporal coding for wireless communication," *IEEE Transactions on Communications*, vol.46, no.3, pp.357-366, March 1998.
- [35] Ye Li; J. H. Winters, and N. R. Sollenberger, "Signal detection for MIMO-OFDM wireless communications," *IEEE International Conference on Communications*, vol.10, pp.3077-3081, 2001.
- [36] M. Guillaud, and D. T. M. Slock, "Multi-stream coding for MIMO OFDM systems with space-time-frequency spreading," *The 5th International Symposium on Wireless Personal Multimedia Communications*, vol.1, pp. 120-124, October. 2002.
- [37] A. F. Molisch, M. Z. Win, and J. H. Winters, "Space-time-frequency (STF) coding for MIMO-OFDM systems," *IEEE Communications Letters*, vol.6, no.9, pp. 370-372, September 2002.
- [38] M. Jiang and L. Hanzo, "Multiuser MIMO-OFDM for next-generation wireless systems," *Proceedings of the IEEE*, vol. 95, no. 7, pp. 1430-1469, July 2007.
- [39] H. Sampath, S. Talwar, J. Tellado, V. Erceg, and A. J. Paulraj, "A fourth-generation MIMO-OFDM broadband wireless system: Design, performance, and field trial results," *IEEE Communications Magazine*, vol. 40, no. 9, pp. 143-149, September 2002.
- [40] G. L. Stuber, J. R. Barry, S. W. McLaughlin, Y. Li, M. A. Ingram, and T. G. Pratt, "Broadband MIMO-OFDM wireless communications," *Proceedings of the IEEE*, vol. 92, no. 2, pp. 271-294, February 2004.

- [41] S. Verdu, *Multiuser Detection*, Cambridge University Press, New York, NY, USA, 2nd edition, 1998.
- [42] S. Verdu, "Minimum probability of error for asynchronous Gaussian multiple access channels", *IEEE Transactions on Information Theory*, vol. 32, pp. 85-96, January 1986.
- [43] W. K. Ma, T. N. Ching, and Z. Ding, "Semidefinite relaxation based multiuser detection for M-ary PSK multiuser systems", *IEEE Transactions on Signal Processing*, vol. 52, no. 10, pp. 2862-2872, October 2004.
- [44] F. Hasegawa, J. Luo, K. Pattipati, P. Willett, and D. Pham, "Speed and accuracy comparison of techniques for multiuser detection in synchronous CDMA", *IEEE Transactions on Communications*, vol. 52, no. 4, pp. 540-545, April 2004.
- [45] B. M. Hochwald, and S. ten Brink, "Achieving Near-Capacity on a Multiple-Antenna Channel", *IEEE Transactions on Communications*, vol. 51, no. 3, pp. 389-399, March 2003.
- [46] P. M. Grant, S. Mowbray, and R. D. Pringle, "Multipath and co-channel CDMA interference cancellation", in *IEEE International Symposium on Spread Spectrum Techniques and Applications*, pp. 83-86, November 1992.
- [47] J. M. Holtzman, "DS/CDMA successive interference cancellation", in *IEEE International Symposium on Spread Spectrum Techniques and Applications*, pp. 69-78, July 1994.
- [48] P. Patel and J. Holtzman, "Analysis of a simple successive interference cancellation scheme in a DS/CDMA system", *IEEE Journal on Selected Areas on Communications*, no. 12, pp. 976-807, June 1994.
- [49] S. J. Baines, *Linear Multi-User Detection in CDMA Cellular Systems*, PhD thesis, Department of Electronics, University of York, YORK, YO10 5DD, UK, September 1997.
- [50] M. K. Varanasi and B. Aazhang, "Multistage detection in asynchronous code division multiple access communications", *IEEE Transactions on Communications*, vol. 38, no. 4, pp. 509-519, April 1990.
- [51] Y. C. Yoon, R. Kohno, and H. Imai, "A spread-spectrum multi-access system with a cascade of co-channel interference cancelers for multipath fading channels", in

- IEEE International Symposium on Spread Spectrum Techniques and Applications*, pp. 87-90, November 1992.
- [52] Y. C. Yoon, R. Kohno and H. Imai, "A spread-spectrum multiaccess system with cochannel interference cancellation for multipath fading channels", *IEEE Journal on Selected Areas in Communications*, vol. 11, pp. 1067-1075, September 1993.
- [53] M. Kawabe, T. Kato, A. Kawahashi, T. Sato, and A. Fukasawa, "Advanced CDMA scheme based on interference cancellation", in *IEEE Vehicular Technology Conference*, pp. 448-451, May 1993.
- [54] R. M. Buehrer, N. S. Correal-Mendoza, and B. D. Woerner, "A simulation comparison of multiuser receivers for cellular CDMA", *IEEE Transactions on Vehicular Technology*, vol. 49, no. 4, pp. 1065-1085, July 2000.
- [55] D. Guo, L. K. Rasmussen, and T. J. Lim, "Linear parallel interference cancellation in long-code CDMA multiuser detection", *IEEE Journal on Selected Areas in Communications*, vol. 17, no. 12, pp. 2074-2081, December 1999.
- [56] A. Nahler, R. Irmer, and G. Fettweis, "Reduced and differential parallel interference cancellation for CDMA systems", *IEEE Journal on Selected Areas in Communications*, vol. 20, no. 2, pp. 237-247, February 2002.
- [57] D. Divsalar, M. K. Simon, and D. Raphaeli, "Improved parallel interference cancellation for CDMA", *IEEE Transactions on Communications*, vol. 46, no. 2, pp. 258-268, February 1998.
- [58] G. Xue and J. Weng, "Adaptive multistage parallel interference cancellation for CDMA over multipath fading channels", in *IEEE Vehicular Technology Conference*, pp. 1251-1255, July 1999.
- [59] R. M. Buehrer and S. P. Nicoloso, "Comments on 'partial parallel interference cancellation for CDMA'", *IEEE Transactions on Communications*, vol. 47, pp. 658-661, May 1999.
- [60] P. Elias, "Coding for noisy channels," *IRE Convention Record*, vol. 4, pp. 37-47, 1955.
- [61] A. J. Viterbi, "Error bounds for convolutional codes and an asymptotically optimum decoding algorithm," *IEEE Transactions on Information Theory*, vol.13, no.2, pp. 260- 269, April 1967.

- [62] S. Lin and D. J. Costello, *Error Control Coding*, Prentice Hall, 2004.
- [63] C. E. Shannon, "A mathematical theory of communication," *Bell System Technical Journal*, vol. 27, pp. 379-423, July 1948.
- [64] C. Berrou, A. Glavieux, and P. Thitimajshima, "Near Shannon limit error-correcting coding and decoding: Turbo codes," in *Proceedings of IEEE International Conference on Communications*, vol. 2, pp. 1064-1070, May 1993.
- [65] A. G. Burr, "Turbo-codes: The Ultimate Error Control Codes?" *Electronics and Communication Engineering Journal*, Vol. 13, No. 4, pp. 155-165, August 2001.
- [66] K. Andrews, C. Heegard, and D. Kozen, "A Theory of Interleavers," Cornell University computer science technical report, January 1997.
- [67] S. Benedetto, G. Montorsi, and D. Divsalar, "Concatenated convolutional codes with interleavers," *IEEE Communications Magazine*, vol. 41, no. 8, pp. 102-109, August 2003.
- [68] H. R. Sadjadpour, A. Sloane, M. Salehi, and G. Nebe, "Interleaver design for turbo codes," *IEEE Journal on Selection Areas in Communications*, vol. 19, no. 5, pp. 831-837, May 2001.
- [69] D. Divsalar and F. Pollara, "Turbo codes for PCS applications", in *IEEE International Conference on Communications*, Seattle, pp. 54-99, 1995.
- [70] F. Said, A. Aghvami, and W. Chambers, "Improving the Random Interleaver for Turbo Codes," *Electronics Letters*, vol. 35, no. 25, pp. 2194-2195, 1999.
- [71] J. Yuan, B. Vucetic, and W. Feng, "Combined Turbo Codes and Interleaver Design," *IEEE Transactions on Communications*, vol. 47, no. 4, pp. 484-487, April 1999.
- [72] 3GPP, "Technical Specification, Group Radio Access Network (Multiplexing and Channel Coding for FDD)," *Technical Report, 3rd Generation Partnership Project*, 1999.
- [73] J. Sun and O. Y. Takeshita, "Interleavers for turbo codes using permutation polynomials over integer rings," *IEEE Transactions on Information Theory*, vol. 51, no. 1, pp. 101-119, January 2005.
- [74] S. Dolinar and D. Divsalar, "Weight distributions for turbo codes using random and nonrandom permutations", *JPL Technical Report*, August 1995.

- [75] L. Bahl, J. Cocke, F. Jelinek, and J. Raviv, "Optimal decoding of linear codes for minimizing symbol error rate," *IEEE Transactions on Information Theory*, vol. IT-20(2), pp. 284-287, March 1974.
- [76] S. ten Brink, "Convergence behavior of iteratively decoded parallel concatenated codes," *IEEE Transactions on Communications*, vol. 49, October 2001.
- [77] P. Robertson and P. Hoeher, "Optimal and sub-optimal maximum a posteriori algorithms suitable for turbo decoding," *European Transactions on Telecommunications*, vol. 8, no. 2, pp. 119-125, 1996.
- [78] P. Robertson, "Improving Decoder and Code Structure of Parallel Concatenated Recursive Systematic (Turbo) Codes," *IEE Trans. of International Conference on Universal Personal Communications*, pp. 183-187, September 1994.
- [79] P. Jung, "Comparison of Turbo Code Decoders Applied to Short Frame Transmission," *IEEE Journal on Selection Areas in Communications*, vol. 14, no. 3, pp. 530-537, April 1996.
- [80] N. Wiberg, *Codes and decoding on general graphs*, Linkoping University, Sweden, 1996.
- [81] R. Nambiar and A. Goldsmith, "Iterative weighted interference cancellation for CDMA systems with RAKE reception," *IEEE Vehicular Technology Conference*, vol.2, pp.1232-1236, July 1999.
- [82] M. Mostofa, K. Howlader, and B. D. Woerner, "Iterative interference cancellation and decoding using a soft cancellation factor for DS-CDMA," *IEEE Vehicular Technology Conference*, vol.3, pp.2076-2080, 2000.
- [83] A. Nakajima, D. Garg, and F. Adachi, "Turbo coded MIMO multiplexing with iterative adaptive soft parallel interference cancellation," *IEEE Vehicular Technology Conference*. vol.2, pp.1410-1414, September 2004.
- [84] P. The-Hanh, A. Nallanathan, and B. Kannan, "An iterative interference cancellation scheme for STBC multirate multiuser systems," *IEEE Wireless Communications and Networking Conference*, vol.1, pp.521-526, March 2005.
- [85] Ci-Ye Tso, J. M. Wu, and P. A. Ting, "Iterative Interference Cancellation for STBC-OFDM Systems in Fast Fading Channels," *IEEE GLOBECOM*, pp.1-5, December 2009.

- [86] C. H. Yih, "Iterative Interference Cancellation for OFDM Signals With Blanking Nonlinearity in Impulsive Noise Channels," *IEEE Signal Processing Letters*, vol.19, no.3, pp.147-150, March 2012.
- [87] Y. Chen, and S. ten Brink, "Enhanced MIMO subspace detection with interference cancellation," *IEEE Wireless Communications and Networking Conference*, pp.267-271, April 2012.
- [88] N. Noels, and M. Moeneclaey, "Iterative Multiuser Detection of Spectrally Efficient FDMA CPM," *IEEE Transactions on Signal Processing*, vol.60, no.10, pp.5254-5267, October 2012.
- [89] P. Li, J. Liu, and R.C. De Lamare, "Adaptive iterative decision multi-feedback detection for multi-user MIMO systems," *IEEE International Conference Acoustics, Speech and Signal Processing*, pp.3037-3040, March 2012.
- [90] O. Goussevskaia, and R. Wattenhofer, "Scheduling Wireless Links with Successive Interference Cancellation," *International Conference on Computer Communication Networks*, pp.1-7, August 2012.
- [91] X. Dai, "Enhancing the Performance of the SIC-MMSE Iterative Receiver for Coded MIMO Systems via Companding," *IEEE Communication Letters*, vol.16, no.6, pp.921-924, June 2012.
- [92] M. Moher, "An iterative multiuser decoder for near-capacity communications", *IEEE Transactions on Communications*, vol. 46, pp. 870-880, July 1998.
- [93] P. H. Tan, L. K. Rasmussen, and T. J. Lim, "Constrained maximum-likelihood detection in CDMA," *IEEE Transactions on Communication*, vol.49, no.1, pp.142-153, January 2001.
- [94] H. Liao, "Sphere Decoding Assisted GA-Based Multiuser Detection for Synchronous LAS Multicode System," *Wireless Communications, Networking and Mobile Computing*, pp.1-4, September 2009.
- [95] C. Wei, L. Wang, and L. Hanzo, "Iterative Irregular Sphere Detection in High-Rate Downlink SDMA Systems," *IEEE Transactions on Vehicular Technology*, vol.58, no.7, pp.3855-3861, September 2009.
- [96] X. Wang and H. V. Poor, "Iterative (Turbo) soft interference cancellation and decoding for coded CDMA", *IEEE Transactions on Communications*, vol. 49, no. 7,

- pp. 1046-1061, July 1999.
- [97] I. Wormsbecker and C. Williamson, "On Channel Selection Strategies for Multi-Channel MAC Protocols in Wireless Ad Hoc Networks," *Wireless and Mobile Computing, Networking and Communications*, pp.212-220, June 2006.
- [98] Fen Hou and Jianwei Huang, "Dynamic Channel Selection in Cognitive Radio Network with Channel Heterogeneity," *IEEE GLOBECOM*, pp.1-6, December 2010.
- [99] D. Piazza and L. Milstein, "Multiuser diversity-mobility tradeoff: Modeling and performance analysis of a proportional fair scheduling," *IEEE GLOBECOM*, vol. 1, pp. 906-910, November 2002.
- [100] Yanlei Shang; Chuanchang Liu, "An adaptive transmission scheme in multiple input multiple output system," *IEEE International Conference on Broadband Network & Multimedia Technology*, pp.755,759, October 2009
- [101] Kai Zhang; Zhisheng Niu, "Adaptive transmission in spatial multiplexing system with zero forcing receiver," *International Symposium on Multi-Dimensional Mobile Communications Proceedings*, vol.1, pp.301-304, August 2004.
- [102] W. Jaafar, W. Ajib, and D. Haccoun, "Adaptive transmission in cooperative wireless communications," *2009 2nd IFIP Wireless Days*, pp.1-5, December 2009.
- [103] Jianguo Liu; Daofeng Xu; Rui Zhao; Luxi Yang, "Adaptive Transmission for Finite-Rate Feedback MIMO Systems," *IEEE Wireless Communications and Networking Conference*, pp.666-671, March 2008.
- [104] A. Duel-Hallen, "Fading Channel Prediction for Mobile Radio Adaptive Transmission Systems," *Proceedings of the IEEE*, vol.95, no.12, pp.2299-2313, December 2007.
- [105] Min Chen and A. G. Burr, "Low-Complexity Iterative Detection for Overloaded Uplink Multiuser MIMO OFDM System," *International ITG Workshop on Smart Antennas*, Dresden, Germany, March 2012.
- [106] Min Chen and A. G. Burr, "Low-Complexity Channel selection and Iterative Detection for Overloaded Uplink Multiuser MIMO OFDM System," *IEEE Vehicular Technology Conference*, Dresden, Germany, June 2013.
- [107] Li Ping, K. Y. Wu, L. Liu, and W. K. Leung, "A simple, unified approach to nearly optimal multiuser detection and space-time coding," *Proceedings of IEEE*

- Information Theory Workshop*, pp. 53-56, October 2002.
- [108] Li Ping, Q. Guo, and J. Tong, "The OFDM-IDMA approach to wireless communication systems," *IEEE Wireless Communications*, vol. 14, no. 3, pp. 18-24, June 2007.
- [109] L. Linton, P. Conder, and M. Faulkner, "Multiuser communications for underwater acoustic networks using MIMO-OFDM-IDMA," *International Conference on signal Processing and Communication Systems*, pp. 1-8, December 2008.
- [110] J. Shikida, S. Suyama, H. Suzuki, and K. Fukawa, "Iterative Receiver Employing Multiuser Detection and Channel Estimation for MIMO-OFDM IDMA," *IEEE Vehicular Technology Conference*, pp. 1-5, May 2010.
- [111] Z. Luo, and X. Xiong, "Analysis of the effect of carrier frequency offsets on the performance of SC-FDMA-IDMA systems," *CECNet 2nd International Conference*, pp. 889-893, April 2012.
- [112] H. Poveda, G. Ferre, and E. Grivel, "Frequency synchronization and channel equalization for an OFDM-IDMA uplink system," *International Conference Acoustics, Speech and Signal Processing*, pp. 3209-3212, March 2012.
- [113] J. Dang, L. Yang, and Z. Zhang, "Improved SNR Evolution for OFDM-IDMA Systems," *IEEE Wireless Communication Letters*, vol. 1, no. 2, pp. 65-68, April 2012.
- [114] Li Ping, Lihai Liu, K. Y. Wu, and W. K. Leung, "Interleave-Division Multiple-Access (IDMA) Communications," *IEEE Transactions on Wireless Communications*, vol. 5, no. 4, pp. 938-947, April 2006.
- [115] Min Chen and A. G. Burr, "Low-Complexity Iterative Interference Cancellation Multiuser Detection for Overloaded MIMO OFDM IDMA System," *International ITG Workshop on Smart Antennas*, Stuttgart, Germany, March 2013.
- [116] O. Edfors, M. Sandell, J. Beek, S. K. Wilson, and P.O. Borjesson, "OFDM Channel estimation by singular value decomposition", *IEEE Transactions on Communications*, vol. 46, July 1998.
- [117] Yu Zhang, *Code-aided Iterative Techniques in OFDM systems*, Ph.d. Thesis, University of York, 2007.

- [118] J. K. Cavers, "An analysis of pilot symbol assisted modulation for Rayleigh fading channels", *IEEE Transaction on Vehicular Technology*, vol. 40, pp. 686-693, November 1991.
- [119] W. C. Jakes, *Mobile Microwave Communication*, New York: Wiley, 1973.
- [120] L. L. Scharf, "Statistical signal processing: detection, estimation and time series analysis", 1991, Addison-Wesley.
- [121] M. C. Valenti and B. D. Woerner, "Iterative channel estimation and decoding of pilot symbol assisted turbo codes over flat-fading channels", *IEEE Journal on Selected Areas in Communications* vol. 19, pp. 1697-1705, September 2001.
- [122] H. J. Su and E. Geraniotis, "Low-complexity joint channel estimation and decoding for pilot symbol-assisted modulation and multiple differential detection systems with correlated Rayleigh fading", *IEEE Transactions on Communications*, vol. 50, pp. 249-261, February 2002.
- [123] S. M. Kay, *Fundamentals of statistical signal processing: estimation theory*, Prentice Hall, 1993.
- [124] S. Bruck, U. Sorger, S. Gligorevic, and N. Stolte, "Interleaving for outer convolutional codes in DS-CDMA Systems," *IEEE Transactions on Communications*, vol 48, pp. 1100-1107, July 2000.
- [125] A. Tarable, G. Montorsi, and S. Benedetto, "Analysis and design of interleavers for CDMA systems," *IEEE Communications Letters*, vol. 5, pp. 420-422, October 2001.
- [126] F. N. Brannstrom, T. M. Aulin, and L. K. Rasmussen, "Iterative multiuser detection of trellis code multiple access using a posteriori probabilities," in *Proceedings of IEEE International Conference on Communications*, Finland, pp. 11-15, June 2001.